

# Study of Ecological and Epidemiological Models in Presence of Noise

---

*Abhijit Majumder*



# Study of Ecological and Epidemiological Models in Presence of Noise

Thesis submitted for the award  
of the degree of

**Doctor of Philosophy**

by

**Abhijit Majumder**

*Under the supervision of*

**Prof. Nandadulal Bairagi**



Center for Mathematical Biology and Ecology  
Department of Mathematics

Jadavpur University

Kolkata - 700 032, INDIA

September 2022





*To my beloved parents*  
**Smt. Susmita Majumder**  
*and*  
**Sri Ashis Majumder**



## **Declaration**

I, hereby, declare that this thesis represents my own work which has been done after registration for the degree of Ph.D. at Jadavpur University and has not been previously included in any thesis or dissertation for the purpose of earning a degree, diploma, or any other credential.

Abhijit Majumder

যা দ ব পু র বি শ্ব বি দ্যা ল য়

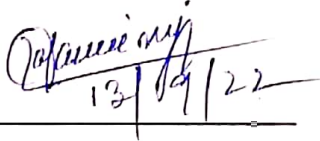
FACULTY OF SCIENCE  
DEPARTMENT OF MATHEMATICS



JADAVPUR UNIVERSITY  
Kolkata-700 032, India  
Telephone : 91 (33) 2414 6717

**CERTIFICATE FROM THE SUPERVISORS**

This is to certify that the thesis entitled “Study of Ecological and Epidemiological Models in Presence of Noise” submitted by Sri Abhijit Majumder, who got his name registered (Ref. No. Email (dated 16/11/2021) & Index No. 69/18/Maths./25) on 20<sup>th</sup> February, 2018 for the award of Ph.D. (Science) degree of Jadavpur University, is absolutely based upon his own work under our supervision and that neither this thesis nor any part of it has been submitted for either any degree / diploma or any other academic award anywhere before.

  
13/09/22

**Dr. Nandadulal Bairagi**  
Professor  
Department of Mathematics  
Jadavpur University  
Kolkata-700 032, India

Nandadulal Bairagi (Ph. D.)  
Professor, Dept. of Mathematics  
Jadavpur University  
Kolkata-700032



## Acknowledgments

I would first like to express my greatest thanks and appreciation to my advisor Prof. (Dr.) Nandadulal Bairagi, whose excellent mentorship was integral to my completion of this thesis and the other requirements associated with my degree. His patient guidance has helped me grow as a researcher, a scientific communicator, and most importantly as a critical thinker. I could not have accomplished this milestone in my education and in my personal and professional development without his close association, invaluable help and continuous support.

I am grateful to the Centre for Mathematical Biology and Ecology, Department of Mathematics, Jadavpur University and to all my teachers of the Department of Mathematics, Jadavpur University, for providing me the platform to work there.

I am grateful to the Council for scientific and industrial research (CSIR), Govt. of India for supporting me financially through a research fellowship.

I thank my senior researchers Dr. Suman Saha and Dr. Debadatta Adak for their sincere help and support. I also thank my fellow researchers, co-workers and friends Dr. Bhaskar Chakraborty, Dr. Shuvojit Mondal for a constant source of encouragement and help; Mr. Chittaranjan Mondal, Ms. Priyanka Saha, Mr. Santanu Bhattacharya for letting me dare to be an open book in front of them with the faith that they would understand me just perfectly; and Mr. Sounov Marick, Mr. Debjit Pal, Mr. Ayanava Basak and Mr. Chirodeep Mondal for adding fun in my otherwise boring life at Jadavpur.

Finally, I thank my parents, my elder brother Mr. Abhik Majumder for supporting me in every aspect of life, enduring my whims with a smile and tolerated my tantrums happily.

August, 2022

Abhijit Majumder



# Contents

<b>1</b>	<b>Introduction</b>	<b>1</b>
1.1	Brief History of Stochastic Differential Equation . . . . .	1
1.2	Basics of Probability . . . . .	5
1.3	Stochastic Process . . . . .	10
1.3.1	Stationary Stochastic Processes . . . . .	10
1.3.1.1	Strict-sense stationary process . . . . .	10
1.3.1.2	Wide-sense stationary process . . . . .	11
1.3.2	Ergodic Stochastic Processes . . . . .	11
1.3.3	Filtrations . . . . .	11
1.3.4	Martingale . . . . .	11
1.3.5	Markov Process . . . . .	12
1.4	Symmetric Random Walk . . . . .	13
1.5	Brownian Motion . . . . .	13
1.5.1	Brownian Motion as the Limit of Symmetric Random Walk . . . . .	13
1.5.2	Defining Brownian Motion or Wiener Process . . . . .	14
1.5.3	Properties of Wiener Process . . . . .	15
1.5.4	Transformation of Wiener Process . . . . .	16
1.5.5	Non-differentiability of Wiener Process . . . . .	16
1.6	Stochastic Integration: The Itô Integral . . . . .	17
1.6.1	Properties of Ito Integral . . . . .	20
1.6.2	Ito's Lemma . . . . .	20
1.7	Different Types of Stochastic Models . . . . .	21
1.7.1	Continuous Time and Discrete State Process (CTMC) . . . . .	22
1.7.2	Discrete Time Markov Chain (DTMC) . . . . .	23
1.7.3	Continuous Time and Continuous State Process . . . . .	23
1.7.3.1	A heuristic approach of formulation of SDE . . . . .	24



---

1.7.4	Solution of SDEs and it’s Uniqueness . . . . .	24
1.7.4.1	Addition of noise in deterministic ODE . . . . .	25
1.7.5	Solution of Some Well-known Stochastic Differential Equations	27
1.7.5.1	Geometric Brownian motion . . . . .	27
1.7.5.2	Orstein-Uhlenbeck process . . . . .	28
1.7.5.3	Mean reverting Ornstein–Uhlenbeck (OU) process . .	28
1.7.6	Some Important Inequalities, Theorems, Lemmas and Definitions Used in the Study . . . . .	29
1.8	Some Basic Definitions and Tools Used For the Deterministic Study .	33
1.8.1	Mathematical Tools . . . . .	33
1.8.2	Optimization Techniques . . . . .	37
1.8.2.1	Fminsearch Algorithm . . . . .	37
1.8.2.2	Lsqcurvefit Algorithm . . . . .	38
1.8.2.3	Partial Rank Correlation Coefficient (PRCC) . . . .	39
1.8.2.4	Latin Hypercube Sampling (LHS) . . . . .	40
1.8.2.5	Parameter estimation technique . . . . .	41
1.9	Literature Review and Motivation . . . . .	42
1.10	Aim of the Thesis . . . . .	47
1.11	Thesis Overview . . . . .	48
<b>2</b>	<b>Phytoplankton-zooplankton interaction under environmental stochasticity: Survival, extinction and stability</b>	<b>51</b>
2.1	Introduction . . . . .	51
2.2	Analysis of the deterministic model . . . . .	54
2.2.1	Positivity and boundedness of solutions . . . . .	54
2.2.2	Equilibria and their stabilities . . . . .	55
2.3	Analysis of the stochastic model . . . . .	58
2.3.1	Existence and uniqueness of positive solution . . . . .	58
2.3.2	Stochastic bounds of the solutions . . . . .	60
2.3.3	Stochastic persistence . . . . .	63
2.3.4	Stationary distribution . . . . .	67
2.4	Numerical Simulations . . . . .	69
2.5	Stochastic perturbation around an equilibrium point . . . . .	75
2.6	Numerical Simulations . . . . .	79
2.7	A case study . . . . .	81

## CONTENTS

---

2.8	Discussion . . . . .	82
<b>3</b>	<b>Persistence and extinction of infection in stochastic SIS host-parasite epidemic model with horizontal and imperfect vertical transmissions</b>	<b>87</b>
3.1	Introduction . . . . .	87
3.2	The model . . . . .	88
3.3	Study of the deterministic model . . . . .	90
3.4	Study of the stochastic model . . . . .	94
3.5	Simulation results . . . . .	103
3.6	Discussion . . . . .	110
<b>4</b>	<b>Persistence and extinction of species in a disease-induced ecological system under environmental stochasticity</b>	<b>113</b>
4.1	Introduction . . . . .	113
4.2	The model . . . . .	115
4.2.1	Deterministic model . . . . .	115
4.2.2	Equilibrium and their local stability . . . . .	117
4.2.3	Incorporating stochasticity . . . . .	119
4.3	Mathematical results . . . . .	119
4.4	Simulation results . . . . .	132
4.4.1	Effect of environmental noise on the persistence and extinction of species . . . . .	132
4.4.2	Red grouse: A case study . . . . .	139
4.5	Discussion . . . . .	141
<b>5</b>	<b>Persistence and extinction criteria of Covid-19 pandemic: India as a case study</b>	<b>147</b>
5.1	Introduction . . . . .	147
5.2	Mathematical results . . . . .	152
5.2.1	Deterministic results . . . . .	152
5.2.1.1	Basic reproduction number . . . . .	152
5.2.1.2	Existence and stability of equilibrium points . . . . .	154
5.2.2	Stochastic results . . . . .	157
5.3	Case study . . . . .	173
5.4	Discussion . . . . .	179

<b>6 Is large-scale vaccination sufficient for controlling the Covid-19 pandemic with uncertainties? A model-based study</b>	<b>181</b>
6.1 Introduction . . . . .	181
6.2 The model . . . . .	183
6.3 Results . . . . .	185
6.3.1 Basic reproduction number of the deterministic system . . . . .	185
6.3.2 Stochastic study . . . . .	186
6.4 Case study . . . . .	195
6.5 Discussion . . . . .	202
<b>7 Future Work</b>	<b>205</b>
<b>References</b>	<b>207</b>
<b>AUTHOR'S PUBLICATIONS</b>	<b>241</b>

# Chapter 1

## Introduction

### 1.1 Brief History of Stochastic Differential Equation

The stochastic differential equation is an area of mathematics that includes randomness in a deterministic system to make the result more realistic. Before one can run, one must first learn to walk. The ordinary differential equation (ODE) plays a crucial role in modelling different natural phenomena and problems in engineering fields. ODE equations describing natural processes always contain some coefficients as a parameter or a functioning part which characterize some aspects of physical phenomena or environmental factors that should be experimentally determined. Therefore, a more generalized realistic formulation of the differential equation must be done by considering the uncertainties and random noise associated with the process. This leads to the development of the stochastic differential equation (SDE), a differential equation for a stochastic process. Therefore, a stochastic differential equation consists of a random part. However, the statistical properties of this random part should be known beforehand. This random part can be either a random variable or a random process. Consequently, the realization of an SDE is also a stochastic process, and the central goal of the theory of SDE is to find the properties of its solutions.

The origin of stochastic differential equations is linked to physics-related issues. We want to start by mentioning the Gibbsian ensemble method, described by J. W. Gibbs in 1903, which is a probabilistic approach to the problem of the time evolution of a large number of material particles (represented by the Hamilton differential equations) in classical statistical mechanics ([Gibbs \[1906\]](#)). Although this dynamical

model merely considers the statistical aspect of a system's initial state (governing Hamiltonian equations are deterministic), it should nonetheless be regarded as the first successful attempt to combine differential equations and probability theory. A statistical description of a system's motion has been adopted due to the challenges in precisely determining the dynamical variables and the fact that the systems considered in statistical physics contain a relatively large number of particles. The so-called phase probability density is typically introduced to do this analysis (Sobczyk [2001]). As a result, the issue with classical statistical mechanics can be expressed by stochastic processes. In a physical system, if the system is open, meaning it interacts with an external field, the Hamiltonian is changed to include the excitations from the external field (Sobczyk [2001]). As a consequence, random fluctuations are added to the system of equations relevant to the external field with which the system interacts. The external fields' interaction should frequently be treated as randomly fluctuating in time. The one-dimensional Langevin equation for the Brownian motion (of a microscopic particle suspended in a liquid) is one of the most basic examples of the description mentioned above (Ullersma [1966]). The stochastic differential equations are typically thought to have their roots in the Langevin equation and the Brownian motion phenomenon (Dunkel and Hänggi [2009]). One of the most intriguing examples of random physical processes is the Brownian motion phenomenon, which was experimentally discovered by the Scottish botanist R. Brown in 1827 (Sobczyk [2001]). Numerous physicists and mathematicians focused their attention on the mathematical modelling of this phenomenon. The first successful outcomes are associated with Einstein and Smoluchowski (Einstein [1956], Nelson [1966]), who came up with a partial differential equation for the probability density of the Brownian particle's displacement. Paul Langevin developed a phenomenological description of the erratic motion of a heavy "Brownian" particle submerged in a liquid almost simultaneously in 1908 (Lavenda [1985]). He believed that the Newtonian equation for the particle could explain this erratic behaviour. The interaction of the surrounding fluid with the Brownian particle produces two separate forces: a dissipative force (owing to dynamic friction in the course of a particle's path through a viscous fluid) and a fluctuating force (arising from molecular collisions). Therefore, Langevin added a random process while formulating the ODE, generally called white noise, with zero mean and finite variance (Lemons and Gythiel [1997]). This method, which was historically connected to Bernstein's work from the 1930s (Perrin [1934]), was systematically developed by Ito in the early 1940s (Itô [1944]) and is now referred to as a theory of the

## 1.1. Brief History of Stochastic Differential Equation

---

Ito stochastic differential equations.

The theory of stochastic differential equations began in mathematics as a means of constructing diffusion Markov processes based on the Brownian motion process (Sobczyk [2001]). This theory also serves as a foundation for a rigorous analysis of equations of the Langevin type, where a random component is idealized as the so-called "white noise." Since the early 1960s, stochastic differential equations have gained widespread acceptance as a crucial mathematical tool for modelling and analysis in finance, biological issues, to a variety of processes in engineering, particularly in control and mechanical systems. Propagation of radio waves through an atmosphere with small density fluctuations has been extensively studied using the stochastic theory (Lighthill [1953], Tatarski [2016], Keller et al. [1964]). Stochastic analysis is required when the parameters of the circuit, i.e., the coefficients in the equation related to circuit theory, fluctuate in mechanical and electromechanical control systems (Van Kampen [1976]). Light waves in the atmosphere are bent by the fluctuations in the atmosphere, as evidenced by the twinkling of stars. In theory, the three-dimensional wave equation covers this. Still, in practice, the geometrical optics approximation is used, resulting in stochastic nonlinear equations for the paths of the light rays (Chernov et al. [1960]). Sound transmission in the atmosphere or the ocean is also of practical interest (Horton Sr [1969]). On the other hand, sonar is less impacted by density variations than by scattering on randomly located objects such as fish due to its short wavelength. One is interested in the consequent "reverberation" (backscattering into the receiver) and signals attenuation. The reflection of the bottom and the waves on the surface results in stochastic boundary conditions (Kohler [1975], kra [1975]). Similar issues arise in the study of thermo-elastic waves, gravity waves, and the transmission of sonic booms (Pierce and Maglieri [1972], Wenzel [1975]). Differential equations with random initial conditions are naturally present in many other domains (e.g., chemical kinetics, structural mechanics, heat conduction, etc.). In this context, one of the earliest stochastic problems for partial differential equations dealt with heat conduction in an infinite beam when the beam's temperature was characterized by a random function (Kampe de Ferie [1955]). Stochastic functions also model diffusion in moving fluid. In the electromagnetic theory, the incident photon beam determines the amount of charge carried in a photoconductor's conduction band. The probability distribution of that number obeys a linear equation (Chapman—Kolmogorov or master equation) if the photon arrival times are uncorrelated (shot noise) (Van Kampen [1976]). If the arrival times are correlated,

## 1. Introduction

---

the linear equation coefficients must be considered stochastic time functions (Ubbink [1971]). A vast application of stochastic modelling can also be found in the study of the spectral lines emitted and absorbed by an atom in an ionized gas in the field of kinetic theory (Van Kampen [1976]), in studying the motion of a spin in a solid in the field of magnetic resonance theory (Bloch [1946], Wangsness and Bloch [1953]), in describing the energy loss in the theory of laser under electromagnetic field (Haken and Weidlich [1969], Haken [1970]). Stochasticity, it is also observed in Maxwell's equations for a medium (Landau and Lifshitz [1960]), in the Boltzmann equation (Khalatnikov et al. [1958], Bixon and Zwanzig [1969], Fox and Uhlenbeck [1970]), in the equations for the gravitational field of the universe (Nariai [1974, 1975]), in economics and finance; stocks and currency options, bonds, interest rates (by continuous time stochastic process, for example, Black-Scholes model, Mean Reverting Process) (Klebaner [2012]), in studying the stochastic effects to the stability problems related to neural network dynamics (Liao and Mao [1996b,a]).

In biological sciences, the stochastic analysis also has numerous applications. Discrete-time Markov chain models, continuous-time Markov chain models, and stochastic differential equation (SDE) models are the three most prevalent types of stochastic models used to analyze population dynamics (Panik [2017]). The first mathematical model in epidemiology that incorporated randomness was suggested by McKendrick [1925]. This is the first model that modified a deterministic general epidemic model into a stochastic continuous time version. An early discrete time model that incorporates randomness is the Binomial chain model of Reed and Frost, where the number of infectives in future time follows a Binomial distribution (Bailey et al. [1975]). In 1949, seminal work of Bartlett [1949] opened up a new horizon. He extensively analyzed the continuous time stochastic version of the model proposed by McKendrick [1925]. This work has given the idea of studying the stochastic properties of various models. After a solid mathematical and logical foundation laid by Itô [1944, 1951], Doob [1953], Hunt [1957] and others, the application of stochastic differential equations is implemented in many different fields. In ecology, Levins [1969] & Capocelli and Ricciardi [1974] first analyzed the well-known logistic or Pearl-Verhulst model in a stochastic environment by considering a multiplicative noise. Stochastic analysis of the fishing model with a fish harvesting term started with the pioneering work of Beddington and May [1977]. An early study of the stochastic phytoplankton zooplankton model was initiated by Parker [1974]. In this paper, the author developed a stochastic zooplankton model by considering the relationships of the

## 1.2. Basics of Probability

---

nutrients, the algae and environmental factors like temperature and light intensity. Among the first line of work on the phytoplankton-zooplankton modelling, [Jernigan and Tsokos \[1980\]](#) introduced a linear stochastic process in the deterministic model proposed by [O'Brien and Wroblewski \[1971\]](#). They analyzed the predation dynamics and the stability of the probability distribution of the system. Stochastic calculus was also applied in the development of cancer modelling ([Armitage and Doll \[1957\]](#), [Fisher \[1958\]](#), [Nordling \[1953\]](#), [Knudson Jr \[1971\]](#)). [Garay and Lefever \[1978\]](#) consider a noise-induced stochastic kinetic interaction model between a normal and tumour cell where the immunological interaction is followed by Michaelis–Menten kinetics and then analyze the stochastic stability of the system in different parameter regimes. The earliest work on the stochastic predator-prey system was done by [Leslie and Gower \[1960\]](#), where the stochasticity was considered in the death rate of each species. After developing the theory of stochastic analysis, many contributions have been made to the stochastic studies of ecological and epidemiological models. It is established that stochastic modelling has a better ability to represent natural phenomena. In the following, we present the basic theory of stochastic differential calculus, give several definitions, and present some applications of stochastic differential equations.

## 1.2 Basics of Probability

The concept of experiments and events is covered by probability theory. A process of trial and observation is an experiment. An experiment is said to be random if the results are unpredictable. An event is the result of a random experiment. The sample space of an experiment is the collection of all possible elementary outcomes of a random experiment, generally symbolized by  $\Omega$ . An event is a subset of the sample space. For instance, if we roll a fair die, the possible outcomes are any of the numbers between 1 to 6. Therefore, the sample space is given by

$$\Omega = \{1, 2, 3, 4, 5, 6\}.$$

The event of getting an odd number in rolling a die is a subset of  $\Omega$ , which is given by  $A = \{1, 3, 5\}$ .

To define a structure on the space  $\Omega$ , consider a family of subsets  $\mathcal{E}$  of  $\Omega$  with the following properties:

- (i)  $\phi$  and  $\Omega$  belong to  $\mathcal{E}$ .



- (ii) Complementation of any set of  $\mathcal{E}$  also belongs to that set, i.e., if  $F \in \mathcal{E}$  then  $\bar{F} \in \mathcal{E}$ .
- (iii)  $\mathcal{E}$  is closed under countable union and countable intersections, i.e., if  $F_1, F_2, F_3, \dots$  be a countable collection of events in  $\mathcal{E}$ , the  $\cup_{n=1}^{\infty} F_n$  and  $\cap_{n=1}^{\infty} F_n$  are both in  $\mathcal{E}$ .

Under this structure,  $\mathcal{E}$  is said to be a  $\sigma$ -algebra or  $\sigma$ -field. The pair  $(\Omega, \mathcal{E})$  is called a measurable space. A probability measure  $P$  on the measurable space  $(\Omega, \mathcal{E})$  is a function  $P : \mathcal{E} \rightarrow [0, 1]$  such that

- (i)  $P(\phi) = 0$  and  $P(\Omega) = 1$ ,
- (ii) for any disjoint countable collection of subsets  $A_1, A_2, A_3, \dots \in \mathcal{E}$ ,

$$P\left(\bigcup_{n=1}^{\infty} A_n\right) = \sum_{n=1}^{\infty} P(A_n).$$

The triple  $(\Omega, \mathcal{E}, P)$  is called a probability space. This is said to be a complete probability space if  $\mathcal{E}$  contains all subsets  $B$  of  $\Omega$  such that the  $P$ -outer measure ( $P^*$ ) is zero, i.e.,

$$P^*(B) = \inf\{P(C) : C \in \mathcal{E}, B \subset C\} = 0.$$

**Conditional probability:** For two events  $A$  and  $B$ , the conditional probability of the event  $A$  given event  $B$  is denoted by  $P(A|B)$  and is defined by

$$P(A|B) = \frac{P(A \cap B)}{P(B)} \quad \text{provided } P(B) > 0.$$

**Independence of events:** Two events  $A$  and  $B$  are said to be independent if the occurrence of one event doesn't influence the probability of occurrence of the other event. In the language of conditional probability, if the events  $A$  and  $B$  are independent, then the conditional probability of event  $A$  given that  $B$  has already occurred, i.e.,  $P(A|B)$  is equal to the probability of  $P(A)$ . Therefore, if  $A$  and  $B$  are independent events, then

$$P(A|B) = P(A).$$

Again by the definition of conditional probability,  $P(A|B) = \frac{P(A \cap B)}{P(B)}$ . Therefore, alternatively, we can define that the events  $A$  and  $B$  are independent if

$$P(A \cap B) = P(A)P(B).$$

## 1.2. Basics of Probability

---

**Random variable:** For a random experiment with sample space  $\Omega$ , random variable  $X$  maps a sample point  $\omega \in \Omega$  to a real number. For a rigorous definition, let  $(\Omega, \mathcal{E}, P)$  be a probability space. A random variable  $X$  is a real-valued function from  $\Omega$  to  $\mathbb{R}$  such that for all  $M \in \mathbb{R}$ ,  $X^{-1}(M) \subseteq \mathcal{E}$ . The range of a random variable is called the spectrum of the random variable. If the spectrum is finite or countably infinite, then the random variable is called a discrete random variable. If the range of the random variable is an open or closed subset of  $\mathbb{R}$ , then the random variable is called a continuous random variable.

**Probability distribution function, probability mass function, probability density function:**

Consider  $(\Omega, \mathcal{E}, P)$  to be a probability space. The distribution function  $F$  of random variable  $X$  is defined by

$$F(x) = P(\{\omega \in \Omega : X(\omega) \leq x\}).$$

For a discrete random variable having spectrum  $x_1, x_2, x_3, \dots \in \mathbb{R}$ , distribution function of random variable can be written as

$$F(x) = P(\{\omega \in \Omega : X(\omega) \leq x\}) = \sum_{x_i < x} p(x_i),$$

where  $p$  is called the probability mass function defined by  $p : x_1, x_2, x_3, \dots \rightarrow [0, 1]$  such that  $p(x_i) = p(X = x_i)$ .

For a continuous random variable, distribution function is defined by

$$F(x) = P(\{\omega \in \Omega : X(\omega) \leq x\}) = \int_{-\infty}^x p(t)dt,$$

where  $p(x)$  is a piecewise continuous non-negative function called probability density function.

**Expectations:** The expectation of a random variable  $X$  is denoted by  $\mathbb{E}(X)$  or  $\bar{X}$

and defined by

$$\mathbb{E}(X) = \begin{cases} \sum_i x_i p(x_i), & \text{whenever } X \text{ is discrete} \\ \int_{-\infty}^{\infty} x p(x) dx, & \text{whenever } X \text{ is continuous.} \end{cases}$$

**Variance:** The variance of a random variable is denoted by  $\text{Var}(X)$  and defined by

$$\text{Var}(X) = \mathbb{E}[(X - \bar{X})^2] = \begin{cases} \sum_i (x_i - \bar{X})^2 p(x_i), & \text{whenever } X \text{ is discrete} \\ \int_{-\infty}^{\infty} (x - \bar{X})^2 p(x) dx, & \text{whenever } X \text{ is continuous.} \end{cases}$$

We, here, list some important properties of expectation and variance.

- (i)  $\mathbb{E}(c) = c$ , where  $c$  is any constant.
- (ii)  $\mathbb{E}(a \pm bX) = \mathbb{E}(a) \pm b\mathbb{E}(X)$ ,  $a, b$  are real numbers.
- (iii)  $\mathbb{E}(X_1 + X_2 + \dots + X_n) = \mathbb{E}(X_1) + \mathbb{E}(X_2) + \dots + \mathbb{E}(X_n)$ .
- (iv)  $\text{Var}(X) = \mathbb{E}(X^2) - [\mathbb{E}(X)]^2$ .
- (v)  $\text{Var}(c) = 0$ , where  $c$  is a constant.
- (vi)  $\text{Var}(a \pm bX) = a^2 \text{Var}(X)$ ,  $a$  is a real number.

**Almost sure convergence of sequences of random variables:** Let  $\{X_n\}_{n=1}^{\infty}$  be a sequence of random variables and  $X$  be another random variable defined on a probability space  $(\Omega, \mathcal{E}, P)$ . Define a set  $H = \{\omega \in \Omega : X_n(\omega) \rightarrow X(\omega) \text{ as } n \rightarrow \infty\}$ . Then the sequence  $X_n$  converges to  $X$  almost surely (a.s.) as  $n \rightarrow \infty$  if  $P(H) = 1$ . A sufficient condition for almost sure (a.s.) convergence is :

$$\text{If } \sum_{n=1}^{\infty} P(|X_n - X| \geq \epsilon) < \infty \quad \forall \epsilon > 0, \text{ then } X_n \xrightarrow{a.s.} X.$$

We now discuss two important theorems which are related to the average of random variables.

**Strong Law of Large Numbers:** Let  $\{X_n\}_{n=1}^{\infty}$  be a sequence of independent and identically distributed (i.i.d) random variables defined on some probability space  $(\Omega, \mathcal{E}, P)$ . Let  $\mathbb{E}(X_i) = \mu$  and  $\mathbb{E}|X_i| < \infty$  for all  $i \geq 1$ . Let us define the sum  $S_n =$

## 1.2. Basics of Probability

---

$\sum_{k=1}^n X_k$ . Then  $\frac{S_n}{n}$  converges to  $\mu$  in almost sure sense, i.e.,  $P(\lim_{n \rightarrow \infty} \frac{S_n}{n} = \mu) = 1$ .

**Central limit Theorem:** Let  $\{X_n\}$  be a sequence of i.i.d random variables with finite mean  $\mathbb{E}(X_i) = \mu$  and finite variance  $\text{Var}(X_i) = \sigma^2$ . Define  $S_n = X_1 + X_2 + \dots + X_n$ . Then,  $\mathbb{E}(S_n) = n\mu$  and  $\text{Var}(S_n) = n\sigma^2$ . Define  $Z_n = \frac{S_n - n\mu}{\sigma\sqrt{n}}$ . Then  $Z_n$  is standard random variable with zero mean and unit variance. By Central Limit Theorem, if  $F_{Z_n}(z)$  is the cumulative distribution function of  $Z_n$ , then

$$\lim_{n \rightarrow \infty} F_{Z_n}(z) = \lim_{n \rightarrow \infty} P[Z_n \leq z] = \frac{1}{2\pi} \int_{-\infty}^z e^{-t^2/2} dt,$$

which implies that  $\lim_{n \rightarrow \infty} Z_n \sim N(0, 1)$ , the standard normal distribution.

We, now, state two very useful inequalities in the area of probability theory.

**Markov's inequality:** If  $X$  is a random variable with  $P(X \geq 0) = 1$ , then for any  $\alpha > 0$

$$P(X \geq \alpha) \leq \frac{\mathbb{E}(X)}{\alpha}.$$

Markov's inequality provides an upper bound for the probability that a non-negative function of a random variable is greater than or equal to some positive constant. It takes its name from the Russian mathematician Andrey Markov.

**Chebyshev inequality:** The Chebyshev inequality enables us to obtain bounds on probability when both the mean and variance of a random variable are known. The statement of the inequality is stated as:

Let  $X$  be a random variable with mean  $\mu$  and variance  $\sigma^2$ . Then for any  $\alpha > 0$

$$P(|X - \mu| \geq \alpha) \leq \frac{\sigma^2}{\alpha^2}.$$

This inequality states that the probability of the absolute difference between a random variable and its mean is greater than a real positive real number is bounded by a constant.

## 1.3 Stochastic Process

A stochastic process  $\{X_t\}_{t \in I}$ , also known as a random process, is a parameterized collection of random variables in which  $X_t$  assumes values in a state space  $S$  for each  $t$  in an indexed set (time-space)  $I$ . The nature of the time-space and state space can be used to classify stochastic processes. A discrete-time stochastic process occurs when the time-space is countable or countably infinite. If  $I$  is a real-number interval, the process is known as a continuous-time stochastic process. A stochastic process is called a discrete-state stochastic process if its state space is finite or countably infinite, and a continuous-state stochastic process if its state space is continuous. For example, a discrete-time and the discrete-state stochastic process is flipping a fair coin every second to acquire an outcome. An instance of a continuous-time and discrete-space stochastic process is the number of cars passing through a checkpoint between 9 a.m. and 12 p.m. The value  $X_t$  of a stock price from the start to the close of trading on a specific day is an example of a continuous-time, continuous-state process.

### 1.3.1 Stationary Stochastic Processes

A stationary stochastic process is one whose statistical properties do not change over time. This section will look at two stochastic stationary processes: strict-sense stationary and wide-sense stationary (WSS) processes.

#### 1.3.1.1 Strict-sense stationary process

A stochastic process is strictly stationary if its finite-dimensional distributions are invariant with respect to time displacements, that is

$$F_X(x_1, x_2, \dots, x_n; t_1, t_2, \dots, t_n) = F_X(x_1, x_2, \dots, x_n; t_1 + \tau, t_2 + \tau, \dots, t_n + \tau)$$

for all  $n = 1, 2, \dots$ ,  $x_1, x_2, \dots, x_n \in \mathbb{R}$ ,  $t_1, t_2, \dots, t_n \in I$ ,  $\tau \in \mathbb{R}$  such that  $t_1 + \tau, t_2 + \tau, \dots, t_n + \tau \in I$ .

### 1.3. Stochastic Process

---

#### 1.3.1.2 Wide-sense stationary process

Stochastic processes in which the mean and autocorrelation function are invariant on absolute time are called wide-sense stationary process (WSS) processes.

#### 1.3.2 Ergodic Stochastic Processes

Consider a stochastic process  $\{X_t\}$  whose observed sample paths are  $x(t)$ . The time average of the sample path is defined by

$$\bar{x} = \frac{1}{2T} \int_{-T}^T x(t) dt.$$

The ensemble average is the statistical average of a random process, denoted by  $\mathbb{E}[X(t)]$ . When the process is ergodic, the time average taken along that single sample path equals the ensemble average, i.e. the expected value of the process.

#### 1.3.3 Filtrations

Consider a probability space  $(\Omega, \mathcal{E}, P)$  and a stochastic process  $\{X_t\}_{t \in I}$ . A family of sub- $\sigma$  algebras  $\mathcal{F} = \{\mathcal{F}_t : t \in T\}$  of  $\mathcal{E}$  is a filtration if  $\mathcal{F}_t \subset \mathcal{F}_s$  whenever  $t \leq s$ .

We say that the stochastic process  $\{X_t\}_{t \in I}$  is  $\mathcal{F}_t$ -adapted if for each  $t \in I$ ,  $X_t$  is  $\mathcal{F}_t$ -measurable. Sometimes, an adapted process is called a non-anticipating process—a process that “cannot see in the future.”

#### 1.3.4 Martingale

Consider a stochastic process  $\{X_t\}_{t \in I}$  on the probability space  $(\Omega, \mathcal{E}, P)$  with a filtration  $\{\mathcal{F}_t\}_{t \in I}$ . The stochastic process is a martingale if it satisfies the following properties:

- (i)  $\mathbb{E}[|X_t|] < \infty \forall t \in I$ ,
- (ii)  $\mathbb{E}[X_t | \mathcal{F}_s] = X_s$  a.s. for any  $s \leq t$ .

The stochastic process  $\{X_t\}_{t \in I}$  will be called a super-martingale if

$$\mathbb{E}[X_t | \mathcal{F}_s] \leq X_s.$$

The random process  $\{X_t\}_{t \in I}$  will be called a sub-martingale if

$$\mathbb{E}[X_t | \mathcal{F}_s] \geq X_s.$$

The notion of martingale reflects the idea of fair play in that the player's predicted fortune at any time in the future is the same as his existing fortune, regardless of the player's current and prior fortunes. In contrast, a sub-martingale portrays a favourable game because the expected fortune rises in the future. Still, a super-martingale represents an unfavourable game because the expected fortune declines in the future.

### 1.3.5 Markov Process

Consider a probability space  $(\Omega, \mathcal{E}, P)$  and a stochastic process  $\{X_t\}_{t \in I}$  with the index set  $I$ . Also consider a filtration  $\{\mathcal{F}_t\}_{t \in I}$  of  $\{X_t\}_{t \in I}$ . Then the random process  $\{X_t\}_{t \in I}$  is said to be a Markov process if it satisfies any one of the following equivalent properties:

- (i)  $P(X_t | X_u, 0 \leq u \leq s) = P(X_t | \mathcal{F}_s), s \leq t.$
- (ii)  $P(X_t | X_{t_1} = x_1, \dots, X_{t_{n-1}} = x_{n-1}, X_{t_n} = x_n) = P(X_t | X_{t_n} = x_n)$  for any  $n = 1, 2, \dots; t_1 \leq \dots \leq t_{n-1} \leq t_n \leq t; x_1, \dots, x_{n-1}, x_n \in \mathbb{R}.$
- (iii)  $\mathbb{E}[Y | X_u, 0 \leq u \leq s] = \mathbb{E}[Y | X_s]$  for any  $\mathcal{F}_t$ -measurable and integrable random variable  $Y$  and  $s \leq t.$

The above properties demonstrate that for a Markov process, given the current state of the process, the future state is independent of the past. This is known as the Markov property. Markov processes are categorized based on the nature of the time space and the nature of the state space. It is known as the discrete-state Markov process in discrete state space and the continuous-state Markov process in continuous state space, respectively. Similarly, depending on the nature of time space, it can be referred to as a discrete-time or continuous-time Markov process. A discrete-state Markov process is referred to as a Markov chain.

## 1.4. Symmetric Random Walk

---

### 1.4 Symmetric Random Walk

Let  $\{X_t\}_{t=1}^{\infty}$  be an independent and identically distributed random variables on the probability space  $(\Omega, \mathcal{E}, P)$ , where  $\Omega = \{-1, 1\}$  and  $\mathcal{E} = 2^{\Omega}$ .  $X_t$  assumes the two values 1 and -1 with probability  $\frac{1}{2}$ , i.e.,

$$X_t = \begin{cases} 1, & \text{with probability } \frac{1}{2} \\ -1, & \text{with probability } \frac{1}{2}. \end{cases}$$

By this definition of  $X_t$ , we have  $\mathbb{E}(X_t) = \frac{1}{2} \cdot 1 + \frac{1}{2}(-1) = 0$  and  $\text{Var}(X_t) = 1^2 \cdot \frac{1}{2} + (-1)^2 \cdot \frac{1}{2} = 1$ . Define another random variable  $Z_t = \sum_{j=1}^t X_j$ ,  $t \geq 1$ . One can easily observe that  $\mathbb{E}(Z_t) = 0$ ,  $\text{Var}(Z_t) = t$ , and  $\sigma(Z_t) = \sqrt{t}$ . Therefore,  $\frac{Z_t}{\sqrt{t}} \sim \mathcal{N}(0, 1)$ . Moreover, it is important to observe that  $\{Z_t\}_{t=1}^{\infty}$  is a martingale. Consider  $Z_t = \sum_{j=1}^t X_j$  and a filtration  $\mathcal{F}_t$ , a  $\sigma$ -field generated by  $\{X_1, X_2, \dots, X_t\}$ . Here,  $\mathbb{E}(|Z_t|) < \infty$ ,  $Z_t \in \mathcal{F}_t$ ,  $X_{t+1}$  is independent of  $\mathcal{F}_t$  and  $Z_{t+1} = Z_t + X_{t+1}$ . Using these facts, it follows that  $\mathbb{E}(Z_{t+1} | \mathcal{F}_t) = \mathbb{E}(Z_t | \mathcal{F}_t) + \mathbb{E}(X_{t+1} | \mathcal{F}_t) = Z_t + \mathbb{E}(X_{t+1}) = Z_t$  and therefore,  $\{Z_t\}_{t=1}^{\infty}$  is a martingale.

### 1.5 Brownian Motion

Brownian motion is a continuous-time random process frequently employed in economics, biology, and management science. Brownian motion was originally noticed in the motion of a pollen particle floating in the fluid by the Scottish botanist Robert Brown in 1827. The movement of the pollen particles in his experiment looked to be random. After nearly 80 years, Einstein published a paper in 1905 explaining that the irregular mobility of pollen was caused by pressures exerted on the pollen by the molecules in surrounding fluids. N. Wiener laid the mathematical underpinning of Brownian motion as a stochastic process in 1923; therefore, the Brownian motion is also called the Wiener process.

#### 1.5.1 Brownian Motion as the Limit of Symmetric Random Walk

We will now construct Brownian motion from a symmetric random walk. Divide the half line  $[0, \infty)$  to small sub-intervals of length  $\delta$ . The intervals are  $(0, \delta]$ ,  $(\delta, 2\delta]$ , ...,



$((n-1)\delta, n\delta], \dots$ . Consider that in each time slot, we toss a fair coin and define a random variable  $X_t$  as follows.  $X_t = \sqrt{\delta}$ , if the  $t$ -th coin toss yields a head and  $X_t = -\sqrt{\delta}$ , if the  $t$ -th coin toss results in a tail. Thus, we have

$$X_t = \begin{cases} \sqrt{\delta}, & \text{with probability } \frac{1}{2} \\ -\sqrt{\delta}, & \text{with probability } \frac{1}{2}. \end{cases}$$

Observe that  $\mathbb{E}(X_t) = 0$  and  $\text{Var}(X_t) = \delta$ . Now define a process  $B(t)$  as  $B(0) = 0$  and  $B(t) = B(n\delta) = \sum_{i=1}^n X_i$ . By our construction,  $B(t)$  is the sum of independent and identically distributed random variables. One can easily observe that  $\mathbb{E}(B(t)) = \sum_{i=1}^n \mathbb{E}(X_i) = 0$  and  $\text{Var}(B(t)) = \sum_{i=1}^n \text{Var}(X_i) = n\delta = t$ . For any  $t \in (0, \infty)$  as  $n \rightarrow \infty$   $\delta$  will tend to 0 and therefore, by central limit theorem,  $B(t)$  will become a normal random variable, i.e.,  $B(t) \sim \mathcal{N}(0, t)$ .

Since the coin tossed are independent, we can conclude that  $B(t)$  has independent increment which implies, for all  $0 \leq t_1 < t_2 < t_3 < \dots < t_n < \dots$ , the random variables  $B(t_2) - B(t_1)$ ,  $B(t_3) - B(t_2), \dots, B(t_n) - B(t_{n-1})$  are independent.

A process  $X_t$  has stationary increments if for all  $t_1, t_2 \geq 0$  and  $\epsilon > 0$ , the two random variables  $X(t_2) - X(t_1)$  and  $X(t_2 + \epsilon) - X(t_1 + \epsilon)$  have same distribution. In other words, distribution depends only on the length of the interval and not on the exact location of the interval. To prove this, we argue as follows. For  $0 \leq t_1 < t_2$ , we assume  $t_1 = n_1\delta$  and  $t_2 = n_2\delta$ . One then have  $B(t_1) = B(n_1\delta) = \sum_{t=1}^{n_1} X_t$  and  $B(t_2) = B(n_2\delta) = \sum_{t=1}^{n_2} X_t$ . Thus,  $B(t_2) - B(t_1) = \sum_{t=n_1+1}^{n_2} X_t$ . Therefore,  $\mathbb{E}[(B(t_2) - B(t_1))] = \sum_{t=n_1+1}^{n_2} \mathbb{E}(X_t) = 0$  and  $\text{Var}((B(t_2) - B(t_1))) = \sum_{t=n_1+1}^{n_2} \text{Var}(X_t) = (n_2 - n_1)\text{Var}(X_1) = (n_2 - n_1)\delta = n_2\delta - n_1\delta = t_2 - t_1$ . Thus, for  $0 \leq t_1 < t_2$ , the distribution of  $B(t_2) - B(t_1)$  depends only on the length of the interval  $[t_1, t_2]$  and also  $B(t_2) - B(t_1) \sim \mathcal{N}(0, t_2 - t_1)$ .

We summarize the properties of the Brownian motion as follows.

### 1.5.2 Defining Brownian Motion or Wiener Process

Let  $(\Omega, \mathcal{E}, P)$  be a probability space with filtration  $\{\mathcal{F}_t\}_{t \geq 0}$ . The Brownian motion is an  $\{\mathcal{F}_t\}_{t \geq 0}$ -adapted process  $\{B(t)\}_{t \geq 0}$  with the following properties:

- (i)  $P(B(0) = 0) = 1$ .
- (ii) For  $0 \leq s < t$ , the increment  $B(t) - B(s)$  is independent of  $\mathcal{F}_s$ .

## 1.5. Brownian Motion

---

- (iii) For  $0 \leq s < t$ , the increment  $B(t) - B(s)$  has normal distribution with mean 0 and variance  $t - s$ .
- (iv)  $B(t)$  is continuous for all  $t \geq 0$ .

### 1.5.3 Properties of Wiener Process

- (i) Let  $\{B(t) : t \geq 0\}$  be a standard Wiener process. For all  $s, t \in [0, \infty)$ ,  $\text{Cov}(B(s), B(t)) = \min(s, t)$ .
- (ii) Let  $(\Omega, \mathcal{E}, P)$  be a probability space and  $\{B(t) : t \geq 0\}$  be a standard Wiener process. Then  $B(t)$  is a martingale.
- (iii) Let  $(\Omega, \mathcal{E}, P)$  be a probability space and  $\{B(t) : t \geq 0\}$  be a standard Wiener process. Then  $X_t = B^2(t) - t$  is a martingale.
- (iv) Quadratic variation of a Wiener process over  $[0, t]$  is  $t$ .

We here present the proof of the property (iv) only.

*Proof.* (iv) We divide the interval  $[0, t]$  into  $n$  sub-intervals as  $0 \leq t_0 < t_1 < t_2 < \dots < t_n = t$ .

Now,  $\mathbb{E} \left[ \sum_{i=0}^{n-1} (B(t_{i+1}) - B(t_i))^2 \right] = \sum_{i=0}^{n-1} [t_{i+1} - t_i] = t_n - t_0 = t$ , for all partitions.

We show that the variance will be negligible if we make the partition finer. Observe that

$$\begin{aligned} \text{Var} [(B(t_{i+1}) - B(t_i))^2] &= \text{Var} [\mathcal{N}(0, t_{i+1} - t_i)^2] \\ &= \text{Var} [(t_{i+1} - t_i) \mathcal{N}(0, 1)^2] \\ &= (t_{i+1} - t_i)^2 \text{Var} [\mathcal{N}(0, 1)^2] \\ &= (t_{i+1} - t_i)^2 \mathbb{E}[(\mathcal{N}(0, 1)^2 - 1)^2] \\ &= 2(t_{i+1} - t_i)^2. \end{aligned}$$

However,  $(t_{i+1} - t_i)^2 \leq (t_{i+1} - t_i) \max\{t_{i+1} - t_i\}$ , where  $\max\{t_{i+1} - t_i\} \rightarrow 0$  as  $n \rightarrow \infty$ .

Hence

$$\begin{aligned} \text{Var} \left( \sum_{i=0}^{n-1} (B(t_{i+1}) - B(t_i))^2 \right) &= 2 \sum_{i=0}^{n-1} (t_{i+1} - t_i)^2 \\ &\leq 2t \max\{t_{i+1} - t_i\} \rightarrow 0 \text{ as } n \rightarrow \infty. \end{aligned}$$

Now, consider  $T_n = (B(t_{i+1}) - B(t_i))^2$ . Then

$$\sum_{i=1}^{\infty} \text{Var}(T_n) < \infty \implies \mathbb{E} \left( \sum_{n=1}^{\infty} (T_n - \mathbb{E}(T_n))^2 \right) < \infty. \quad (1.1)$$

Therefore, the series inside the expectation converges almost surely. Hence its terms converge to zero, and we have

$$\begin{aligned} T_n - \mathbb{E}(T_n) &\rightarrow 0 \\ \therefore T_n &\rightarrow t \text{ almost surely.} \end{aligned}$$

Hence the proof is complete. □

### 1.5.4 Transformation of Wiener Process

- (i) (Reflection) Let  $(\Omega, \mathcal{E}, P)$  be a probability space and  $\{B(t) : t \geq 0\}$  be a standard Wiener process. Then under reflection  $X(t) = -B(t)$  is also a standard Wiener process.
- (ii) (Time shifting) Let  $\{B(t) : t \geq 0\}$  be a standard Wiener process. Then  $X(t) = B(t+u) - B(u)$ ,  $u > 0$  is also a standard Wiener process.
- (iii) (Normal scaling) For a standard Wiener process  $\{B(t) : t \geq 0\}$ ,  $X(t) = cB(\frac{t}{c^2})$ ,  $c$  being a non-zero real number, is also a standard Wiener process.
- (iv) (Time inversion) For a standard Wiener process  $\{B(t) : t \geq 0\}$ ,

$$X_t = \begin{cases} 0, & \text{if } t = 0 \\ tB\left(\frac{1}{t}\right), & \text{if } t \neq 0 \end{cases}$$

is also a standard Wiener process.

- (v) (Time reversal) For a standard Wiener process  $\{B(t) : t \geq 0\}$ ,  $X_t = B(1) - B(1-t)$ ,  $t > 0$  is also a standard Wiener process.

### 1.5.5 Non-differentiability of Wiener Process

**Theorem 1.5.1.** *Let  $(\Omega, \mathcal{E}, P)$  be a probability space with a filtration  $\{\mathcal{F}_t\}_{t \geq 0}$  and  $\{B(t) : t \geq 0\}$  be a standard Wiener process. Then the sample paths of a standard*

## 1.6. Stochastic Integration: The Itô Integral

---

*Wiener process is continuous but not differentiable.*

*Proof.* We know that  $B(t) \sim \mathcal{N}(0, t)$  will be continuous in the sense of probability if and only for every  $\epsilon > 0$  and  $t \geq 0$ ,

$$\lim_{\Delta t \rightarrow 0} P(|B(t + \Delta t) - B(t)| \geq \epsilon) = 0.$$

Using the fact that  $B(t)$  is a martingale and applying Chebyshev's inequality, one obtains

$$\begin{aligned} P(|B(t + \Delta t) - B(t)| \geq \epsilon) &= P(|B(t + \Delta t) - \mathbb{E}(B(t + \Delta t)|\mathcal{F}_t)| \geq \epsilon) \\ &\leq \frac{\text{Var}(B(t + \Delta t)|\mathcal{F}_t)}{\epsilon^2} \\ &= \frac{\text{Var}(B(t + \Delta t) - B(t) + B(t)|\mathcal{F}_t)}{\epsilon^2} \\ &= \frac{\text{Var}(B(t + \Delta t) - B(t)|\mathcal{F}_t)}{\epsilon^2} + \frac{\text{Var}(B(t)|\mathcal{F}_t)}{\epsilon^2} \\ &= \frac{\Delta t}{\epsilon^2}, \end{aligned} \tag{1.2}$$

since the increment  $B(t + \Delta t) - B(t)$  is independent of the filtration  $\mathcal{F}_t$  and  $\text{Var}(B(t)|\mathcal{F}_t) = 0$ . Now, taking limit as  $\Delta t \rightarrow 0$  on both sides of (1.2), we get

$$P(|B(t + \Delta t) - B(t)| \geq \epsilon) \rightarrow 0$$

and therefore, the sample path of Wiener process is continuous.

Assume  $\Delta B(t) = B(t + \Delta t) - B(t) = \psi\sqrt{\Delta t}$ , where  $\psi \sim \mathcal{N}(0, 1)$ .

Then  $\lim_{\Delta t \rightarrow 0} \frac{B(t + \Delta t) - B(t)}{\Delta t} = \lim_{\Delta t \rightarrow 0} \psi \frac{\sqrt{\Delta t}}{\Delta t} = \pm\infty$ , depending on the sign of  $\psi$ .

Thus,  $B(t)$  is non-differentiable. □

## 1.6 Stochastic Integration: The Itô Integral

There are several ways to define a stochastic integral. The two most well-known definitions of a stochastic integral are Ito and Stratonovich. Ito's definition of stochastic calculus is named after the Japanese mathematician Kiyoshi Ito (1915-2008), who laid

the major development of the basic theory. The name Stratonovich refers to the Russian physicist Ruslan Stratonovich (1930-1997), who defined an alternative approach to the Ito stochastic integral. Since each of the definitions can be applied to stochastic analysis and each definition leads to a different stochastic calculus, it is, therefore, important to specify whether the calculus refers to the Ito or the Stratonovich definition when speaking of stochastic integrals. In biological examples, Ito definition is mostly preferred (Allen [2007]; Gard [1988]; Øksendal [2003]; Turelli [1977]) and Stratonovich calculi are applied frequently in physics (Gardiner et al. [1985]).

Consider a complete probability space  $(\Omega, \mathcal{E}, P)$  with a filtration  $\{\mathcal{F}_t\}_{t \geq 0}$ . Let  $\{B(t) : t \geq 0\}$  be a Wiener process adapted to the filtration  $\{\mathcal{F}_t\}_{t \geq 0}$  and  $X(t)$  is a  $\mathcal{F}_t$ -adapted random process. The Ito integral deals with the objective to integrate the expression

$$S = \int_0^T g(w, t) dB(t),$$

where  $g(w, t)$  is a stochastic process with  $w \in \{B(t) : t \geq 0\}$  and  $t \in [0, \infty)$ . To evaluate the above integral, when the process  $B(t)$  is not differentiable, we first partitioned the interval  $[0, T]$  into  $n$ -sub-intervals and define Ito integral as a limit of the Riemann sum as follows:

$$S_N(w) = \sum_{i=1}^N g(w, t_{i-1})(B(t_i) - B(t_{i-1})), \quad \text{with } N \rightarrow \infty.$$

The random variable  $S$  will be equal to the Riemann sum as  $N \rightarrow \infty$ , if

$$\lim_{N \rightarrow \infty} \mathbb{E} \left[ S - \sum_{i=1}^N g(w, t_{i-1})(B(t_i) - B(t_{i-1})) \right] = 0$$

for each sequence of partitions  $(t_0, t_1, \dots, t_N)$  of the interval  $[0, T]$  such that  $\max_i(t_i - t_{i-1}) \rightarrow 0$ . Additionally, the above expression will be valid if  $g(w, t)$  is smooth enough so that  $g(w, t_{i-1})$  represent  $g(w, t)$  in the interval  $[t_{i-1}, t_i]$  and  $g(w, t_{i-1})$  requires to be independent of the increment  $B(t_i) - B(t_{i-1})$ .

The limit in the above definition converges to the stochastic integral in the mean-square sense.

## 1.6. Stochastic Integration: The Itô Integral

---

Example: (i) Consider  $g(t) = c$ , a constant for all  $t \geq 0$ .

Then

$$\begin{aligned}
 \int_0^T cdB(t) &= c \lim_{N \rightarrow \infty} \sum_{i=1}^N (B(t_i) - B(t_{i-1})) \\
 &= c \lim_{N \rightarrow \infty} [B(t_1) - B(t_0) + B(t_2) - B(t_1) + \dots + B(t_N) - B(t_{N-1})] \\
 &= c \lim_{N \rightarrow \infty} [B(t_N) - B(t_0)], \tag{1.3}
 \end{aligned}$$

where  $(t_0, t_1, \dots, t_N)$  is a partition of  $[0, T]$ ,  $B(t)$  is standard Wiener process with  $B(0) = 0$  and the expression (1.3) becomes

$$\int_0^T cdB(t) = cB(T).$$

Example: (ii) Let  $g(t) = B(t)$ , the standard Wiener process. Then

$$\begin{aligned}
 \int_0^T B(t)dB(t) &= \lim_{N \rightarrow \infty} \sum_{i=1}^N B(t_{i-1})(B(t_i) - B(t_{i-1})) \\
 &= \lim_{N \rightarrow \infty} \left[ \frac{1}{2} \sum_{i=1}^N (B^2(t_i) - B^2(t_{i-1})) - \frac{1}{2} \sum_{i=1}^N (B(t_i) - B(t_{i-1}))^2 \right] \\
 &= -\frac{1}{2} \lim_{N \rightarrow \infty} \sum_{i=1}^N (B(t_i) - B(t_{i-1}))^2 + \frac{1}{2} B^2(T).
 \end{aligned}$$

By quadratic variation of Wiener process, we have

$$\lim_{N \rightarrow \infty} \sum_{i=1}^N (B(t_i) - B(t_{i-1}))^2 = T$$

and therefore, the equation (1.4) becomes

$$\int_0^T B(t)dB(t) = \frac{1}{2} B^2(T) - \frac{1}{2} T.$$

**Remark 1.6.1.** *This result is in contrast to our intuition from standard calculus. In the case of deterministic integral, we have  $\int_0^T x(t)dx = \frac{1}{2}x^2(T)$  if  $x(0) = 0$ , whereas the Ito integral differs by the term  $-\frac{1}{2}T$ .*

### 1.6.1 Properties of Ito Integral

Consider a complete probability space  $(\Omega, \mathcal{E}, P)$  with a filtration  $\{\mathcal{F}_t\}_{t \geq 0}$  and  $\{B(t) : t \geq 0\}$  be a Wiener process  $\mathcal{F}_t$ -adapted. Let  $X(t)$  be a regular adapted process with  $P\left(\int_0^T X^2(t)dt < \infty\right) = 1$ , then the Ito integral  $\int_0^T X(t)dB(t)$  is defined and has the following properties.

(i) (Linearity) If  $X(t)$  and  $Y(t)$  are Ito integrable and  $a, b$  are two constants, then

$$\int_0^T (aX(t) + bY(t))dB(t) = \int_0^T aX(t)dB(t) + \int_0^T bY(t)dB(t).$$

(ii) (Zero mean property) For an adapted process  $X(t)$  if the condition  $\int_0^T \mathbb{E}(X^2(t))dt < \infty$  holds, then

$$\mathbb{E}\left[\int_0^T X(t)dB(t)\right] = 0.$$

(iii) Under the condition  $\int_0^T \mathbb{E}(X^2(t))dt < \infty$

$$\text{Var}\left[\int_0^T X(t)dB(t)\right] = \int_0^T \mathbb{E}[X^2(t)] dt.$$

(iv) (Isometry) For two stochastic process  $X(t)$  and  $Y(t)$  satisfying  $\int_0^T \mathbb{E}(X^2(t))dt < \infty$  and  $\int_0^T \mathbb{E}(Y^2(t))dt < \infty$ , we have

$$\mathbb{E}\left[\int_0^T X(t)dB(t) \cdot \int_0^T Y(t)dB(t)\right] = \mathbb{E}\int_0^T X(t)Y(t)dt.$$

(v) The stochastic integral  $\int_0^T X(t)dB(t)$  has centered Gaussian distribution, i.e.,

$$\int_0^T X(t)dB(t) \sim \mathcal{N}\left(0, \int_0^T |X(t)|^2 dt\right).$$

### 1.6.2 Ito's Lemma

Let  $(\Omega, \mathcal{E}, P)$  be a probability space with a filtration  $\{\mathcal{F}_t\}_{t \geq 0}$  and  $\{B(t) : t \geq 0\}$  be a Wiener process  $\mathcal{F}_t$ -adapted. Consider a function  $Y(t) = f(t, B(t))$  which is continuously differentiable upto first order in  $t$  and twice differentiable in  $B(t)$ . Then

## 1.7. Different Types of Stochastic Models

---

by Taylor's theorem

$$\begin{aligned} dY(t) &= \frac{\partial f}{\partial t} dt + \frac{\partial f}{\partial B(t)} dB(t) + \frac{1}{2} \frac{\partial^2 f}{\partial t^2} (dt)^2 + \frac{\partial^2 f}{\partial t \partial B(t)} dt dB(t) + \frac{1}{2} \frac{\partial^2 f}{\partial (B(t))^2} (dB(t))^2 \\ &+ \quad (\text{higher order derivatives}). \end{aligned} \tag{1.4}$$

Since  $dt$  is very small we discard all terms involving a  $dt$  to a power greater than 1. Using the quadratic variation property of Wiener process, we have  $(dB(t))^2 = dt$  and  $dB(t)dt = (dt)^{\frac{3}{2}}$ . Therefore, the expression (1.4) becomes

$$dY(t) = \left( \frac{\partial f}{\partial t} + \frac{1}{2} \frac{\partial^2 f}{\partial (B(t))^2} \right) dt + \frac{\partial f}{\partial B(t)} dB(t).$$

## 1.7 Different Types of Stochastic Models

Various techniques exist to construct and analyze the solution of different stochastic processes depending on the structure of their underlying index set and the random variable. As we have previously discussed, while defining a stochastic process, the index set and the random variable can be either discrete or continuous. The processes are classified as

1. both time and the random variables are discrete-valued,
2. time is continuous but random variable is discrete valued,
3. time is discrete but random variable is continuous,
4. both time and random variables are continuous.

Among these four types, stochastic models of type (2) received the most attention in modelling various biological phenomena like cellular activity, molecular activity, genetics, competition, predation, and epidemic processes. Type (4) models are referred to as diffusion processes whose realization is a solution of the stochastic differential equation. The variability in these models can be included through birth, death, immigration, emigration and different environmental factors.

We here briefly discuss these models with examples and will draw their connection with stochastic differential equation models.



### 1.7.1 Continuous Time and Discrete State Process (CTMC)

We here consider the simple birth process, which is continuous in time but discrete in the state. The following assumptions will be considered first to begin with:

1. No individual die.
2. Two different individuals are independent.
3. All individuals have same birth rate  $\lambda$ .

Let  $X_t$  be the random variable denoting the size of the population at time  $t$ . Here the spectrum of  $X_t$  is  $\{0, 1, 2, \dots\}$  and time  $t \in [0, \infty)$  is continuous. Let the probability mass function associated with  $X_t$  be  $\{p_n(t)\}_{n=0}^{\infty}$  defining

$$p_n(t) = \text{Prob}\left(\{X_t = n\}\right).$$

It indicates that the probability of population size will be  $n$  at time  $t$  is  $p_n(t)$ . We further assume that (i) in a sufficiently small span of time  $\Delta t$ , the probability that birth occurs is  $\lambda\Delta t$  and (ii) the probability that more than one birth occurs in time  $\Delta t$  is negligible. At  $t = 0$ , consider the initial population size in terms of probability as  $\text{Prob}\left(\{X_0 = a\}\right) = 1$ . The second assumption states that the probability of getting more than one birth is negligible, implying that the actual birth will be  $\lambda\Delta t + o(\Delta t)$ . The probability that the population size increases from  $n$  to  $n + 1$  in the interval  $(t, t + \Delta t)$  is approximately  $\lambda\Delta t \times n$ . Therefore, the probability that the population fails to increase in the interval  $(t, t + \Delta t)$  will be  $(1 - \lambda\Delta t \times n)$ . Thus, the probability of attaining a population size equal to  $n$  at time  $t + \Delta t$  depends on two factors, viz.,

1. either, the population size was  $n - 1$  at time  $t$  and there is a birth in the intermediate time span  $(t, t + \Delta t)$ , or
2. the population size was  $n$  and there is no birth in the time span  $(t, t + \Delta t)$ .

Considering this two possibilities, the stochastic equation of population size becomes

$$p_n(t + \Delta t) = p_{n-1}(t)\lambda(n - 1)\Delta t + p_n(t)(1 - \lambda n\Delta t). \quad (1.5)$$

## 1.7. Different Types of Stochastic Models

---

Subtracting  $p_n(t)$  from both sides of (1.5), dividing by  $\Delta t$  and letting  $\Delta t \rightarrow 0$ , we obtain a system of differential equation

$$\frac{dp_n(t)}{dt} = \lambda(n-1)p_{n-1}(t) - \lambda np_n(t), \quad n = 1, 2, 3, \dots \quad (1.6)$$

which is known as the forward Kolmogorov differential equations. It can be shown that the solution of the equation (1.6) form a negative binomial distribution for each fixed time  $t$ .

### 1.7.2 Discrete Time Markov Chain (DTMC)

In this stochastic process both the state variable and the time are discrete valued. We know that a discrete time stochastic process  $\{X_n\}_{n=0}^{\infty}$  is said to have Markov property if

$$\text{Prob}\{X_n = i_n | X_0 = i_0, \dots, X_{n-1} = i_{n-1}\} = \text{Prob}\{X_n = i_n | X_{n-1} = i_{n-1}\}.$$

We here give an example of a stochastic DTMC model. Consider  $I_n$  denotes the number of infected individuals at instant  $n$ . The state space is also discrete, and we consider the state space as a set  $\{0, 1, 2, \dots, N\}$ . Let  $\Delta t$  be a sufficiently short time during which at most one change is possible in  $I_n$ . If  $I_n = i$  then  $I_{n+1}$  can be equal to any one of  $i-1, i, i+1$ . We define the one-step transition probability as

$$\begin{aligned} p_{i+1,i} &= \text{Prob}\{I_{n+1} = i+1 | I_n = i\} = \beta i \left(1 - \frac{i}{N}\right), \\ p_{i-1,i} &= \text{Prob}\{I_{n+1} = i-1 | I_n = i\} = (b + \gamma)i, \\ p_{i,i} &= \text{Prob}\{I_{n+1} = i | I_n = i\} = 1 - \beta i \left(1 - \frac{i}{N}\right) - (b + \gamma)i, \end{aligned}$$

for  $i = 1, 2, \dots, N-1$  and  $p_{j,i} = 0$  if  $j \neq i-1, i, i+1$ . Here the one step transition probability  $p_{j,i}$  is defined by  $p_{j,i} = \text{Prob}\{X_{n+1} = j | X_n = i\}$ .

### 1.7.3 Continuous Time and Continuous State Process

We now discuss the most well-known process used in stochastic modelling. The Brownian motion, often known as the Wiener process, is an example of a continuous time and state stochastic process. The Wiener process, commonly known as the diffusion process, assumes a continuous sample path with an infinitesimal mean and a finite variance. The Ito stochastic differential equation is formed using the generalised

definition of the Wiener process explained in 1.5.2. A DTMC model can also be used to develop an Ito stochastic differential equation for more than one interacting species Allen [2010]. The following section discusses a heuristic method for formulating the Ito SDE.

### 1.7.3.1 A heuristic approach of formulation of SDE

The mathematical model of the stochastic differential equation actually originated from the physical phenomena of microscopic motions of a particle suspended in a fluid. Molecules in the fluid move with different velocities, colliding with the suspended particle and resulting in a random movement in the suspended particles. This movement further intensifies if the temperature increases. Consider  $X(t)$  denotes the displacement of a particle in one direction from its initial position at time  $t$ .  $\sigma(x, t)$  denotes the measurement of temperature at time  $t$  at a point  $x$ . Then the displacement of the suspended particle due to collision in a small time interval  $[t, t + \Delta t]$  can be modeled as  $\sigma(x, t)(B(t + \Delta t) - B(t))$ , where  $B(t)$  is the Wiener process that captures such erratic movement. If the velocity of the fluid at  $x$  and at time  $t$  be  $\mu(x, t)$ , then the displacement of the suspended particle due to the movement of the fluid in the time span  $[t, t + \Delta t]$  is given by  $\mu(x, t)dt$ . Therefore, the total displacement of the particle from its initial position at time  $t$  is given by

$$X(t + \Delta t) - X(t) \approx \mu(x, t)\Delta t + \sigma(x, t)(B(t + \Delta t) - B(t)). \quad (1.7)$$

Assume  $\Delta X(t) = X(t + \Delta t) - X(t)$  and  $\Delta B(t) = B(t + \Delta t) - B(t)$ . Taking  $\Delta t$  infinitesimally small, a stochastic differential equation is obtained heuristically from the above relation (1.7) in the following form

$$dX(t) = \mu(x, t) dt + \sigma(x, t) dB(t).$$

### 1.7.4 Solution of SDEs and it's Uniqueness

From the above discussion, we can now propose the general form of stochastic differential equation as

$$dX(t) = \mu(X(t), t)dt + \sigma(X(t), t)dB(t), \quad X(0) = x_0, \quad (1.8)$$

## 1.7. Different Types of Stochastic Models

---

where  $\mu(X(t), t)$  and  $\sigma(X(t), t)$  are called respectively the drift and the diffusion coefficient and  $B(t), t \geq 0$ , is a Wiener process.

An adapted and continuous process  $X(t), t \geq 0$ , is a solution to the equation (1.8) if the integrals  $\int_0^t \mu(X(s), s)ds$  and  $\int_0^t \sigma(X(s), s)dB(s)$  exist and

$$X(t) = x_0 + \int_0^t \mu(X(s), s)ds + \int_0^t \sigma(X(s), s)dB(s).$$

If the coefficients of the equation (1.8) satisfies

(i) (Global Lipschitz condition)  $\|\mu(x, t) - \mu(y, t)\| + \|\sigma(x, t) - \sigma(y, t)\| \leq k_1(\|x - y\|),$   
 $k_1 > 0,$

(ii) (Monotone condition)  $\|\mu(x, t)\|^2 + \|\sigma(x, t)\|^2 \leq k_2^2(1 + \|x\|)^2, k_2 > 0,$

for every  $x, y \in \mathbb{R}^n, t \geq 0$ , then the stochastic differential equation (1.8) admits an unique solution.

### 1.7.4.1 Addition of noise in deterministic ODE

**(A) Adding white noise into the parameter of ODE:** Consider an ODE

$$\frac{dx(t)}{dt} = ax(t) \quad \text{with } x(0) = x_0, \quad \text{where } a \text{ is a constant.} \quad (1.9)$$

Expressing the above equation in differential form, we get

$$dx(t) = ax(t)dt \quad \text{with } x(0) = x_0.$$

Now we perturb the parameter by a white noise process say  $\xi(t), t \geq 0$  in the way that ' $a$ ' changes to ' $a + \xi(t)$ ' and also using the differential relation of Wiener process and white noise given by  $dB(t) = \xi(t)dt$ , the above differential form becomes

$$dx(t) = ax(t)dt + x(t)dB(t) \quad \text{with } x(0) = x_0.$$

Here the noise term is multiplied with the state variable, and this kind of perturbation is called multiplicative perturbation. One advantage of this perturbation is that the solution of this SDE contains noise term in the exponent, so the solution is

always non-negative.

**(B) Adding white noise directly into the ODE:** We can add noise directly into the system in the equation (1.9). The differential form would be like

$$dx(t) = ax(t)dt + dB(t) \quad \text{with } x(0) = x_0.$$

This kind of perturbation is called additive noise. One disadvantage of this perturbation is that the solution can be negative if the initial condition is very small and the noise has high negative fluctuation.

**(C) Adding white noise perturbation around the equilibrium:** Assume that the above ODE (1.9) has an equilibrium point  $\bar{x}$ , which is the solution of  $f(x) = 0$ . One can add the perturbation in the ODE as

$$dx(t) = ax(t)dt + (x(t) - \bar{x})dB(t) \quad \text{with } x(0) = x_0.$$

It can be easily seen that this stochastic perturbation is a combination of additive and multiplicative noises. The unique feature of this type of stochastic model is that the equilibrium of the deterministic and stochastic models coincides. Another advantage of this type of stochastic disturbance is that it makes the equilibrium robust.

In our study, we have applied stochasticity in two methods, namely, (i) adding stochastic perturbation in terms of white noise in the parameter, (ii) adding stochastic perturbation around the equilibrium point of the deterministic system.

In the above discussion, we have considered perturbation of ODE by white noise. For a white noise process, auto-covariance function  $Cov(t) = 0$  for  $t \neq 0$ .  $\Delta B(t)/\Delta t$  has variance  $\Delta t/(\Delta t)^2 = 1/\Delta t$  which tends to  $\infty$  as  $\Delta t$  tends to zero. As a result, auto-covariance of white noise at  $t = 0$  is  $Cov(0) = \infty$ . We can, therefore, characterize the covariance function as the *Dirac – delta* function. White noise has a constant spectral density because its Fourier transform is a constant function. Coloured noises have a non-constant spectral density, small non-zero auto-correlations between two neighbour times of a realization of the process, and the auto-covariance function with a finite peak at the origin. If this peak is sharp, the Dirac delta function—which has an infinite peak at the origin—can be used to closely approximate the auto-covariance function and, consequently, the related coloured noise. It should be mentioned that

## 1.7. Different Types of Stochastic Models

---

the perturbation can be made through any colour of noise. However, the white noise and Wiener process are more mathematically tractable, and a colour noise can be approximated by white noise (Braumann [2019]). We have used white noise perturbation throughout our study.

### 1.7.5 Solution of Some Well-known Stochastic Differential Equations

#### 1.7.5.1 Geometric Brownian motion

Consider the stochastic differential equation

$$dS(t) = \mu S(t)dt + \sigma S(t)dB(t). \quad (1.10)$$

We define  $Y(t) = \ln(S(t)) = f(S(t))$ .

Then  $\frac{\partial f}{\partial S} = \frac{1}{S}$ ,  $\frac{\partial^2 f}{\partial S^2} = -\frac{1}{S^2}$ ,  $\frac{\partial f}{\partial t} = 0$ . Applying Ito's lemma on  $Y(t)$  and using the equation (1.10), we have

$$\begin{aligned} dY(t) &= \left( \frac{\partial f}{\partial t} + \frac{\partial f}{\partial S} \mu S(t) + \frac{1}{2} \frac{\partial^2 f}{\partial S^2} \sigma^2 S^2(t) \right) dt + \frac{\partial f}{\partial S} \sigma S(t) dB(t) \\ &= \left( \mu - \frac{1}{2} \sigma^2 \right) dt + \sigma dB(t). \end{aligned} \quad (1.11)$$

Integrating both sides of (1.11) between  $[0, t]$ , we have

$$Y(t) = y_0 + \int_0^t \left( \mu - \frac{1}{2} \sigma^2 \right) dt + \int_0^t \sigma dB(t).$$

From,  $S(t) = e^{Y(t)}$ , we have

$$\therefore S(t) = S(0)e^{(\mu - \frac{1}{2}\sigma^2)t + \sigma B(t)}.$$

Thus, mean of the process is given by

$$\mathbb{E} \left( S(0)e^{(\mu - \frac{1}{2}\sigma^2)t + \sigma B(t)} \right) = S(0)e^{(\mu - \frac{1}{2}\sigma^2)t} \mathbb{E} \left( e^{\sigma B(t)} \right) = S(0)e^{(\mu - \frac{1}{2}\sigma^2)t} e^{\frac{\sigma^2 t}{2}} = S(0)e^{\mu t}$$

and the variance is given by

$$\begin{aligned} \text{Var}(S(t)) &= \mathbb{E}(S^2(t)) - (\mathbb{E}(S(t)))^2 = S^2(0)e^{2(\mu - \frac{1}{2}\sigma^2)t} \mathbb{E} \left( e^{2\sigma B(t)} \right) - S^2(0)e^{2\mu t} = \\ &= S^2(0)e^{2(\mu - \frac{1}{2}\sigma^2)t} e^{\frac{(2\sigma)^2 t}{2}} - S^2(0)e^{2\mu t} = S^2(0)e^{2\mu t} \left( e^{\sigma^2 t} - 1 \right). \end{aligned}$$

### 1.7.5.2 Ornstein-Uhlenbeck process

The Ornstein-Uhlenbeck model (see Uhlenbeck and Ornstein (1930)) appeared in 1930 as an improvement on Einstein's model (Braumann [2019]). The OU process is used in statistical mechanics to describe the velocity of a particle in a fluid. It is the most commonly used model for random movement toward a concentration point. It is also known as a continuous-time Gauss-Markov process, where a Gauss-Markov process is a stochastic process that meets the criteria for both the Gaussian and the Markov process (Ibe [2013]).

The Ornstein-Uhlenbeck process is described by the following stochastic differential equation

$$dX(t) = -\sigma X(t)dt + \mu dB(t), \quad \text{with } X(0) = X_0.$$

A closed-form solution of this SDE is of the form

$$X(t) = X_0 e^{-\sigma t} + e^{-\sigma t} \int_0^t \mu e^{\sigma s} dB(s).$$

The mean of this process is  $X_0 e^{-\sigma t}$  and the variance of this process is  $\frac{\mu^2}{2\sigma} [1 - e^{-2\sigma t}]$ .

### 1.7.5.3 Mean reverting Ornstein-Uhlenbeck (OU) process

A process that tends to drift toward its long-term mean over time is called a mean-reverting process. Finance's idea that an asset's price would often tend to converge to the average price over time is known as mean reversion. The selection of the trading range for an asset and the computation of the average price using quantitative methods are both necessary when utilising mean reversion as a timing strategy. The phenomena of mean reversion may be seen in a wide range of financial time-series data, including price, earnings, and book value data. When the current market price is less than the historical average, investors are enticed to buy the asset in the hope that the price will increase. When the current market price is higher than the previous average price, a decline in the market price is anticipated. In other words, it is anticipated that price variations would return to the average, and the structural underpinning of the OU process has an exact resemblance to this phenomenon.

The mean reverting process is described by the following stochastic differential equa-

## 1.7. Different Types of Stochastic Models

---

tion

$$dX(t) = \alpha\{\mu - X(t)\}dt + \beta dB(t) \quad \text{with } X(0) = X_0,$$

where  $\mu$  is the long run mean of  $X(t)$  and  $\alpha$  is the rate of mean reversion. A closed form solution of this mean-reverting process is given by

$$X(t) = X_0 e^{-\alpha t} + \int_0^t \alpha \mu e^{-\alpha(t-s)} ds + \int_0^t \beta e^{-\alpha(t-s)} dB(s).$$

The mean of this process is  $\mu + e^{-\alpha t}(X_0 - \mu)$  and variance is  $\frac{\beta^2}{2\alpha}(1 - e^{-2\alpha t})$ .

### 1.7.6 Some Important Inequalities, Theorems, Lemmas and Definitions Used in the Study

**Lemma 1.7.1. (Borel-Cantelli's)** Consider a probability space  $(\Omega, \mathcal{E}, P)$ .

1. If  $\{A_k\} \subset \mathcal{E}$  and  $\sum_{k=1}^{\infty} P(A_k) < \infty$ , then

$$P(\limsup_{k \rightarrow \infty} A_k) = 0.$$

2. If  $\{A_k\} \subset \mathcal{E}$  is independent and  $\sum_{k=1}^{\infty} P(A_k) = \infty$ , then

$$P(\limsup_{k \rightarrow \infty} A_k) = 1.$$

Here  $P(\limsup A_k)$  is the probability that the events  $A_k$  occur "infinitely often (i.o.)" and is denoted by  $P(A_k \text{ i.o.})$ . Therefore, the first case of the theorem states that the set of all outcomes that are "repeated" infinitely many times must occur with probability 0 if the sum of the probabilities of the events  $A_k$  is finite. The second case represents a partial converse of the first case of the Borel-Cantelli lemma. The second case reads: If the events  $A_k$  are independent and their total of probabilities diverges to infinity, then the probability that an infinite number of them will occur is 1.

**Theorem 1. (Doob's Martingale inequality)** Let  $\{M_t\}_{t \geq 0}$  be a martingale in  $\mathbb{R}^n$  and let  $[a, b]$  be a bounded interval in  $\mathbb{R}_+$ . If  $p \geq 1$  and  $\mathbb{E}|M_t|^p < \infty$ , then

$$P \left\{ w : \sup_{a \leq t \leq b} |M_t(w)| \geq c \right\} \leq \frac{\mathbb{E}|M_b|^p}{c^p}$$



for all  $c > 0$ .

Doob's martingale inequality, also known as Kolmogorov's submartingale inequality, provides a bound on the probability that a martingale will exceed any given value over a given time interval. This result is usually used when the process is a martingale, but it is also valid for submartingales.

**Theorem 2. (Burkholder-Davis-Gundy)** Let  $\{f(t)\}_{t \geq 0}$  be a stochastic process which satisfies  $\int_0^T |f(t)|^p dt < \infty$  a.s.. Define for  $t \geq 0$

$$x(t) = \int_0^t f(s)dB(s), \quad \text{and} \quad A(t) = \int_0^t |f(s)|^2 ds,$$

where  $\{B(t)\}_{t \geq 0}$  is a Wiener process. Then for every  $p > 0$ , there exists positive constants  $c_p, C_p$  (depending on  $p$ ), such that

$$c_p \mathbb{E}|A(t)|^{\frac{p}{2}} \leq \mathbb{E} \left( \sum_{0 \leq s \leq t} |x(s)|^p \right) \leq C_p \mathbb{E}|A(t)|^{\frac{p}{2}}$$

for all  $t \geq 0$ .

The Burkholder-Davis-Gundy inequality is a remarkable result relating to the bounds of a local martingale. The inequalities are frequently used in martingale theory, harmonic analysis and Fourier analysis.

**Theorem 3. (Gronwall's inequality)** Let  $T > 0$  and  $c \geq 0$ . Let  $u(\cdot)$  be a real-valued continuous function defined on  $[0, T]$  and let  $v(\cdot)$  be a non-negative integrable function on  $[0, T]$ . If

$$u(t) \leq c + \int_0^t v(s)u(s)ds \quad \text{for all } 0 \leq t \leq T,$$

then

$$u(t) \leq c \exp \left( \int_0^t v(s)ds \right) \quad \text{for all } 0 \leq t \leq T.$$

Gronwall's inequality (also known as Gronwall's lemma or the Gronwall-Bellman inequality) allows one to bound a function that is known to satisfy a particular differential or integral inequality by solving the corresponding differential or integral equation. The lemma can be expressed in two ways: differentially and integrally. We only state the integral form here. Gronwall's inequality is a useful tool in the theory

## 1.7. Different Types of Stochastic Models

---

of ordinary and stochastic differential equations for obtaining various estimates. In particular, Gronwall's inequality can be used to demonstrate the uniqueness of a solution to the initial value problem.

**Persistence and extinction of species from an ecological perspective:** From a mathematical point of view, the persistence of species may be weak or strong. Suppose the function  $g(t)$  represents a population at any time  $t$  and  $g(t) > 0$  for all  $t \geq 0$  then  $\frac{1}{t} \int_0^t g(\theta) d\theta$  is the average value of population in the time span  $[0, t]$ . The population is said to be strongly persistent if the infimum of these limiting averages is always positive. Therefore, the eventual average population size will always remain away from zero, ensuring the existence of populations for all time. In the case of weak persistence, the supremum of these eventual averages is always positive. It, however, does not guarantee that the average population will always remain away from zero, and therefore population may be arbitrarily closed to zero. Non-persistent implies that the supremum of these eventual averages is zero. However, extinction is guaranteed if the supremum of these eventual averages becomes negative. In the following, we give the formal definition of persistency.

**Definition 1.7.2.** (*Liu and Wang [2011c]*) Let  $f(t)$  be a function such that it represents a population at any time  $t$  and  $f(t) > 0$  for all  $t \in [0, \tau_e)$ . Then

- (i)  $f(t)$  is said to be extinct in the mean if  $\lim_{t \rightarrow \infty} f(t) = 0$ ,
- (ii)  $f(t)$  is said to be non-persistent in the mean if  $\limsup_{t \rightarrow \infty} \int_0^t f(\theta) d\theta = 0$ ,
- (iii)  $f(t)$  is said to be weakly persistent in the mean if  $\limsup_{t \rightarrow \infty} \int_0^t f(\theta) d\theta > 0$ ,
- (iv)  $f(t)$  is said to be strongly persistent in the mean if  $\liminf_{t \rightarrow \infty} \int_0^t f(\theta) d\theta > 0$ .

The following Lemma will be used throughout the thesis to derive the conditions for persistence and extinction.

**Lemma 1.7.3.** (*Liu et al. [2013]*) Suppose  $w(t) \in C(\Omega \times [0, \infty), \mathbb{R}_+^0)$ , where  $\mathbb{R}_+^0 = \{p \mid p > 0, p \in \mathbb{R}\}$ .

(1) If there exist two positive constants  $T$  and  $\kappa_0$  such that

$$\ln(w(t)) \leq \kappa t - \kappa_0 \int_0^t w(\theta) d\theta + \sum_{i=1}^n \alpha_i B_i(t), \quad \forall t \geq T,$$

where  $\alpha_i$  ( $1 < i < n$ ) are constants, then

$$\begin{cases} \limsup_{t \rightarrow \infty} \frac{1}{t} \int_0^t w(\theta) d\theta \leq \frac{\kappa}{\kappa_0} \text{ almost surely (a.s.), if } \kappa \geq 0; \\ \lim_{t \rightarrow \infty} w(t) = 0 \text{ a.s., if } \kappa < 0. \end{cases}$$

(2) If there exist three positive constants  $T$ ,  $\kappa$ ,  $\kappa_0$  such that

$$\ln(w(t)) \geq \kappa t - \kappa_0 \int_0^t w(\theta) d\theta + \sum_{i=1}^n \alpha_i B_i(t), \quad \forall t \geq T,$$

then

$$\liminf_{t \rightarrow \infty} \frac{1}{t} \int_0^t w(\theta) d\theta \geq \frac{\kappa}{\kappa_0} \text{ a.s.}$$

In proving the stationary distribution and the ergodic nature of stochastic differential equation throughout this thesis, we make the following assumption due to [Khasminskii \[2011\]](#). First we give the following definition of the diffusion matrix.

**Definition 1.7.4.** (*Khasminskii [2011]*) Let  $W(t)$  be a time-homogeneous Markov process in  $E_l$  ( $E_l$  denotes the Euclidean  $l$  space) governed by the following stochastic differential equation:

$$dW(t) = g(W(t))dt + \sum_{k=1}^p \sigma_k(W(t))dB_k(t).$$

The diffusion matrix is defined as follows:

$$M(w(t)) = (m_{ij}(w)), \quad m_{ij}(w) = \sum_{k=1}^p \sigma_k^i(w) \sigma_k^j(w), \quad \forall w \in E_l.$$

**Lemma 1.7.5.** *There exists a bounded domain  $U \subset E_l$  with regular boundary  $\Gamma$  having the following properties:*

(A1) *In the domain  $U$  and some neighborhood thereof, the smallest eigenvalue of the diffusion matrix  $M(w)$  is bounded away from zero.*

(A2) *If  $w \in E_l \setminus U$ , the mean time  $\tau$  at which a path starting from  $w$  reaches the set  $U$  is finite and  $\sup_{w \in K} E_w \tau < \infty$  for every compact subset  $K \subset E_l$ .*

If Lemma 1.7.5 holds, then the Markov process  $W(t)$  has a stationary distribution

## 1.8. Some Basic Definitions and Tools Used For the Deterministic Study

$\pi(\cdot)$ . Let  $f(\cdot)$  be a function integrable with respect to the measure  $\pi$  then

$$P_w \left( \lim_{T \rightarrow \infty} \frac{1}{T} \int_0^T f(W^w(t)) = \int_{E_l} f(w) \pi(dw) \right) = 1, \forall w \in E_l.$$

**Remark 1.7.6.** To validate (A1) of Lemma 1.7.5, it is sufficient to prove that  $F$  is uniformly elliptical in  $U$ , where  $F_u = g(w) \cdot u_w + [\text{tr}(A(w)u_{xx})/2]$ , i.e., there is a positive number  $M$  such that  $\sum_{i,j=1}^k a_{ij}(w) \xi_i \xi_j \geq M |\xi|^2$ ,  $w \in U$ ,  $\xi \in \mathbb{R}^p$ . To verify (A2) of Lemma 1.7.5, it suffices to show that there exists some neighborhood  $U$  and a non-negative  $C^2$  function  $V$  such that for any  $w \in E_l \setminus U$ ,  $LV$  is negative, where  $L$  is the Ito differential operator (Zhu and Yin [2007]).

**Lemma 1.7.7.** (Petrov [1969]) Let  $M = \{M\}_{t \geq 0}$  be a continuous valued local martingale and vanishing at  $t = 0$ , then

$$\lim_{t \rightarrow \infty} \langle M, M \rangle_t = \infty \implies \lim_{t \rightarrow \infty} \frac{M_t}{\langle M, M \rangle_t} = 0,$$

and

$$\limsup_{t \rightarrow \infty} \frac{\langle M, M \rangle_t}{t} < \infty \implies \lim_{t \rightarrow \infty} \frac{M_t}{t} = 0 \text{ a.s.}$$

The first part of this lemma means that if the expectation of  $M^2$  is equal to  $\infty$ , then  $\frac{M_t}{\langle M, M \rangle_t}$  tends to 0 as  $t \rightarrow \infty$ . The second part of this lemma indicates that if the expectation of  $M^2$  is equal to  $O(t)$ , then  $M_t/t$  converges to 0 almost surely, where  $O(\cdot)$  is the big  $O$  notation also called as Bachmann–Landau notation.

## 1.8 Some Basic Definitions and Tools Used For the Deterministic Study

We state here some basic definitions and Theorems that have been used throughout this thesis.

### 1.8.1 Mathematical Tools

**Definition 1. (Dynamical System)** A dynamical system is an evolution rule that defines a trajectory as a function of a single parameter (time) on a set of states (the phase space).

**Definition 1.8.1. (Deterministic System)** A dynamical system is called deterministic if, for each state in the phase space, there is a unique consequent, i.e., the evolution rule of the deterministic dynamical system is a function taking a given state to a unique subsequent state.

In deterministic systems, for each time  $t$ , the evolution rule is a mapping from the phase space to the phase space given by

$$\xi(x, t) \equiv \xi_t(x) : A \longrightarrow A,$$

where  $t \in \mathbb{R}$  is the continuous time variable,  $A$  is the phase space,  $x(t) = \xi_t(x_0)$  denotes the position of the system at time  $t$  that started at  $x_0$ . Moreover, we assume that  $t \geq 0$  and at  $t = 0$ ,  $\xi_t(x_0) = x_0$ .

**Definition 1.8.2. (Equilibrium point)** Consider a dynamical system

$$\frac{dx}{dt} = \dot{x} = f(x) \quad \text{with } x(0) = x_0, \tag{1.12}$$

where  $x \in \mathbb{R}^n$ , and  $f = (f_1, f_2, \dots, f_n)^T$ .

A point  $\bar{x}$  is called an equilibrium point of the above system if

$$\dot{x} = f(\bar{x}) = 0.$$

**Definition 1.8.3. (Local Stability)** An equilibrium solution  $\bar{x}$  of (1.12) is said to be locally stable if for each  $\epsilon > 0$  there exists a  $\delta > 0$  such that every solution  $x(t)$  of (1.12) with initial condition  $x(0) = x_0$  and  $\|x_0 - \bar{x}\| < \delta \Rightarrow \|x(t) - \bar{x}\| < \epsilon$  for all  $t > 0$ , where  $\|\cdot\|$  is the Euclidean norm. If the equilibrium solution is not locally stable, it is said to be unstable.

**Definition 1.8.4. (Local Asymptotic Stability)** An equilibrium solution  $\bar{x}$  of (1.12) is said to be locally asymptotically stable if it is locally stable and if there exists a  $\sigma > 0$  such that  $\|x_0 - \bar{x}\| < \sigma \Rightarrow \lim_{t \rightarrow \infty} \|x(t) - \bar{x}\| = 0$ .

**Definition 1.8.5. (Instability)** An equilibrium solution  $\bar{x}$  of (1.12) is called unstable if it is not stable.

**Definition 1.8.6.** For the system (1.12), we assume  $f$  is  $C^1$  function and  $\bar{x}$  is an equilibrium point. Then the linearization of  $\dot{x} = f(x)$ ,  $x \in \mathbb{R}^n$  at the equilibrium point

## 1.8. Some Basic Definitions and Tools Used For the Deterministic Study

$\bar{x}$  can be expressed as

$$\dot{x} = JX(t),$$

where the Jacobian matrix or variational matrix evaluated at  $\bar{x}$  is given by

$$J = \begin{pmatrix} \frac{\partial f_1}{\partial x_1} & \frac{\partial f_1}{\partial x_2} & \cdots & \frac{\partial f_1}{\partial x_n} \\ \frac{\partial f_2}{\partial x_1} & \frac{\partial f_2}{\partial x_2} & \cdots & \frac{\partial f_2}{\partial x_n} \\ \cdot & \cdot & \cdot & \cdot \\ \cdot & \cdot & \cdot & \cdot \\ \cdot & \cdot & \cdot & \cdot \\ \frac{\partial f_n}{\partial x_1} & \frac{\partial f_n}{\partial x_2} & \cdots & \frac{\partial f_n}{\partial x_n} \end{pmatrix}_{x=\bar{x}}$$

and

$$X = \begin{pmatrix} x_1 \\ x_2 \\ \cdot \\ \cdot \\ \cdot \\ x_n \end{pmatrix}.$$

**Theorem 1.8.7. (Routh-Hurwitz Criteria)** Given the  $n$ -th degree polynomial

$$P(\lambda) = \lambda^n + a_1\lambda^{n-1} + a_2\lambda^{n-2} + \dots + a_{n-1}\lambda + a_n,$$

where the coefficients  $a_i$  are real constants,  $i = 1, 2, \dots, n$ . Hurwitz matrices are defined by using the coefficients of  $P(\lambda)$  as

$$H_k = \begin{pmatrix} a_1 & 1 & 0 & 0 & \cdots & 0 \\ a_3 & a_2 & a_1 & 1 & \cdots & 0 \\ a_5 & a_4 & a_3 & a_2 & \cdots & 0 \\ \cdot & \cdot & \cdot & \cdot & \cdots & 0 \\ \cdot & \cdot & \cdot & \cdot & \cdots & 0 \\ \cdot & \cdot & \cdot & \cdot & \cdots & 0 \\ 0 & 0 & 0 & 0 & \cdots & a_k \end{pmatrix},$$

where  $k = 1, 2, \dots, n$  and  $a_k = 0$  if  $k > n$ . All the roots of the polynomial  $P(\lambda)$  will have negative real parts if and only if the determinants of all Hurwitz matrices are positive, i.e.,  $\det(H_k) > 0$ ,  $k = 1, 2, \dots, n$ . Following are the Routh-Hurwitz criteria for

$n = 2, 3$  and 4.

- $n = 2$ ;  $a_1 > 0$ ,  $a_2 > 0$ .
- $n = 3$ ;  $a_1 > 0$ ,  $a_3 > 0$ ,  $a_1 a_2 - a_3 > 0$ .
- $n = 4$ ;  $a_1 > 0$ ,  $a_3 > 0$ ,  $a_4 > 0$ ,  $a_1 a_2 a_3 - a_3^2 - a_1^2 a_4 > 0$ .

**Theorem 1.8.8. (Local Stability Using Routh-Hurwitz Criteria)** Let  $\bar{x}$  be an equilibrium of the system (1.12) and the characteristic equation of the variational matrix satisfies the Routh-Hurwitz criteria. Then the equilibrium  $\bar{x}$  is said to be locally asymptotically stable.

**Definition 1.8.9. (Global Asymptotic Stability)** An equilibrium solution  $\bar{x}$  of (1.12) is said to be globally asymptotically stable if it is locally asymptotically stable and if  $\|x_0 - \bar{x}\| < \infty$  implies  $\lim_{t \rightarrow \infty} \|x(t) - \bar{x}\| = 0$ .

**Theorem 1.8.10. (Lyapunov Stability Theorem)** Let  $\bar{x}$  be an equilibrium of the system (1.12) and  $V$  be a  $C^1$  function given by  $V : E \rightarrow \mathbb{R}$ , where  $E$  is an open subset of  $\mathbb{R}^n$  containing the equilibrium  $\bar{x}$  with  $V(\bar{x}) = 0$  and  $V(x) > 0$  for  $x \neq \bar{x}$ .

1. If  $\frac{dV}{dt} \leq 0$  for all  $x \in E \setminus \{\bar{x}\}$  then  $\bar{x}$  is said to be locally stable.  $V$ , in this case, is called a ‘weak Lyapunov function’.
2. If  $\frac{dV}{dt} < 0$  for all  $x \in E \setminus \{\bar{x}\}$  then  $\bar{x}$  is said to be locally asymptotically stable. In this case,  $V$ , is called a ‘strict Lyapunov function’.
3. If  $\frac{dV}{dt} > 0$  for all  $x \in E \setminus \{\bar{x}\}$  then  $\bar{x}$  is unstable.

**Theorem 1.8.11. (Hopf Bifurcation Theorem)** Consider an autonomous system of ordinary differential equations

$$\dot{x} = f(x, \mu), x \in \mathbb{R}^n, \mu \in \mathbb{R}, \quad (1.13)$$

where  $f$  is continuously differentiable. Suppose, the system (1.13) has an equilibrium  $\bar{x}(\mu)$ . Moreover, the Jacobian matrix evaluated at  $\bar{x}(\mu)$  has one pair of complex eigenvalues

$$\xi_{1,2} = A(\mu) + \pm B(\mu)$$

such that for some  $\mu = \mu^*$  it becomes purely imaginary, i.e.,

$$A(\mu^*) = 0 \quad \text{and} \quad B(\mu^*) \neq 0.$$

## 1.8. Some Basic Definitions and Tools Used For the Deterministic Study

Then the eigenvalues will cross the imaginary axis with nonzero speed if (transversality condition)

$$\left. \frac{dA(\mu)}{d\mu} \right|_{\mu=\mu^*} \neq 0.$$

Then the system of differential equations (1.13) will undergo a Hopf bifurcation around  $\bar{x}(\mu)$  for  $\mu = \mu^*$  and will possess a periodic solution with approximate period  $T = \frac{2\pi}{B(\mu^*)}$  as  $\mu$  crosses  $\mu^*$ . The parameter  $\mu$  is called the bifurcation parameter and the value  $\mu^*$  is called the bifurcation point.

### 1.8.2 Optimization Techniques

#### 1.8.2.1 Fminsearch Algorithm

Fminsearch is a MatLab inbuilt toolbox, which uses the Nelder-Mead simplex algorithm, as described in Lagarias et al. [1998]. For  $n$ -dimensional vectors  $x$ , this approach employs a simplex of  $n + 1$  points. The approach first constructs a simplex around the initial guess  $y_0$  by adding 5% of each component  $y_0(i)$  ( $i = 1, 2, \dots, n + 1$ ) to  $y_0$  and uses these  $n$  vectors as simplex elements alongside  $y_0$ . The algorithm then repeatedly updates the simplex using the following approach.

1. Let the list of points in the current simplex be represented by  $y(i)$ ,  $i = 1, \dots, n+1$ .
2. Sort the simplex points from lowest function value  $g(y(1))$  to highest function value  $g(y(n + 1))$ . The procedure adds a new point to the simplex at each iteration and discards the worst point at the moment,  $y(n + 1)$ . [Or, in the case of step 7 below, all  $n$  points with values higher than  $g(y(1))$  are changed.]
3. Generate the reflected point

$$r = 2m - y(n + 1),$$

where  $m = \sum x(i)/n$ ,  $i = 1 \dots n$ , and compute  $g(r)$ .

4. Iteration terminates if  $g(y(1)) \leq g(r) < g(y(n))$  and accept  $r$ .
5. If  $g(r) < g(y(1))$ , calculate the expansion point

$$s = m + 2(m - x(n + 1)),$$



and calculate  $g(s)$ . For  $g(s) < g(r)$ , accept  $s$  and iteration is terminated. Otherwise, accept  $r$  and terminate the iteration.

6. If  $g(r) \geq g(y(n))$ , perform a contraction between  $m$  and either  $y(n+1)$  or  $r$ , depending on which has the lower objective function value. If  $g(r) < g(y(n+1))$  (that is,  $r$  is better than  $y(n+1)$ ), calculate

$$c = m + \frac{(r-m)}{2}$$

and calculate  $g(c)$ . If  $g(c) < g(r)$ , accept  $c$  and terminate the iteration. Otherwise, go with Step 7.

If  $g(r) \geq g(y(n+1))$ , calculate

$$cc = m + \frac{(x(n+1)-m)}{2}$$

and calculate  $g(cc)$ . If  $g(cc) < g(y(n+1))$ , accept  $cc$  and terminate the iteration. Otherwise, continue with Step 7

7. Calculate the  $n$  points  $u(i) = y(1) + \frac{(y(i)-y(1))}{2}$  and calculate  $g(u(i))$ ,  $i = 2, \dots, n+1$ . The simplex at the next iteration is  $y(1), u(2), \dots, u(n+1)$ .

One disadvantage of this technique is that `fminsearch` can often handle discontinuity, especially if it occurs not near the solution. Because `fminsearch` is a local optimization technique, it may only provide local solutions.

### 1.8.2.2 Lsqcurvefit Algorithm

The Matlab `lsqcurvefit` function is used to solve least-squares non-linear curve fitting problems. To put it another way, given input data ( $xdata$ ) and observed output ( $ydata$ ), we will find coefficients  $x$  that "best-fit" the equation

$$\min_x ||F(x, xdata) - ydata||^2 = \min_x \sum_i [F(x, xdata_i) - ydata_i]^2,$$

where  $F(x, xdata)$  is a vector valued function. Because the component  $x$  may contain a parameter, it may have a lower and higher bound. The user-defined func-

## 1.8. Some Basic Definitions and Tools Used For the Deterministic Study

tion  $F(x, xdata)$  is required by the `lsqcurvefit` function, and the size of this vector must be equal to  $xdata$  and  $ydata$ . The `lsqcurvefit` solver's basic syntax is  $x = \text{lsqcurvefit}(fun, x0, xdata, ydata)$ . The function  $fun$  is to be fitted with the observation or experimental values in this case.  $fun$  is a function that takes two inputs, a vector or matrix  $x$  and a matrix  $xdata$ , and returns the function  $F$ . `lsqcurvefit` computes the sum of squares of differences between the user-defined function and the given experimental or observed values. The user specifies the initial point,  $x0$ , as a vector or array. For the optimization, by default, `lsqcurvefit` selects an algorithm from the 'trust-region-reflective' and 'Levenberg-Marquardt' families. The interior-reflective Newton method presented in Coleman and Li [1996, 1994] serves as the foundation for the trust-region-reflective method. Each iteration includes approximating the solution of a large linear problem using the preconditioned conjugate gradients approach. The trust-region-reflective technique does not permit an under-determined system. For this, the number of equations must be at least equal to the number of variables. The Levenberg-Marquardt curve-fitting method is a hybrid of two minimization techniques: gradient descent and the Gauss-Newton method (Moré [1978]). The gradient descent approach reduces the sum of squared errors by updating the parameters in the steepest descent direction. The sum of squared errors is decreased in the Gauss-Newton approach by assuming that the least squares function is locally quadratic and finding the minimum of the quadratic. When the parameters are far from their optimal value, the Levenberg-Marquardt technique behaves more like a gradient-descent method, and when the parameters are close to their optimal value, it behaves more like the Gauss-Newton method.

### 1.8.2.3 Partial Rank Correlation Coefficient (PRCC)

The strength of the relationship between the input and the outcome measures in a model is assessed using the statistical technique of correlation. After discounting the linear effects of the LHS parameters (inputs)  $x_j$  on the outcome measure (outputs)  $y$ , partial correlation, which uses the residuals from the regression procedure, describes the linear relationship between the LHS parameters and the outcome measure (Marino et al. [2008]). Given that there is little to no correlation between the inputs, PRCC is a reliable sensitivity measure for nonlinear but monotonic relationships between  $x_j$  and  $y$  (Marino et al. [2008]). A correlation coefficient (CC) between  $x_j$  and  $y$  is

calculated as follows:

$$r_{x_j y} = \frac{Cov(x_j, y)}{\sqrt{Var(x_j) \cdot Var(y)}} = \frac{\sum_{i=1}^N (x_{ij} - \bar{x})(y_i - \bar{y})}{\sqrt{\sum_{i=1}^N (x_{ij} - \bar{x})^2 \sum_{i=1}^N (y_i - \bar{y})^2}}, \quad j = 1, 2, \dots, k.$$

which varies between  $-1$  and  $+1$  (Marino et al. [2008]). The coefficient  $r$  is referred to as the sample or Pearson correlation coefficient when applied to raw data of  $x_j$  and  $y$ . A Spearman or rank correlation coefficient is the result for rank-transformed data. It should be emphasised that, in the process of rank transforming of data, sampled model inputs can have real values or can take on a variety of alternative values. When the linear effects on  $y$  of the other inputs are discounted, the partial correlation is nothing more than the linear relationship between input  $x_j$  and output  $y$ . Whereas the partial correlation coefficient (PCC) between  $x_j$  and  $y$  is the CC between the two residuals given by  $(x_j - \hat{x}_j)$  and  $(y - \hat{y})$ , where  $\hat{x}_j$  and  $\hat{y}$  has the following linear regression models:

$$\hat{x}_j = c_0 + \sum_{p=1, p \neq j}^k c_p x_p \quad \text{and} \quad \hat{y} = b_0 + \sum_{p=1, p \neq j}^k b_p x_p.$$

The term "partial rank correlation" refers to a partial correlation on rank transformed data, where  $x_j$  and  $y$  must first be rank transformed before the above two equations be used to create linear regression models. This robust sensitivity applies when the relationship between  $x_j$  and  $y$  is nonlinear and monotone. We may evaluate the sensitivity of the model outcome with respect to parameter variation using the combination of uncertainty analysis and PRCC (Marino et al. [2008]).

#### 1.8.2.4 Latin Hypercube Sampling (LHS)

In partial rank correlation coefficient sensitivity analysis, Latin hypercube sampling (LHS) is employed (Marino et al. [2008]). It was developed by McKay et al. [1979] and belonged to the Monte Carlo sampling method class. With the advantage of utilising fewer samples to achieve the same accuracy as simple random sampling, this method offers an unbiased estimate of the average model output (McKay et al. [1979]). This method divides the random parameter distributions into  $N$  equal probability intervals, which are then sampled, where  $N$  is the sample size. Although values of  $N$  should be larger to assure accuracy (McKay et al. [1979], Blower and Dowlatabadi [1994]). This number  $N$  should be more than or equal to  $k + 1$ , where  $k$  is the number of

## 1.8. Some Basic Definitions and Tools Used For the Deterministic Study

parameters adjusted. The sample can be calculated on a log scale to prevent under-sampling at the outer ranges of the interval when the parameter assumes very small values in a vast region of variation for any parameter. Despite the development of a technique for imposing correlations on sampled values, the LHS technique necessitates that sampling for each parameter be done independently (Iman and Conover [1982], Iman and Davenport [1982]). The sampling values are chosen at random from each probability density function. To cover the whole range for each parameter, each interval must be sampled exactly once, without replacement. This sampling yields the LHS matrix, which has  $N$  rows for the number of simulations and  $k$  columns for the number of changed parameters. Each row of the LHS matrix, or each combination of parameter values, is then used to simulate the  $N$  model solutions. Finally, the model output of interest is collected for each model run.

### 1.8.2.5 Parameter estimation technique

We, here, discuss the method adopted to estimate the parameters of an SDE. For the estimation of the parameter set of an SDE, we first find the best-fit parameters for the corresponding deterministic system through the least square method such that the sum of the squared difference of deterministic model output and experimental data would be minimized. Consider the multi-dimensional parameter set of deterministic system as  $\theta = (\theta_1, \theta_2, \dots, \theta_n)$  and  $(t_1, y_1), (t_2, y_2), \dots, (t_n, y_n)$  be the given set of experimental data points. If we assume  $h(t_j, \theta)$  be the model output at the  $t_j$  time step, then our objective is to minimize the squared sum of errors (SSE):

$$\text{SSE}(\theta) = \sum_{i=1}^n (h(t_i, \theta) - y_i)^2.$$

Starting from an initial guess of  $\theta$ , we will find the best parameter set iteratively using either the `fminsearch` or the `lsqcurvefit` algorithm toolbox of MATLAB. After the estimation of parameters for the deterministic system, we will search for a proper noise intensity of the stochastic system to obtain a good agreement between stochastic system output and experimental data. In the quest for suitable noise strength, we compute the sum of squared errors (SSE), the total sum of squares (SST) and the corresponding r-squared value for stochastic simulation data and experimental data. The statistical measure of fit r-squared is computed from the relation (Motulsky and

Christopoulos [2004])

$$r\text{-squared} = 1 - \frac{\text{SSE}}{\text{SST}}.$$

We consider 10,000 different random values of noise intensities between 0 to 1 through Latin hypercube sampling. Then for each of these 10,000 values of noise intensities, the stochastic system is simulated 1000 times. Taking the mean of the 1000 simulations,  $r$ -squared is computed between the average stochastic simulation output and the experimental data. We choose the particular values of noise intensity for which the  $r$ -squared value is closest to 1 as our required noise intensity.

## 1.9 Literature Review and Motivation

Population models have drawn interest among researchers around for almost two hundred years. Some of the founders of these models were [Malthus \[1798\]](#), [Verhulst \[1838\]](#), [Pearl and Reed \[1920\]](#), and then [Lotka \[1925\]](#) and [Volterra \[1926\]](#). Lotka and Volterra explored several population models, including their famous work on the predator-prey system. An enormous contribution of Lotka and Volterra's work was making assumptions to simplify these population models into solvable equations ([Edelstein-Keshet \[2005\]](#)). Ecological and epidemiological models can be divided naturally into deterministic and stochastic models. The primary difference between the two is that the deterministic model has no chance effects ([Tuckwell \[2018\]](#)). Deterministic models assume that the present status of the population completely determines the model's behaviour. Yet the earliest mathematical models were deterministic rather than stochastic for the equally obvious reason that one must learn to walk before running. The deterministic models have been a stimulus for both abstract and experimental work ([Hritonenko et al. \[1999\]](#), [Foppa \[2016\]](#)). One can forecast the population actions if we know everything about that population at a particular instant. These deterministic models have given us much of our understanding of biological systems. There are some limitations to the deterministic model. Werner Heisenberg ([Heelan \[2012\]](#)) found that purely deterministic models are not worthy enough to study physical/biological systems. The problem is that one cannot exactly describe a physical system at any given instant. Deterministic models deliver an average population behaviour ([Feynman et al. \[1965\]](#)), implying that the deterministic models are based on the mean-field theory. This averaging of quantity is

## 1.9. Literature Review and Motivation

---

valid if the system population is large but becomes invalid if the population is small (Rand and Wilson [1991]) because a small population behaves differently compared to its larger counterpart due to the loss of heterogeneity. There are three types of stochasticity considered in ecological systems: demographic stochasticity, measurement stochasticity and environmental stochasticity. The first type of stochasticity is due to endogenous causes and may appear through random variation in fecundity or survival due to genetic factors, disproportionate sex ratio, sexual selection, etc. It has a strong effect on small population (Legendre [1999]). The measurement stochasticity is caused by factors that randomly cause measurements of the variables up and down. The most important is the environmental stochasticity caused by exogenous factors. Stochasticity in the physical and biological environment may cause significant fluctuations even in a large population (Engen et al. [1998]). But it has been observed that random fluctuations due to environmental noise or demographic stochasticity are inherent in species dynamics and the spread of infection. For example, rainfall, humidity and temperature affect food production and species growth (Sibly and Hone [2002], Dexter [2003]). Growth of many pathogens and their virulence is dependent on temperature (Blanford et al. [2003], Baron et al. [2001]). Due to this environmental noise or stochasticity, the population density generally does not attain a fixed value but rather fluctuates around some average value (Renshaw [1993]). These shortcomings of the deterministic model led to the development of probabilistic or stochastic models (Olinick [1978]).

After the development of the full-fledged theory of stochastic analysis, many valuable contributions have been made by considering randomness into deterministic models in ecology and epidemiology. The nature of the noise may be additive or multiplicative. The critical difference between additive and multiplicative noises is that the noise is directly added to the system in the former case. In the latter case, it is multiplied with the state variables (Grigoriu [2013]). The main disadvantage of additive noise is that, with an initial very low population density, a negative noise fluctuation could make the solution of the stochastic system negative, which is non-physical in population biology because population density cannot be negative. In contrast, the multiplicative noise always ensures the non-negativity of the solution, even if there are initial negative fluctuations, because the noise appears in the exponential function. More specifically, for a linear multiplicative stochastic differential equation, the solution is purely exponential, and the fluctuating term (i.e., the Wiener process) appears in the exponent, while for a nonlinear system, a functional at the

exponent (Mikhailov and Loskutov [2013]). Moreover, as the stochastic solution for multiplicative noise is exponential, the zero population density becomes a barrier to the solution. Strong negative fluctuation can bring the solution to zero density for specific system parameters and noise strength levels. Understanding the effectiveness of multiplicative noise in population dynamics, it is prudent to use this kind of noise to construct the stochastic system from its deterministic population model.

Introduction of stochasticity in a population model may be done in various ways, e.g., following Markov process (Hernandez-Suarez [2002], Clancy [2014], Laskey and Myers [2003]) and parameter perturbation technique (Liang et al. [2016], Gray et al. [2011], Majumder et al. [2020a]). Stochasticity can also be introduced in a deterministic model where the stochastic perturbations are proportional to the distance of the state variable from the deterministic steady state (Carletti [2002], Chakraborty et al. [2012]). One can also consider the environmental fluctuation that would be manifested solely in the parameters. In such a case, a constant parameter of the deterministic system is replaced by its average value plus an error term (Beddington and May [1977], Mao [2011]). In general, the error term follows a normal distribution (by the well-known central limit theorem), and hence one can approximate the error term by white noise (Liu and Wang [2011a]). This stochastic perturbations technique has been widely applied in biological systems (Saha and Bandyopadhyay [2008], Tapaswi and Mukhopadhyay [1999], Ji et al. [2011a], Liu and Wang [2011c], Li et al. [2019b]). Alternatively, a stochastic perturbation can be added to the growth equation of each state variable, where the perturbation is proportional to the distance of the state variable from its deterministic equilibrium value (Beretta et al. [1998]). Using this technique of stochasticity in a deterministic model, one can verify the robustness of various dynamics obtained from the deterministic system and can observe the asymptotic stochastic nature of equilibrium points for stochastic models (Carletti [2002]). For such advantage, this method of stochastic perturbation has received great attention from the researchers (Beretta et al. [2000], Bandyopadhyay and Chattopadhyay [2005], Carletti [2006], Chatterjee et al. [2008], Adnani et al. [2013], Yu et al. [2009], Carletti [2002]).

Planktons are omnipresent in the aquatic environment and therefore have attracted researchers' attention to exploring the interaction between phytoplankton and zooplankton (Rosenzweig [1971], Gounand et al. [2014], Gilpin and Rosenzweig [1972], May [1972], Roy and Chattopadhyay [2007], Bairagi et al. [2019]). It is reported that environmental fluctuations may affect the intrinsic growth rate, death rate, compe-

## 1.9. Literature Review and Motivation

---

tition coefficient, and other parameters involved in the model system (May [2001], Ruokolainen et al. [2009a]). Experimental evidence also supports the claim of the impact of environmental noise (Ripa and Lundberg [2000]). An apparent difference between the above-mentioned stochastic models is that there is no equilibrium point in the first system and the second system has the same equilibrium point as in the case of the deterministic system. It is, therefore, interesting to know how environmental noise affects deterministic dynamics. And how different types of stochasticities affect differently when applied to an identical system. Another interesting question in population dynamics is to find whether the addition of stochasticity makes an unstable equilibrium of the deterministic system stable. By considering a stochastic model of phytoplankton-zooplankton interaction, we search for the answers to these questions.

Epidemic models deal with the transmission of infection in a population. They are frequently used to gain insights into disease dynamics and control mechanisms. The susceptible-infective (SI) type deterministic compartmental models, where rate parameters are constant, have been extensively used to explore infection-related issues in different populations (Anderson and May [1981], Lipsitch et al. [1995], Dunn and Smith [2001], Restif and Koella [2003], Miller et al. [2007]). However, disease transmission is a random process, which is difficult to describe by a well-defined rule and subject to vary randomly due to exogenous factors. For example, it is reported that disease transmission is significantly affected by environmental factors like temperature, humidity, rainfall etc. (Fayer [1994], Memarzadeh [2012]). Since we cannot biologically explain all the unknown perturbations involved in disease transmission, one must consider an epidemic model with random variations.

The transmission of disease from one infected individual to another susceptible individual is a significant issue, and the persistence of parasites and their virulence largely depend on this transmission mechanism (Lipsitch et al. [1996], Chen et al. [2006], Ewald et al. [1994], Clayton and Tompkins [1994]). We intend to explore how uncertainty affects the disease dynamics in an SIS epidemic model, where the infection spreads through horizontal and vertical transmissions. The relative fecundity of parasites has been demonstrated to play a crucial role in disease persistence (Ebert et al. [2000], Tompkins and Begon [1999]). So our quest is to know how the relative fecundity affects the parasite fitness under environmental noise.

The world has been under immense pressure since 2020 due to the extraordinary respiratory pathogen SARS-CoV-2, which emerged from Wuhan, China and spread over the globe. This exceptional virus has stunning transmission capability from



human to human, which has infected more than 198 million people worldwide, with 4.2 million deaths as of July 29, 2021.

Mathematical models are vital in understanding the disease dynamics and can be used as a tool in predicting the covid cases along with the time frame for the same. The model can predict the probable time of the epidemic peak, incidence and duration ([Grassly and Fraser \[2008\]](#)). Such information is vital for the health care management authority. Based on the information, they can take necessary steps for designing effective control measures and facility development so that the health care system does not collapse due to the surge of covid cases, and optimum treatment can be provided to the thousands of infected people ([Adam \[2020\]](#)). Many mathematical models have been developed to give early-stage epidemic predictions for the ongoing Covid-19 pandemic ([Prem et al. \[2020\]](#), [Paul et al. \[2020b\]](#), [Chatterjee et al. \[2020\]](#)-[Khajanchi and Sarkar \[2020\]](#)), ([Fanelli and Piazza \[2020\]](#), [Paul et al. \[2020a\]](#), [Mondal et al. \[2020\]](#), [Peng et al. \[2020\]](#), [Chen et al. \[2020\]](#), [Pang et al. \[2020\]](#), [Sardar et al. \[2020\]](#), [Zhou et al. \[2020b\]](#), [Rabajante \[2020\]](#), [Lin et al. \[2020\]](#), [Mandal et al. \[2020\]](#), [Paul et al. \[2020b\]](#), [Ivorra et al. \[2020\]](#)). All these models are deterministic types and do not consider uncertainty and variations in the parameters though it is obvious in the case of a growing epidemic. In particular, it has been shown that uncertainty is certain in the disease transmission rate, in the infectious period, in the recovery rate of Covid-19, and there is a large variation in its range ([Anderson et al. \[2020\]](#), [Zhang et al. \[2020a\]](#), [Manski and Molinari \[2021a\]](#)). However, understanding the dynamics of a novel virus is insufficient if the inherent noise in the rate parameters is not considered. We, therefore, consider uncertainties in the various rate parameters and analyze the early transmission model of COVID-19 disease.

A massive vaccination program started at the beginning of 2021, hoping that the disease would be controlled. Though the morbidity and mortality of the covid disease reduced significantly due to vaccination, the disease eradication or control is far from expected. Earlier Covid-19 epidemic models did not consider the effect of vaccination. Consequently, such models can no longer be used to determine the course of the epidemic once the full-fledged Covid-19 vaccination has started. Studies show that vaccine-induced immunity is significantly reduced after six to eight months post-vaccination. As a result, vaccinated people are subject to reinfection. There is uncertainty regarding the rate of immunity loss among the vaccinated population. Therefore, considering such uncertainties/fluctuations in the SARS-CoV-2 epidemic models with vaccine-induced immunity loss is essential. It is therefore important to

## 1.10. Aim of the Thesis

---

analyze the effect of vaccination in controlling the Covid-19 epidemic when there is significant variation in the disease transmission rate and uncertainty in the vaccine-induced immunity loss.

## 1.10 Aim of the Thesis

The present thesis aims to understand the dynamic behaviour of various biological systems by applying stochastic calculus. More precisely, this thesis is devoted to capturing the role of stochasticity by using two methods: adding white noise perturbation into system parameters and adding white noise perturbation around the equilibrium in different ecological and epidemiological models. We analytically studied stochastic models to achieve various statistical and biological phenomena, including extinction, persistence, and stability. Numerically, we would give insights into this mathematical analysis. Additionally, to deepen our understanding of the dynamics of the model, we will study some intriguing phenomena numerically, such as the extinction time of diseases and the distribution of extinction times. We intend to use real-world data to validate the model's output. We will consider the available data on phytoplankton-zooplankton interaction in ecology to verify how our model and its output can capture the natural system dynamics. In an eco-epidemiological case, we will utilize the well-known red grouse data to validate the viability of our model. In this thesis, we are also interested in formulating stochastic models of Covid-19 taking into account the epidemiological status of individuals of a given geographical region and then analyzing it to provide various insights into the persistence and eradication of the disease. The SARS-CoV-2 infection has kept the world under pressure for the last two years. We, therefore, like to propose mathematical models to predict the course of the Covid-19 pandemic considering the uncertainty in the disease transmission & recovery rates. Motivated by the fact that there is uncertainty in vaccine-induced immunity loss, we would like to propose a stochastic epidemic model to decipher the interrelationship between vaccine efficacy and disease transmissibility. Our objective is to demonstrate how disease persistence and eradication are affected due to the uncertainty in the rate parameters like immunity loss and disease transmission coefficient. In all cases, we would like to present a simple but tractable method for calibrating stochastic model output with the actual Covid-19 pandemic data to estimate system parameters and provide insightful conclusions from the obtained results.

## 1.11 Thesis Overview

The whole thesis is divided into several chapters. The **Chapter 1** contains the origin and development of stochastic calculus, and the thesis ends with the future direction. Various mathematical tools & techniques which are used throughout this thesis are also discussed in the first chapter.

In **Chapter 2**, we study a minimal deterministic model of phytoplankton-zooplankton (prey and predator, respectively) interaction and compare its dynamics with its stochastic version formulated by two different stochastic perturbation techniques. In the first method, two parameters of the deterministic system are replaced by its average value plus an error term. In the second method, the stochastic perturbation is considered proportional to the distance of state variables from their deterministic equilibrium value. We analyze both stochastic models and explore their dynamics. In particular, we determine sufficient conditions for extinction probability, stochastic persistence of populations, and the existence of stationary distribution of the first stochastic system. We determine sufficient conditions for the asymptotic mean square stability for the other system by defining a suitable Lyapunov function. Different analytical results are illustrated numerically and interpreted biologically. The stochastic behaviours of the system are compared with their deterministic counterpart. A case study has also been done considering the 24 months of data of phytoplankton-zooplankton interaction in Lake Trasimeno, Italy. It is shown that the stochastic model's output can capture the seasonal fluctuations of plankton populations of Lake Trasimeno.

Epidemic models are used to understand the dynamics of disease transmission and explore the possible measures for preventing the spread of infection. Disease transmission is intrinsically random and severely affected by (changing) environmental factors. In **Chapter 3**, we study a stochastic SIS (susceptible-infected-susceptible) type model, where infection transmits through horizontal and vertical transmission modes. White multiplicative noise is considered in the horizontal disease transmission term to incorporate stochasticity in the system. We prove that noise intensity, disease transmissibility and recovery rates are potential routes for eradicating the disease. Furthermore, it is shown that parasites reduce their fitness for some fixed noise if the relative fecundity of infected hosts and the disease transmissibility are low, but observe an enhanced fitness if any of them is increased.

## 1.11. Thesis Overview

---

In **Chapter 4**, we consider a Leslie-Gower type prey-predator model with parasitic infection in prey. Here, we consider stochasticity in the growth rate of susceptible prey, the parasite-induced death rate of infected prey, and the growth rate of the predator. Population extinction is a serious issue both from theoretical and practical points of view. We explore how environmental noise influences the persistence and extinction of interacting species in the presence of a pathogen, even when the populations remain stable in their deterministic counterpart. Multiplicative white noise is introduced in a deterministic predator-prey-parasite system by randomly perturbing three biologically important parameters. It is revealed that the extinction criterion of species may be satisfied in multiple ways, indicating various routes to extinction, and disease eradication may be possible with the right environmental noise. Even when its focal prey strongly persists, the predator population cannot survive if its growth rate is lower than some critical value, measured by half of the corresponding noise intensity. It is shown that the average extinction time of the population decreases with increasing noise intensity and the probability distribution of the extinction time follows the log-normal density curve. A case study on red grouse (prey) and fox (predator) interaction in the presence of the parasites *trichostrongylus tenuis* of grouse is presented to demonstrate that the model well fits the field data.

Novel coronavirus has altered the socio-economic condition of the whole world through its devastating effects on the human population. Mathematical models and computation techniques may play an essential role in understanding this epidemic and contribute much to policy-making to control the infection more systematically and effectively. In **Chapter 5**, we have proposed a deterministic mathematical model for the Covid-19 pandemic taking into account the different epidemiological status of individuals of a given geographical region and analysing it with respect to the basic reproduction number. Uncertainty is obvious in the case of a growing epidemic, and it multiplies if the disease etiology is unknown. Taking into account the uncertainty in the epidemiological parameters, we extended the deterministic system into a stochastic system through random parameter perturbations in three epidemiological parameters. Analysing the model, we determined the disease persistence and eradication conditions. The stochastic solution's asymptotic behaviour around the deterministic model's coexistence equilibrium was also presented. As a case study, we considered the Covid-19 pandemic in India and estimated the model parameters

from the epidemic data for the period 1<sup>st</sup> March to 6<sup>th</sup> December, 2020. We demonstrated different analytical results and predicted the course of the epidemic.

A massive vaccination program against SARS-CoV-2 infection started at the beginning of 2021. Studies show that vaccinated people are subject to reinfection, and there is uncertainty in the rate of immunity loss, the force of infection, recovery rate, and vaccine efficacy. In **Chapter 6**, we study a six-dimensional stochastic epidemic model with vaccine-induced immunity loss to demonstrate the effect of vaccination in controlling the Covid-19 epidemic. It is shown that the disease persists for a long time if the stochastic basic reproduction number (SBRN) is greater than unity. We have also proved a sufficient condition for disease eradication. Our analysis shows that the disease cannot persist if  $R_{0V}^{ext} < 1$ . Noticeably, this condition may not hold if the infectivity increases or/and the vaccine-induced immunity loss increases. Two case studies were done: one with Indian Covid-19 data and the other with the data of Italy. Both Indian and Italian Covid-19 case studies are used to estimate the model parameters and noise intensities. It is revealed that the mean extinction time increases with the increasing rate of immunity loss and force of infection. For the case of India, a nontrivial observation is that mass vaccination cannot eradicate the disease if the vaccine-induced immunity loss is higher than 23 %. The case is almost similar if the infectivity is also high. Similarly, for Italy, it is observed that if the vaccine-induced immunity loss is higher than 12 %, the new cases will increase rapidly. It implies that the infection will last long unless a long-lasting vaccine candidate appears or a low infectious variant replaces the highly contagious variant.

The thesis ends with the future direction of research in **Chapter 7**.

# Chapter 2

## Phytoplankton-zooplankton interaction under environmental stochasticity: Survival, extinction and stability.<sup>1</sup>

### 2.1 Introduction

Planktons are floating organisms that occupy the first trophic level of any aquatic food chain and therefore received a significant amount of research interest. Mathematical models are frequently used to understand the complex interaction of the food chain and have been proven to be useful in having a deeper understanding of such interactions. There are different types of studies with plankton models. The bloom phenomenon and paradox of enrichment have been explained with the help of mathematical models (Rosenzweig [1971], Gounand et al. [2014], Gilpin and Rosenzweig [1972], May [1972], Roy and Chattopadhyay [2007], Bairagi et al. [2019]). Some researchers have observed the role of different aquatic virus (Suttle and Chan [1993], Beltrami and Carroll [1994], Rhodes and Martin [2010]) and the effect of toxin released by several phytoplanktons (Chattopadhyay et al. [2002], Bairagi et al. [2008b]). Mathematical models were also developed to study the allelopathic effect of plankton community (Fistarol et al. [2003], Mukhopadhyay et al. [1998], Chen et al. [2007]).

---

<sup>1</sup>The bulk of this chapter has been published in *Applied Mathematical Modelling*, 89 (2021), 1382-1404.

## 2. Phytoplankton-zooplankton interaction under environmental stochasticity: Survival, extinction and stability

---

Fish predation on zooplankton plays an important role in phytoplankton-zooplankton interaction and has been addressed by many researchers to show the zooplankton community structure (Brooks and Dodson [1965], Scheffer et al. [2000], Vanni [1987], Malchow et al. [2002]).

Scheffer [1991] proposed the following minimal model to describe the zooplankton-phytoplankton interaction in the presence of nutrient and fish predation:

$$\begin{aligned}\frac{dx}{dt} &= r \frac{n}{n+h_n} x - cx^2 - py \frac{x}{x+h_a} = f_1(x, y), \quad x(0) > 0, \\ \frac{dy}{dt} &= pey \frac{x}{x+h_a} - my - F \frac{y^2}{y^2+h_y^2} = f_2(x, y), \quad y(0) > 0,\end{aligned}\tag{2.1}$$

where  $x(t)$  and  $y(t)$  are, respectively, the phytoplankton and zooplankton biomass at time  $t$ . This model says that phytoplankton grows logistically in the absence of zooplankton by consuming nutrients, where the carrying capacity of phytoplankton,  $\frac{rn}{c(n+h_n)}$ , is dependent on the nutrient level. Zooplankton feeds on phytoplankton following a type II functional response. Fish predation is dependent on zooplankton biomass and follows a type III response function. Here fish was considered as a static predator because the generation time of fish is much higher compared to that of zooplankton (Bairagi et al. [2019]) and therefore the rate equation of fish population was not considered. All parameters (see Table 2.1) are positive for biological demands. Further description of the model can have in Scheffer [1991].

**Table 2.1:** Parameter descriptions and their default values (Scheffer [1991])

Parameter	Description	Default value	Dimension
$n$	Nutrient level of the system	0.5	relative unit
$r$	Maximum growth rate of phytoplankton	varies	$d^{-1}$
$c$	Intra-species competition	0.05	$mg^{-1} dw^{-1} l d^{-1}$
$p$	Maximum grazing rate of zooplankton	0.7	$d^{-1}$
$e(0 < e < 1)$	Conversion efficiency of zooplankton	varies	dimension less
$m$	Natural mortality rate of zooplankton	0.175	$d^{-1}$
$F$	Maximum zooplankton predation rate by fish	0.2	$mg dw l^{-1} d^{-1}$
$h_n$	Half-saturation constant of nutrient limitation	0.6	relative unit
$h_a$	Half-saturation constant of zooplankton's response function	0.6	$mg dw l^{-1}$
$h_y$	Half-saturation constant of response function for fish predation	0.6	$mg dw l^{-1}$
$x(0)$	Initial phytoplankton biomass	0.5	$mg dw l^{-1}$
$y(0)$	Initial zooplankton biomass	0.3	$mg dw l^{-1}$

## 2.1. Introduction

---

In this chapter, we extend the minimal model of [Scheffer \[1991\]](#) by two types of stochastic perturbation techniques for a deeper understanding of phytoplankton-zooplankton interaction in the natural aquatic system. We first assume that fluctuations in the environment mainly affect the intrinsic growth rate ( $r$ ) of phytoplankton population and the death rate ( $m$ ) of zooplankton so that the parameters  $r$  and  $m$  are replaced by  $r \rightarrow r + \sigma_1 \dot{B}_1(t)$ ,  $m \rightarrow m + \sigma_2 \dot{B}_2(t)$ , where  $\sigma_1$  and  $\sigma_2$  are small positive numbers representing the intensities of white noise on phytoplankton and zooplankton, respectively;  $B_1(t), B_2(t)$  are mutually independent Brownian motions defined on a complete probability space  $(\Omega, \mathcal{F}, \mathcal{P})$  with a filtration  $\{\mathcal{F}_t\}_{t \in R_+}$  satisfying the usual condition (i.e, it is increasing as well as right continuous, while  $\mathcal{F}_0$  contains all  $\mathcal{P}$ -null sets) ([Liu and Wang \[2011a\]](#)). Under such circumstances, the stochastic extension of the deterministic model (2.1) reads

$$\begin{aligned} dx &= \left( r \frac{n}{n+h_n} x - cx^2 - py \frac{x}{x+h_a} \right) dt + \sigma_1 \frac{n}{n+h_n} x dB_1(t), \\ dy &= \left( pey \frac{x}{x+h_a} - my - F \frac{y^2}{y^2+h_y^2} \right) dt - \sigma_2 y dB_2(t). \end{aligned} \quad (2.2)$$

In the second case, we assumed the stochastic perturbation in the state variables as  $\sigma_1(x - \hat{x})\dot{B}_1(t)$  and  $\sigma_2(y - \hat{y})\dot{B}_2(t)$ , where  $\hat{x}, \hat{y}$  are components of the positive equilibrium point of system (2.1) and  $\sigma_1, \sigma_2, B_1(t), B_2(t)$  carry the same meanings as stated earlier. The transformed system in this case has the form

$$\begin{aligned} dx &= \left( r \frac{n}{n+h_n} x - cx^2 - py \frac{x}{x+h_a} \right) dt + \sigma_1 (x - \hat{x}) dB_1(t), \\ dy &= \left( pey \frac{x}{x+h_a} - my - F \frac{y^2}{y^2+h_y^2} \right) dt + \sigma_2 (y - \hat{y}) dB_2(t). \end{aligned} \quad (2.3)$$

One important characteristic of the stochastic mode (2.2) is that it has no precise steady-state, but the model (2.3) has equilibrium points that coincide with the equilibrium points of the deterministic system (2.1). Here we analyze both the stochastic systems and explore their dynamics. More specifically, we determine the extinction probability, stochastic persistence of populations and stochastic stability of the system (2.2). For the system (2.3), we determine the sufficient conditions for the asymptotic mean square stability by defining a suitable Lyapunov function. The stochastic behavior of the systems (2.2) and (2.3) are also compared with the deterministic behavior of the system (2.1).



## 2. Phytoplankton-zooplankton interaction under environmental stochasticity: Survival, extinction and stability

---

The rest of the chapter is organized as follows. In Section 2.2, we state some basic stability results of the deterministic system (2.1). Different results of stochastic system (2.2), like the existence and uniqueness of the positive solutions and their bounds, sufficient conditions for extinction, weak and strong persistence, existence of stationary distribution, are presented in Section 2.3. Simulations results of the systems are also given to illustrate the analytical results in Section 2.4. In Section 2.5, the second stochastic model (2.3) is analysed and sufficient conditions are derived for mean square stability and the results are illustrated numerically. The chapter ends with a discussion in Section 2.6.

## 2.2 Analysis of the deterministic model

### 2.2.1 Positivity and boundedness of solutions

**Proposition 2.2.1.** *All solutions of system (2.1) are positively invariant and uniformly bounded in the domain  $M$ , where*

$$M = \left\{ (x, y) \in \mathbb{R}_+^2 \mid 0 < x(t) \leq \frac{r}{c} \left( \frac{n}{n+h_n} \right), 0 \leq y(t) \leq \frac{2r^2e}{cR} \left( \frac{n}{n+h_n} \right)^2 \right\},$$

$$R = \min \left\{ m, \frac{rn}{n+h_n} \right\}.$$

**Proof** From (2.1), one can easily show

$$x(t) = x(0)e^{\int_0^t \left[ r \frac{n}{n+h_n} x(u) - cx^2(u) - py(u) \frac{x(u)}{x(u)+h_a} \right] d\nu},$$

$$y(t) = y(0)e^{\int_0^t \left[ pey(u) \frac{x(u)}{x(u)+h_a} - my(u) - F \frac{y^2(u)}{y^2(u)+h_y^2} \right] d\nu}.$$

Therefore, as  $x(0) > 0$ ,  $y(0) > 0$  then  $x(t) > 0$ ,  $y(t) > 0$  for all  $t \geq 0$ . We now show that all solutions of (2.1) are ultimately bounded in the region  $M$ . The first equation of (2.1) yields

$$\frac{dx}{dt} \leq x(t) \left( \frac{rn}{n+h_n} - cx(t) \right) \Rightarrow \limsup_{t \rightarrow \infty} x(t) \leq \frac{r}{c} \left( \frac{n}{n+h_n} \right).$$

## 2.2. Analysis of the deterministic model

---

For the bound of  $y(t)$ , we have

$$\begin{aligned}
\frac{d}{dt}(ex(t) + y(t)) &= r \frac{n}{n+h_n} ex - cex^2 - my - \frac{Fy^2}{y^2+h_y^2} \\
&\leq r \frac{n}{n+h_n} ex - my \\
&= 2r \frac{n}{n+h_n} ex - r \frac{n}{n+h_n} ex - my \\
&\leq 2r \frac{n}{n+h_n} ex - R(ex+y), R = \min\left\{r \frac{n}{n+h_n}, m\right\} \\
\therefore \frac{d(ex+y)}{dt} + R(ex+y) &\leq 2r \frac{n}{n+h_n} ex \leq \frac{2r^2 e}{c} \left\{ \frac{n}{n+h_n} \right\}^2 \\
&\Rightarrow \limsup_{t \rightarrow \infty} y(t) \leq \limsup_{t \rightarrow \infty} [ex(t) + y(t)] \leq \frac{2r^2 e}{cR} \left\{ \frac{n}{n+h_n} \right\}^2.
\end{aligned}$$

Hence the proposition is proved.

### 2.2.2 Equilibria and their stabilities

The equilibrium points of the system (2.1) are the nonnegative solutions of the simultaneous equations

$$\frac{dx}{dt} = r \frac{n}{n+h_n} x - cx^2 - py \frac{x}{x+h_a} = 0 = \frac{peyx}{x+h_a} - my - F \frac{y^2}{y^2+h_y^2} = \frac{dy}{dt}.$$

It is trivial to show that the equilibrium point  $E^0(0,0)$  is always unstable and the predator-free equilibrium  $E^1(\hat{x}, 0)$ , where  $\hat{x} = \frac{rn}{c(n+h_n)}$ , is locally asymptotically stable if  $\frac{pe\hat{x}}{\hat{x}+h_a} - m < 0$ .

For the existence of a unique positive interior equilibrium point  $E^*(x^*, y^*)$ , we show that the equations  $r \frac{n}{n+h_n} - cx - \frac{py}{x+h_a} = 0$  and  $\frac{pex}{x+h_a} - m - F \frac{y}{y^2+h_y^2} = 0$  have exactly one intersection in the first quadrant. The first equation gives a parabola

$$\left[ x - \frac{1}{2c^{3/2}} \left( \frac{rn}{n+h_n} - ch_a \right) \right]^2 = -\frac{p}{c^2} \left[ y - \frac{1}{p} \left( \frac{1}{4c} \left( \frac{rn}{n+h_n} - ch_a \right)^2 + \frac{rn h_a}{n+h_n} \right) \right]$$

having vertex at  $\left( \frac{1}{2c^{3/2}} \left( \frac{rn}{n+h_n} - ch_a \right), \frac{1}{p} \left( \frac{1}{4c} \left( \frac{rn}{n+h_n} - ch_a \right)^2 + \frac{rn h_a}{n+h_n} \right) \right)$  and the second equation can be expressed as  $x = \frac{h_a(my^2 + Fy + mh_y^2)}{(pe-m)y^2 - Fy + (pe-m)h_y^2}$ , which has a vertical asymptote  $x = \frac{mh_a}{pe-m}$ . From the second equation,  $x$  will be positive if  $pe - m > 0$ ,

## 2. Phytoplankton-zooplankton interaction under environmental stochasticity: Survival, extinction and stability

---

$0 < F < 2h_y(pe - m)$  and its slope  $\frac{dy}{dx} = \frac{peh_a(y^2+h_y^2)^2}{F(x+h_a)^2(y+h_y)} \frac{1}{h_y-y}$  is positive (negative) for  $y < h_y$  ( $y > h_y$ ). This curve has a tangent parallel to the vertical axis at  $y = h_y$ , where  $x = \frac{h_a(F+2mh_y)}{2(pe-m)h_y-F}$ . Therefore, if

$$\frac{rn}{n+h_n} < \frac{ch_a(F+2mh_y)}{2(pe-m)h_y-F} + \frac{ph_y(2(pe-m)h_y-F)}{h_a[F(p-1)+2h_y(pm+pe-m)]}, pe-m > 0, \text{ and}$$

$0 < F < 2h_y(pe - m)$  hold, the system (2.1) has a unique positive interior equilibrium  $E^*$ .

At the coexistence equilibrium  $E^*$ , the Jacobian matrix is

$$J(E^*) = \begin{pmatrix} A & B \\ C & D \end{pmatrix}, \quad (2.3)$$

where  $A = \frac{rn}{n+h_n} - 2cx^* - \frac{ph_ay^*}{(x^*+h_a)^2}$ ,  $B = -\frac{px^*}{x^*+h_a}$ ,  $C = \frac{peh_ay^*}{(x^*+h_a)^2}$  and  $D = \frac{pex^*}{x^*+h_a} - m - \frac{Fy^*h_y^2}{(y^*+h_y)^2}$ . The characteristic polynomial of the Jacobian matrix can be written as

$$P(\lambda) = \lambda^2 + p_1\lambda + p_2, \quad (2.4)$$

where  $p_1 = -(A+D)$  and  $p_2 = AD-BC$ . The equilibrium  $E^*$  is locally asymptotically stable if  $\text{trace}(J(E^*)) < 0$  and  $\det(J(E^*)) > 0$ , implying

$$\frac{ph_ay^*}{(x^*+h_a)^2} + \frac{Fy^{*3}}{(y^{*2}+h_y^2)^2} < cx^* + \frac{Fh_y^2y^*}{(y^{*2}+h_y^2)^2} \quad \text{and} \quad \frac{Fy^*(y^{*2}-h_y^2)}{(y^{*2}+h_y^2)^2} + \frac{pex^*}{x^*+h_a} > 0,$$

respectively.

The Hopf bifurcation result is an important topic in the qualitative theory of differential equations. It arises if the sign of the real parts of a pair of complex roots changes when a system parameter is smoothly varied. One can easily prove the following theorem in relation to the Hopf bifurcation of the interior equilibrium  $E^*$  of the system (2.1).

**Theorem 2.2.2.** (*Martcheva [2015]*) Assume that  $f_1$  and  $f_2$  defined in (2.1) have continuous third order derivative in  $x$  and  $y$ . Also, let  $\lambda(r) = q_1(r) \pm iq_2(r)$  be the root of (2.4) and satisfy the following conditions at a certain value  $r_c$  of the parameter  $r$

## 2.2. Analysis of the deterministic model

---

such that

$$(i) \ q_1(r_c) = 0, \quad q_2(r_c) = v \neq 0 \quad (\text{Nonhyperbolicity}), \quad (ii) \ \left. \frac{d}{dr}q_1(r) \right|_{r=r_c} = l \neq 0$$

(Transversality) and (iii)  $s \neq 0$  (Generecity), where  $s = \frac{1}{16}(f_{1_{xxx}} + f_{1_{xyy}} + f_{2_{xxy}} + f_{2_{yyy}}) + \frac{1}{16v}(f_{1_{xy}}(f_{1_{xx}} + f_{1_{yy}}) - f_{2_{xy}}(f_{2_{xx}} + f_{2_{yy}}) - f_{1_{xx}}f_{2_{xx}} + f_{1_{yy}}f_{2_{yy}})$  and  $f_{1_{xy}} = \left. \frac{\partial^2 f_1(x^*, y^*)}{\partial x \partial y} \right|_{r=r_c}$ . Then the system (2.1) has a periodic solution around the equilibrium point  $(x^*, y^*)$  for  $r > r_c$  if  $ls < 0$  and for  $r < r_c$  if  $ls > 0$ . The bifurcation periodic solution is stable (unstable) and said to be supercritical (subcritical) if  $ls < 0$  ( $ls > 0$ ).

No bifurcation will occur and the interior equilibrium  $E^*$  will be globally asymptotically stable if conditions of the following theorem hold.

**Theorem 2.2.3.** *The interior equilibrium point  $E^*(x^*, y^*)$ , whenever it exists, is globally asymptotically stable if  $y^* < \min (ch_a^2/p, h_y^2/L)$ , where  $L$  is the upper bound of  $y(t)$  given in Proposition 2.2.1.*

**Proof** We consider the positive definite Lyapunov function

$$V = \left( x - x^* - x^* \ln \frac{x}{x^*} \right) + \frac{(x^* + h_a)}{e} \left( y - y^* - y^* \ln \frac{y}{y^*} \right).$$

The time derivative of  $V$  along the solutions of system (2.1) is

$$\begin{aligned} \frac{dV}{dt} &= -c(x - x^*)^2 + py^* \frac{(x - x^*)^2}{(x^* + h_a)(x + h_a)} + \frac{F(x^* + h_a)}{e(y^2 + h_y^2)(y^{*2} + h_y^2)} (y - y^*)^2 (yy^* - h_y^2) \\ &\leq \left( \frac{py^*}{h_a^2} - c \right) (x - x^*)^2 + \frac{F(x^* + h_a)}{h_y^4 e} (yy^* - h_y^2) (y - y^*)^2 \\ &\leq \left( \frac{py^*}{h_a^2} - c \right) (x - x^*)^2 + \frac{F(x^* + h_a)}{h_y^4 e} (Ly^* - h_y^2) (y - y^*)^2, \end{aligned}$$

where  $L = \frac{2r^2 e}{cR} \left( \frac{n}{n+h_n} \right)^2$ . Therefore,  $\frac{dV}{dt}$  will be negative definite if  $\left( \frac{py^*}{h_a^2} - c \right) < 0$  and  $(Ly^* - h_y^2) < 0$ , implying  $y^* < \min (ch_a^2/p, h_y^2/L)$ . Hence, following LaSalle's invariance principle,  $E^*$  is globally asymptotically stable whenever it exists and given condition holds. This completes the theorem.

## 2.3 Analysis of the stochastic model

We rewrite the stochastic model (2.2) for convenience

$$\begin{aligned} dx &= \left( r \frac{n}{n+h_n} x - cx^2 - py \frac{x}{x+h_a} \right) dt + \sigma_1 \frac{n}{n+h_n} x dB_1(t), \quad x(0) > 0, \\ dy &= \left( pey \frac{x}{x+h_a} - my - F \frac{y^2}{y^2+h_y^2} \right) dt - \sigma_2 y dB_2(t), \quad y(0) > 0. \end{aligned} \quad (2.5)$$

### 2.3.1 Existence and uniqueness of positive solution

**Theorem 2.3.1.** *For any initial value  $(x(0), y(0)) \in \mathbb{R}_+^2$ , there exists a unique solution  $(x(t), y(t)) \in \mathbb{R}_+^2$  for the system (2.5) on  $t \geq 0$  and the solution will remain in  $\mathbb{R}_+^2$  with probability 1, i.e.,  $(x(t), y(t)) \in \mathbb{R}_+^2$  for all  $t \geq 0$  almost surely (a.s.).*

**Proof** Since the coefficients of the equation are locally Lipschitz continuous, for any initial value  $(x(0), y(0)) \in \mathbb{R}_+^2$ , there is a unique local solution  $(x(t), y(t)) \in \mathbb{R}_+^2$  for all  $t \in [0, \tau_e)$ , where  $\tau_e$  is the explosion time (Mao [2007]). Now to verify that the solution is global, we need to prove  $\tau_e = \infty$  a.s.

Let  $\kappa_0 > 0$  be sufficiently large for every coordinate  $(x(0), y(0))$  lying within the interval  $\left[ \frac{1}{\kappa_0}, \kappa_0 \right]$ . Now for every integer  $\kappa > \kappa_0$ , we define the stopping time

$$\tau_\kappa = \inf \left\{ t \in [0, \tau_e) : x(t) \notin \left( \frac{1}{\kappa}, \kappa \right) \text{ or } y(t) \notin \left( \frac{1}{\kappa}, \kappa \right) \right\}. \quad (2.6)$$

Here  $\tau_\kappa$  is increasing as  $\kappa \rightarrow \infty$ . Set  $\lim_{\kappa \rightarrow \infty} \tau_\kappa = \tau_\infty$ , when  $\tau_\infty \leq \tau_e$  a.s. Therefore, if we can show that  $\tau_\infty = \infty$ , we will obtain  $\tau_e = \infty$  and  $(x(t), y(t)) \in \mathbb{R}_+^2$  a.s. for all  $t \geq 0$ . To prove  $\tau_\infty = \infty$ , let us assume that the result is not true. Hence there exist two constants  $T > 0$  and  $\epsilon \in (0, 1)$  such that

$$P(\tau_\infty \leq T) > \epsilon. \quad (2.7)$$

Thus, there exists an integer  $\kappa_1 \geq \kappa_0$  such that

$$P(\tau_\kappa \leq T) \geq \epsilon, \quad \forall \kappa \geq \kappa_1. \quad (2.8)$$

Define

$$V = x + 1 - \ln x + y + 1 - \ln y. \quad (2.9)$$

### 2.3. Analysis of the stochastic model

---

As  $u + 1 - \ln u > 0$  for all  $u > 0$ , the function  $V$  is positive definite for all  $(x(t), y(t)) \in \mathbb{R}_+^2$ . Applying Ito's formula, one can calculate

$$\begin{aligned}
dV &= \left(1 - \frac{1}{x}\right) dx + \frac{1}{2x^2}(dx)^2 + \left(1 - \frac{1}{y}\right) dy + \frac{1}{2y^2}(dy)^2 \\
&= \left[ (x-1) \left( r \frac{n}{n+h_n} - cx - \frac{py}{x+h_a} \right) + (y-1) \left( \frac{pex}{x+h_a} - m - \frac{Fy}{y^2+h_y^2} \right) \right. \\
&\quad \left. + \frac{\sigma_1^2 n^2}{2(n+h_n)^2} + \frac{\sigma_2^2}{2} \right] dt + \frac{\sigma_1 n}{n+h_n} (x-1) dB_1(t) - \sigma_2 (y-1) dB_2(t) \\
&\leq \left[ m + (r+c)x + \left( pe + \frac{p}{h_a} + \frac{F}{h_y^2} \right) y + \frac{\sigma_1^2 + \sigma_2^2}{2} \right] dt + \sigma_1 (x-1) dB_1(t) \\
&\quad - \sigma_2 (y-1) dB_2(t).
\end{aligned}$$

Observe that  $u \leq 2(u + 1 - \ln u)$  for all  $u > 0$ . Hence one can write

$$\begin{aligned}
dV &\leq \left[ \left( m + \frac{\sigma_1^2 + \sigma_2^2}{2} \right) + 2(r+c)(x+1 - \ln x) + 2 \left( pe + \frac{p}{h_a} + \frac{F}{h_y^2} \right) (y+1 - \ln y) \right] dt \\
&\quad + \sigma_1 (x-1) dB_1(t) - \sigma_2 (y-1) dB_2(t).
\end{aligned}$$

Let  $\Delta_1 = m + \frac{\sigma_1^2 + \sigma_2^2}{2}$  and  $\Delta_2 = \max \left\{ 2(r+c), 2 \left( pe + \frac{p}{h_a} + \frac{F}{h_y^2} \right) \right\}$ . Then

$$dV \leq (\Delta_1 + \Delta_2 V) dt + \sigma_1 (x-1) dB_1(t) - \sigma_2 (y-1) dB_2(t).$$

Again, define  $\Delta_3 = \max\{\Delta_1, \Delta_2\}$ . Hence

$$dV \leq \Delta_3 (1 + V) dt + \sigma_1 (x-1) dB_1(t) - \sigma_2 (y-1) dB_2(t). \quad (2.10)$$

Integrating both sides of (2.10) from 0 to  $t_1 \wedge \tau_\kappa$  for any  $t_1 \leq T$  and taking expectation,

## 2. Phytoplankton-zooplankton interaction under environmental stochasticity: Survival, extinction and stability

---

we obtain

$$\begin{aligned}
& EV\left(x(t_1 \wedge \tau_\kappa), y(t_1 \wedge \tau_\kappa)\right) \\
& \leq V\left(x(0), y(0)\right) + \Delta_3 E \int_0^{t_1 \wedge \tau_\kappa} (1 + V) dt \\
& \leq V\left(x(0), y(0)\right) + \Delta_3 t_1 + \Delta_3 E \int_0^{t_1 \wedge \tau_\kappa} V dt \\
& \leq V\left(x(0), y(0)\right) + \Delta_3 T + \Delta_3 E \int_0^{t_1} V(x(\tau_\kappa \wedge t), y(\tau_\kappa \wedge t)) dt \\
& = V\left(x(0), y(0)\right) + \Delta_3 T + \Delta_3 \int_0^{t_1} EV(x(\tau_\kappa \wedge t), y(\tau_\kappa \wedge t)) dt.
\end{aligned}$$

Therefore, applying Gronwall's inequality

$$EV(x(t_1 \wedge \tau_\kappa), y(t_1 \wedge \tau_\kappa)) \leq (V(x(0), y(0)) + \Delta_3 T) e^{\Delta_3(t_1 \wedge \tau_\kappa)} = \Delta_4 \text{ (say)}. \quad (2.11)$$

Set  $\Omega_\kappa = \{\tau_\kappa \leq T\}$  for all  $\kappa \geq \kappa_1$ . Thus, following (2.8), we get  $P(\Omega_\kappa) \geq \epsilon$  for all  $\omega \in \Omega_\kappa$ . Clearly, at least one of  $x(\tau_\kappa, \omega)$ ,  $y(\tau_\kappa, \omega)$  is equal to either  $\kappa$  or  $\frac{1}{\kappa}$ . Hence  $V(x(\tau_\kappa), y(\tau_\kappa))$  is no less than  $\min\{\kappa + 1 - \ln \kappa, \frac{1}{\kappa} + 1 + \ln \kappa\}$ . Finally, from (2.7) and (2.11), we obtain

$$\Delta_4 \geq E[1_{\Omega_\kappa} V(x(\tau_\kappa, \omega), y(\tau_\kappa, \omega))] \geq \epsilon \left[ (\kappa + 1 - \ln \kappa) \wedge \left( \frac{1}{\kappa} + 1 + \ln \kappa \right) \right],$$

where  $1_{\Omega_\kappa}$  is the indicator function of  $\Omega_\kappa$ . Therefore, letting  $\kappa \rightarrow \infty$ , we get  $\infty > \Delta_4 = \infty$ . Thus, we get a contradiction and so  $\tau_\infty = \infty$  a.s.

### 2.3.2 Stochastic bounds of the solutions

**Theorem 2.3.2.** *Solution of the system (2.5) are stochastically ultimately bounded for any positive initial value  $(x(0), y(0)) \in \mathbb{R}_+^2$ .*

**Proof** First we show that any solution  $(x(t), y(t))$  of system (2.5) with any positive initial value  $(x(0), y(0))$  is uniformly bounded in mean. Observe that

$$dx(t) \leq x(t)(r - cx(t))dt + \sigma_1 x(t)dB_1(t).$$

### 2.3. Analysis of the stochastic model

---

Let

$$\Phi(t) = \frac{e^{\left(r - \frac{\sigma_1^2}{2}\right)t + \sigma_1 B_1(t)}}{\frac{1}{x(0)} + c \int_0^t e^{\left(r - \frac{\sigma_1^2}{2}\right)\theta + \sigma_1 B_1(\theta)} d\theta}. \quad (2.12)$$

Then  $\Phi(t)$  is the unique solution of the equation

$$\begin{cases} d\Phi(t) = \Phi(t)(a - b\phi(t))dt + \sigma_1 dB_1(t), \\ \Phi(0) = x(0). \end{cases} \quad (2.13)$$

By the comparison theorem of stochastic differential equations, we get  $x(t) \leq \Phi(t)$  a.s. for all  $t \in [0, \tau_e)$ . Following (Jiang et al. [2008]), we state the following lemma.

**Lemma 2.3.3.** *Let  $\Phi(t)$  be a solution of system (2.13). Then*

$$\limsup_{t \rightarrow \infty} E[\Phi(t)] \leq \frac{r}{c}.$$

Considering Lemma 2.3.3 and  $x(t) \leq \Phi(t)$  a.s. for all  $t \in [0, \tau_e)$ , we get

$$\limsup_{t \rightarrow \infty} E[x(t)] \leq \frac{r}{c} \quad \text{a.s.} \quad (2.14)$$

Let  $G(t) = ex(t) + y(t)$ . The time derivative of  $G(t)$  along the system (2.5) is given by

$$\begin{aligned} dG(t) &= \left( re \frac{n}{n+h_n} x - cex^2 - pey \frac{x}{x+h_a} \right) + \left( pey \frac{x}{x+h_a} - my - F \frac{y^2}{y^2+h_y^2} \right) \\ &\quad + x(t) \frac{\sigma_1 ne}{n+h_n} dB_1(t) - y(t) \sigma_2 dB_2(t) \\ &\leq x(t)(re - cex(t)) - my(t) + x(t) \sigma_1 e dB_1(t) - y(t) \sigma_2 dB_2(t) \\ &\leq (2rex(t) - rex(t) - cex^2(t) - my(t))dt + \sigma_1 ex(t) \sigma_1 dB_1(t) - y(t) \sigma_2 dB_2(t) \\ &= (2rex(t) - cex^2(t))dt - \xi(ex(t) + y(t)) + \sigma_1 ex(t) \sigma_1 dB_1(t) - y(t) \sigma_2 dB_2(t). \end{aligned}$$

where  $\xi = \min(r, m)$ . Integrating both sides from 0 to  $t$ , we get

$$G(t) \leq G(0) + \int_0^t [2rex(\theta) - cex^2(\theta) - \xi G(\theta)] d\theta + \sigma_1 e \int_0^t x(\theta) dB_1(\theta) - \sigma_2 \int_0^t y(\theta) dB_2(\theta).$$

Thus,

$$E[G(t)] \leq G(0) + \int_0^t E[2rex(\theta) - cex^2(\theta) - \xi G(\theta)] d\theta$$



## 2. Phytoplankton-zooplankton interaction under environmental stochasticity: Survival, extinction and stability

---

and

$$\frac{dE[G(t)]}{dt} \leq 2reE[x(t)] - ceE[x^2(t)] - \xi E[G(t)].$$

Now,  $\max\{2reE[x(t)] - ce(E[x(t)])^2\} = \frac{r^2e}{c}$  and therefore

$$\begin{aligned} \frac{dE[G(t)]}{dt} \leq \frac{r^2e}{c} - \xi E[G(t)] &\Rightarrow 0 \leq \limsup_{t \rightarrow \infty} E[G(t)] \leq \frac{r^2e}{c\xi} \\ &\Rightarrow \limsup_{t \rightarrow \infty} E[ex(t) + y(t)] \leq \frac{r^2e}{c\xi} \text{ a.s.} \end{aligned} \quad (2.15)$$

Hence,  $y(t)$  is also uniformly bounded in mean a.s. Now, following Markov's inequality, we assert that for any positive constant  $\alpha$ , we get some  $\beta > 0$  such that

$$P(x > \alpha) \leq \frac{E(x)}{\beta} \Rightarrow \limsup_{t \rightarrow \infty} P(x > \alpha) \leq \frac{r}{c\beta} \text{ [following (2.14)] a.s.} \quad (2.16)$$

Define  $\delta_1 = \frac{r}{c\beta}$ . Therefore, for any positive constant  $\alpha > 0$ , we get an arbitrary  $\delta_1 > 0$  such that

$$\limsup_{t \rightarrow \infty} P(x > \alpha) \leq \delta_1 \text{ a.s.}$$

Hence,  $x(t)$  of system (2.5) is stochastically ultimately bounded and there exists a positive constant  $\bar{x} > 0$  such that for all  $t \in [0, \tau_e)$

$$\limsup_{t \rightarrow \infty} x(t) \leq \bar{x} \text{ a.s.} \quad (2.17)$$

Arguing in a similar manner, we can show that  $y(t)$  of system (2.5) is also stochastically ultimately bounded and there exists a positive constant  $\bar{y} > 0$  such that for all  $t \in [0, \tau_e)$

$$\limsup_{t \rightarrow \infty} y(t) \leq \bar{y} \text{ a.s.} \quad (2.18)$$

Hence the lemma is proved.

## 2.3. Analysis of the stochastic model

---

### 2.3.3 Stochastic persistence

To obtain the persistence results for our system, we consider the following auxiliary system and prove the lemma stated below:

$$\begin{aligned} dX &= (rX - cX^2)dt + \sigma_1 X dB_1(t), \\ dY &= \left( \frac{pe}{h_a} XY - mY - \frac{FY^2}{\bar{y}^2 + h_y^2} \right) dt - \sigma_2 Y dB_2(t), \end{aligned} \quad (2.19)$$

where  $\bar{y}$  is the stochastic upper bound of  $y$ . Clearly,  $x \leq X$ ,  $y \leq Y$  for  $t \geq 0$  a.s.

**Lemma 2.3.4.** *If  $\frac{pe}{ch_a} \left( r - \frac{\sigma_1^2}{2} \right) - \left( m + \frac{\sigma_1^2}{2} \right) > 0$ , then*

$$\lim_{t \rightarrow \infty} \frac{1}{t} \int_0^t X(u) du = \frac{1}{c} \left( r - \frac{\sigma_1^2}{2} \right), \quad \lim_{t \rightarrow \infty} \frac{1}{t} \int_0^t Y(u) du = \frac{\frac{pe}{ch_a} \left( r - \frac{\sigma_1^2}{2} \right) - \left( m + \frac{\sigma_1^2}{2} \right)}{\frac{F}{\bar{y}^2 + h_y^2}}.$$

**Proof** Applying Ito's formula to system (2.19), we obtain

$$d \ln X = \left( r - cX - \frac{\sigma_1^2}{2} \right) dt + \sigma_1 dB_1(t). \quad (2.20)$$

Integration on both sides from 0 to  $t$  gives

$$\ln \frac{X(t)}{X(0)} = \left( r - \frac{\sigma_1^2}{2} \right) t - c \int_0^t X(u) du + \sigma_1 B_1(t). \quad (2.21)$$

Observe that the assumption  $\frac{pe}{ch_a} \left( r - \frac{\sigma_1^2}{2} \right) - \left( m + \frac{\sigma_1^2}{2} \right) > 0$  implies  $\left( r - \frac{\sigma_1^2}{2} \right) > 0$ . Applying Lemma 1.7.3, we then have

$$\lim_{t \rightarrow \infty} \frac{1}{t} \int_0^t X(u) du = \frac{1}{c} \left( r - \frac{\sigma_1^2}{2} \right). \quad (2.22)$$

Substituting (2.22) in (2.21) and using  $\lim_{t \rightarrow \infty} \frac{B_1(t)}{t} = 0$ , one gets

$$\lim_{t \rightarrow \infty} \frac{\ln X(t)}{t} = 0. \quad (2.23)$$

## 2. Phytoplankton-zooplankton interaction under environmental stochasticity: Survival, extinction and stability

---

A similar application of Ito's formula to the second equation of (2.19) gives

$$\lim_{t \rightarrow \infty} \frac{1}{t} \int_0^t Y(u) du = \frac{\frac{pe}{ch_a} \left( r - \frac{\sigma_1^2}{2} \right) - \left( m + \frac{\sigma_1^2}{2} \right)}{\frac{F}{\bar{y}^2 + h_y^2}}. \quad (2.24)$$

**Theorem 2.3.5.** *The following results are true for the solution  $x(t)$  of the system (2.5).*

- (i) *If  $r < \frac{\sigma_1^2}{2}$  then  $x(t)$  will go to extinction a.s.*
- (ii) *If  $r = \frac{\sigma_1^2}{2}$  then  $x(t)$  is non-persistent in the mean a.s.*
- (iii) *If  $\frac{rn}{n+h_n} > \frac{\sigma_1^2}{2} + \frac{p\bar{y}}{h_a}$  then  $x(t)$  is strongly persistent in the mean a.s.*

**Proof** From the first equation of the system (2.5), it follows that

$$dx(t) \leq x(t)[r - cx(t)]dt + x(t)\sigma_1 dB_1(t).$$

Clearly, the righthand side is a logistic system. Hence, following the comparison theorem of stochastic differential equations and using the results of Liu and Wang [2011c], one can easily prove (i) and (ii).

(iii) From the first equation of (2.5), we have

$$\begin{aligned} d \ln x &\geq \left( \frac{rn}{n+h_n} - cx - \frac{p}{h_a} y - \frac{\sigma_1^2}{2} \right) dt + \frac{\sigma_1 n}{n+h_n} dB_1(t) \\ \Rightarrow \ln \frac{x(t)}{x(0)} &\geq \left( \frac{rn}{n+h_n} - \frac{p\bar{y}}{h_a} - \frac{\sigma_1^2}{2} \right) t - c \int_0^t x(\theta) d\theta + \frac{\sigma_1 n}{n+h_n} B_1(t). \end{aligned}$$

Therefore, if  $\frac{rn}{n+h_n} - \frac{p\bar{y}}{h_a} - \frac{\sigma_1^2}{2} > 0$  then, by applying Lemma 1.7.3, we obtain

$$\liminf_{t \rightarrow \infty} \frac{1}{t} \int_0^t x(\theta) d\theta \geq \frac{1}{c} \left( \frac{rn}{n+h_n} - \frac{p\bar{y}}{h_a} - \frac{\sigma_1^2}{2} \right) > 0.$$

Evidently,  $x(t)$  is strongly persistent in the mean if  $\frac{rn}{n+h_n} > \frac{\sigma_1^2}{2} + \frac{p\bar{y}}{h_a}$ .

**Theorem 2.3.6.** *The following results are true for the solution  $y(t)$  of (2.5).*

- (I) *If  $r \leq \frac{\sigma_1^2}{2}$  then  $y(t)$  will go to extinction a.s.*
- (II) *If  $r > \frac{\sigma_1^2}{2}$  then*
  - (i)  *$y(t)$  will go to extinction a.s. if  $pe \left( r - \frac{\sigma_1^2}{2} \right) < ch_a \left( m + \frac{\sigma_2^2}{2} \right)$ ,*
  - (ii)  *$y(t)$  is non-persistent in the mean a.s. if  $pe \left( r - \frac{\sigma_1^2}{2} \right) = ch_a \left( m + \frac{\sigma_2^2}{2} \right)$ ,*

### 2.3. Analysis of the stochastic model

---

(iii)  $y(t)$  is strongly persistent in the mean a.s. if  $\frac{pe}{\bar{x}+h_a} \left( \frac{rn}{n+h_n} - \frac{\sigma_1^2}{2} \right) > c \left( m + \frac{\sigma_2^2}{2} \right)$ .

**Proof** (I) Suppose  $r - \frac{\sigma_1^2}{2} \leq 0$ . Then from Theorem 2.3.5 (i), one can note that  $x(t)$  is extinct a.s, i.e.,  $\limsup_{t \rightarrow \infty} \frac{1}{t} \int_0^t x(\theta) d\theta < 0$ , following Definition 1.7.2 (i). Now, the second equation of (2.5) yields

$$\begin{aligned} \frac{\ln y(t) - \ln y(0)}{t} &\leq \left( -m - \frac{\sigma_2^2}{2} \right) + \frac{pe}{h_a t} \int_0^t x(\theta) d\theta - \sigma_2 \frac{B_2(t)}{t} \\ \Rightarrow \limsup_{t \rightarrow \infty} \frac{\ln y(t)}{t} &\leq \left( -m - \frac{\sigma_2^2}{2} \right) < 0 \Rightarrow \lim_{t \rightarrow \infty} y(t) = 0. \end{aligned}$$

Thus, the extinction of  $x(t)$  implies the extinction of  $y(t)$  under the same restriction.

(II) Consider  $r - \frac{\sigma_1^2}{2} > 0$ .

(i) From the first equation of (2.5), one then obtains

$$\frac{\ln x(t) - \ln x(0)}{t} \leq r - \frac{\sigma_1^2}{2} - \frac{c}{t} \int_0^t x(\theta) d\theta + \sigma_1 \frac{B_1(t)}{t}.$$

Lemma 1.7.3 then leads to

$$\limsup_{t \rightarrow \infty} \frac{1}{t} \int_0^t x(\theta) d\theta \leq \frac{r - \frac{\sigma_1^2}{2}}{c}. \quad (2.25)$$

Again from (2.5), we have

$$\begin{aligned} \frac{\ln y(t) - \ln y(0)}{t} &\leq \left( -m - \frac{\sigma_2^2}{2} \right) + \frac{pe}{h_a t} \int_0^t x(\theta) d\theta - \frac{F}{(\bar{y}^2 + h_y^2)t} \int_0^t y(\theta) d\theta - \sigma_2 \frac{B_2(t)}{t} \\ \Rightarrow \limsup_{t \rightarrow \infty} \frac{1}{t} \int_0^t y(\theta) d\theta &\leq (\bar{y}^2 + h_y^2) \frac{[pe \left( r - \frac{\sigma_1^2}{2} \right) - ch_a \left( m + \frac{\sigma_2^2}{2} \right)]}{Fch_a}. \end{aligned} \quad (2.26)$$

Thus, if  $pe \left( r - \frac{\sigma_1^2}{2} \right) < ch_a \left( m + \frac{\sigma_2^2}{2} \right)$  then  $\lim_{t \rightarrow \infty} y(t) = 0$ .

(ii) Assume,  $\limsup_{t \rightarrow \infty} \frac{1}{t} \int_0^t y(\theta) d\theta \geq 0$ . For sufficiently small  $\nu > 0$ , there exists  $T_1 > 0$  such that for all  $t > T_1$

$$\frac{1}{t} \int_0^t x(\theta) d\theta < \limsup_{t \rightarrow \infty} \frac{1}{t} \int_0^t x(\theta) d\theta + \nu. \quad (2.27)$$

## 2. Phytoplankton-zooplankton interaction under environmental stochasticity: Survival, extinction and stability

---

Using Ito's formula on the second equation of (2.5) and substituting the inequality (2.27), we have

$$\begin{aligned} \frac{\ln y(t) - \ln y(0)}{t} &\leq \left(-m - \frac{\sigma_2^2}{2}\right) + \frac{pe}{h_a t} \int_0^t x(\theta) d\theta - \frac{F}{(\bar{y}^2 + h_y^2)t} \int_0^t y(\theta) d\theta - \sigma_2 \frac{B_2(t)}{t} \\ &\leq \left(-m - \frac{\sigma_2^2}{2}\right) + \limsup_{t \rightarrow \infty} \frac{pe}{h_a t} \int_0^t x(\theta) d\theta + \frac{pe}{h_a} \nu - \frac{F}{(\bar{y}^2 + h_y^2)t} \int_0^t y(\theta) d\theta \\ &\quad - \sigma_2 \frac{B_2(t)}{t}. \end{aligned}$$

By Lemma 1.7.3

$$\limsup_{t \rightarrow \infty} \frac{1}{t} \int_0^t y(\theta) d\theta \leq \frac{\left(-m - \frac{\sigma_2^2}{2}\right) + \limsup_{t \rightarrow \infty} \frac{pe}{h_a t} \int_0^t x(\theta) d\theta + \frac{pe}{h_a} \nu}{\frac{F}{\bar{y}^2 + h_y^2}}. \quad (2.28)$$

As  $\nu$  is arbitrary, from (2.25), we get

$$\limsup_{t \rightarrow \infty} \frac{1}{t} \int_0^t y(\theta) d\theta \leq \frac{(\bar{y}^2 + h_y^2) \left[ pe \left( r - \frac{\sigma_1^2}{2} \right) - ch_a \left( m + \frac{\sigma_2^2}{2} \right) \right]}{Fch_a}.$$

Thus, whenever  $pe \left( r - \frac{\sigma_1^2}{2} \right) = ch_a \left( m + \frac{\sigma_2^2}{2} \right)$ ,  $\limsup_{t \rightarrow \infty} \frac{1}{t} \int_0^t y(\theta) d\theta = 0$ , implying  $y(t)$  is non-persistent in the mean a.s.

(iii) From the two equations of (2.5), one can obtain

$$\begin{aligned} \ln \frac{x(t)}{x(0)} &= \left( \frac{rn}{n + h_n} - \frac{\sigma_1^2 n^2}{2(n + h_n)^2} \right) t - c \int_0^t x(\theta) d\theta - \int_0^t \frac{py(\theta)}{x(\theta) + h_a} d\theta + \frac{\sigma_1 n}{n + h_n} B_1(t), \\ \ln \frac{y(t)}{y(0)} &= - \left( m + \frac{\sigma_2^2}{2} \right) t + pe \int_0^t \frac{x(\theta)}{x(\theta) + h_a} d\theta - \int_0^t \frac{Fy(\theta)}{y^2(\theta) + h_y^2} d\theta - \sigma_2 B_2(t). \end{aligned}$$

Hence

$$\begin{aligned} \frac{pe}{\bar{x} + h_a} \ln \frac{x(t)}{x(0)} + c \ln \frac{y(t)}{y(0)} &\geq \left[ \frac{pe}{\bar{x} + h_a} \left( \frac{rn}{n + h_n} - \frac{\sigma_1^2}{2} \right) - c \left( m + \frac{\sigma_2^2}{2} \right) \right] t \\ &\quad - \left( \frac{p^2 e}{h_a(\bar{x} + h_a)} + \frac{cF}{h_y^2} \right) \int_0^t y(\theta) d\theta + \frac{pe\sigma_1 n}{(\bar{x} + h_a)(n + h_n)} B_1(t) - c\sigma_2 B_2(t). \end{aligned}$$

### 2.3. Analysis of the stochastic model

By virtue of Lemma 2.3.4,  $\limsup_{t \rightarrow \infty} \frac{\ln x(t)}{t} \leq 0$  implies  $\frac{\ln x(t)}{t} \leq 0$ . Thus, we get

$$\begin{aligned} \ln \frac{y(t)}{y(0)} &\geq \frac{1}{c} \left[ \frac{pe}{\bar{x} + h_a} \left( \frac{rn}{n + h_n} - \frac{\sigma_1^2}{2} \right) - c \left( m + \frac{\sigma_2^2}{2} \right) \right] t \\ &\quad - \frac{1}{c} \left( \frac{p^2e}{h_a(\bar{x} + h_a)} + \frac{cF}{h_y^2} \right) \int_0^t y(\theta) d\theta + \frac{pe\sigma_1 n}{c(\bar{x} + h_a)(n + h_n)} B_1(t) - \sigma_2 B_2(t). \end{aligned}$$

Assuming  $\frac{pe}{\bar{x} + h_a} \left( \frac{rn}{n + h_n} - \frac{\sigma_1^2}{2} \right) > c \left( m + \frac{\sigma_2^2}{2} \right)$ , it follows from Lemma 1.7.3,

$$\liminf_{t \rightarrow \infty} \frac{1}{t} \int_0^t y(\theta) d\theta \geq \frac{\frac{pe}{\bar{x} + h_a} \left( \frac{rn}{n + h_n} - \frac{\sigma_1^2}{2} \right) - c \left( m + \frac{\sigma_2^2}{2} \right)}{\frac{p^2e}{h_a(\bar{x} + h_a)} + \frac{cF}{h_y^2}}.$$

Clearly,  $\liminf_{t \rightarrow \infty} \frac{1}{t} \int_0^t y(\theta) d\theta > 0$  if  $\frac{pe}{\bar{x} + h_a} \left( \frac{rn}{n + h_n} - \frac{\sigma_1^2}{2} \right) > c \left( m + \frac{\sigma_2^2}{2} \right)$ , implying  $y(t)$  is strongly persistent in the mean.

#### 2.3.4 Stationary distribution

**Theorem 2.3.7.** *The system (2.5) has a stationary distribution and it is ergodic if (i)  $h_y^2 > \bar{y}y^*$ , (ii)  $0 < \delta < \min \{\Theta_1, \Theta_2\}$ , where  $A = x^* + h_a$ ,  $L = cA + \frac{py^*}{\bar{x} + h_a}$ ,  $M = \frac{FA}{h_y^4 e} (h_y^2 - \bar{y}y^*)$ ,  $\Theta_1 = L \left( x^* + \frac{\sqrt{\Theta}}{L^{3/2}} \right)^2$ ,  $\Theta_2 = M (y^* + \Theta)^2$ ,  $\Theta = \frac{p}{h_a} (\bar{x} - x^*) (2\bar{x}y^* - x^*y^*) + \frac{A\sigma_1^2 n^2 x^*}{2(n + h_n)^2} + \frac{A\sigma_2^2 y^*}{2}$ ,  $\delta = \Theta \left( 1 + \frac{1}{L^2} \right)$  and  $\bar{x}, \bar{y}$  is the stochastic bound of  $x$  and  $y$ .*

**Proof** System (2.5) can be written as

$$\begin{aligned} d \begin{pmatrix} x(t) \\ y(t) \end{pmatrix} &= \begin{pmatrix} x \left( r \frac{n}{n + h_n} - cx \right) - py \frac{x}{x + h_a} \\ pey \frac{x}{x + h_a} - my - F \frac{y^2}{y^2 + h_y^2} \end{pmatrix} dt + \begin{pmatrix} \frac{n\sigma_1}{n + h_n} x(t) \\ 0 \end{pmatrix} dB_1(t) \\ &\quad + \begin{pmatrix} 0 \\ -\sigma_2 y(t) \end{pmatrix} dB_2(t) \end{aligned} \quad (2.29)$$

and the diffusion matrix is

$$A' = \begin{pmatrix} \frac{n^2 \sigma_1^2}{(n + h_n)^2} x^2 & 0 \\ 0 & \sigma_2^2 y^2 \end{pmatrix}. \quad (2.30)$$

Define

$$\bar{V}(x, y) = V_1(x, y) + V_2(x, y),$$

## 2. Phytoplankton-zooplankton interaction under environmental stochasticity: Survival, extinction and stability

---

where

$$V_1 = A \left[ x - x^* - x^* \ln \frac{x}{x^*} \right], \quad V_2 = \frac{A}{e} \left[ y - y^* - y^* \ln \frac{y}{y^*} \right].$$

Again at  $E^*$ , we have

$$\frac{rn}{n + h_n} = cx^* + \frac{py^*}{x^* + h_a}, \quad m = \frac{pex^*}{x^* + h_a} - \frac{Fy^*}{y^{*2} + h_y^2}. \quad (2.31)$$

Using (2.31), one can calculate

$$\begin{aligned} L\bar{V} &= A \left( \frac{x - x^*}{x} \right) \left[ \frac{rn}{n + h_n} x - cx^2 - \frac{pxy}{x + h_a} \right] + \frac{\sigma_1^2 n^2 Ax^*}{2(n + h_n)^2} \\ &\quad + \frac{A}{e} \left( \frac{y - y^*}{y} \right) \left[ \frac{pexy}{x + h_a} - my - \frac{Fy^2}{y^2 + h_y^2} \right] + \frac{Ay^* \sigma_2^2}{2e} \\ &\leq -cA(x - x^*)^2 - \frac{py^*}{x + h_a} (x - x^*)^2 + p \frac{(x - x^*)(2xy^* - x^*y^* - x^*y)}{x + h_a} \\ &\quad - \frac{ph_a}{x + h_a} (x - x^*)(y - y^*) + \frac{n\sigma_1^2 Ax^*}{2(n + h_n)^2} + \frac{ph_a}{x + h_a} (x - x^*)(y - y^*) \\ &\quad + \frac{FA(yy^* - h_y^2)(y - y^*)^2}{e(y^2 + h_y^2)(y^{*2} + h_y^2)} + \frac{Ay^* \sigma_2^2}{2e} \\ &\leq -L(x - x^*)^2 - M(y - y^*)^2 + p \frac{(x - x^*)(2xy^* - x^*y^* - x^*y)}{x + h_a} + \frac{n\sigma_1^2 Ax^*}{2(n + h_n)^2} + \frac{Ay^* \sigma_2^2}{2e} \\ &\leq -L \left( x - \left( x^* + \frac{\sqrt{\Theta}}{L^{3/2}} \right) \right)^2 - M(y - (y^* + \Theta))^2 + \delta, \end{aligned}$$

where  $0 < \delta < \min \{\Theta_1, \Theta_2\}$  and  $\Theta_1, \Theta_2, \Theta$  are as in the theorem. Therefore, if  $h_y^2 > \bar{y}y^*$  (i.e.,  $M > 0$ ) and  $0 < \delta < \min \{\Theta_1, \Theta_2\}$  then the ellipse

$$L \left( x - \left( x^* + \frac{\sqrt{\Theta}}{L^{3/2}} \right) \right)^2 + M(y - (y^* + \Theta))^2 = \delta$$

lies entirely in  $\mathbb{R}_+^2$ . We choose  $U$  to be a neighborhood of this ellipse such that  $\bar{U} \subseteq E_2 = \mathbb{R}_+^2$  and for all  $(x, y) \in E_2 \setminus U$ ,  $L\bar{V} \leq 0$  which implies that (A2) of Lemma 1.7.5 is satisfied. Besides, there is a  $M = \min \left\{ \frac{n^2}{(n+h_n)^2} \sigma_1^2 x^2, \sigma_2^2 y^2; (x, y) \in \bar{U} \right\} > 0$  such that

$$\Sigma_{i,j=1}^2 a_{ij} \xi_i \xi_j = \frac{n^2}{(n + h_n)^2} \sigma_1^2 x^2 \xi_1^2 + \sigma_2^2 y^2 \xi_2^2 \geq M \|\xi\|^2, \quad \forall (x, y) \in \bar{U}, \quad \xi \in \mathbb{R}^2,$$

## 2.4. Numerical Simulations

---

satisfying (A1) of Lemma 1.7.5. Therefore, the stochastic system (2.5) has a stationary distribution  $\pi(\cdot)$  and it is ergodic.

**Remark 2.3.8.** *It is to be mentioned that whenever the conditions of Theorem 2.3.5 (i) and Theorem 2.3.6 I, II(i) hold then both  $x$  and  $y$  go to extinction and therefore no question of satisfying the conditions of Theorem 2.3.7. However, if the conditions of Theorem 2.3.5 (i) and Theorem 2.3.6 I, II(i) do not hold then  $x$  and  $y$  may be non-persistent (following Theorem 2.3.5 (ii) and Theorem 2.3.6 II(ii)) and the conditions of Theorem 3.5 will not hold; but the conditions of Theorem 2.3.7 will hold if the conditions of Theorem 2.3.5 (iii) and Theorem 2.3.6 II(iii) hold simultaneously.*

## 2.4 Numerical Simulations

In this section, we numerically simulate the system (2.5) to support and visualize the analytical results. We first present various dynamic behaviors of the deterministic system (2.1). With the parameter values as in Table 2.1, we plot the stability domain (central figure of Fig. 2.1) of the equilibrium points in the  $r - e$  parametric plane. Here the magenta, green, and red colour regions represent, respectively, the stability of  $E^1$ , stability of  $E^*$  and instability of  $E^*$ . It shows that zooplankton can not survive, even when the phytoplankton growth rate ( $r$ ) is high, because of its low conversion efficiency ( $e$ ). Zooplankton, however, coexists with phytoplankton in a stable state if its conversion efficiency is high. Both populations coexist in an oscillatory state if phytoplankton's growth rate and zooplankton's conversion efficiency both are high. Representative behaviors of the solutions in each region is plotted in Figs. 2.1(a-c) for some particular values of  $r$  and  $e$ . Stability switching through the Hopf bifurcation of the interior equilibrium  $E^*$ , arising due to variation in the growth rate ( $r$ ), is shown in the bifurcation diagram Fig. 2.1(d). It shows that the system loses its stability at the critical value  $r_c = 0.5995$  when other parameters are fixed. Notice that all conditions of Theorem 2.2.2 are satisfied with  $q_1(r_c) = 0.0005 \approx 0$ ,  $q_2(r_c) = 0.0952 \neq 0$ ,  $\frac{d}{dr}q_1(r)|_{r=r_c} = 0.2272 = l \neq 0$ ,  $s = -0.0113 \neq 0$  and  $ls = -0.0026 < 0$ . Thus, following Theorem 2.2.2, the system (2.1) experiences a supercritical Hopf bifurcation. Similar stability switching for variation in zooplankton's conversion efficiency ( $e$ ) is given in Fig. 2.1(e). The stability is lost here at the critical value  $e_c = 0.6015$ . For the stochastic system, we use Milstein's scheme (Higham [2001]), which has a higher order of convergence, to find the solution of system (2.5). The numerical scheme of



## 2. Phytoplankton-zooplankton interaction under environmental stochasticity: Survival, extinction and stability

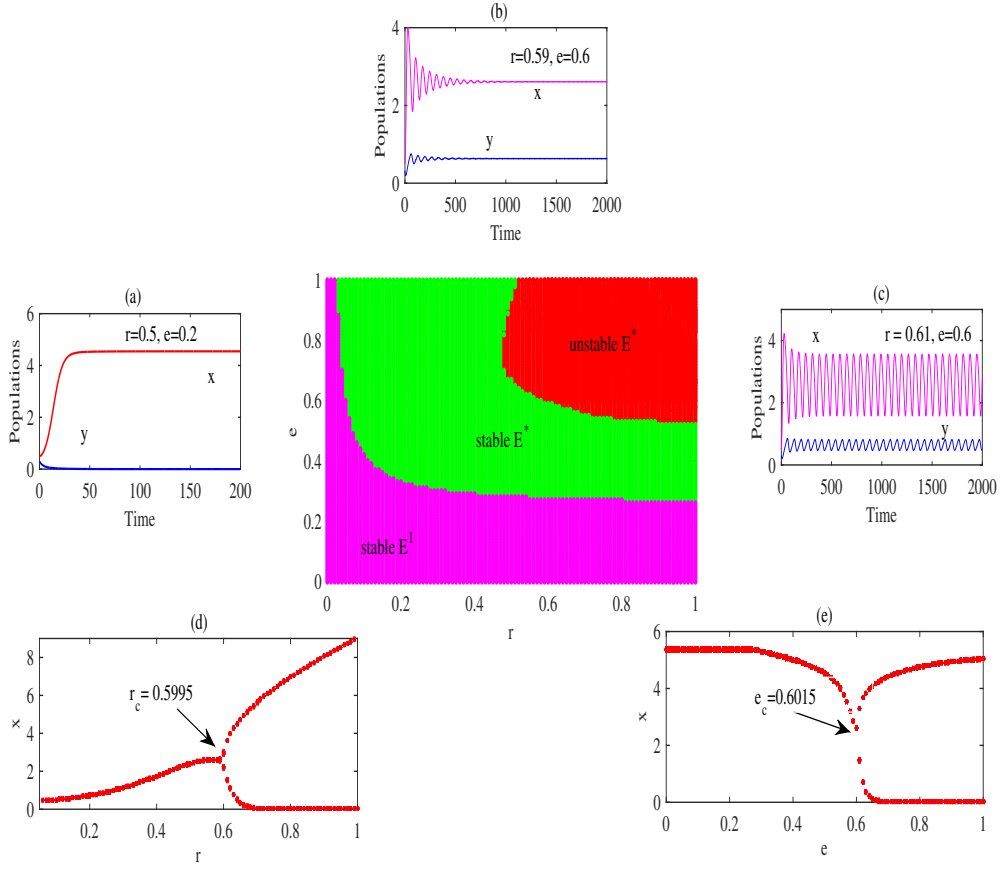


**Figure 2.1:** Centre: stability and instability region of equilibrium points  $E^1$  and  $E^*$  of the system (2.1) in  $r - e$  parametric plane. Left: Solution converges to  $E^1$  for  $r = 0.5, e = 0.2$ . Upper: Solution converges to  $E^*$  for  $r = 0.59, e = 0.6$ . Right: unstable oscillatory behavior of the solution for  $r = 0.61, e = 0.6$ . Below: bifurcation diagrams of  $x$  population with respect to  $r$  (left) and  $e$  (right). Parameters are as in Table 2.1 and the initial value is  $(0.5, 0.3)$ .

Milstein's method provides the following discretized system corresponding to system (2.5):

$$\begin{aligned}
 x_{k+1} &= x_k + \left( r \frac{n}{n + h_n} x_k - c x_k^2 - p y_k \frac{x_k}{x_k + h_a} \right) \Delta t + \sigma_1 \frac{n}{n + h_n} x_k \sqrt{\Delta t} \xi_k \\
 &\quad + \frac{\sigma_1^2 n^2}{2(n + h_n)^2} x_k (\xi_k^2 - 1) \Delta t, \\
 y_{k+1} &= y_k + \left( p e y_k \frac{x_k}{x_k + h_a} - m y_k - F \frac{y_k^2}{y_k^2 + h_y^2} \right) \Delta t - \sigma_2 y_k \sqrt{\Delta t} \eta_k \\
 &\quad + \frac{1}{2} \sigma_2^2 y_k (\eta_k^2 - 1) \Delta t,
 \end{aligned} \tag{2.32}$$

## 2.4. Numerical Simulations

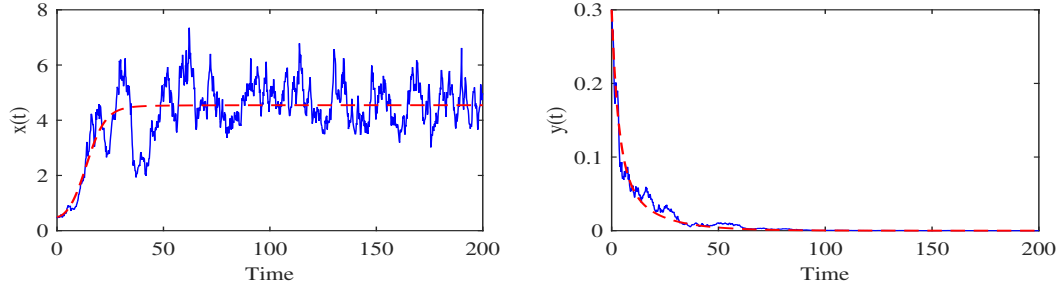


**Figure 2.2:** Solid and broken lines represent, respectively, the solutions of the stochastic system (2.5) and deterministic system (2.1). Here  $\sigma_1 = 0.3$ ,  $\sigma_2 = 0.2$  and other parameters are as in Table 2.1 with  $r = 0.5$ ,  $e = 0.2$ . Initial value is considered as  $(0.5, 0.3)$ .

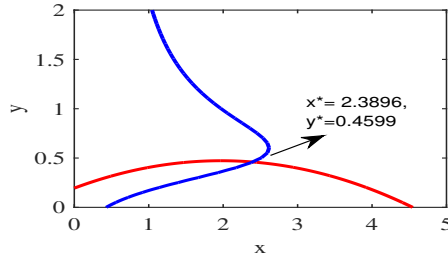


**Figure 2.3:** Existence of a unique positive interior equilibrium point  $E^* = (2.3896, 0.4599)$  of the system (2.1) for the parameter values of Fig. 2.1(b).

where  $\xi_k$  and  $\eta_k$  are two independent Gaussian random variables that follow  $N(0, 1)$ . The parameter and initial values are considered as in Table 2.1 and the time-step is taken as  $\Delta t = 0.01$ . Choosing  $e = 0.2$ ,  $r = 0.5$  (corresponding to Fig. 2.1(a)) and setting the environmental forcing intensities as  $\sigma_1 = 0.3$ ,  $\sigma_2 = 0.2$ , we present the result of one simulation run in Fig. 2.2. It shows that the zooplankton population of both the deterministic (broken line) and stochastic (solid line) systems goes extinct simultaneously, but the phytoplankton population of the stochastic system (solid line) fluctuates around the deterministic steady-state value  $\hat{x} = 4.545$  (broken line). The parameter values of Fig. 2.1(b) satisfy the existence criterion of a unique interior equilibrium point  $E^*$  and consequently Fig. 2.3 shows such positive interior equilibrium point  $E^* = (x^*, y^*) = (2.3896, 0.4599)$  of the system (2.1). To demonstrate the environmental effect on the coexistence equilibrium  $E^*$ , we consider the environmental forcing intensities as  $\sigma_1 = 0.01$  and  $\sigma_2 = 0.01$  so that these values satisfy the conditions of stochastic persistence and existence of stationary distribution of Theorems 2.3.5 (iii), 2.3.6 (iii), 2.3.7. Time series solutions of system (2.5) (Fig.

## 2. Phytoplankton-zooplankton interaction under environmental stochasticity: Survival, extinction and stability

---

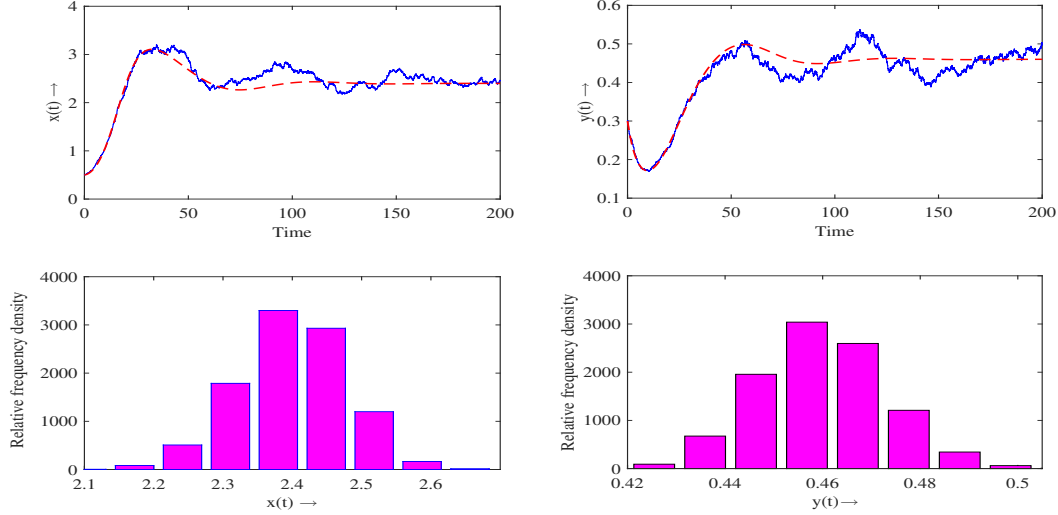


**Figure 2.4:** Upper panel: Time evolutions of systems populations of (2.1) and (2.5) are plotted with parameters as in Table 2.1 with  $\sigma_1 = 0.01$ ,  $\sigma_2 = 0.01$ . The solid blue curve represents the stochastic solution and the red broken line represents the deterministic solution. Lower panel: Frequency distribution of plankton populations obtained at  $t = 200$  from 10,000 simulation runs. Parameters are  $r = 0.5$ ,  $n = 0.5$ ,  $c = 0.05$ ,  $e = 0.6$ ,  $p = 0.7$ ,  $m = 0.175$ ,  $h_a = 0.6$ ,  $h_y = 0.6$ ,  $h_n = 0.6$ ,  $F = 0.2$  and initial value is  $(0.5, 0.3)$ .

(2.4, upper panel) show that the population densities fluctuate around the deterministic steady state  $(x^*, y^*)$ . Keeping all the parameters fixed, we repeat the simulation 10,000 times and plot the relative frequency density of both populations at  $t = 200$  in the lower panel of Fig. 2.4. Observe that the phytoplankton and zooplankton population densities are distributed in the range  $(2.1, 2.6)$  and  $(0.42, 0.5)$ , respectively, around the deterministic steady state  $x^* = 2.3896$ ,  $y^* = 0.4599$ . The population fluctuation around the deterministic steady-state value increases with the increasing strength of the environmental forcing term (see Fig. 2.5). The corresponding relative frequency densities are plotted in the lower panel of Fig. 2.5 and it indicates that both the phytoplankton and zooplankton population densities are distributed in a wider range  $(0.5, 4)$  and  $(0.1, 1)$ , respectively.

Following further increase in the noise intensity of  $\sigma_1 (= 1.3)$ , the parameter values satisfy the condition of Theorem 2.3.5(i). In this case, the phytoplankton population goes to extinction and the extinction time for this simulation is 72 units of time (Fig. 2.6, left panel). This value of the time unit may, however, differ from another simulation run with the same parameter set, though the extinction of the phytoplank-

## 2.4. Numerical Simulations

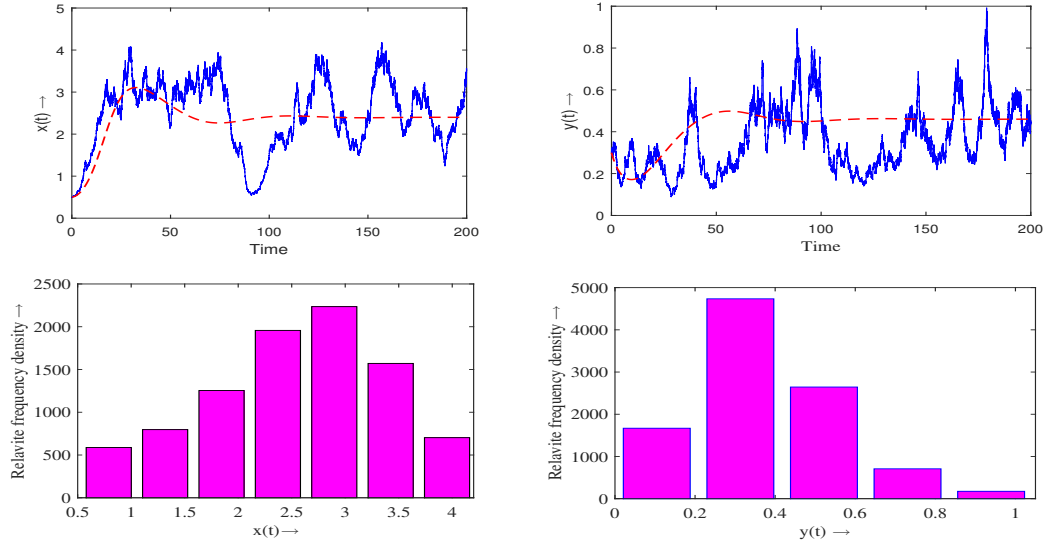


**Figure 2.5:** Upper panel: Time series behavior of systems populations of (2.1) and (2.5) are plotted with forcing intensities  $\sigma_1 = 0.2$ ,  $\sigma_2 = 0.2$ . Stochastic and deterministic solutions are represented by solid blue and broken red curves, respectively. Lower panel: Frequency distribution of both populations at  $t = 200$  for 10,000 simulation runs. Parameters are as in Fig. 2.4.

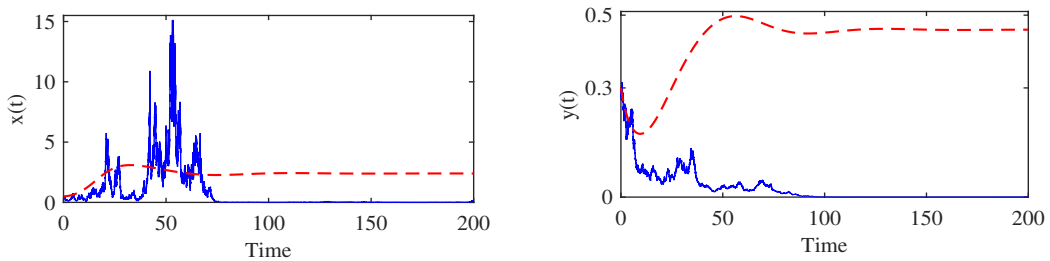


**Figure 2.6:** Left: Phytoplankton population of system (2.5) goes to extinction for  $\sigma_1 = 1.3$ ,  $\sigma_2 = 0.2$ . Right: The corresponding zooplankton population also dies out for this same forcing intensity. Both populations, however, maintain their steady state values in the deterministic case (red broken line). Parameters are as in Fig. 2.4.

ton population is always confirmed in each simulation. Extinction of zooplankton is followed due to scarcity of food (Theorem 2.3.6 (I)). Thus, both species may go to extinction due to environmental stochasticity. However, extinction of both species is never possible in the deterministic system as  $(0, 0)$  equilibrium is always unstable.

In the next case, we select  $\sigma_1 = 0.9$  and  $\sigma_2 = 1.6$ , keeping all other parameters unchanged, to satisfy Theorem 2.3.6 II(i). Notice that the zooplankton population

## 2. Phytoplankton-zooplankton interaction under environmental stochasticity: Survival, extinction and stability

---

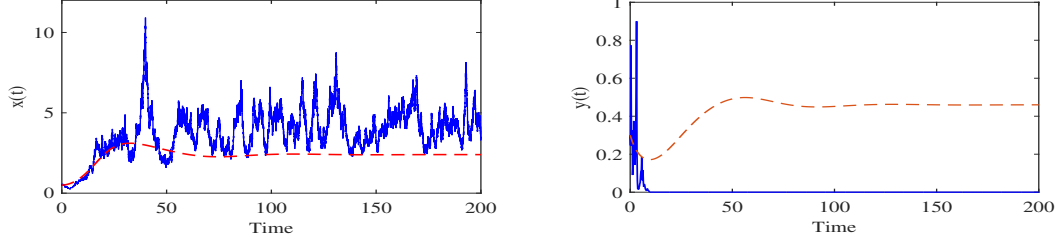


**Figure 2.7:** Left: The time evolution of the phytoplankton population of system (2.5) for  $\sigma_1 = 0.9$  and  $\sigma_2 = 1.6$  shows that the stochastic trajectory fluctuates around some fuzzy value. Right: Solution curve of zooplankton population of system (2.5) for  $\sigma_1 = 0.9$ ,  $\sigma_2 = 1.6$  exhibits extinction scenario. The deterministic steady state value is represented by the red broken line. Parameters are as in Fig. 2.4.

becomes extinct with extinction time 11 units, as presented in the right block of Fig. 2.7. In this case, the phytoplankton population survives (as  $r > \frac{1}{2}\sigma_1^2$ ) and its density most of the time remains above the deterministic steady-state value. It shows that the predator population goes to extinction when the noise intensity in the predator's equation is higher, but both the prey and predator coexist in a stable state in the absence of environmental noise.

So far, we have selected parameter values from the stability region of  $E^*$ . It would be interesting to observe the stochastic behavior of the solutions if the parameter values are selected from the unstable region of  $E^*$ . Figure 2.1(d) shows that stability switching occurs at  $r = r_c = 0.5995$  for a fixed value of  $e = 0.6$ . Thus, the equilibrium

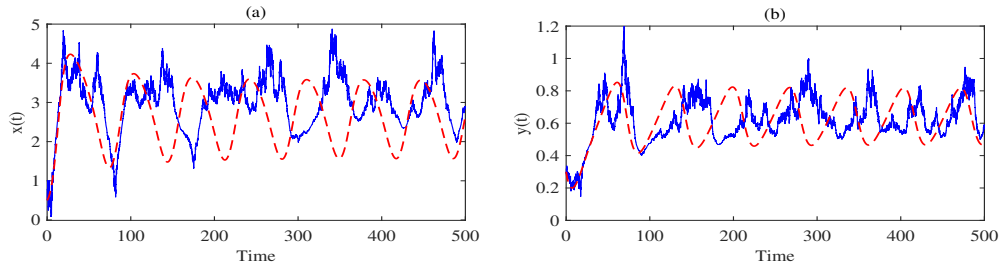


**Figure 2.8:** Phytoplankton and zooplankton populations both fluctuate simultaneously for  $e = 0.6$  and  $r = 0.61$ . Here the environmental forcing intensities are  $\sigma_1 = 0.2$  and  $\sigma_2 = 0.2$  and other parameters are as in Table 2.1. The deterministic solution is represented by the red broken line and the stochastic solution is represented by the blue solid line. Parameters are as in Fig. 2.4.

$E^*$  shows unstable oscillatory behaviour for the value of  $e = 0.6$ ,  $r = 0.61$ . Here the

## 2.5. Stochastic perturbation around an equilibrium point

---

stochastic solutions (blue solid line) fluctuate similarly with the deterministic solution with some phase lag (Fig. 2.8).

## 2.5 Stochastic perturbation around an equilibrium point

For convenience, we first rewrite the model (2.3), where the stochastic perturbation is considered proportional to the distances of state variables from their respective equilibrium value:

$$\begin{aligned} dx &= f_1(x, y)dt + \sigma_1(x - \hat{x})dB_1(t), \\ dy &= f_2(x, y)dt + \sigma_2(y - \hat{y})dB_2(t), \end{aligned} \quad (2.33)$$

where  $f_1, f_2$  are defined in (2.1) and  $\hat{E} = (\hat{x}, \hat{y})$  is a generic equilibrium of the deterministic system. The stochastic system can be centered at its positive equilibrium point by the following change in variables:

$$u_1 = x - \hat{x}, \quad u_2 = y - \hat{y}. \quad (2.34)$$

The linearized counterpart of the nonlinear SDE system (2.33) about  $(\hat{x}, \hat{y})$  reads

$$\begin{aligned} du_1 &= \left[ u_1 \frac{\partial f_1(\hat{x}, \hat{y})}{\partial x} + u_2 \frac{\partial f_1(\hat{x}, \hat{y})}{\partial y} \right] dt + \sigma_1 u_1 dB_1(t), \\ du_2 &= \left[ u_1 \frac{\partial f_2(\hat{x}, \hat{y})}{\partial x} + u_2 \frac{\partial f_2(\hat{x}, \hat{y})}{\partial y} \right] dt + \sigma_2 u_2 dB_2(t). \end{aligned} \quad (2.35)$$

Note that the stability of the zero solution of (2.35) is equivalent to the stability property of the equilibrium solution  $(\hat{x}, \hat{y})$  of (2.33). The system (2.35) can be expressed as

$$du(t) = f(u(t))dt + g(u(t))dB(t), \quad (2.36)$$

where  $u(t) = [u_1, u_2]^T$  and

$$f(u(t)) = \begin{bmatrix} \frac{\partial f_1}{\partial x} u_1 + \frac{\partial f_1}{\partial y} u_2 \\ \frac{\partial f_2}{\partial x} u_1 + \frac{\partial f_2}{\partial y} u_2 \end{bmatrix}_{(\hat{x}, \hat{y})}, \quad g(u(t)) = \begin{bmatrix} \sigma_1 u_1 & 0 \\ 0 & \sigma_2 u_2 \end{bmatrix}, \quad dB(t) = \begin{bmatrix} dB_1(t) \\ dB_2(t) \end{bmatrix},$$

## 2. Phytoplankton-zooplankton interaction under environmental stochasticity: Survival, extinction and stability

---

and

$$\begin{aligned}\hat{A} &= \frac{\partial f_1}{\partial x} = r \frac{n}{n+h_n} - 2cx - \frac{pyh_a}{(x+h_a)^2}, & \hat{B} &= \frac{\partial f_1}{\partial y} = -\frac{px}{x+h_a}, & \hat{C} &= \frac{\partial f_2}{\partial x} = \frac{peyh_a}{(x+h_a)^2}, \\ \hat{D} &= \frac{\partial f_2}{\partial y} = \frac{pex}{x+h_a} - m - \frac{2Fyh_y^2}{(y^2+h_y^2)^2}.\end{aligned}\tag{2.37}$$

One can state the following theorem for the stability of different equilibrium points of the stochastic system (2.33).

**Theorem 2.5.1.** (I) *Equilibrium  $E^*$  of system (2.33) is asymptotically 2-stable or mean square stable if*

$$(i) \sigma_1 < \sqrt{-2\hat{A}}, \quad \hat{A} < 0, \quad (ii) \sigma_2 < \sqrt{-2\hat{D}}, \quad \hat{D} < 0,\tag{2.38}$$

where  $\hat{A}$ ,  $\hat{B}$ ,  $\hat{C}$  and  $\hat{D}$  are evaluated from (2.37) at the equilibrium point  $E^* = (x^*, y^*)$ . (II) *Equilibrium  $E^1$  of the system (2.33) are asymptotically 2-stable or mean square stable if they are deterministically stable and*

$$(i) \sigma_1 < \sqrt{-2\hat{A}}, \quad \hat{A} < 0, \quad (ii) \sigma_2 < \sqrt{-2\hat{D}}, \quad \hat{D} < 0,\tag{2.39}$$

where  $\hat{A}$ ,  $\hat{B}$ ,  $\hat{C}$  and  $\hat{D}$  are evaluated from (2.37) at the equilibrium point  $E_1 = (\hat{x}, 0)$ .

**Proof** We here make use of the following well-known theorem concerning the  $p$ -stability of the trivial solution of the stochastic system (2.36).

**Theorem 2.5.2.** (Afanasev et al. [1996]) *The trivial solution of system (2.36) is asymptotically  $p$ -stable in probability if there exists a function  $W(t, u(t)) \equiv W(t, u) \in C_2^0(\Delta)$  satisfying the inequalities*

$$K_1|u|^p \leq W(t, u) \leq K_2|u|^p,\tag{2.40}$$

$$L(W(t, u)) \leq -K_3|u|^p,\tag{2.41}$$

where  $\Delta = (t \geq t_0) \times \mathbb{R}^n$ ,  $t_0 \in \mathbb{R}^+$ ,  $K_i, i = 1, 2, 3$ , and  $p$  are positive constants. Then the trivial solution of (2.36) is exponentially  $p$ -stable for  $t \geq 0$ . Moreover, if  $p = 2$ , then the trivial solution is asymptotically mean square stable. The differential

## 2.5. Stochastic perturbation around an equilibrium point

---

operator  $L$  is defined as

$$L \equiv \frac{\partial}{\partial t} + (fu(t))^T \frac{\partial}{\partial u} + \frac{1}{2} \text{Tr} \left[ g^T \frac{\partial^2}{\partial u^2} g \right], \quad (2.42)$$

where  $f, g$  are given in (2.36),  $u(t) = \begin{pmatrix} u_1(t) \\ u_2(t) \end{pmatrix}$ ,  $T \equiv \text{Transpose}$  and  $\text{Tr} \equiv \text{Trace}$  of a matrix, respectively.

Moreover,

$$\frac{\partial W}{\partial u} = \begin{pmatrix} \frac{\partial W}{\partial u_1} \\ \frac{\partial W}{\partial u_2} \end{pmatrix}, \quad \frac{\partial^2 W}{\partial u^2} = \begin{pmatrix} \frac{\partial^2 W}{\partial u_1^2} & \frac{\partial^2 W}{\partial u_1 u_2} \\ \frac{\partial^2 W}{\partial u_2 u_1} & \frac{\partial^2 W}{\partial u_2^2} \end{pmatrix}. \quad (2.43)$$

Using Theorem 2.5.2, one can prove the following theorem concerning the stability of the zero solution of (2.36).

We define a Lyapunov function

$$V(t) = \frac{1}{2}(\omega_1 u_1^2 + \omega_2 u_2^2), \quad (2.44)$$

where  $\omega_1$  and  $\omega_2$  are positive real constants to be determined. One can express

$$V = \frac{1}{2} \begin{pmatrix} u_1 & u_2 \end{pmatrix} Q \begin{pmatrix} u_1 \\ u_2 \end{pmatrix}, \quad (2.45)$$

where

$$Q = \begin{pmatrix} \omega_1 & 0 \\ 0 & \omega_2 \end{pmatrix}.$$

Let  $\lambda_1(Q)$  and  $\lambda_2(Q)$  be the smallest and largest eigenvalues of  $Q$ , respectively, and then we have

$$\frac{1}{2} \lambda_1(Q)(u_1^2 + u_2^2) \leq V \leq \frac{1}{2} \lambda_2(Q)(u_1^2 + u_2^2). \quad (2.46)$$

Define  $K_1 = \frac{\lambda_1(Q)}{2}$  and  $K_2 = \frac{\lambda_2(Q)}{2}$  so that the inequality (2.40) is satisfied for  $p = 2$ , where  $|u|^2 = u_1^2 + u_2^2$ .

Again, since  $V$  does not depend on  $t$  explicitly, following (2.43), we have

$$\frac{\partial V}{\partial t} = 0, \quad \frac{\partial V}{\partial u} = \begin{pmatrix} \omega_1 u_1 \\ \omega_2 u_2 \end{pmatrix}, \quad \frac{\partial^2 V}{\partial u^2} = \begin{pmatrix} \omega_1 & 0 \\ 0 & \omega_2 \end{pmatrix}. \quad (2.47)$$



## 2. Phytoplankton-zooplankton interaction under environmental stochasticity: Survival, extinction and stability

---

From (2.42), we obtain

$$\begin{aligned}
 L(V(u)) &= \begin{pmatrix} \hat{A}u_1 + \hat{B}u_2 \\ \hat{C}u_1 + \hat{D}u_2 \end{pmatrix}^T \begin{pmatrix} \omega_1 u_1 \\ \omega_2 u_2 \end{pmatrix} + \frac{1}{2} \text{Tr} \begin{pmatrix} \sigma_1^2 u_1^2 \omega_1 & 0 \\ 0 & \sigma_2^2 u_2^2 \omega_2 \end{pmatrix} \\
 &= \left( \hat{A} + \frac{\sigma_1^2}{2} \right) \omega_1 u_1^2 + \left( \hat{D} + \frac{\sigma_2^2}{2} \right) \omega_2 u_2^2 + (\hat{B}\omega_1 + \hat{C}\omega_2) u_1 u_2 \\
 &= -u^T M u,
 \end{aligned} \tag{2.48}$$

where the symmetric matrix  $M$  is defined as

$$M = \begin{pmatrix} -\left( \hat{A} + \frac{\sigma_1^2}{2} \right) \omega_1 & -\frac{1}{2}(\hat{B}\omega_1 + \hat{C}\omega_2) \\ -\frac{1}{2}(\hat{B}\omega_1 + \hat{C}\omega_2) & -\left( \hat{D} + \frac{\sigma_2^2}{2} \right) \omega_2 \end{pmatrix}. \tag{2.49}$$

Now we choose  $\omega_1$  and  $\omega_2$  in such a manner that  $M$  becomes positive definite. In doing so, we will find some conditions so that all the principal minors of  $M$  become positive.

For the interior equilibrium point  $E^*(x^*, y^*)$ , we have  $\hat{A} = \frac{px^*y^*}{(x^*+h_a)^2} - cx^*$ ,  $\hat{B} = -\frac{px^*}{x^*+h_a} < 0$ ,  $\hat{C} = \frac{peh_a y^*}{(x^*+h_a)^2} > 0$ ,  $\hat{D} = \frac{Fy^*(y^{*2}-h_y^2)}{(y^{*2}+h_y^2)^2}$ . Since  $\hat{B}\hat{C} < 0$ , it is possible to choose suitable values of  $\omega_1$  and  $\omega_2$  so that  $M$  becomes positive definite. We select  $\omega_1 = -\frac{1}{\hat{B}}$  and  $\omega_2 = \frac{1}{\hat{C}}$ . Then the corresponding principal minors of  $M$  become  $m_{11} = -\left( \hat{A} + \frac{\sigma_1^2}{2} \right) \omega_1$  and  $m_{22} = \left( \hat{A} + \frac{\sigma_1^2}{2} \right) \left( \hat{D} + \frac{\sigma_2^2}{2} \right) \omega_1 \omega_2$ . Positivity of the first principal minor  $m_{11}$  forces  $\sigma_1 < \sqrt{-2\hat{A}}$  and  $\hat{A} < 0$ . Clearly, if  $\hat{D} < 0$ , then the second principal minor will be positive when  $\sigma_2 < \sqrt{-2\hat{D}}$ . Thus,  $M$  becomes positive definite if  $\sigma_1 < \sqrt{-2\hat{A}}$  and  $\sigma_2 < \sqrt{-2\hat{D}}$  with  $\hat{A} < 0$  and  $\hat{D} < 0$ .

For the axial equilibrium  $E_1 = (\hat{x}, 0)$ , we obtain  $\hat{A} = -\frac{rn}{n+h_n} < 0$ ,  $\hat{B} = -\frac{p\hat{x}}{\hat{x}+h_a} < 0$ ,  $\hat{C} = 0$ ,  $\hat{D} = \frac{pe\hat{x}}{\hat{x}+h_a} - m$ . Principal minors of  $M$  are  $m_{11} = -\left( \hat{A} + \frac{\sigma_1^2}{2} \right) \omega_1$  and  $m_{22} = \left( \hat{A} + \frac{\sigma_1^2}{2} \right) \left( \hat{D} + \frac{\sigma_2^2}{2} \right) \omega_1 \omega_2 - \frac{\hat{B}^2 \omega_1^2}{4}$ . One can easily observe that the first principal minor is positive if  $\sigma_1 < \sqrt{-2\hat{A}}$ . Since  $\left( \hat{A} + \frac{\sigma_1^2}{2} \right)$  is negative and  $\omega_1, \omega_2$  are chosen to be positive, we select  $\omega_1 = \frac{1}{\hat{B}^2}$  and  $\omega_2 = \frac{1}{\left( \hat{A} + \frac{\sigma_1^2}{2} \right) \left( \hat{D} + \frac{\sigma_2^2}{2} \right)}$ . Note that  $\omega_1$  is positive,

and  $\omega_2$  will be positive under the condition  $\sigma_2 < \sqrt{-2\hat{D}}$  with  $\hat{D} < 0$ . Hence the positivity of both principle minors imply the positive definiteness of  $M$  subject to the conditions  $\sigma_1 < \sqrt{-2\hat{A}}$ ,  $\sigma_2 < \sqrt{-2\hat{D}}$  with  $\hat{D} < 0$ ,  $\hat{A} < 0$ . Therefore, all eigenvalues of  $M$  becomes positive irrespective of the values of  $\hat{B}$  and  $\hat{C}$ . Hence, from (2.48), we

## 2.6. Numerical Simulations

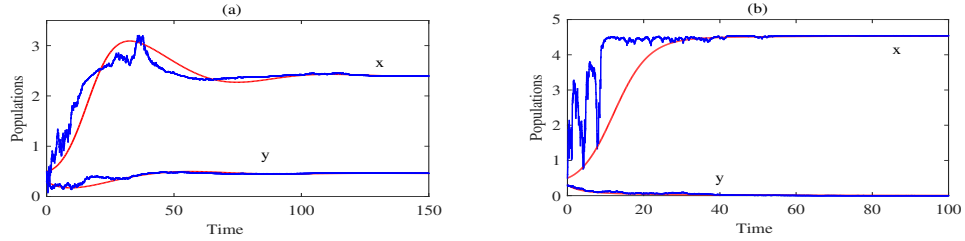


**Figure 2.9:** Time evolutions of the deterministic system (2.1) and stochastic system (2.33). (a) Trajectories of both the stochastic and deterministic systems converge to coexistence equilibrium  $E^*$  for  $\sigma_1 = 0.2$ ,  $\sigma_2 = 0.2$ . Parameters and initial values are as in Table 2.1 with  $r = 0.5$ ,  $e = 0.6$ . (b) All trajectories converges to predator-free equilibrium point  $E^1$  for  $\sigma_1 = 0.2$ ,  $\sigma_2 = 0.2$ . Parameters are as in Table 2.1 with  $r = 0.5$ ,  $e = 0.2$ .

have

$$L(V(u)) < -\lambda_1(M)|u|^2, \quad (2.50)$$

where  $\lambda_1(M)$  is the smallest eigenvalue of  $M$  and  $\lambda_1(M) > 0$ . Following Theorem 2.5.2, the zero solution of system (2.36) and consequently the equilibrium  $\hat{E}$  of (2.33) is asymptotically 2-stable or mean square stable if  $\sigma_1 < \sqrt{-2\hat{A}}$ ,  $\sigma_2 < \sqrt{-2\hat{D}}$ ,  $\hat{A} < 0$ ,  $\hat{D} < 0$ . Hence the theorem.

## 2.6 Numerical Simulations

For numerical simulations of system (2.33), we consider the parameter set as in Table 2.1 with  $r = 0.5$ ,  $e = 0.6$  so that the solution of the deterministic system (2.1) converges to the interior equilibrium point  $E^* = (2.3896, 0.4599)$ . For the stochastic system, after computing the bounds of the noise intensities  $\sqrt{-2\hat{A}} = 0.2608$  and  $\sqrt{-2\hat{D}} = 0.2306$ , we choose  $\sigma_1 = 0.2 (< \sqrt{-2\hat{A}})$ ,  $\sigma_2 = 0.2 (< \sqrt{-2\hat{D}})$  and plot the solution of the stochastic system (2.33) in Fig. 2.9(a) with the same initial value. Observe that the solution trajectories converge to the corresponding deterministic solution after some initial fluctuations. For the axial equilibrium point  $E^1(\hat{x}, 0)$ , we choose the same parameter set as in Table 2.1 with  $r = 0.5$ ,  $e = 0.2$  and fix  $\sigma_1 = 0.2 < \sqrt{-2\hat{A}} = 0.2345$  and  $\sigma_2 = 0.2 < \sqrt{-2\hat{D}} = 0.2045$ . Solutions of both the deterministic and stochastic systems (Fig. 2.9(b)) converge to the predator-free solution of the deterministic system. It is to be observed here that the phytoplankton population of the stochastic system oscillates significantly before converging to

## 2. Phytoplankton-zooplankton interaction under environmental stochasticity: Survival, extinction and stability

---

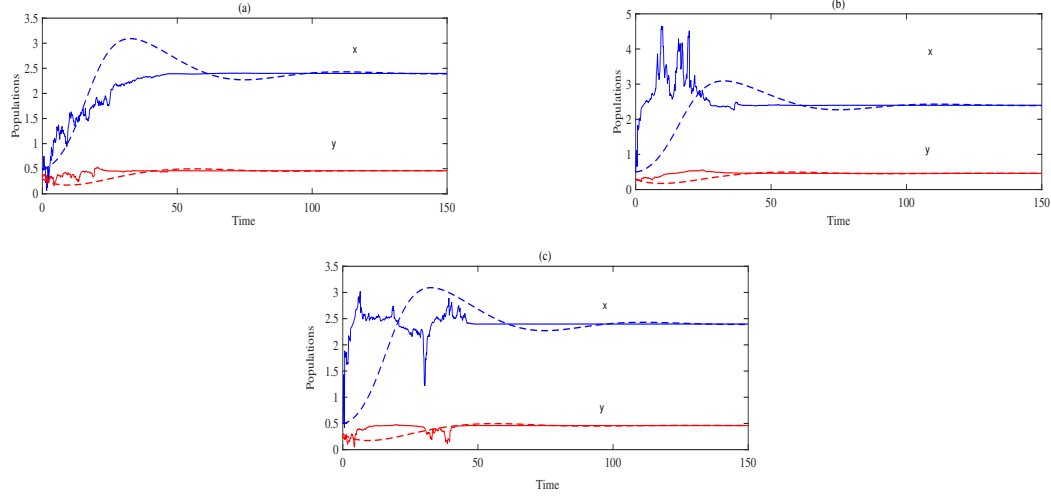


**Figure 2.10:** Comparison of solutions between the deterministic (dotted line) system (2.1) and stochastic (solid line) system (2.33) with higher noise intensities: (a)  $\sigma_1 = 0.2$ ,  $\sigma_2 = 0.6$ , (b)  $\sigma_1 = 0.6$ ,  $\sigma_2 = 0.2$ , (c)  $\sigma_1 = 0.6$ ,  $\sigma_2 = 0.6$ . Parameters are as in Table 2.1 with  $r = 0.5, e = 0.2$ .

its deterministic steady-state value, whereas the zooplankton population goes extinct simultaneously. One can compare Fig. 2.9(a) with the time series solutions given in Fig. 2.5 for the same parameter and initial values. In the first case, the stochastic solutions do not converge to its deterministic solution, but in the later case it does.

The mean square stability conditions prescribed in Theorem 2.5.1 are sufficient conditions, it says that if the noises do not exceed the given bounds, then the equilibrium point will definitely be mean square stable. It, however, does not say that the equilibrium will be unstable if the noise exceeds its bound. Therefore, we verified the mean square stability of the interior equilibrium point if either or both bounds of the noise cross the respective analytical bounds. If noise in the phytoplankton population is within its bound ( $\sigma_1 < 0.2608$ ) but the noise intensity in zooplankton population is significantly higher from its analytical bound ( $\sigma_2 > 0.2306$ ) then a considerable amount of fluctuation is observed in zooplankton population density but mild fluctuation is observed in phytoplankton (Fig. 2.10(a)). They, however, eventually coincide with the deterministic equilibrium density. Similar behaviour is observed (Fig. 2.10(b)) when the noise is very high in the  $x$  population, but noise in the  $y$  population is within the analytical bound. When both populations are subject to higher environmental noise, larger fluctuation is observed in both populations

## 2.7. A case study

---

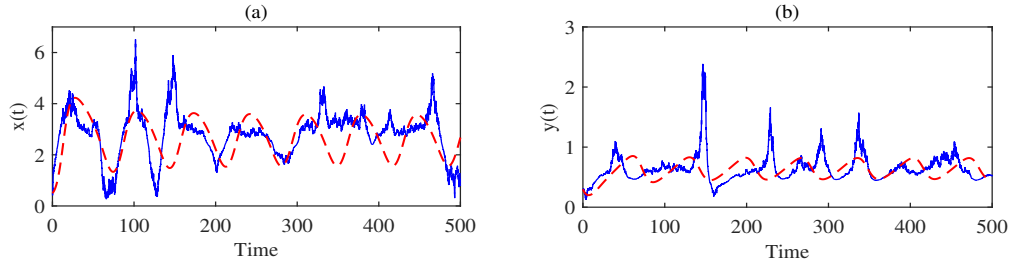


**Figure 2.11:** Phytoplankton and zooplankton populations both fluctuate simultaneously for  $e = 0.6$  and  $r = 0.61$ . Here the environmental forcing intensities are  $\sigma_1 = 0.2$  and  $\sigma_2 = 0.2$  and other parameters are as in Table 2.1. The deterministic solution is represented by the red broken line and the stochastic solution is represented by the blue solid line.

at initial stage, but the asymptotic nature remains the same with the deterministic counterpart. Thus, the long time behavior of the stochastic system is independent of the noise intensity. This result is consistent with the global stability result of the equilibrium  $E^*$  in the deterministic case. The only difference in the solution is observed at the initial stage of the solution. We also compare the solution's behavior of both the deterministic system (2.1) and stochastic system (2.33) when the parameter values show an unstable oscillatory behavior of the interior equilibrium for the deterministic system. Fig. 2.11 shows that the qualitative behaviors of both the deterministic and stochastic solutions are similar except some occasional higher peak values in the latter case. Fluctuations in the population density are however less here compared to the stochastic results of the system (2.5) given in Fig. 2.8 for the same parameter values.

## 2.7 A case study

In this section, we fit our stochastic model with a data set of 24 months on phytoplankton-zooplankton interaction in the Lake Trasimeno, Umbria, Italy. This lake is eutrophic, having abundant phytoplankton species mostly dominated by dinoflagellates, chlorophytes and cyanobacteria and various zooplankton species with cycloids and cladocera as dominant ones. The data set was taken from the study of Havens et al. [2009]. We here considered the recorded data given on a monthly basis from January 1991 to December 1992 (24 months). We first scaled the real data set in logarithmic scale and then compared the qualitative behavior of the actual dynam-

## 2. Phytoplankton-zooplankton interaction under environmental stochasticity: Survival, extinction and stability

---

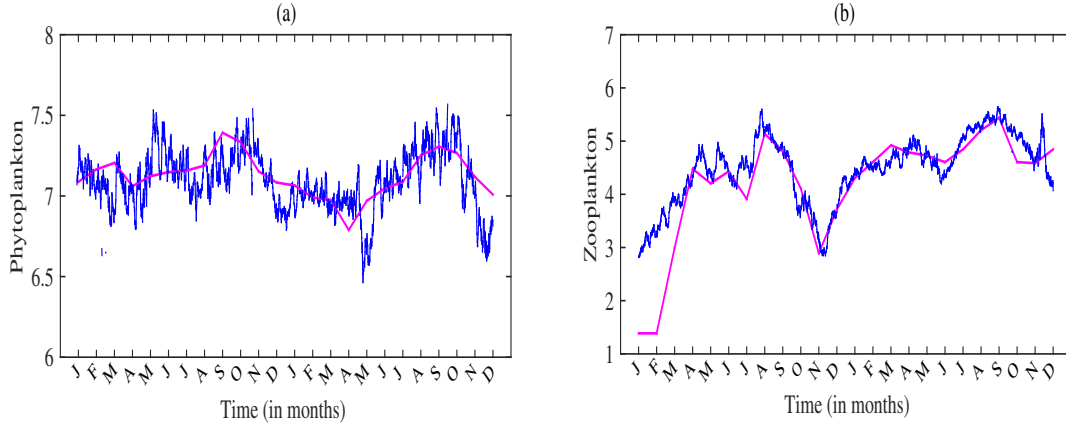


**Figure 2.12:** Field data of (a) phytoplankton population and (b) zooplankton population are plotted with red line and the simulation results of the stochastic model (2.5) are represented by blue solid line.

ics of plankton species with our model simulated dynamics. Using the Fminsearch optimization toolbox in Matlab, we find the best fit parameters. The best-fit parameter values using Fminsearch optimization toolbox for the Lake Trasimeno are  $r = 1.10347, n = 1.59211, h_n = 0.61218, c = 0.07493, p = 0.51678, h_a = 1.33862, e = 0.24659, m = 0.04273, F = 0.25373, h_z = 0.78108$ . In the left panel of Fig. 2.12, we plotted the real time series (red colour) and simulated time series (blue color) and the same for zooplankton are plotted in the right panel. It is reported that phytoplankton biomass becomes maximum during autumn in every sampling year (Reynolds [2006]). From the simulated and original time series, one can see that our stochastic solution can capture the seasonal fluctuations of phytoplankton with the coefficient of determination  $R^2 = 0.5722$ . Zooplankton species biomass becomes higher especially in winter or spring (Reynolds [2006]) and can be seen from the field data plot in right panel Fig. 2.12b. It is notable that our stochastic model (2.5) can capture this seasonal variability with the coefficient of determination  $R^2 = 0.7989$ . Thus, our stochastic model can reproduce the quantitative and qualitative behaviour of the real system with seasonal fluctuations.

## 2.8 Discussion

Acknowledging the limitations of a deterministic model, we have extended here the minimal deterministic model of phytoplankton-zooplankton interaction to its stochastic version following two approaches. Since environmental fluctuations may affect the

## 2.8. Discussion

---

birth rate and death rate of a species, we have replaced these two parameters of the deterministic system by their respective average values plus an error term represented by a white noise. The Gaussian white noise has been theoretically preferred to model environmental fluctuations as it is very irregular in nature and thus a good approximation to rapidly fluctuating phenomena (Jonsson and Wennergren [2019]). In the second case, we constructed a stochastic model corresponding to the same deterministic model by adding stochastic perturbations proportional to the distances of state variables from their respective equilibrium values. An obvious difference between these two stochastic models is that there is no equilibrium point in the first system and the second system has the same equilibrium point as in the case of the deterministic system. The objective is to understand how environmental noise affects the deterministic system dynamics and how different types of stochasticities affect differently when applied to an identical system.

The deterministic model considered here was proposed by Scheffer [1991] to study the effect of nutrient and fish predation on algal biomass through numerical simulations. We here first present briefly the stability results of different equilibrium points and show the existence of Hopf bifurcation that causes periodic oscillations in the system populations. However, there will be no oscillation and both planktons will coexist in a stable state, implying the global stability of the coexistence equilibrium ( $E^*$ ), if the equilibrium zooplankton density is not too high.

For the stochastic model (2.5) with parameter noise, we established a set of sufficient conditions for weak & strong persistence as well as non-persistence in the mean for both plankton species. We observed that the environmental forcing intensities primarily act as a regulatory mechanism behind the survival and extinction of both plankton species, and this analytical finding have been substantiated through numerical simulations. We also investigated the stochastic stability of the model (2.5). It is worthy to mention that the noise-induced stochastic system (2.5) lacks of steady state value. We, therefore, examined the probabilistic 'smoke cloud' (Fig. 2.13 (a)) around the deterministic steady state. It shows that species densities are mostly concentrated in a neighbourhood of the deterministic equilibrium value (red point) if the noise intensity is low but the population density sparse and is distributed over a larger area (Fig. 2.13 (b)) around the deterministic equilibrium value if the noise intensity is higher.

It may be recalled that the stochastic model (2.33) has the same equilibrium points as in the corresponding deterministic model (2.1). For this system, we per-

## 2. Phytoplankton-zooplankton interaction under environmental stochasticity: Survival, extinction and stability

---

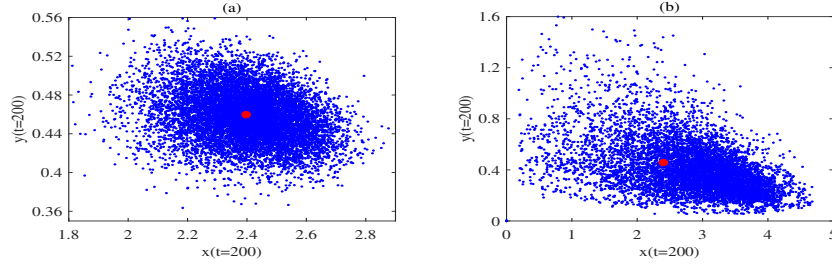


**Figure 2.13:** Probabilistic smoke cloud of phytoplankton and zooplankton populations of system (2.5) around the deterministic steady state (red dot) in both figures. (a) For  $\sigma_1 = 0.01$ ,  $\sigma_2 = 0.01$ , (b) for  $\sigma_1 = 0.2$ ,  $\sigma_2 = 0.2$ .

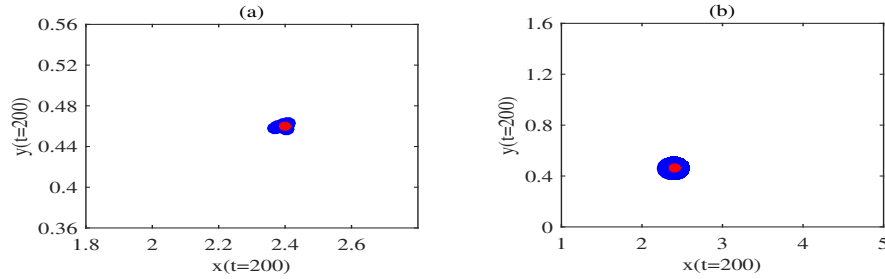


**Figure 2.14:** Probabilistic smoke cloud of phytoplankton and zooplankton populations of the system (2.33) around the deterministic steady state (red dot) in both figures. (a) For  $\sigma_1 = 0.01$ ,  $\sigma_2 = 0.01$ , (b) for  $\sigma_1 = 0.2$ ,  $\sigma_2 = 0.2$ .

formed the stability analysis by defining a suitable Lyapunov function and showed that the system (2.33) is asymptotically mean square stable if the forcing intensities are less than some threshold value. Even if the noise exceeds the limit, the stability result does not change (Fig. 2.10). Our simulation experiments showed that the system populations fluctuate considerably at the initial stage, but their asymptotic behavior remains same with the deterministic counterpart. In this case, a concentrated probabilistic 'smoke cloud' (Fig. 2.14) converges to the deterministic steady state value. It is interesting to note that either zooplankton or both phytoplankton and zooplankton can go to extinction (Figs. 2.6, 2.7) in the parameter noise-induced stochastic model (2.5) depending on the intensity of environmental noise even when the deterministic system is stable. Both the phytoplankton and zooplankton (prey and predator, respectively) can not go to extinction simultaneously (i.e.,  $(0, 0)$  equilibrium is unstable) under any parametric restriction in the deterministic system, however, parameter noise can do it in the stochastic system (see Fig. 2.6). Thus, stochasticity makes an unstable equilibrium of the deterministic system stable and

## 2.8. Discussion

---

the species persistency largely depends on the environmental noise. Data analysis in the aquatic regions has also found fluctuations in plankton populations due to different changes in climate ([Rasconi et al. \[2017\]](#), [Benedetti et al. \[2019\]](#)). A data set of 24 months on phytoplankton-zooplankton interaction in Lake Trasimeno, Umbria, Italy, also shows variation in the count of plankton species with seasonal peaks of phytoplankton and zooplankton. We fit our stochastic model with the data and show that our simulated dynamics well fit the actual dynamics of phytoplankton and zooplankton with seasonal variation.

The environmental forcing intensities primarily act as a regulatory mechanism behind the survival and extinction of phytoplankton and zooplankton species. Species densities are concentrated mainly in a neighbourhood of the deterministic equilibrium value if the noise intensity is low, but the population density is sparse over a larger area if the noise intensity is higher. A stochastic system exhibits more realistic dynamics, which a deterministic system fails to show. Different types of stochasticities, however, affected the dynamics differently when applied to the same deterministic system.

In the next chapter, we analyze a stochastic SIS epidemic model, where the infection spreads through two modes: (i) horizontal mode, where transmission of disease occurs from one infected individual to another susceptible individual and (ii) vertical mode, where the infection spreads through birth. Assuming the uncertainty in the infection transmission coefficient, we explore disease persistency and eradication conditions.





## Chapter 3

# Persistence and extinction of infection in stochastic SIS host-parasite epidemic model with horizontal and imperfect vertical transmissions<sup>2</sup>

### 3.1 Introduction

The transmission of disease from one infected individual to another susceptible individual is a significant issue, and the persistence of parasites, as well as their virulence, largely depend on this transmission mechanism ([Lipsitch et al. \[1996\]](#), [Chen et al. \[2006\]](#), [Ewald et al. \[1994\]](#), [Clayton and Tompkins \[1994\]](#)). Horizontal and vertical transmissions are two utterly distinct disease transmission modes that are usually followed by different pathogens. Here, we consider a homogeneous mixture of susceptible and infected populations, where a disease spreads following horizontal and vertical transmissions. In the case of horizontal transmission, the infection spreads through contact. On the contrary, vertical transmission occurs through birth only. Though many parasites spread disease through multiple pathways, horizontal transmission is the predominant infection spreading mode ([Antonovics et al. \[2017\]](#)). Infected hosts can give birth to susceptible and infected individuals so that the ver-

---

<sup>2</sup>*The bulk of this chapter has been communicated in a peer reviewed journal.*

### 3. Persistence and extinction of infection in stochastic SIS host-parasite epidemic model with horizontal and imperfect vertical transmissions

---

tical transmission may be imperfect (Lipsitch et al. [1996]). It is mentionable that an SIS model is more realistic compared to its SI counterpart because an infected individual may recover from the infection due to its immune mechanism or due to some external measures like using antibiotics, pesticides or fungicides (Hua and Reylea [2014], Djéballi and Belhassen [2010]). We thus focus on an SIS epidemic model with uncertainty in the horizontal disease transmission term. The main objective is to study the SIS stochastic epidemic model and prescribe the feasible disease eradication and persistence criteria. We also determine the local and global stabilities of the corresponding deterministic system to compare its results with the stochastic model. Another purpose of this study is to determine a set of conditions under which the deterministic solution becomes a limiting case of the stochastic solution. To know whether the disease extinction time follows any law is another intention of this work. Parasites evolve to increase their fitness. It is experimentally demonstrated that the relative fecundity of parasites plays a significant role in the persistence of infection and survival of both the hosts and parasites (Sorensen and Minchella [1998], Ebert et al. [2000], Tompkins and Begon [1999]). One way to measure such fitness of the parasites is to determine the extinction time of the infected host. We intend to know how the relative fecundity and the disease transmissibility jointly affect the parasite fitness.

The rest of the chapter is organized as follows. The SIS epidemic model to be investigated is presented in the immediate next Section 3.2. A brief study of the deterministic model is presented in Section 3.3. The stochastic system analysis is given in Section 3.4. Numerical illustrations of the analytical results are presented in Section 3.5. The chapter ends with a discussion in Section 3.6.

## 3.2 The model

Assume that the host population is divided into susceptible and infected classes in the presence of some parasitic infection. Let the infected hosts give birth to susceptible and infected individuals at the rates  $b_I$  and  $e$ , respectively. The birth rate of the susceptible host is assumed to be  $b_S$ . Parasites may affect the fecundity and morbidity rates of their host population (Holmes [1972], Lafferty and Morris [1996]). It is therefore assumed that the death rate of infected hosts is never less than that of susceptible hosts, i.e.,  $u_I \geq u_S$ , and the birth rate of susceptible hosts ( $b_S$ ) is higher

### 3.2. The model

---

than the total birth rate of infected hosts, i.e.,  $b_S \geq b_I + e$ . An infected individual may recover from the infection and join the susceptible class to be reinfected. If  $S(t)$  and  $I(t)$  are the densities of the susceptible and infected hosts at any time  $t$  and  $\beta$  is the disease transmission coefficient, then the SIS epidemic model can be represented by the following coupled nonlinear differential equations:

$$\begin{aligned}\frac{dS}{dt} &= b_S S \left[1 - \frac{(S+I)}{K}\right] - u_S S - \beta SI + eI \left[1 - \frac{(S+I)}{K}\right] + \mu I, \\ \frac{dI}{dt} &= b_I I \left[1 - \frac{(S+I)}{K}\right] - u_I I + \beta SI - \mu I.\end{aligned}\quad (3.1)$$

Here  $K$  is the environment's carrying capacity, and  $\mu$  is the recovery rate of infected individuals.

Horizontal disease transmission may occur directly through the effective contact between a susceptible and an infective, or indirectly through the environment and intermediate hosts (Grassly and Fraser [2008]). Such transmissions are primarily unknown and random. Assuming that the disease transmission process is random and directly affects the horizontal disease transmission parameter  $\beta$ , we replace the parameter  $\beta \rightarrow \beta + d\xi_t$ , where  $\xi(t)_{t \geq 0}$  is standard Wiener process defined on a complete probability space  $(\Omega, F, P)$  with a filtration  $\{F_t\}_{t \in \mathbb{R}^+}$  and satisfies  $\langle d\xi(t) \rangle = 0$ ,  $\langle d\xi(t), d\xi(t') \rangle = \delta(t - t')$ , where  $\delta$  is the Dirac delta function. It induces a multiplicative noise and thus avoids the negativity of the solution due to initial negative fluctuations. Zero becomes a lower bound in this case, even if the initial population size is small and there is a negative fluctuation of noise (Mikhailov and Loskutov [2012]). Under this assumption, the deterministic SIS epidemic model (3.1) with imperfect vertical transmission reads

$$\begin{aligned}dS &= \left[ b_S S \left\{1 - \frac{S+I}{K}\right\} - u_S S - \beta SI + eI \left\{1 - \frac{S+I}{K}\right\} + \mu I \right] dt - \sigma SI d\xi_t, \\ dI &= \left[ b_I I \left\{1 - \frac{S+I}{K}\right\} - u_I I + \beta SI - \mu I \right] dt + \sigma SI d\xi_t,\end{aligned}\quad (3.2)$$

where  $\sigma^2$  is a real constant that measures the intensity of the noise. Recently, Gao et al. [2019] analyzed a stochastic SIS epidemic model, where the infection spreads only through horizontal transmission. They considered the constant birth rate of the susceptible population and a nonlinear incidence rate to determine the threshold dynamics of extinction and persistence of disease. A stochastic SIS epidemic model

### **3. Persistence and extinction of infection in stochastic SIS host-parasite epidemic model with horizontal and imperfect vertical transmissions**

with constant birth of susceptible population and no vertical disease transmission was considered in [Lan et al. \[2019\]](#). It is shown that if the stochastic basic reproduction number is less than unity with some other restrictions, eradication of the disease from the system is possible. They also proved the existence criteria of the stationary distribution. A simple stochastic SIR model with horizontal and vertical transmissions was considered in [Miao et al. \[2018\]](#). This model, however, considered the linear birth rate of all populations, contrary to the density-dependent birth considered in (3.2). It is shown that considerable noise is conducive to controlling the infection. [Li et al. \[2015\]](#) analyzed a SIRS epidemic model with nonlinear incidence rate and environmental stochasticity. The model considers the only horizontal spread of infection with density-independent growth of susceptible populations. A set of sufficient conditions for the disease extinction and persistence is provided, and simulation results are presented to illustrate the results. We here analyze the stochastic system (3.2), which considers density-dependent growth of host populations and horizontal as well as imperfect vertical transmissions of infection. We provide the local and global dynamics of the corresponding deterministic system with respect to the deterministic basic reproduction number. The persistence and extinction conditions of disease for the stochastic system are derived. The stochastic process's ergodicity and the stationary distribution criteria are proved. We present different simulation results to illustrate the theoretical results and provide insights into parasites' fitness.

### **3.3 Study of the deterministic model**

The deterministic system (3.1) considers a recovery term of the infected host in the model studied in [Lipsitch et al. \[1995\]](#). Local stability of different equilibrium points of the system (3.1) with no recovery (i.e.,  $\mu = 0$ ) has already been proved ([Lipsitch et al. \[1995\]](#), [Saha and Bairagi \[2018\]](#)). Here we start by recalling (without proof) the local dynamics of the system (3.1), where recovery is considered, and then provide a new global stability result.

#### **Basic reproduction number**

The basic reproductive number in epidemics is an important measure and plays a critical role in eradicating infection. It is defined as the number of new cases arising from a single infected individual when introduced into a group of susceptible ([Anderson](#)

### 3.3. Study of the deterministic model

---

et al. [1992]). If the basic reproduction number is less than unity, then the disease cannot establish in the host population, and in the opposite case, the disease can invade the population. We measure the basic reproduction number of the deterministic system (3.1) by the next-generation matrix (Van den Driessche and Watmough [2002]).

**Proposition 3.3.1.** *The basic reproduction number of the deterministic system (3.1),  $R_0^D$ , is*

$$R_0^D = \frac{b_I u_S + \beta \hat{S} b_S}{b_S (u_I + \mu)}. \quad (3.3)$$

*Proof.* In absence of infection, the susceptible population has equilibrium density  $\hat{S} = K \left(1 - \frac{u_S}{b_S}\right)$ . The Jacobian matrix of the epidemic model (3.1) evaluated at  $(\hat{S}, 0)$  is

$$J_{11} = \begin{pmatrix} b_S - \frac{2b_S \hat{S}}{K} - u_S & e + \mu - \frac{b_S \hat{S}}{K} - \frac{e \hat{S}}{K} - \beta \hat{S} \\ 0 & b_I \left(1 - \frac{\hat{S}}{K}\right) + \beta \hat{S} - (u_I + \mu) \end{pmatrix}. \quad (3.4)$$

The sub-matrix of  $J_{11}$  associated with the infectious compartments is a one-by-one matrix

$$J_{12} = b_I \left(1 - \frac{\hat{S}}{K}\right) + \beta \hat{S} - (u_I + \mu) = F - V,$$

where  $F = b_I \left(1 - \frac{\hat{S}}{K}\right) + \beta \hat{S}$  and  $V = (u_I + \mu)$ . The next generation matrix is then given by

$$FV^{-1} = \frac{1}{u_I + \mu} \left[ b_I \left(1 - \frac{\hat{S}}{K}\right) + \beta \hat{S} \right] = \frac{b_I u_S}{b_S (u_I + \mu)} + \frac{\beta \hat{S}}{u_I + \mu} = \frac{b_I u_S + \beta \hat{S} b_S}{b_S (u_I + \mu)}.$$

The basic reproduction number of the system (3.1) is the spectral radius of the scalar matrix  $FV^{-1}$  (Van den Driessche and Watmough [2002]) and is thus

$$R_0^D = \rho(FV^{-1}) = \frac{b_I u_S + \beta \hat{S} b_S}{b_S (u_I + \mu)}.$$

□

As mentioned earlier, infection will die out if the basic reproduction number is less than 1. A straightforward way to reduce the basic reproduction number is to decrease the transmission coefficient. It is noticeable that the basic reproduction number is

### 3. Persistence and extinction of infection in stochastic SIS host-parasite epidemic model with horizontal and imperfect vertical transmissions

directly proportional to  $\beta$ . The parameter  $\mu$  can also reduce the value of the basic reproduction number, but it is inversely proportional.

#### Local and global stability of the equilibrium points

From a biological point of view and for the model's applicability, the populations should be non-negative for all future time, and the deterministic model solutions should stay bounded. For this, one can easily prove the following result in the line of [Bairagi and Adak \[2015\]](#).

**Proposition 3.3.2.** *Solutions of the system (3.1) are positively invariant and uniformly bounded in the domain  $G \subset \mathbb{R}_+^2$ , where  $G = \left\{ (S, I) \in \mathbb{R}_+^2 \mid 0 \leq S(t), I(t) \leq K \right\}$ .*

The local stability results (without proof) may be summarized as follows.

**Theorem 3.3.3.** *The deterministic SIS model (3.1) has three non-negative equilibrium points.*

- (i) *The trivial equilibrium point  $E_0^{(1)} = (0, 0)$  is locally asymptotically stable if  $b_S < u_S$  and  $b_I < u_I + \mu$ .*
- (ii) *The disease-free equilibrium point  $E_1^{(1)} = (\hat{S}, 0)$ , where  $\hat{S} = K(1 - \frac{u_S}{b_S})$ ,  $u_S < b_S$ , is locally asymptotically stable if  $R_0^D < 1$ .*
- (iii) *The infected (interior) equilibrium point  $E_*^{(1)} = (S^*, I^*)$ , having equilibrium densities  $S^* = \frac{-B}{2A} + \frac{1}{2A}\sqrt{B^2 - 4AC}$  &  $I^* = \frac{1}{b_I}[K(b_I - u_I - \mu) + (\beta K - b_I)S^*]$ , exists and becomes locally asymptotically stable under the parametric restrictions*

$$b_S \geq b_I + e, \mu + u_I < b_I < \beta K \text{ and } R_0^D > 1,$$

$$\text{where } A = \frac{\beta K}{b_I^2} [\beta K(b_I + e) + b_I(b_S - b_I - e)], B = -K(b_S - u_S) + \frac{K}{b_I}[(b_I - u_I - \mu)(K\beta + b_S + e) - (e + \mu)(\beta K - b_I)] + \frac{2K\epsilon(\beta K - b_I)}{b_I^2}(b_I - u_I - \mu), C = -\frac{K^2}{b_I^2}[b_I - u_I - \mu][\mu(b_I + e) + eu_I].$$

Biologically, all populations go to extinction if the birth rate of susceptible hosts is less than its death rate and the ensemble clearance rate of infected hosts exceeds its birth rate. Noticeably, the stability of the trivial equilibrium ceases the existence of

### 3.3. Study of the deterministic model

---

the other two equilibrium points. However, the disease-free equilibrium point exists if the birth rate of susceptible hosts is larger than its death rate and becomes stable if the basic reproduction number is less than unity. It is worth mentioning that local stability criteria of  $E_1^{(1)}$  makes  $E_*^{(1)}$  and  $E_0^{(1)}$  unstable. The infected equilibrium  $E_*^{(1)}$  exists, and both populations persist in a stable state if the birth rate of susceptible hosts is higher than the total birth rate of infected hosts, i.e.,  $b_S \geq b_I + e$ . In addition, the vertical birth rate is higher than its ensemble clearance rate of infected hosts but lower than the maximum disease transmission rate through horizontal transmission, i.e.,  $\mu + u_I < b_I < \beta K$  and the basic reproduction number is greater than unity. Thus, the basic reproduction number  $R_0^{(D)}$  must be less than unity to make the system disease-free, and it is achievable through the parameter  $\mu$ , which is responsible for creating a SI system into an SIS one.

Local asymptotic stability guarantees that the solutions will eventually arrive at equilibrium if they start close to the equilibrium value. However, if the considered initial values are far away from the equilibrium, they may not arrive at the equilibrium point. To assure that the equilibrium point's stability does not depend on the initial values, it is necessary to show its global stability. We prove that the local stability results of different equilibrium points are sufficient for their global stability.

**Theorem 3.3.4.** *Each equilibrium of the deterministic model (3.1) is locally and globally asymptotically stable throughout the domain  $G \subset \mathbb{R}_+^2$ , unless the solution starts from the other two equilibrium points.*

*Proof.* To prove it, we first show that there is no periodic orbit in  $D \subset G$ , where  $D = \{(S, I) : 0 < S < K, 0 < I < K\}$ . For this, we define a continuously differentiable function  $B(S, I)$  in  $D$ , where  $B(S, I) = 1/(SI)$ . Defining  $F = (F_1, F_2)$ , where  $F_1 = b_S \left\{ \left(1 - \frac{S+I}{K}\right) - u_S - \beta I \right\} S + eI \left[1 - \frac{S+I}{K}\right] + \mu I$ ,  $F_2 = b_I I \left[1 - \frac{S+I}{K}\right] - u_I I + \beta SI - \mu I$ , and noting that  $I \leq K$  by Proposition 3.3.2, one then have

$$\operatorname{div}(BF) = \frac{\partial(BF_1)}{\partial S} + \frac{\partial(BF_2)}{\partial I} = -\frac{b_S}{KI} - \frac{b_I}{KS} - \frac{\mu}{S^2} + \frac{e}{S^2} \frac{(I-K)}{K} < 0. \quad (3.5)$$

Hence, by Bendixson-Dulac criteria (Kot [2001]), the system (3.1) has no periodic orbit in the interior of  $D$ . Since  $E_0^{(1)}$  is the only stable equilibrium, there is no periodic orbit in the domain of definition. Therefore  $E_0^{(1)}$  is globally asymptotically stable whenever it is locally asymptotically stable. Similar arguments prove that local stability criteria of  $E_1^{(1)}$  and  $E_*^{(1)}$  also assure their global stability if the solutions are



### 3. Persistence and extinction of infection in stochastic SIS host-parasite epidemic model with horizontal and imperfect vertical transmissions

not started from the equilibrium point  $E_*^{(1)}$  for the first case and  $E_1^{(1)}$  for the second case.  $\square$

## 3.4 Study of the stochastic model

In this section, we present our main results of the SIS epidemic model with both modes of disease transmission, which have not been studied earlier. We will use the Lyapunov analysis method, Ito's formula, Chebyshev's inequality, the law of large number, along with the other standard techniques to obtain various results for our system (3.2).

Populations explosion may occur in the case of a multiplicative noise (Valenti et al. [2004a]). It is, therefore, necessary to show that such an explosion does not happen here. Also, biological populations should always be nonnegative. For this, we prove the global existence, positivity and boundedness of the stochastic solutions in the following.

**Proposition 3.4.1.** *For any initial value  $(S(0), I(0)) \in \mathbb{R}_+^2$ , there exists a unique solution  $(S(t), I(t))$  of the system (3.2) for  $t \geq 0$  and the solution remains in  $\mathbb{R}_+^2$  with probability 1.*

*Proof.* Since the coefficients of system (3.2) satisfy the local Lipschitz conditions, there is a unique positive local solution on  $[0, \nu_e)$ , where  $\nu_e$  is the explosion time (Mao [2007]). We show that this solution is global, meaning  $\nu_e = \infty$ . One gets from (3.2)

$$\begin{aligned} \frac{d}{dt}(S + I) &= b_S S \left(1 - \frac{S + I}{K}\right) + eI \left(1 - \frac{S + I}{K}\right) + b_I I \left(1 - \frac{S + I}{K}\right) - u_S S - u_I I \\ &\leq \{b_S S + eI + b_I I\} \left(1 - \frac{S + I}{K}\right) - u_S S - u_I I \\ &\leq \{b_S S + (b_I + e)I\} \left(1 - \frac{S + I}{K}\right) \\ &\leq b_S(S + I) - \frac{b_S}{K}(S + I)^2 \quad [\because b_S \geq b_I + e], \end{aligned}$$

giving

$$0 \leq \lim_{t \rightarrow \infty} (S(t) + I(t)) \leq K, \implies 0 \leq \lim_{t \rightarrow \infty} S(t), \lim_{t \rightarrow \infty} I(t) \leq K.$$

Let  $m_0 > 0$  be sufficiently large so that  $S(0), I(0)$  lie within the interval  $[\frac{1}{m_0}, m_0]$ . For

### 3.4. Study of the stochastic model

---

any integer  $m \geq m_0$ , define a sequence of stopping times by

$$\nu_m = \inf \left\{ t \in [0, \nu_e] : S(t) \notin \left( \frac{1}{m}, m \right) \text{ or } I(t) \notin \left( \frac{1}{m}, m \right) \right\},$$

where we set  $\inf \Phi = \infty$  ( $\Phi$  represents the empty set). Since  $\nu_m$  is non-decreasing as  $m \rightarrow \infty$ , one gets  $\nu_\infty = \lim_{m \rightarrow \infty} \nu_m$ . Then  $\nu_\infty \leq \nu_e$  almost surely (a.s.). Now, we prove that  $\nu_\infty = \infty$  a.s. If this statement is violated, then there exists  $M > 0$  and  $\delta \in (0, 1)$  such that  $P\{\nu_\infty \leq M\} > \delta$ . Thus, there is an integer  $m_1 \geq m_0$  such that

$$P\{\nu_m \leq M\} \geq \delta \quad \forall m \geq m_1. \quad (3.6)$$

Define a  $C^2$  function  $V : \mathbb{R}_+^2 \rightarrow \mathbb{R}_+$  by

$$V(S, I) = (S - 1 - \log S) + (I - 1 - \log I).$$

Using Ito's formula, we have

$$\begin{aligned} dV(S, I) &= \left(1 - \frac{1}{S}\right) \left[ b_S S \left(1 - \frac{S+I}{K}\right) - u_S S - \beta SI + eI \left(1 - \frac{S+I}{K}\right) + \mu I \right] dt \\ &\quad + \frac{1}{2} \sigma^2 I^2 dt + \frac{1}{2} \sigma^2 S^2 dt + \left(1 - \frac{1}{I}\right) \left[ b_I I \left(1 - \frac{S+I}{K}\right) - u_I I + \beta SI - \mu I \right] dt \\ &\quad - \sigma \left(1 - \frac{1}{S}\right) SI d\xi(t) + \sigma \left(1 - \frac{1}{I}\right) SI d\xi(t) \\ &\leq \left[ (u_S + u_I + \mu) + (b_S + b_I + e + \beta)K + \sigma^2 K^2 \right] dt + \sigma(I - S) d\xi(t). \end{aligned} \quad (3.7)$$

Let  $U = (u_S + u_I + \mu) + (b_S + b_I + e + \beta)K + \sigma^2 K^2$ . Integrating both sides of (3.7) from 0 to  $\nu_m \wedge M$ , one gets

$$\int_0^{\nu_m \wedge M} dV(S(u), I(u)) \leq \int_0^{\nu_m \wedge M} U du + \int_0^{\nu_m \wedge M} (\sigma S d\xi_1(u) + \sigma I d\xi_2(u)). \quad (3.8)$$

Expectation in both sides yields

$$\mathbb{E}(V(S(\nu_m \wedge M), I(\nu_m \wedge M))) \leq V(S(0), I(0)) + UM.$$

Set  $G_m = \{\nu_m \leq M\}$  for  $m \geq m_1$  and from (3.6), we have  $\mathbb{P}(G_m) \geq \delta$ . For every  $\tau \in G_m$ ,  $S(\nu_m, \tau)$ ,  $I(\nu_m, \tau)$  are equal to  $m$  or  $\frac{1}{m}$ , implying that  $V(S(\nu_m, \tau), I(\nu_m, \tau))$

### 3. Persistence and extinction of infection in stochastic SIS host-parasite epidemic model with horizontal and imperfect vertical transmissions

---

is no less than  $\min \{m - 1 - \ln(m), 1/m - 1 - \ln(1/m)\}$ . Therefore, we have

$$V(S(0), I(0)) + UM \geq \mathbb{E} (1_{G_m(\tau)} V(S(\nu_m), I(\nu_m))) \geq \delta \min \left\{ m - 1 - \ln m, \frac{1}{m} - 1 - \ln \frac{1}{m} \right\}, \quad (3.9)$$

where  $1_{G_m(\tau)}$  is the indicator function of  $G_m$ . Then  $m \rightarrow \infty$  leads to the contradiction

$$\infty = V(S(0), I(0)) + UM < \infty.$$

Therefore,  $\nu_\infty = \infty$  a.s. This completes the proof.  $\square$

**Proposition 3.4.2.** *Solutions of the system (3.2) are stochastically bounded on any time interval for any initial value  $(S(0), I(0)) \in \mathbb{R}_+^2$ .*

*Proof.* From equation (3.2), we have

$$\begin{aligned} d(S + I) &= b_S S \left(1 - \frac{S + I}{K}\right) + (b_I + e)I \left(1 - \frac{S + I}{K}\right) - u_S S - u_I I \\ &\geq M(S + I) \left(1 - \frac{S + I}{K}\right) - N(S + I), \end{aligned} \quad (3.10)$$

where  $M = \min \{b_S, b_I + e\}$ ,  $N = \min \{u_S, u_I\}$

$$= (M - N)(S + I) - \frac{M}{K}(S + I)^2.$$

Therefore,  $\lim_{t \rightarrow \infty} (S + I) \geq \frac{K}{M}(M - N) = \bar{L}$  (say).

Define the function

$$W(S, I) = e^t (S^\theta + I^\theta) = e^t U(S, I),$$

for  $(S, I) \in \mathbb{R}_+^2$ ,  $\theta > 1$  and  $U(S, I) = S^\theta + I^\theta$ . By Ito's formula, we have

$$\begin{aligned} dW(S, I) &= e^t \left[ \theta S^{\theta-1} \left( b_S S \left(1 - \frac{S + I}{K}\right) - u_S S - \beta SI + eI \left(1 - \frac{S + I}{K}\right) + \mu I \right) \right. \\ &\quad \left. + \theta I^{\theta-1} \left( b_I I \left(1 - \frac{S + I}{K}\right) - u_I I + \beta SI - \mu I \right) \right. \\ &\quad \left. + \frac{\theta(\theta - 1)}{2} \left( \sigma^2 S^\theta I^2 + \sigma^2 I^\theta S^2 \right) \right] dt + e^t \theta \left[ -\sigma S^\theta I d\xi(t) + \sigma I^\theta S d\xi(t) \right] \\ &\leq e^t \left[ \theta K^{\theta-1} (b_S + e + \mu) K + \theta K^{\theta-1} (b_I + \beta K) K + \theta(\theta - 1) \sigma^2 K^{\theta+2} \right] dt \end{aligned}$$

### 3.4. Study of the stochastic model

---

$$\begin{aligned}
& +e^t\theta \left[-\sigma S^\theta I d\xi(t) + \sigma I^\theta S d\xi(t)\right] \\
= & Ae^t dt + \theta\sigma e^t \left[-S^\theta I d\xi(t) + I^\theta S d\xi(t)\right], \tag{3.11}
\end{aligned}$$

where  $A = \theta K^{\theta-1}(b_S + e + \mu)K + \theta K^{\theta-1}(b_I + \beta K)K + \theta(\theta - 1)\sigma^2 K^{\theta+2}$ .

Using Proposition 3.4.1 and from (3.11), one gets

$$\mathbb{E} \left( e^{t \wedge \nu_m} U(S(t \wedge \nu_m), I(t \wedge \nu_m)) \right) \leq W(S(0), I(0)) + A \mathbb{E} \left( \int_0^{t \wedge \nu_m} e^u du \right).$$

Making  $m \rightarrow \infty$ , we have

$$\mathbb{E} \left( e^t U(S(t), I(t)) \right) \leq W(S(0), I(0)) + A(e^t - 1),$$

implying

$$\mathbb{E} \left( U(S(t), I(t)) \right) \leq e^{-t} W(S(0), I(0)) + A - Ae^{-t}.$$

Defining  $|Y(t)| = (S^2(t) + I^2(t))^{\frac{1}{2}}$  and noting that  $|Y(t)|^\theta = (S^2(t) + I^2(t))^{\frac{\theta}{2}} \leq 2^{\frac{\theta}{2}} \max \{S^\theta(t), I^\theta(t)\} \leq 2^{\frac{\theta}{2}} (S^\theta + I^\theta)$ , we obtain

$$\mathbb{E} \left( |Y(t)|^\theta \right) \leq 2^{\frac{\theta}{2}} \left( e^{-t} W(S(0), I(0)) + A - Ae^{-t} \right).$$

Thus,  $\limsup_{t \rightarrow \infty} \mathbb{E} \left( |Y(t)|^\theta \right) \leq 2^{\frac{\theta}{2}} A < \infty$ . Therefore, there exists a positive constant  $\eta$  such that  $\limsup_{t \rightarrow \infty} \mathbb{E} \left( \sqrt{Y(t)} \right) < \eta$ . For any  $\nu > 0$ ,  $\omega = \frac{\eta^2}{\nu^2} > 0$ , and using the Chebyshev's inequality,  $\mathbb{P}(|Y(t)| > \omega) \leq \frac{\mathbb{E}(\sqrt{Y(t)})}{\sqrt{\omega}}$ , one gets

$$\limsup_{t \rightarrow \infty} \mathbb{P} \left( |Y(t)| > \omega \right) \leq \frac{\eta}{\sqrt{\omega}} = \nu.$$

Hence the result. □

### Stochastic extinction and persistence of infection

One important concern in epidemiology is the eradication of infection from the system. The average infected population in the time interval  $[0, t]$  is  $\frac{1}{t} \int_0^t I(\kappa) d\kappa$ . The infected population is said to be strongly non-persistent or extinct if the supremum of its limiting average population is zero. In this case, the infection is said to be removed from the system. On the other hand, if the infimum of its limiting average population

### 3. Persistence and extinction of infection in stochastic SIS host-parasite epidemic model with horizontal and imperfect vertical transmissions

---

is always positive, then the  $I$  population is said to be strictly persistent (Liu and Wang [2011d]). In this case, the eventual average  $I$  will always stay away from zero, and the infection consistently remains present in the system. In the following two theorems, we provide sufficient conditions so that the disease is eliminated or persists almost surely in the stochastic system (3.2).

Using the definition 1.7.2 of extinction and the Lemma 1.7.3(i), we present a vital result that guarantees disease eradication in the stochastic system.

**Theorem 3.4.3.** *If  $R_0^S = \frac{\beta^2 + b_I}{2\sigma^2 + u_I + \mu} < 1$ , then the infected population of the model (3.2) goes to extinction almost surely.*

*Proof.* Let  $(S(t), I(t))$  be a solution of the system (3.2) with initial value  $(S(0), I(0))$ . Applying Ito's formula in the second equation of system (3.2), we have

$$\begin{aligned} d(\ln I(t)) &= \left[ b_I \left( 1 - \frac{S+I}{K} \right) - u_I + \beta S - \mu - \frac{1}{2} \sigma^2 S^2 \right] dt + \sigma S d\xi(t) \\ &= \left[ b_I - \frac{\sigma^2}{2} \left( S - \frac{\beta}{\sigma^2} \right)^2 + \frac{\beta^2}{2\sigma^2} - (u_I + \mu) - \frac{b_I}{K} (S+I) \right] dt + \sigma S d\xi(t) \\ &\leq \left[ \frac{\beta^2}{2\sigma^2} + b_I - (u_I + \mu) \right] dt + \sigma S d\xi(t). \end{aligned} \quad (3.12)$$

Integration on the both sides of (3.12) from 0 to  $t$ , and division by  $t$  yields

$$\frac{\ln I(t)}{t} \leq \left[ \frac{\beta^2}{2\sigma^2} + b_I - (u_I + \mu) \right] + \frac{\ln I(0)}{t} + \frac{M(t)}{t}, \quad (3.13)$$

where,  $M(t) = \int_0^t \sigma S(\tau) d\xi(\tau)$  is the local martingale with  $M(0) = 0$ . Moreover,  $\langle M, M \rangle_t = \left( \int_0^t \sigma S(\tau) d\xi(\tau) \right)^2 = \int_0^t \sigma^2 S^2(\tau) d\tau \leq \sigma^2 K^2 t$ . One then have

$$\limsup_{t \rightarrow \infty} \frac{\langle M, M \rangle_t}{t} \leq \sigma^2 K^2 < \infty \quad \text{a.s.}$$

Therefore, by the law of large number (Petrov [1969]),  $\lim_{t \rightarrow \infty} \frac{M(t)}{t} = 0$  a.s. Taking limit superior on both sides of (3.13) and using the Lemma 1.7.3, we obtain

$$\limsup_{t \rightarrow \infty} \frac{\ln I(t)}{t} \leq \frac{\beta^2}{2\sigma^2} + b_I - (u_I + \mu) < 0,$$

whenever  $R_0^S = \frac{\beta^2 + b_I}{2\sigma^2 + u_I + \mu} < 1$ . Thus, we have  $\lim_{t \rightarrow \infty} I(t) = 0$  for  $R_0^S < 1$ . This

### 3.4. Study of the stochastic model

---

completes the proof.  $\square$

The condition  $R_0^S < 1$  may be considered the equivalent basic reproduction number for the stochastic system. The stochastic basic reproduction number ( $R_0^S$ ) prescribe some restriction on the system parameters and noise. If the condition is satisfied, the infected population will be extinct, and the system will be disease-free. One can easily observe that  $R_0^S$  is a decreasing function of the recovery rate,  $\mu$ , and the noise intensity,  $\sigma$ . The recovery rate may be increased by taking suitable external measures; consequently,  $R_0^S$  can be made less than unity to make the eradication process possible. Similarly, additional noise may also be helpful in disease elimination. However, the disease transmission parameter  $\beta$  and the birth rate  $b_I$  of the infected host are positively correlated with  $R_0^S$ .

Ergodicity of a stationary process means that the long-time average value of sample paths of the process converges to the expected value of the process (Braumann [2019]). The following theorem is a kind of ergodic behaviour of  $I$  population of the stochastic system (3.2).

**Theorem 3.4.4.** *If  $\frac{b_I - u_I - \mu}{\frac{b_I}{K} + \frac{A(b_I + e)}{b_S} - \frac{Au_I}{b_S}} > 0$ , the infected population  $I$  persists in mean a.s., and*

$$\liminf_{t \rightarrow \infty} \langle I(t) \rangle = \frac{b_I - u_I - \mu}{\frac{b_I}{K} + \frac{A(b_I + e)}{b_S} - \frac{Au_I}{b_S}}, \quad \text{where } A = \min \left\{ \beta - \frac{b_I}{K}, \frac{K\sigma^2}{2} \right\}.$$

*Proof.* Integrating both the equations of (3.2) from 0 to  $t$  and dividing by  $t$ , one obtains

$$\begin{aligned} \frac{S(t) - S(0)}{t} + \frac{I(t) - I(0)}{t} &= b_S \left\langle S \left( 1 - \frac{S+I}{K} \right) \right\rangle - u_S \langle S \rangle + e \left\langle I \left( 1 - \frac{S+I}{K} \right) \right\rangle \\ &+ b_I \left\langle I \left( 1 - \frac{S+I}{K} \right) \right\rangle - u_I \langle I \rangle, \end{aligned} \quad (3.14)$$

where  $\langle x(t) \rangle = \frac{1}{t} \int_0^t x(s) ds$ . Since  $S$  and  $I$  are stochastically ultimately bounded, therefore  $\lim_{t \rightarrow \infty} \frac{S(t) - S(0)}{t} = 0$  and  $\lim_{t \rightarrow \infty} \frac{I(t) - I(0)}{t} = 0$ . Eq. (3.14) then becomes

$$\begin{aligned} b_S \left\langle \left( S - \frac{S^2}{K} \right) \right\rangle + e \langle I \rangle + b_I \langle I \rangle - u_I \langle I \rangle &\geq b_S \left\langle S \left( 1 - \frac{S+I}{K} \right) \right\rangle \\ - u_S \langle S \rangle + e \left\langle I \left( 1 - \frac{S+I}{K} \right) \right\rangle + b_I \left\langle I \left( 1 - \frac{S+I}{K} \right) \right\rangle - u_I \langle I \rangle. \end{aligned} \quad (3.15)$$

### 3. Persistence and extinction of infection in stochastic SIS host-parasite epidemic model with horizontal and imperfect vertical transmissions

---

Taking limit as  $t$  goes to  $\infty$ , we have

$$\lim_{t \rightarrow \infty} \left\langle \left( S - \frac{S^2}{K} \right) \right\rangle \geq \frac{u_I - (b_I + e)}{b_S} \langle I \rangle. \quad (3.16)$$

Using Ito's formula in the second equation of the system (3.2), one gets

$$\begin{aligned} d(\ln I(t)) &= \left[ (b_I - u_I - \mu) + \left( \beta S - \frac{b_I}{K} S - \frac{1}{2} \sigma^2 S^2 \right) - \frac{b_I}{K} I \right] dt + \sigma S d\xi(t) \\ &\geq \left[ (b_I - u_I - \mu) + A \left( S - \frac{S^2}{K} \right) - \frac{b_I}{K} I \right] dt + \sigma S d\xi(t), \end{aligned} \quad (3.17)$$

where  $A = \min \left\{ \beta - \frac{b_I}{K}, \frac{K\sigma^2}{2} \right\}$ . Integrating both sides of (3.17) from 0 to  $t$ , dividing by  $t$ , and using (3.16), we get

$$\frac{\ln I(t)}{t} \geq (b_I - u_I - \mu) - \left\{ \frac{b_I}{K} + \frac{A(b_I + e)}{b_S} - \frac{Au_I}{b_S} \right\} \langle I \rangle + \frac{\ln I(0)}{t} + \frac{\sigma}{t} \int_0^t S(\tau) d\xi(\tau).$$

Since  $I$  is bounded,  $\lim_{t \rightarrow \infty} \frac{\ln I(0)}{t} = 0$  and by the argument given previously,

$$\lim_{t \rightarrow \infty} \frac{\sigma}{t} \int_0^t S(\tau) d\xi(\tau) = 0.$$

Therefore, using Lemma 1.7.3, we have

$$\liminf_{t \rightarrow \infty} \langle I(t) \rangle \geq \frac{b_I - u_I - \mu}{\frac{b_I}{K} + \frac{A(b_I + e)}{b_S} - \frac{Au_I}{b_S}}. \quad (3.18)$$

Thus, if the condition stated in the theorem holds then the infected population persists almost surely for all future time.  $\square$

### Stochastic asymptotic stability

It is worth mentioning that the stochastic system (3.2) has no explicit equilibrium density like the deterministic system (3.1). Instead, the stochastic solution fluctuates around the deterministic equilibrium or fixed value. One may find it interesting to determine the conditions under which the behaviour of the stochastic solution will be similar to that of the deterministic equilibrium solution. For this, we provide the following theorem.

### 3.4. Study of the stochastic model

**Theorem 3.4.5.** *Let  $(S(t), I(t))$  be the solution of (3.2) with initial value  $(S(0), I(0)) \in \mathbb{R}_+^2$  and the stability criteria of  $E^*$  hold. If  $\frac{b_S}{K}(S^* + 1) + g_1 \bar{L} + \frac{b_I I^*}{K} + u_S - (\frac{3}{2}b_s + e + b_I) > 0$ ,  $\frac{e}{K}(S^* + I^*) + \frac{(b_S + b_I)S^*}{K} + \frac{b_I I^*}{K} + g_2 \bar{L} + \frac{c_1 b_I}{K} + u_I - (\frac{b_S}{2} + 2(e + b_I)) > 0$  and  $\frac{2S^* b_S}{K} + \frac{e(S^* + I^*)}{K} + \frac{b_I(S^* + I^*)}{K} - b_S - b_I - e > 0$ , then*

$$\limsup_{t \rightarrow \infty} \frac{1}{t} \int_0^t [(S(\tau) - S^*)^2 + (I(\tau) - I^*)^2] d(\tau) \leq G_1 \sigma^2 \quad a.s., \quad (3.19)$$

where  $E^* = (S^*, I^*)$  is the endemic equilibrium of the deterministic system and  $G_1 = \frac{K^2(K^2 + \frac{c_1}{2}I^*)}{H}$ ,  $H = \min \left\{ \frac{b_S}{K}(S^* + 1) + g_1 \bar{L} + \frac{b_I I^*}{K} + u_S - (\frac{3}{2}b_s + e + b_I), \frac{e}{K}(S^* + I^*) + \frac{(b_S + b_I)S^*}{K} + \frac{b_I I^*}{K} + g_2 \bar{L} + \frac{c_1 b_I}{K} + u_I - (\frac{b_S}{2} + 2(e + b_I)) \right\}$ ,  $g_1 = \min \left\{ \frac{e}{K}, \frac{b_S}{K} \right\}$ ,  $g_2 = \min \left\{ \frac{e}{K}, \frac{b_I}{K} \right\}$  and  $\bar{L} = \frac{K}{M}(M - N)$ .

*Proof.* Define a positive function  $G = \frac{1}{2}(S - S^* + I - I^*)^2 + c_1 (I - I^* - I^* \log \frac{I}{I^*})$ , where  $c_1$  is a positive constant to be determined later. At  $(S^*, I^*)$ , we have

$$\begin{aligned} b_S S^* \left(1 - \frac{S^* + I^*}{K}\right) + e I^* \left(1 - \frac{S^* + I^*}{K}\right) &= u_S S^* + \beta S^* I^* - \mu I^* \\ \beta S^* I^* + b_I I^* \left(1 - \frac{S^* + I^*}{K}\right) &= u_I I^* + \mu I^*. \end{aligned} \quad (3.20)$$

Using (3.20) and Ito's formula, one obtains

$$\begin{aligned} dG &= (S - S^* + I - I^*) \left[ b_S S \left(1 - \frac{S + I}{K}\right) - u_S S + e I \left(1 - \frac{S + I}{K}\right) \right. \\ &\quad \left. + b_I I \left(1 - \frac{S + I}{K}\right) - u_I I \right] dt + \sigma^2 S^2 I^2 dt + c_1 \left(1 - \frac{I}{I^*}\right) \left[ \left\{ b_I I \left(1 - \frac{S + I}{K}\right) \right. \right. \\ &\quad \left. \left. - u_I I + \beta S I - \mu I \right\} dt + \sigma S I d\xi(t) \right] + \frac{c_1}{2} \sigma^2 S^2 I^* dt \\ &= \left[ b_s - \frac{b_S}{K}(S + S^* + 1) - \frac{eI}{K} - \frac{b_I I^*}{K} - u_S \right] (S - S^*)^2 + \left[ e + b_I - \frac{e}{K}(S^* + I^* + I) \right. \\ &\quad \left. - \frac{(b_S + b_I)S^*}{K} - \frac{b_I(I + I^*)}{K} - \frac{c_1 b_I}{K} - u_I \right] (I - I^*)^2 \end{aligned} \quad (3.21)$$



### 3. Persistence and extinction of infection in stochastic SIS host-parasite epidemic model with horizontal and imperfect vertical transmissions

$$\begin{aligned}
& + \left[ b_S - \frac{b_S}{K}(2S^* + S + I) + e - \frac{e}{K}(S^* + I^* + 2I) + b_I - \frac{b_I}{K}(s^* + I^* + 2I) \right. \\
& - u_I - u_S + c_1 \left( \beta - \frac{b_I}{K} \right) \left. \right] (S - S^*)(I - I^*) + \sigma^2 S^2 I^2 dt + \frac{c_1}{2} \sigma^2 S^2 I^* dt \\
& + c_1 \sigma (I - I^*) S d\xi(t) \\
& \leq \left[ b_S - \frac{b_S}{K}(S^* + 1) - g_1 \bar{L} - \frac{b_I I^*}{K} - u_S \right] (S - S^*)^2 + \left[ e + b_I - \frac{e}{K}(S^* + I^*) \right. \\
& - \frac{(b_S + b_I)S^*}{K} - \frac{b_I I^*}{K} - g_2 \bar{L} - \frac{c_1 b_I}{K} - u_I \left. \right] (I - I^*)^2 + \left[ b_S - \frac{2S^* b_S}{K} + e \right. \\
& - \frac{e(S^* + I^*)}{K} + b_I - \frac{b_I(S^* + I^*)}{K} + c_1 \left( \beta - \frac{b_I}{K} \right) \left. \right] (S - S^*)(I - I^*) \\
& + \left[ \frac{b_S}{K}(S + I) + \frac{2(e + b_I)I}{K} \right] |(S - S^*)(I - I^*)| + \sigma^2 S^2 I^2 dt + \frac{c_1}{2} \sigma^2 S^2 I^* dt \\
& + c_1 \sigma (I - I^*) S d\xi(t).
\end{aligned}$$

Choosing  $c_1 = \frac{1}{\beta - \frac{b_I}{K}} \left[ \frac{2S^* b_S}{K} + \frac{e(S^* + I^*)}{K} + \frac{b_I(S^* + I^*)}{K} - b_S - b_I - e \right] > 0$  and using  $|(S - S^*)(I - I^*)| \leq \frac{1}{2} ((S - S^*)^2 + (I - I^*)^2)$ , (3.21) becomes

$$\begin{aligned}
dG & \leq - \left\{ \left[ \frac{b_S}{K}(S^* + 1) + g_1 \bar{L} + \frac{b_I I^*}{K} + u_S - \left( \frac{3}{2} b_S + e + b_I \right) \right] (S - S^*)^2 \right. \\
& + \left[ \frac{e}{K}(S^* + I^*) + \frac{(b_S + b_I)S^*}{K} + \frac{b_I I^*}{K} + g_2 \bar{L} \right. \\
& + \left. \left. \frac{c_1 b_I}{K} + u_I - \left( \frac{b_S}{2} + 2(e + b_I) \right) \right] (I - I^*)^2 \right\} + \sigma^2 S^2 I^2 dt + \frac{c_1}{2} \sigma^2 S^2 I^* dt \\
& + c_1 \sigma (I - I^*) S d\xi(t), \tag{3.22}
\end{aligned}$$

where  $\bar{L} = \frac{K}{M}(M - N)$ .

Define  $H = \min \left\{ \frac{b_S}{K}(S^* + 1) + g_1 \bar{L} + \frac{b_I I^*}{K} + u_S - \left( \frac{3}{2} b_S + e + b_I \right), \frac{e}{K}(S^* + I^*) + \frac{(b_S + b_I)S^*}{K} + \frac{b_I I^*}{K} + g_2 \bar{L} + \frac{c_1 b_I}{K} + u_I - \left( \frac{b_S}{2} + 2(e + b_I) \right) \right\}$ . Integrating (3.22) from 0 to  $t$ , one gets

$$\begin{aligned}
G(t) - G(0) & \leq -H \int_0^t [(S(\tau) - S^*)^2 + (I(\tau) - I^*)^2] d\tau + \sigma^2 K^2 \left( K^2 + \frac{c_1}{2} I^* \right) t \\
& + c_1 \sigma \int_0^t (I(\tau) - I^*) S(\tau) d\xi(\tau).
\end{aligned}$$

### 3.5. Simulation results

---

$$\begin{aligned} \therefore \int_0^t [(S(\tau) - S^*)^2 + (I(\tau) - I^*)^2] d(\tau) &\leq \frac{G(0)}{H} + \frac{\sigma^2 K^2 (K^2 + \frac{c_1}{2} I^*) t}{H} \\ &+ \frac{c_1 \sigma}{H} \int_0^t (I(\tau) - I^*) S(\tau) d\xi(\tau) \end{aligned} \quad (3.23)$$

Let  $N_1(t) = \int_0^t (I(\tau) - I^*) S(\tau) d\xi(\tau)$ , which is a continuous martingale and  $N_1(0) = 0$ . Also,  $\langle N_1, N_1 \rangle_t = \left( \int_0^t (I(\tau) - I^*) S(\tau) d\xi(\tau) \right)^2 = \int_0^t (I(\tau) - I^*)^2 S^2(\tau) d(\tau) \leq 4K^4 t$  and  $\limsup_{t \rightarrow \infty} \frac{\langle N_1, N_1 \rangle_t}{t} \leq 4K^4 < \infty$  a.s. Therefore, by the law of large number (Petrov [1969]),  $\lim_{t \rightarrow \infty} \frac{N_1(t)}{t} = 0$  a.s. Combining these results and then dividing (3.23) by  $t$  and taking limit superior, we have

$$\limsup_{t \rightarrow \infty} \frac{1}{t} \int_0^t [(S(\tau) - S^*)^2 + (I(\tau) - I^*)^2] d(\tau) \leq G_1 \sigma^2 \quad \text{a.s.}$$

where  $G_1 = \frac{K^2(K^2 + \frac{c_1}{2} I^*)}{H}$ . Hence the theorem is proven.  $\square$

Furthermore, if  $\sigma \rightarrow 0$  then

$$\limsup_{t \rightarrow \infty} \frac{1}{t} \int_0^t [(S(\tau) - S^*)^2 + (I(\tau) - I^*)^2] d(\tau) \rightarrow 0.$$

Therefore,  $\lim_{t \rightarrow \infty} S(t) \rightarrow S^*$ ,  $\lim_{t \rightarrow \infty} I(t) \rightarrow I^*$  and the stochastic solution tends to the deterministic equilibrium solution. It implies that if the noise intensity is low, the stochastic system behaves similarly to the asymptotic solution of the deterministic system, provided the restrictions in the above theorem hold.

### 3.5 Simulation results

In support of the previous analytical results, we present here different simulation results of the stochastic model (3.2) for the parameter values taken from Lipsitch et al. [1996]. The following system parameters are considered fixed unless it is stated:

$$b_S = 0.2, \quad b_I = 0.1, \quad u_S = 0.1, \quad u_I = 0.3, \quad e = 0.02, \quad K = 2, \quad \beta = 0.5, \quad \mu = 0.1.$$

### 3. Persistence and extinction of infection in stochastic SIS host-parasite epidemic model with horizontal and imperfect vertical transmissions

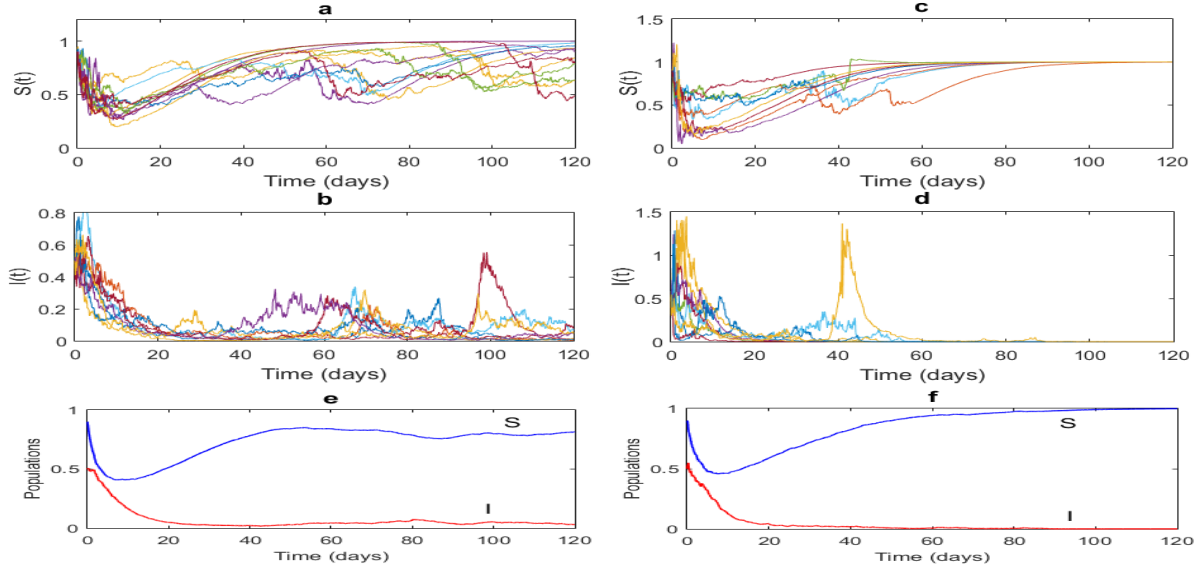


**Figure 3.1:** Time series of ten runs of the stochastic system (3.2) for  $\sigma = 0.4$  (first column) and  $\sigma = 0.65$  (second column). Each figure shows that the solution trajectories are different for each run even though the parameter set remains unchanged. Third row: Average susceptible and infected populations of 100 time series of the stochastic system with  $\sigma = 0.4$  (Fig. e) and  $\sigma = 0.65$  (Fig. f). Figures in the left column show that the disease persists and the same in the right column shows that the disease goes to extinction.

The time evolution of a stochastic system is different for each run; however, that of the deterministic system is unique for a given initial and parameter values. Thus, due to inherent randomness, there may exist a considerable disagreement between the solutions of the stochastic system for different runs. To illustrate this, we have presented 10 simulation results for two distinct noises in the first two rows of Figure 3.1. The first column shows that the disease persists for low values of the noise ( $\sigma = 0.4$ ) when the parameter set satisfies the conditions of the Theorem 3.4.4 with  $\frac{b_I - u_I - \mu}{\frac{b_I}{K} + \frac{A(b_I + e)}{b_S} - \frac{Au_I}{b_S}} = 3.1915 > 0$ . The second column illustrates that the disease dies out for higher values of the noise ( $\sigma = 0.65$ ) when the parameter set satisfies the conditions of Theorem 3.4.3 with  $R_0^S = 0.9896 < 1$ . Observe that the solution trajectories differ in each simulation though the initial condition and parameter values remain the same. It is, therefore, more justified to present the average behaviour of the stochastic solutions. In the last row, we have presented the mean value of 100 solutions of the stochastic system (3.2) for  $\sigma = 0.4$  (left figure) and  $\sigma = 0.65$  (right figure).

### 3.5. Simulation results

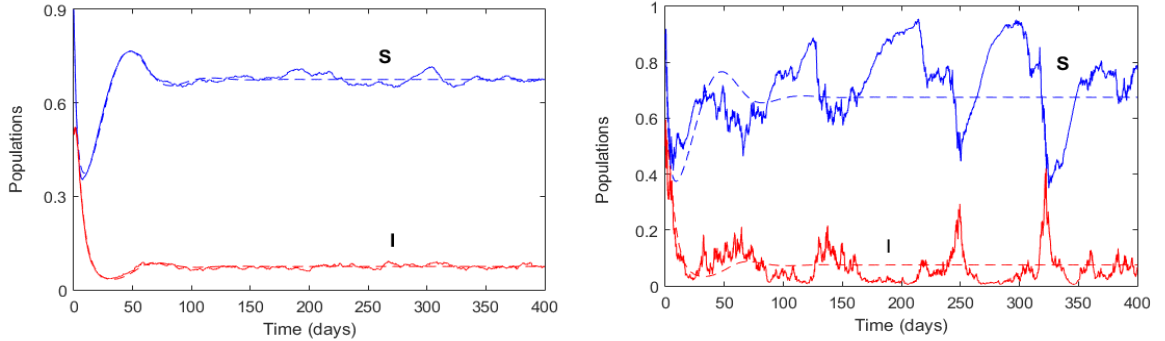


**Figure 3.2:** Asymptotic behaviour of the stochastic system (3.2) (solid line) and the deterministic system (3.1) (dashed line) for low noise intensity,  $\sigma = 0.05$  (left figure) and higher noise  $\sigma = 0.4$  (right figure). It shows that the stochastic solution is very close to the deterministic equilibrium solution ( $S^* = 0.675, I^* = 0.075$ ) for low noise but significantly differs when it is high. Other parameters are as in Fig. 3.1.

It is worth mentioning that the noise-induced stochastic system (3.2) has no steady-state value. In Theorem 3.4.5, we have proven that the stochastic and deterministic systems behave similarly if the noise intensity is low. However, if the noise intensity is high, the stochastic solution largely deviates from its deterministic counterpart. We illustrate such behaviour of the system in Figure 3.2 for two different noises:  $\sigma = 0.05$  and  $\sigma = 0.4$ . It is mentionable that the conditions of the stationary distribution (Theorem 3.4.5) are satisfied here. We further examined the probabilistic smoke cloud around the deterministic steady state. It shows the strength of the stabilizing factors of the population interaction compared to the diffusive effects of the random environmental fluctuations (May [2019]). The probability cloud is compact if the interaction strength can overcome the noise. However, if the interaction strength is weak compared to the intensity of the environmental variance, the cloud is dispersed (see Fig. 3.3). To illustrate this, we repeat the simulation 10,000 times and plot the values of  $S$  and  $I$  at  $t = 120$ . This figure shows that species densities are mostly concentrated in the neighborhood of deterministic equilibrium value  $(S^*, I^*) = (0.675, 0.075)$  (blue point) if the noise intensity is low ( $\sigma = 0.05$ ). Observe that the frequency distribution of the susceptible population ( $S$ ) is distributed in the range  $0.6 - 0.8$  around its equilibrium value  $S^* = 0.675$  (Fig. 3.3b), and the same for infected population ( $I$ ) is distributed in the range  $0.05 - 0.11$  around its equilibrium value  $I^* = 0.075$  (Fig. 3.3c). Here, the widths and heights of rectangles represent various classes and frequencies. The population densities, however, become

### 3. Persistence and extinction of infection in stochastic SIS host-parasite epidemic model with horizontal and imperfect vertical transmissions

more sparse around the deterministic steady-state and are spread over a larger area (Fig. 3.3d) if the noise intensity is high ( $\sigma = 0.15$ ). The corresponding frequency distributions (Figs. 3.3e, f) show that  $S$  and  $I$  are distributed over a more extensive range of  $0.35 - 0.1$  and  $0.005 - 0.32$ , respectively, around their deterministic equilibrium values. It reveals that the stochastic system does not deviate too much from its deterministic system if the noise is low, but it does if it is high.

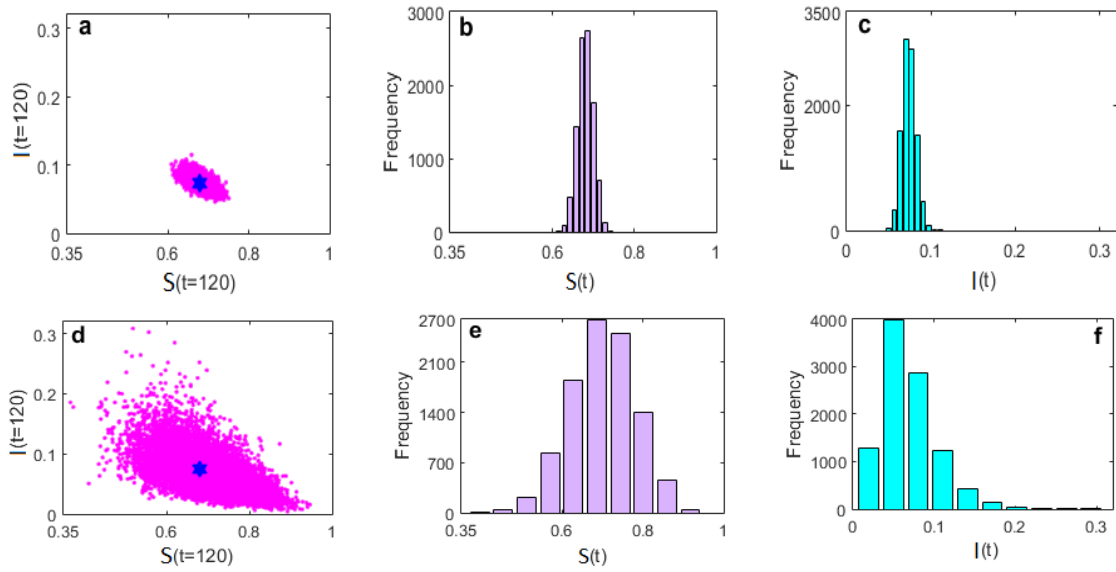


**Figure 3.3:** Scatter plot of susceptible and infected populations of system (3.2) around the deterministic steady state (blue dot) and the corresponding frequency plot obtained at  $t = 120$  for 100 simulations. Upper row: For the lower value of  $\sigma = 0.05$ , frequency distribution shows small fluctuations around the deterministic steady state value  $(S^*, I^*) = (0.675, 0.075)$ . Lower row: Frequency distribution shows larger variations around  $(S^*, I^*)$  for higher noise intensity,  $\sigma = 0.15$ . Here  $\beta = 0.5$ ,  $\mu = 0.1$  and other parameters are as in Fig. 3.1.

It is observed that the noise intensity ( $\sigma$ ) and the disease transmission rate ( $\beta$ ) play a pivotal role in the extinction and persistence of the disease. We present in Fig 3.4a the mean extinction time of the infected population of the stochastic system (3.2) with the variations in  $\beta$  and  $\sigma$ . In order to find the extinction time numerically, we repeated the simulation 100 times for each pair of  $(\beta, \sigma)$  and plotted the mean of the extinction time of 100 simulations. The infected population was considered extinct if it went below 0.0001. It is to be noted that  $R_0^S < 1$  is satisfied throughout the considered range of  $\beta$  and  $\sigma$ . Fig. 3.4a shows that if  $\beta$  is high and  $\sigma$  is low, the extinction time is longer. However, the extinction time decreases if  $\beta$  is low or  $\sigma$

### 3.5. Simulation results

is high. We have also investigated how disease extinction time is influenced by the parameter variation  $\beta$  and  $b_I$ . We have selected four different values of  $\sigma$ , namely, 0.2, 0.4, 0.6, 0.8. For each of these  $\sigma$  values, we varied  $\beta$  and  $b_I$  jointly and recorded the mean extinction time for 100 simulations (see Fig. 3.4, second and third rows). It has been observed that disease extinction takes a shorter time if both  $\beta$  and  $b_I$  are low. But disease extinction time is prolonged for higher values of  $\beta$  and  $b_I$ . We further observe that when  $\sigma$  is low, disease extinction time in the whole parametric space of  $\beta$  and  $b_I$  is high compared to the higher value of  $\sigma$ . It reveals that stronger environmental noise helps eradicate the disease from the system early, implying that the environmental noise may act as a regulatory mechanism to control the disease.

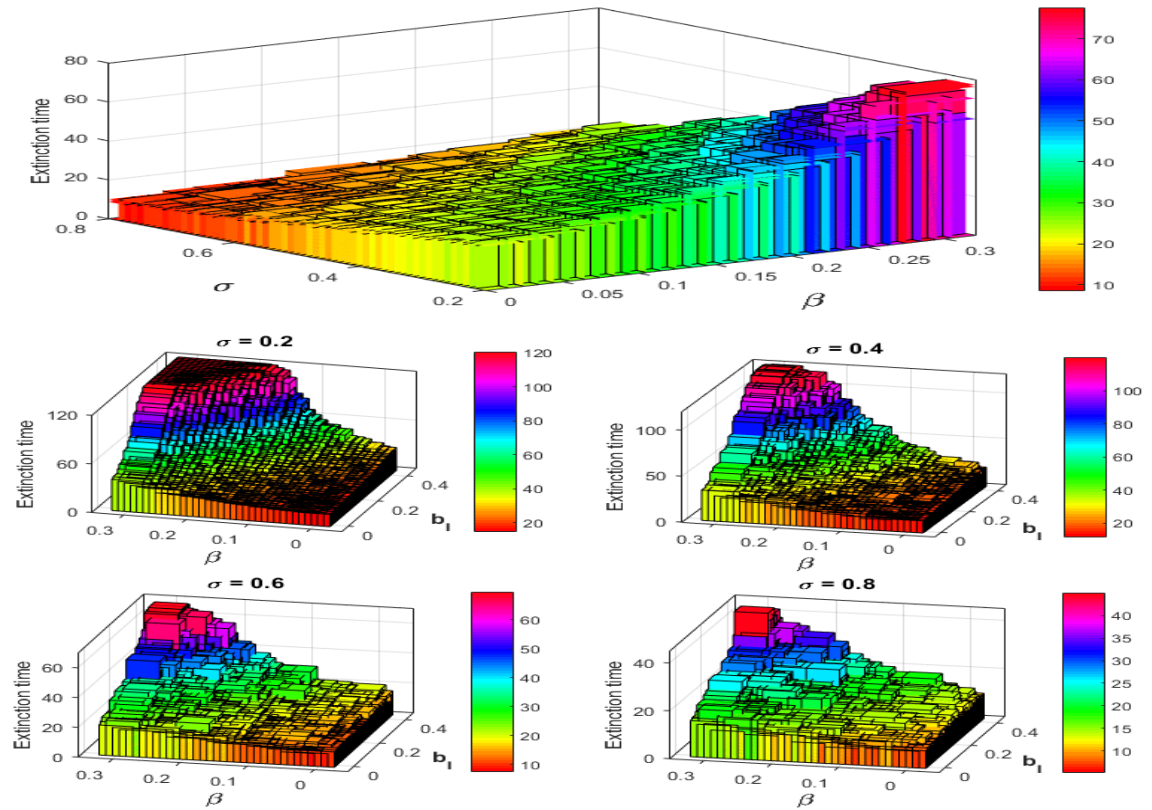


**Figure 3.4:** Left: Mean extinction time distribution calculated from 100 simulations of the infected population of the stochastic system (3.2) for different  $\beta$  and  $\sigma$ , keeping other parameters fixed as in Fig. 3.1. It reveals that extinction time decreases as the noise intensity increases, but the case is the opposite for the disease transmission coefficient. Right: For four different values of  $\sigma$ , extinction time is calculated in the  $\beta$  and  $b_I$  plane. It shows that as  $\beta$  and  $b_I$  are both high, disease extinction takes a long time to eradicate.

### 3. Persistence and extinction of infection in stochastic SIS host-parasite epidemic model with horizontal and imperfect vertical transmissions

To unveil the underlying law of extinction time, we plotted the mean of extinction time of 100 simulations with the variation of  $\sigma$  for three particular values of  $\beta$ , 0.1, 0.2 and 0.3 (Fig. 3.5a). Mean extinction time gradually decreases as  $\sigma$  increases and fits the negative exponential curve. A similar figure was drawn with three fixed values of  $\sigma$ , 0.2, 0.5 and 0.8 for the variation of  $\beta$  (Fig. 3.5b). In this latter case, the disease extinction time gradually increases with the increase of the disease transmission coefficient. The mean extinction time in this case fits the positive exponential curve.

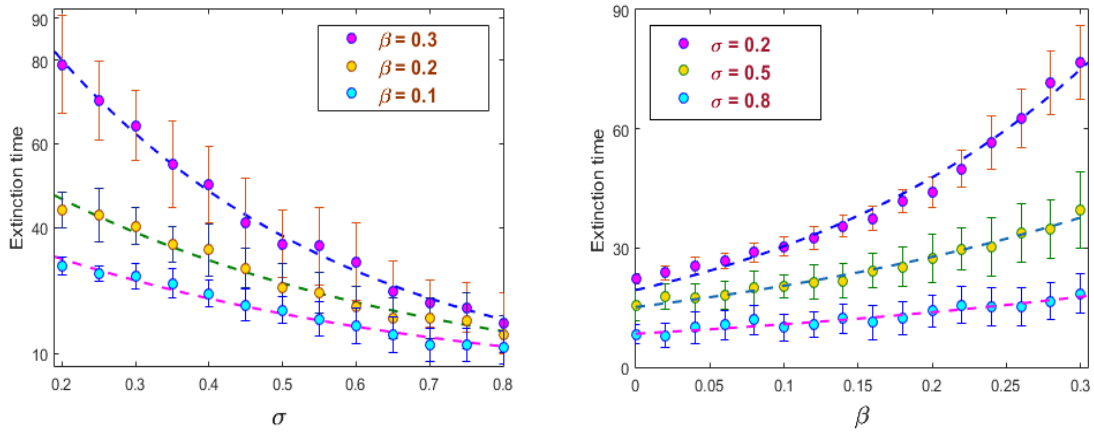


**Figure 3.5:** (a) Dashed lines are the best-fitted curve for three particular values of  $\beta$  (0.1, 0.2 and 0.3) due to the variations in the environmental noise. It indicates that the extinction time follows the negative exponential law. (b) Similar curves are drawn to show exponential increase in the extinction time for  $\sigma = 0.2, 0.5, 0.8$  due to the variations in the noise intensity,  $\sigma$ . It shows that the extinction time follows the positive exponential law. The error bars indicate standard deviations from the average of 100 simulations. Other parameters remain fixed as in Fig. 3.1.

It is shown that  $R_0^S$  is a decreasing function of the recovery rate,  $\mu$ . Here we explore the disease extinction scenario for  $\mu$  for different values of  $\sigma$  and  $\beta$ . Fig. 3.6 shows that the extinction time curves have two distinct natures for the variations in  $\mu$ . If  $\sigma$  is high or  $\beta$  is low, the extinction time follows the negative exponential law. On the contrary, if  $\sigma$  is low or  $\beta$  is high, the extinction time follows the Gaussian law. All these have a long tail, implying that a shorter extinction time of the disease is possible for an extended range of  $\mu$ .

### 3.5. Simulation results

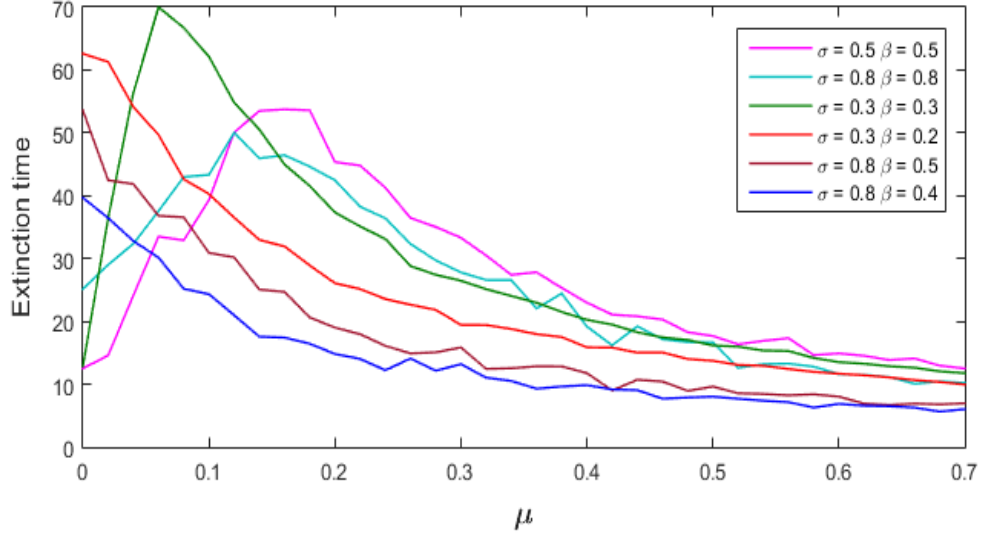


**Figure 3.6:** The plot of the infected population’s extinction time for the variation of  $\mu$  for different pairs of  $(\sigma, \beta)$ , keeping other parameters fixed as in Fig. 3.1. It shows two distinct natures of extinction time.

As mentioned earlier, parasites’ infectivity and the relative fecundity of infected hosts are critical for parasite fitness. The survival fitness of parasites depends on how long the infected hosts persist in the system. For this, we plotted (see Fig. 3.7) the extinction time of infected hosts from the system for the simultaneous variations in  $\beta$  and  $\frac{b_I+e}{b_S}$ . It is to be recalled that the ensemble fecundity of the infected population is  $b_I+e$  and that of the susceptible is  $b_S$ . The ratio  $\frac{b_I+e}{b_S}$  denotes the relative fecundity of infected host. By our assumption,  $b_S \geq b_I+e$  and therefore, the ratio  $\frac{b_I+e}{b_S}$  is always less than or equal to 1. It is observed that if the force of infection is not too high ( $\beta < 0.6$ ), then the infection eradication time increases with the increasing relative fecundity of the infected host for some fixed value of noise. However, for the higher force of infection ( $\beta > 0.6$ ), the relative fecundity of infected hosts has a negligible effect on extinction time. The trend remains the same if the noise intensity is altered. Thus, the parasite fitness is low if the relative fecundity and disease transmissibility are low but gradually increase if any of them increases.



### 3. Persistence and extinction of infection in stochastic SIS host-parasite epidemic model with horizontal and imperfect vertical transmissions

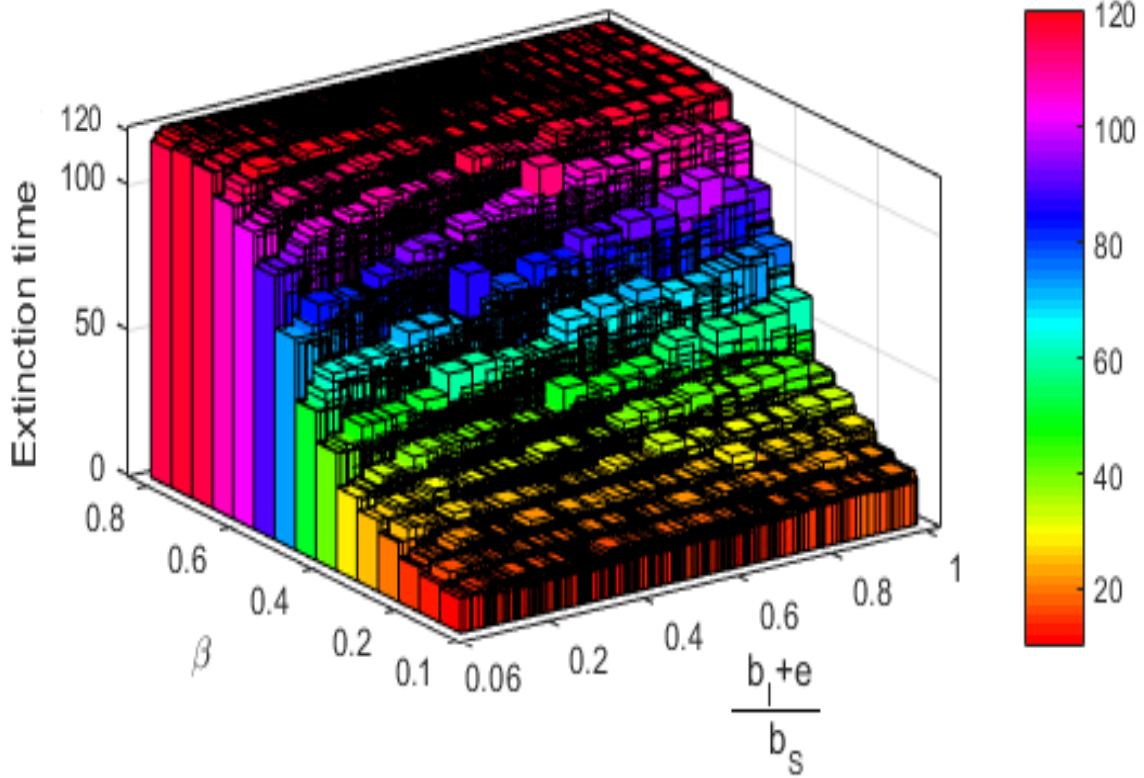


**Figure 3.7:** Parasite fitness is measured in terms of the extinction time of infected host. Mean extinction time of the infected hosts is calculated from 100 simulations of the stochastic system (3.2) for different  $\beta$  and  $\frac{b_I + e}{b_S}$ , keeping other parameters fixed as in Fig. 3.1 with  $\sigma = 0.5$ . It shows that parasite fitness increases with the increasing values of  $\beta$  and  $\frac{b_I + e}{b_S}$ .

## 3.6 Discussion

Mathematical models for the diseased system have helped understand the underlying disease dynamics. After the benchmark work of [Kermack and McKendrick \[1927\]](#), many mathematical models have been proposed and analyzed considering the epidemiological demands. Most of these models are deterministic types represented by ordinary differential equations. The deterministic models have been criticized for viewing all the rate parameters as constant even when knowing the fact that these rate constants constantly fluctuate due to the various unknown environmental noises. Uncertainty is an integral part of modelling biological phenomena due to the complexity and lack of knowledge of microscopic events involved in the system. In partic-

### 3.6. Discussion

---

ular, the disease transmission phenomena are entirely random, and the transmission rate depends on various factors. Incorporating such randomness in a model leads to stochastic differential equations models.

This chapter considers an SIS-type stochastic epidemic model, where the disease is transmitted through horizontal and vertical transmission modes. To incorporate stochasticity in the model, we introduced a white noise in the horizontal disease transmission term, which is the predominant disease transmission mechanism. The fluctuation in the transmission rate usually occurs around some mean value, and therefore, the error term follows a normal distribution, allowing to approximate of it by a white noise (Liu and Wang [2011a]).

Eradication or controlling of various emerging and reemerging diseases is a global challenge. Environmental factors like temperature, humidity, rainfall, and pollution significantly affect disease persistence. Knowing the different routes for theoretically eradicating an infection from the system is essential. Our mathematical analysis revealed that the system could be disease-free by modulating some parameters and the noise intensity. We have shown that if the stochastic basic reproduction number,  $R_0^S$ , can be made less than unity, the system can be disease-free. It is observed that noise intensity plays a pivotal role in eradicating and has an inverse relationship with  $R_0^S$ . The environmental noise can make a system disease-free if it significantly affects the transmission mechanism and make  $R_0^S < 1$ . On the contrary,  $R_0^S$  is directly proportional to the disease transmission coefficient. Thus,  $R_0^S$  may exceed the threshold value, 1, if the disease transmissibility increase. Therefore, the management strategy should be to reduce horizontal disease transmissibility. Our numerical computations revealed that the disease eradication time follows a negative exponential law with the increasing noise intensity. In contrast, the disease transmission coefficient follows the positive exponential law.

Furthermore, disease eradication is also possible with respect to the controllable parameter  $\mu$ . This parameter measures the recovery rate of the infected population and can be used in the disease eradication process. It is mentionable that an infected host may recover from the infection due to its immune mechanism. Recovery of infected hosts is also possible with the help of some external measures. For some given noise and disease transmissibility values, the extinction time may follow either a negative exponential law or a Gaussian law. In the former case, the noise must be high, or the transmission coefficient must be low. In the latter case, the effects of noise and disease transmissibility should be reversed. The eradication time will

### **3. Persistence and extinction of infection in stochastic SIS host-parasite epidemic model with horizontal and imperfect vertical transmissions**

be significantly quicker if the recovery rate is high. On the other hand, disease management would be more challenging if the noise intensity is low and the disease transmissibility is high.

Several studies have demonstrated that parameters have a detrimental effect on the host fecundity. The survival of parasites depends on the infected host density and the extinction time of the infected host population. So it is expected that parasites will evolve towards higher relative fecundity of the infected host to enhance fitness. Parasites can also increase their fitness by evolving towards higher transmissibility. Our simulation result for simultaneous variation of disease transmission coefficient and relative fecundity rate shows that parasite fitness increases with increasing relative fecundity of parasites when the transmissibility is low. The relative fecundity of infected hosts, however, has a negligible effect on the extinction time of the infected host and, consequently, on the parasite survival fitness if disease transmissibility of parasites is high. A similar trend is also maintained if the noise intensity is altered.

In the next chapter, we consider a three-dimensional predator-prey parasite (PPP) model, where the infection spreads in the prey species. We then randomly perturb three crucial system parameters and then analyze the system to determine the population extinction routes in a PPP system due to environmental stochasticity.

# Chapter 4

## Persistence and extinction of species in a disease-induced ecological system under environmental stochasticity<sup>2</sup>

### 4.1 Introduction

Predator-prey (PP) interactions in presence of infection are common in natural system (Moore [2002], Kabata et al. [1985], Kaiser [1999], Lafferty and Morris [1996], Hudson et al. [1992], Lafferty [1992]) and consequently a large number of mathematical models of predator-prey interactions have appeared in the recent past taking into account the effect of disease (Greenman and Hoyle [2010], Chattopadhyay and Bairagi [2001], Greenhalgh et al. [2017], Bairagi et al. [2007], Chattopadhyay and Pal [2002], Venturino [2002], Haque and Venturino [2006], Xiao and Chen [2002], Yongzhen et al. [2011], Bairagi et al. [2008a]). Study of such predator-prey models in presence of infection, popularly known as predator-prey-parasites (PPP) model or eco-epidemiological models, is extremely important because it encapsulates both the ecological and epidemiological issues simultaneously. Mathematical models of PPP interactions extend, in most of the cases, the basic predator-prey model of either Rosenzweig-MacArthur (RM) type or Leslie-Gower (LG) type (also known as Holling–Tanner type). In the first case, only prey has logistic (i.e., density-dependent) growth limited by a prede-

---

<sup>2</sup>The bulk of this chapter has been published in *Physical Review E* 103, no. 3 (2021): 032412.

#### 4. Persistence and extinction of species in a disease-induced ecological system under environmental stochasticity

---

terminated constant value,  $K$ , called the environmental carrying capacity, but not the predator. On the other hand, the logistic growth of both the populations is considered in the second type of PP models. In fact, the carrying capacity of predator is not a constant here rather depends on the prey density, known as the emerging carrying capacity (Sieber et al. [2014]). Another distinguishing feature of these PP models lies in the fact that predator in an LG model is a generalist one while in an RM model, it is a specialist one. In an LG type PP model, the predator has a focal prey, which predators prefer to consume when in abundance, though it has other secondary food (Ji et al. [2009]) on which predator can survive in absence of its focal prey. RM model, however, assumes a single prey for its predator (Turchin [2003]).

All the PPP models mentioned earlier consider that the models are deterministic and therefore all model parameters (viz. birth rate, death rate, etc.) are constant. In a real ecosystem, however, these parameters are not constant due to various environmental noises and therefore fluctuate around some mean value (May [2001], Ruokolainen et al. [2009b]). Experimental evidence also supports the claim of such impact of environmental noise (Ripa and Lundberg [2000]). To make the models closer to reality, stochastic population models, therefore, have received significant attention from the researchers. There are few stochastic PPP models which either assume that predator consumes infected prey only or the predator's functional response (prey attack rate) is type I (Wei et al. [2018], Li and Wang [2015], Mukherjee [2003], Ji and Jiang [2013]). These assumptions are simplifications of actual phenomena and usually done to make the analysis tractable. For example, Wei et al. [2018] recently considered a predator-prey-parasite model with prey infection, where a predator feeds only on infected prey following Beddington-DeAngelis (BD) response function and LG type growth of predator. They have shown that the corresponding stochastic model has a unique positive global solution and established conditions for disease eradication and its persistence. Li and Wang [2015] also studied a similar stochastic predator-prey model with disease in the predator, where the predator-prey relationship was modelled with RM type interaction. A stochastic predator-prey model with prey infection and type I response function was analysed in Mukherjee [2003]. It is shown that the deterministic stability results are preserved in the stochastic system. Ji and Jiang [2013] considered an RM type PPP model, where predator consumes only infected prey with type II response function. It is shown that both the deterministic system and its stochastic counterpart (with parameter perturbation in the disease transmission coefficient) have similar behaviour if the noise intensity is low but the stability

## 4.2. The model

---

may be lost if the noise intensity is high. A four-dimensional deterministic predator-prey model with infection in both the prey and predator and type I response function was analyzed by [Jang and Baglama \[2009\]](#). They also simulated the corresponding continuous-time Markov chain model to study the population interaction under random effects but did not study it analytically. Stochastic predator-prey (PP) models with different biological attributes, however, have been studied extensively ([Ji et al. \[2009\]](#), [Wu et al. \[2014\]](#), [Yu et al. \[2018\]](#), [Wang and Liu \[2020\]](#), [Yu et al. \[2019\]](#), [Zhao et al. \[2016\]](#), [Zhou and Shi \[2013\]](#), [Ji et al. \[2011b\]](#)). Though these studies have made significant contributions in the theory and application of noise-induced population dynamics, none of these stochastic PP or PPP models has tried to fit the model with experimental data and therefore these models and the corresponding outcomes remained unverified.

Various studies ([Denaro et al. \[2013b\]](#), [Giuffrida et al. \[2009\]](#), [Denaro et al. \[2013a\]](#), [Caruso et al. \[2005\]](#)) show that stochastic model improves the predictive features of the models analyzed and fits the data well by mimicking the random fluctuations. In this chapter, we first theoretically analyze an LG-type stochastic PPP model, where predator consumes both the susceptible and infected preys with type II response function, and then validate our model with empirical data of long time population interaction.

The rest of the chapter is organized as follows. In the next Section 4.2 of this chapter, we discussed the deterministic model's equilibrium and their stability and introduced stochasticity into deterministic model. Mathematical results corresponding to stochastic model is discussed in the Section 4.3. Numerical simulations to support the analytic study is given in Section 4.4. The chapter ends with a discussion in Section 4.5.

## 4.2 The model

### 4.2.1 Deterministic model

We consider an LG type predator-prey model with  $x$  and  $z$  as the prey and predator densities at time  $t$ , where prey follows density-dependent growth and predator follows

#### 4. Persistence and extinction of species in a disease-induced ecological system under environmental stochasticity

---

type II response function:

$$\begin{aligned}\frac{dx}{dt} &= ax - bx^2 - \frac{cxz}{m_1 + x}, \\ \frac{dz}{dt} &= z\left[r - \frac{fz}{m_2 + x}\right],\end{aligned}\tag{4.1}$$

where  $a$  is the intrinsic growth rate of prey,  $b$  is the intra-species competition coefficient,  $c$  is the predator's attack rate,  $r$  is the intrinsic growth rate of the predator,  $f$  is the intra-species competition of predator,  $m_2$  is the half-saturation constant of the predator. A parasitic infection divides the prey population into a susceptible group and an infected group. The disease spreads horizontally, having disease transmissibility  $\lambda$ , and there is no vertical transmission. Infection may cause various modifications to its host, e.g., conspicuousness, castration, lower competitive ability, higher mortality, altered behaviour, increased vulnerability etc. (Moore [2002], Kabata et al. [1985], Kaiser [1999], Lafferty and Morris [1996], Hudson et al. [1992], Lafferty [1992]). Based on this empirical evidence, it is assumed that infected preys are unable to give birth and do not recover. Infected prey dies due to infection at a rate of  $\gamma$  and has intra-species competition but no inter-species competition. Predators are not affected by the parasites and they consume that prey which is readily available. Both the susceptible and infected preys give the same reproductive gain to the predator population. These assumptions provide the following PPP model:

$$\begin{aligned}\frac{dx}{dt} &= ax - bx^2 - \lambda xy - \frac{cxz}{m_1 + x + y}, \\ \frac{dy}{dt} &= \lambda xy - my^2 - \frac{eyz}{m_1 + x + y} - \gamma y, \\ \frac{dz}{dt} &= z\left[r - \frac{fz}{m_2 + x + y}\right],\end{aligned}\tag{4.2}$$

where  $y$  is the density of the infected prey at time  $t$ . The parameter  $m$  is the intra-species competition coefficient of infected prey and  $e$  is the predation rate of infected prey. This model has similarity to the models (Haque and Venturino [2006], Sarwardi et al. [2011]). In fact, Haque and Venturino [2006] did not consider the inter- and intra-species competition between and among the hosts, while it was considered in Sarwardi et al. [2011]. Inclusion of inter- and intra-species competitions produces product terms like  $xy$  and  $x^2, y^2$ , respectively, which may be combined to deduce the model (4.2) from Sarwardi et al. [2011]. They mainly studied the stability and

## 4.2. The model

---

instability (through Hopf bifurcation) of different equilibrium points. Global stability of the interior equilibrium has been shown under nontrivial parametric restrictions. The basic reproduction number, secondary cases produced by an infected individual, for the deterministic system is shown to be  $R_0^D = \frac{a\lambda}{b\gamma}$ , and infection eradication is possible if  $R_0^D < 1$  (Sarwardi et al. [2011]). It was pointed out that the competition coefficient,  $b$ , contributes positively in the disease eradication process and makes a difference with the earlier study (Haque and Venturino [2006]) which does not contain the intraspecific competition. Similar PPP systems, however, may show more complicated dynamics (including chaos) in presence of disease transmission delay (Bairagi and Adak [2016]). Recent study (Adak et al. [2020]), however, shows that chaos in a delay-induced PPP system may be suppressed through proper harvesting of prey species. It is mentionable that all these studies are described in a deterministic setting and have not been explored under environmental stochasticity.

### 4.2.2 Equilibrium and their local stability

Existence of a unique interior equilibrium point  $E^*(x^*, y^*, z^*)$  of the system (4.3) and its stability can be deduced from Sarwardi et al. [2011]. The equilibrium population densities are  $y^* = \frac{(ae+\gamma c)-(be+\lambda c)x^*}{\lambda e-mc}$ ,  $z^* = \frac{r}{f}(m_2 + x^* + y^*)$ , and  $x^*$  is the unique positive root of the quadratic equation  $B_1x^{*2} - B_2x^* - B_3 = 0$ , where

$$\begin{aligned} B_1 &= \frac{be + \lambda c}{\lambda e - mc} \left[ b + \lambda - \frac{\lambda(be + \lambda c)}{\lambda e - mc} \right] - b = \frac{(\lambda^2 + mb)c}{(\lambda e - mc)^2} [\lambda(e - c) - (eb + mc)], \\ B_2 &= \frac{be + \lambda c}{\lambda e - mc} \left( a - \lambda m_1 - \frac{rc}{f} \right) + (b + \lambda) \frac{ae + \gamma c}{\lambda e - mc} - \left( a - \lambda m_1 - \frac{rc}{f} \right) \\ &\quad - 2\lambda \frac{(ae + \gamma c)(be + \lambda c)}{(\lambda e - mc)^2}, \\ B_3 &= -\left( am_1 - \frac{rcm_2}{f} \right) - \frac{ae + \gamma c}{\lambda e - mc} \left( a - \lambda m_1 - \frac{rc}{f} \right) + \lambda \left( \frac{ae + \gamma c}{\lambda e - mc} \right)^2 \\ &= \frac{c(ma + \gamma\lambda)}{\lambda e - cm} \left[ m_1 + \frac{ae + \gamma c}{\lambda e - cm} \right] + \frac{rc}{f} \left[ m_2 + \frac{ae + \gamma c}{\lambda e - cm} \right]. \end{aligned}$$

The last equation will have a unique positive root if  $B_1 > 0$  and  $B_3 > 0$ . One can observe that  $B_1 > 0$  holds if  $m < \frac{1}{c}\{\lambda(e - c) - be\} = m^*$  (say) and  $e > c$ .  $y^*$  will be positive if  $x^* < \frac{ae+\gamma c}{be+\lambda c}$  and  $\lambda > \frac{mc}{e} = \lambda^*$  (say) Therefore, a set of sufficient conditions



#### 4. Persistence and extinction of species in a disease-induced ecological system under environmental stochasticity

---

for the existence of a unique equilibrium point of system (4.3) are

$$(i) e > c, (ii) \lambda > \lambda^*, (iii) m < m^* \text{ and } (iv) x^* < \frac{ae + \gamma c}{be + \lambda c}.$$

The equilibrium  $E^*$ , whenever exists, is locally asymptotically stable if

$$(i) \frac{z^*(cx^* + ey^*)}{(m_1 + x^* + y^*)^2} < bx^* + my^* + \frac{ey^* - cx^*}{m_1 + x^* + y^*}, (ii) \frac{2cx^*z^*}{(m_1 + x^* + y^*)^2} + \frac{r^2}{f} < (b + \lambda)x^*,$$

$$(iii) \{(\lambda - b)e - (\lambda + m)c\} \left[ -m + \frac{e(m_2 - m_1)z^*}{(m_1 + x^* + y^*)^2(m_2 + x^* + y^*)} \right] + (\lambda e - mc)(\lambda + m) > 0,$$

$$(iv) \frac{2ey^*z^*}{(m_1 + x^* + y^*)^2} + (\lambda - m)y^* < r + \frac{r^2}{f}.$$

We are interested in the equilibrium point  $E^*(x^*, y^*, z^*)$ , where all populations coexist. In the absence of noise, the existence of a unique equilibrium point of the system (4.3) and its stability can be deduced from Sarwardi et al. [2011]. A unique positive interior equilibrium point exists if  $e > c$ ,  $\lambda > \lambda^*$ ,  $m < m^*$  and  $x^* < \frac{ae + \gamma c}{be + \lambda c}$ . The first condition says that the infected prey is predated at a higher rate compared to its healthy counterpart. This is a reasonable restriction because, by assumption, predators do not discriminate between infected and healthy preys, rather they consume that prey which is readily available. Since the infected prey has reduced mobility, so the attack rate is expected to be higher on infected prey compare to healthy prey. Understandably, the infection cannot persist if the force of infection is too weak. Consequently, for the existence of infected class, disease transmission rate should exceed some lower threshold value,  $\lambda^*$ . It is mentionable that the intraspecies competition arises when the same species compete for limited resources. Due to the lower fitness, the intraspecies competition among the infected prey is much smaller than that of the susceptible prey, i.e.,  $m < b$ . The third restriction  $m < m^*$  describes the threshold level of intraspecies coefficient of the infected preys. The last condition prescribes an upper bound in the equilibrium density of healthy prey for the existence of infected prey. Infected prey cannot exist if the last inequality is reversed. In addition to these conditions, the parameters need to satisfy some nontrivial conditions for the local stability of this equilibrium.

### 4.3. Mathematical results

---

#### 4.2.3 Incorporating stochasticity

We, here, consider random perturbations in the growth parameter of susceptible prey, virulence parameter and growth parameter of the predator as

$$a \rightarrow a + \sigma_1 dW_1(t), \quad -\gamma \rightarrow -\gamma + \sigma_2 dW_2(t), \quad r \rightarrow r + \sigma_3 dW_3(t),$$

where  $W_i(t), i = 1, 2, 3$ , are mutually independent Wiener process defined on a complete probability space  $(\Omega, F, P)$  with a filtration  $\{F_t\}_{t \in \mathbb{R}^+}$  and  $\sigma_i^2$  are the intensities of noises. The Wiener process  $dW_i(t)$  satisfies the properties  $\langle dW_i(t) \rangle = 0$  (gives the average value) and  $\langle dW_i(t), dW_i(t') \rangle = \delta(t - t')$  (defines the correlation function), where  $\delta$  is the Dirac delta function. Under these assumptions, the model (4.2) becomes

$$\begin{aligned} dx &= \left[ ax - bx^2 - \lambda xy - \frac{cxz}{m_1 + x + y} \right] dt + \sigma_1 x dW_1(t), \\ dy &= \left[ \lambda xy - my^2 - \frac{eyz}{m_1 + x + y} - \gamma y \right] dt + \sigma_2 y dW_2(t), \\ dz &= \left[ rz - \frac{fz^2}{m_2 + x + y} \right] dt + \sigma_3 z dW_3(t). \end{aligned} \quad (4.3)$$

All parameters are nonnegative. We analyze the stochastic model (4.3) with positive initial conditions  $x(0) > 0$ ,  $y(0) > 0$ ,  $z(0) > 0$ .

### 4.3 Mathematical results

We are mainly concerned about the solutions of the stochastic system (4.3). For any population model, the first thing one needs to investigate is the non-negativity of the stochastic solution and its global existence. Introduction of multiplicative noise can induce population explosion (Spagnolo et al. [2004], Valenti et al. [2004b]). It is, therefore, essential to show the boundedness of solutions, which means that the interacting species will not grow abruptly or exponentially for a long time. We first show that, for any positive initial value  $(x(0), y(0), z(0)) \in \mathbb{R}_+^3$ , that there exists a unique solution  $(x(t), y(t), z(t)) \in \mathbb{R}_+^3$  of the system (4.3) which remains positive and bounded for all  $t \geq 0$  with probability 1. An important aspect of population biology is the extinction and persistence of interacting species. It is important to know whether the species of the system will die out in finite time or survive. In the subsequent

#### 4. Persistence and extinction of species in a disease-induced ecological system under environmental stochasticity

---

theorems, we have shown the persistence and non-persistence of the species

**Theorem 4.3.1.** *For any initial value  $(x(0), y(0), z(0)) \in \mathbb{R}_+^3$ , there exists a unique solution  $(x(t), y(t), z(t)) \in \mathbb{R}_+^3$  of the system (4.3) for all  $t \geq 0$  and the solution remains in  $\mathbb{R}_+^3$  with probability 1, i.e.,  $(x(t), y(t), z(t)) \in \mathbb{R}_+^3$  for all  $t \geq 0$  a.s. (almost surely).*

*Proof.* This theorem can be proved similarly as presented in Theorem 2.3.1 in chapter 2.1. □

**Theorem 4.3.2.** *For any initial value  $(x(0), y(0), z(0)) \in \mathbb{R}_+^3$ , there exists some bound  $(\bar{x}, \bar{y}, \bar{z})$  of the solution  $(x(t), y(t), z(t)) \in \mathbb{R}_+^3$  of the system (4.3) for all  $t \geq 0$ .*

*Proof.* To prove this result, we will use the well known lemma 2.3.3. We now prove that the solutions of system (4.3) are stochastically ultimately bounded for any positive initial value. First we show that any solution  $(x(t), y(t), z(t))$  of system (4.3) with any positive initial value  $(x(0), y(0), z(0)) \in \mathbb{R}_+^3$  is uniformly bounded in mean. Observe that

$$dx(t) \leq x(t)(a - bx(t))dt + \sigma_1 x(t)dW_1(t).$$

Let

$$\Phi(t) = \frac{e^{\left(a - \frac{\sigma_1^2}{2}\right)t + \sigma_1 W_1(t)}}{\frac{1}{x(0)} + b \int_0^t e^{\left(a - \frac{\sigma_1^2}{2}\right)\theta + \sigma_1 W_1(\theta)} d\theta}.$$

Then  $\Phi(t)$  is the unique solution of the equation

$$\begin{cases} d\Phi(t) = \Phi(t)(a - b\phi(t))dt + \sigma_1 dB_1(t), \\ \Phi(0) = x(0). \end{cases}$$

By the comparison theorem of stochastic equation, we get  $x(t) \leq \Phi(t)$  a.s. for all  $t \in [0, \tau_e)$ . Following Lemma 2.3.3, we have

$$\limsup_{t \rightarrow \infty} E[x(t)] \leq \frac{a}{b} \quad \text{a.s.} \quad (4.4)$$

### 4.3. Mathematical results

---

Let  $G(t) = x(t) + y(t)$ . The time derivative of  $G(t)$  along the system (4.3) is given by

$$\begin{aligned} dG(t) &= \left[ x(t)(a - bx(t)) - my^2(t) - \gamma y(t) - \frac{cx(t)z(t)}{m_1 + x(t) + y(t)} - \frac{ey(t)z(t)}{m_1 + x(t) + y(t)} \right] dt \\ &\quad + x(t)\sigma_1 dW_1(t) + y(t)\sigma_2 dW_2(t) \\ &\leq [x(t)(a - bx(t)) - \gamma y(t)]dt + x(t)\sigma_1 dW_1(t) + y(t)\sigma_2 dW_2(t) \\ &\leq [2ax(t) - bx^2(t) - \xi(x(t) + y(t))]dt + x(t)\sigma_1 dW_1(t) + y(t)\sigma_2 dW_2(t), \quad \xi = \min\{a, \gamma\} \\ &= [2ax(t) - bx^2(t) - \xi G(t)]dt + x(t)\sigma_1 dW_1(t) + y(t)\sigma_2 dW_2(t). \end{aligned}$$

Integration of both sides from 0 to  $t$  gives

$$\begin{aligned} G(t) &\leq G(0) + \int_0^t [2ax(\theta) - bx^2(\theta) - \xi G(\theta)]d\theta + \sigma_1 \int_0^t x(\theta)dW_1(\theta) \\ &\quad + \sigma_2 \int_0^t y(\theta)dW_2(\theta). \end{aligned}$$

Taking expectation, one gets

$$E[G(t)] \leq G(0) + \int_0^t E[2ax(\theta) - bx^2(\theta) - \xi G(\theta)]d\theta.$$

On differentiation, we have

$$\begin{aligned} \frac{dE[G(t)]}{dt} &\leq 2aE[x(t)] - bE[x^2(t)] - \xi E[G(t)] \\ &\leq 2aE[x(t)] - b(E[x(t)])^2 - \xi E[G(t)]. \end{aligned}$$

As,  $\max\{2aE[x(t)] - b(E[x(t)])^2\} = \frac{a^2}{b}$ ,

$$\begin{aligned} \frac{dE[G(t)]}{dt} \leq \frac{a^2}{b} - \xi E[G(t)] &\implies 0 \leq \limsup_{t \rightarrow \infty} E[G(t)] \leq \frac{a^2}{b\xi} \\ &\implies \limsup_{t \rightarrow \infty} E[x(t) + y(t)] \leq \frac{a^2}{b\xi} \quad \text{a.s.} \end{aligned}$$

Hence,  $y(t)$  is also uniformly bounded in mean a.s. Now, following Markov's inequality, for any positive constant  $\alpha$  there exists  $\beta > 0$  such that  $P(x > \alpha) \leq \frac{E(x)}{\beta}$ . Following (4.4), we then have

$$\limsup_{t \rightarrow \infty} P(x > \alpha) \leq \delta_1 \quad \text{a.s., where } \delta_1 = \frac{a}{b\beta}.$$

#### 4. Persistence and extinction of species in a disease-induced ecological system under environmental stochasticity

---

Therefore, for any positive constant  $\alpha > 0$ , there is a  $\delta_1 > 0$  such that

$$\limsup_{t \rightarrow \infty} P(x > \alpha) \leq \delta_1 \text{ a.s.}$$

Hence,  $x(t)$  of system (4.3) is stochastically ultimately bounded and there exists a positive constant, say  $\bar{x} (>0)$ , such that for all  $t \in [0, \tau_e)$

$$\limsup_{t \rightarrow \infty} x(t) \leq \bar{x} \text{ a.s.}$$

In a similar manner, we can show that  $y(t)$  is also stochastically ultimately bounded and there exists a positive constant, say  $\bar{y} (>0)$ , such that for all  $t \in [0, \tau_e)$

$$\limsup_{t \rightarrow \infty} y(t) \leq \bar{y} \text{ a.s.}$$

To show  $z(t)$  is also uniformly bounded in mean, we observe that

$$dz(t) = z \left( r - \frac{fz}{m_2 + x + y} \right) + \sigma_3 z dW_3(t) \leq z \left( r - \frac{fz}{m_2 + \bar{x} + \bar{y}} \right) + \sigma_3 z dW_3(t).$$

Proceeding as before, we then obtain

$$\limsup_{t \rightarrow \infty} E[z(t)] \leq \frac{r(m_2 + \bar{x} + \bar{y})}{f} \text{ a.s.}$$

Hence  $z(t)$  of system (4.3) is stochastically ultimately bounded and there exists a positive constant  $\bar{z} > 0$  such that for all  $t \in [0, \tau_e)$

$$\limsup_{t \rightarrow \infty} z(t) \leq \bar{z} \text{ a.s.}$$

Hence the theorem is proven. □

**Theorem 4.3.3.** (i) If  $a < \frac{\sigma_1^2}{2}$  then  $x(t)$  will go to extinction a.s.

(ii) If  $a = \frac{\sigma_1^2}{2}$  then  $x(t)$  is non-persistent in the mean a.s.

(iii) If  $a > \frac{\sigma_1^2}{2} + \lambda\bar{y} + \frac{c\bar{z}}{m_1}$  then  $x(t)$  is strongly persistent in the mean a.s.

**Proof** (i) From the first equation of system (4.3), it follows that

$$dx(t) \leq x(t)(a - bx(t))dt + \sigma_1 x(t)dW_1(t).$$

### 4.3. Mathematical results

---

If we consider the system

$$dY(t) = Y(t)(a - bY(t))dt + \sigma_1 Y(t)dW_1(t), Y(0) = Y_0$$

then

$$Y(t) = \frac{e^{\left(a - \frac{\sigma_1^2}{2}\right)t + \sigma_1 W_1(t)}}{\frac{1}{Y_0} + b \int_0^t e^{\left(a - \frac{\sigma_1^2}{2}\right)s + \sigma_1 W_1(s)} ds}.$$

Obviously  $x(t) \leq Y(t) \quad \forall t$  and if  $a - \frac{\sigma_1^2}{2} < 0$ , then  $\lim_{t \rightarrow \infty} Y(t) = 0$  and since  $x(t)$  is non-negative, we have  $\lim_{t \rightarrow \infty} x(t) = 0$ .

(ii) We have from the first equation of system (4.3)

$$\begin{aligned} d(\ln(x)) &= \left[ a - bx - \lambda y - \frac{cz}{m_1 + x + y} - \frac{\sigma_1^2}{2} \right] dt + \sigma_1 dW_1(t) \\ \frac{\ln(x(t))}{t} &= \left( a - \frac{\sigma_1^2}{2} \right) - \frac{b}{t} \int_0^t x(s) ds - \frac{\lambda}{t} \int_0^t y(s) ds - \frac{c}{t} \int_0^t \frac{z(s)}{m_1 + x(s) + y(s)} ds \\ &\quad + \frac{\int_0^t \sigma_1 dW_1(t)}{t} + \frac{\ln x(0)}{t}. \end{aligned}$$

$$\therefore \ln x(t) - \ln x(0) \leq \left( a - \frac{\sigma_1^2}{2} \right) t - b \int_0^t x(s) ds + M_1, \quad (4.5)$$

where  $M_1 = \int_0^t \sigma_1 dW_1(t)$ . By strong law of large number for Martingales yields

$$\lim_{t \rightarrow \infty} \frac{M_1(t)}{t} = 0 \quad \text{a.s.}$$

From the property of limit, for arbitrary  $\epsilon_1 > 0$ ,  $\exists T_1 > 0$  such that  $\forall t \geq T_1$ ,  $\frac{M_1(t)}{t} \leq \epsilon_1$ . From (4.5), under the assumption  $a - \frac{\sigma_1^2}{2} = 0$ , we have

$$\begin{aligned} \frac{1}{t} \ln \frac{x(t)}{x(0)} &\leq \epsilon_1 - b \frac{x(0)}{t} \int_0^t \frac{x(s)}{x(0)} ds. \\ \therefore \limsup_{t \rightarrow \infty} \frac{1}{t} \int_0^t x(s) ds &\leq \epsilon_1. \end{aligned}$$

#### 4. Persistence and extinction of species in a disease-induced ecological system under environmental stochasticity

---

Since  $\epsilon_1$  is arbitrary and  $x(t)$  is non-negative, we therefore have

$$\limsup_{t \rightarrow \infty} \frac{1}{t} \int_0^t x(s) ds = 0$$

and  $x(t)$  is non-persistent in mean.

(iii) Again, from the first equation

$$\begin{aligned} d \ln x &\geq \left( a - bx - \lambda y - \frac{cz}{m_1} - \frac{\sigma_1^2}{2} \right) dt + \sigma_1 dW_1(t) \\ \Rightarrow \ln \frac{x(t)}{x(0)} &\geq \left( a - \lambda \bar{y} - \frac{c\bar{z}}{m_1} - \frac{\sigma_1^2}{2} \right) t - b \int_0^t x(\theta) d\theta + \sigma_1 W_1(t). \end{aligned}$$

Therefore, if  $a - \lambda \bar{y} - \frac{c\bar{z}}{m_1} - \frac{\sigma_1^2}{2} > 0$  then by applying Lemma 1.7.3, we obtain

$$\liminf_{t \rightarrow \infty} \frac{1}{t} \int_0^t x(t) \geq \frac{1}{b} \left( a - \lambda \bar{y} - \frac{c\bar{z}}{m_1} - \frac{\sigma_1^2}{2} \right) > 0.$$

Evidently,  $x(t)$  is strongly persistent in the mean if  $a > \frac{\sigma_1^2}{2} + \lambda \bar{y} + \frac{c\bar{z}}{m_1}$ .

**Theorem 4.3.4.** (a) For  $a < \frac{\sigma_1^2}{2}$ ,  $y(t)$  will go to extinction a.s.

(b) For  $a > \frac{\sigma_1^2}{2}$ ,

(i) if  $\lambda \left( a - \frac{\sigma_1^2}{2} \right) < b \left( \gamma + \frac{\sigma_2^2}{2} \right)$  then  $y(t)$  will go to extinction a.s.

(ii) if  $\lambda \left( a - \frac{\sigma_1^2}{2} \right) = b \left( \gamma + \frac{\sigma_2^2}{2} \right)$  then  $y(t)$  is non-persistent in the mean a.s.

(iii) if  $\lambda \left( a - \frac{\sigma_1^2}{2} \right) > b \left( \gamma + \frac{\sigma_2^2}{2} \right) + \lambda^2 \bar{y} + (\lambda c + be) \frac{\bar{z}}{m_1}$  then  $y(t)$  is strongly persistent in the mean a.s.

**Proof** (a) Suppose  $a - \frac{\sigma_1^2}{2} < 0$ . From Theorem 4.3.3, one can easily see that

$$\limsup_{t \rightarrow \infty} \frac{1}{t} \int_0^t x(\theta) d\theta < 0.$$

Integration of second equation of system (4.3) yields

$$\begin{aligned} \frac{\ln(y(t))}{t} &= \frac{\lambda}{t} \int_0^t x(s) ds - \frac{m}{t} \int_0^t y(s) ds - \gamma - \frac{\sigma_2^2}{2} - \frac{e}{t} \int_0^t \frac{z(s)}{m_1 + x(s) + y(s)} ds \\ &\quad + \frac{\int_0^t \sigma_2 dW_2(t)}{t} + \frac{\ln y(0)}{t}. \end{aligned} \tag{4.6}$$

### 4.3. Mathematical results

---

Then the equation (4.6) coupled with the extinction condition of  $x(t)$  yields

$$\begin{aligned} \frac{\ln y(t) - \ln y(0)}{t} &\leq \left(-\gamma - \frac{\sigma_2^2}{2}\right) + \frac{\lambda}{t} \int_0^t x(\theta) d\theta + \sigma_2 \frac{\int_0^t dW_2(t)}{t} \\ \Rightarrow \limsup_{t \rightarrow \infty} \frac{1}{t} \int_0^t y(\theta) d\theta &\leq \left(-\gamma - \frac{\sigma_2^2}{2}\right) < 0 \\ \Rightarrow \lim_{t \rightarrow \infty} y(t) &= 0. \end{aligned}$$

Therefore, extinction of  $x(t)$  implies the extinction of  $y(t)$ .

(b) (i) If we consider  $a - \frac{\sigma_1^2}{2} > 0$  then from the first equation of (4.3)

$$\frac{\ln x(t) - \ln x(0)}{t} \leq a - \frac{\sigma_1^2}{2} - \frac{b}{t} \int_0^t x(\theta) d\theta + \sigma_1 \frac{\int_0^t dW_1(t)}{t}. \quad (4.7)$$

Lemma 1.7.3 then leads to

$$\limsup_{t \rightarrow \infty} \frac{1}{t} \int_0^t x(\theta) d\theta \leq \frac{a - \frac{\sigma_1^2}{2}}{b}. \quad (4.8)$$

Again from (4.3), we have

$$\begin{aligned} \frac{\ln y(t) - \ln y(0)}{t} &\leq \left(-\gamma - \frac{\sigma_2^2}{2}\right) + \frac{\lambda}{t} \int_0^t x(\theta) d\theta - \frac{m}{t} \int_0^t y(\theta) d\theta + \sigma_2 \frac{W_2(t)}{t} \\ \therefore \limsup_{t \rightarrow \infty} \frac{1}{t} \int_0^t y(\theta) d\theta &\leq \frac{\lambda \left(a - \frac{\sigma_1^2}{2}\right) - b \left(\gamma + \frac{\sigma_2^2}{2}\right)}{mb}. \end{aligned} \quad (4.9)$$

Thus, if  $\lambda \left(a - \frac{\sigma_1^2}{2}\right) < b \left(\gamma + \frac{\sigma_2^2}{2}\right)$  then  $\lim_{t \rightarrow \infty} y(t) = 0$ .

(ii) Assume  $\limsup_{t \rightarrow \infty} \frac{1}{t} \int_0^t y(\theta) d\theta \geq 0$ . For sufficiently small  $\eta > 0$ , there exists  $T > 0$  such that for all  $t > T$ ,

$$\frac{\lambda}{t} \int_0^t x(\theta) d\theta < \limsup_{t \rightarrow \infty} \frac{\lambda}{t} \int_0^t x(\theta) d\theta + \eta.$$



#### 4. Persistence and extinction of species in a disease-induced ecological system under environmental stochasticity

---

Second equation of (4.3) then yields

$$\begin{aligned} \frac{\ln y(t) - \ln y(0)}{t} &\leq \left(-\gamma - \frac{\sigma_2^2}{2}\right) + \frac{\lambda}{t} \int_0^t x(\theta) d\theta - \frac{m}{t} \int_0^t y(\theta) d\theta + \sigma_2 \frac{W_2(t)}{t} \\ &\leq \left(-\gamma - \frac{\sigma_2^2}{2}\right) + \limsup_{t \rightarrow \infty} \frac{\lambda}{t} \int_0^t x(\theta) d\theta + \eta - \frac{m}{t} \int_0^t y(\theta) d\theta + \sigma_2 \frac{W_2(t)}{t}. \end{aligned}$$

By Lemma 1.7.3, one have

$$\limsup_{t \rightarrow \infty} \frac{1}{t} \int_0^t y(\theta) d\theta \leq \frac{\left(-\gamma - \frac{\sigma_2^2}{2}\right) + \limsup_{t \rightarrow \infty} \frac{\lambda}{t} \int_0^t x(\theta) d\theta + \eta}{m}.$$

If  $\lambda \left(a - \frac{\sigma_1^2}{2}\right) = b \left(\gamma + \frac{\sigma_2^2}{2}\right)$  then we must have  $a > \frac{\sigma_1^2}{2}$ . As  $\eta$  is arbitrary, we get form (4.8)

$$\limsup_{t \rightarrow \infty} \frac{1}{t} \int_0^t y(\theta) d\theta \leq \frac{-b \left(\gamma + \frac{\sigma_2^2}{2}\right) + \lambda \left(a - \frac{\sigma_1^2}{2}\right)}{bm} = 0,$$

provided  $\lambda \left(a - \frac{\sigma_1^2}{2}\right) = b \left(\gamma + \frac{\sigma_2^2}{2}\right)$ . Thus,  $y(t)$  is non-persistent in the mean a.s. if  $\lambda \left(a - \frac{\sigma_1^2}{2}\right) = b \left(\gamma + \frac{\sigma_2^2}{2}\right)$ .

(iii) From the second equations of (4.3), we have

$$\begin{aligned} \frac{1}{t} \ln \frac{y(t)}{y(0)} &= - \left(\gamma + \frac{\sigma_2^2}{2}\right) + \frac{\lambda}{t} \int_0^t x(\theta) d\theta - \frac{m}{t} \int_0^t y(\theta) d\theta - \frac{1}{t} \int_0^t \frac{ez(\theta)}{m_1 + x(\theta) + y(\theta)} d\theta \\ &\quad + \sigma_2 \frac{W_2(t)}{t} \\ &\geq - \left(\gamma + \frac{\sigma_2^2}{2}\right) + \liminf_{t \rightarrow \infty} \frac{\lambda}{t} \int_0^t x(\theta) d\theta - \frac{m}{t} \int_0^t y(\theta) d\theta \\ &\quad - \frac{1}{t} \int_0^t \frac{ez(\theta)}{m_1 + x(\theta) + y(\theta)} d\theta + \sigma_2 \frac{W_2(t)}{t} \\ &\geq - \left(\gamma + \frac{\sigma_2^2}{2}\right) + \frac{\lambda}{b} \left(a - \lambda \bar{y} - \frac{e\bar{z}}{m_1} - \frac{\sigma_1^2}{2}\right) - \frac{e\bar{z}}{m_1} - \frac{m}{t} \int_0^t y(\theta) d\theta + \sigma_2 \frac{W_2(t)}{t}. \end{aligned}$$

### 4.3. Mathematical results

---

Assuming  $\lambda \left( a - \frac{\sigma_1^2}{2} \right) > b \left( \gamma + \frac{\sigma_2^2}{2} \right) + \lambda^2 \bar{y} + (\lambda c + be) \frac{\bar{z}}{m_1}$ , from Lemma 1.7.3, it follows

$$\liminf_{t \rightarrow \infty} \frac{1}{t} \int_0^t y(\theta) d\theta \geq \frac{\lambda \left( a - \frac{\sigma_1^2}{2} \right) - b \left( \gamma + \frac{\sigma_2^2}{2} \right) - \left( \lambda^2 \bar{y} + (\lambda c + be) \frac{\bar{z}}{m_1} \right)}{mb}.$$

Clearly,  $y(t)$  is strongly persistent in the mean if  $\lambda \left( a - \frac{\sigma_1^2}{2} \right) > b \left( \gamma + \frac{\sigma_2^2}{2} \right) + \lambda^2 \bar{y} + (\lambda c + be) \frac{\bar{z}}{m_1}$ .

The proof of Theorem 4.3.5 is similar to that of Theorem 4.3.3 and hence omitted.

**Theorem 4.3.5.** (i) If  $r < \frac{\sigma_2^2}{2}$  then  $z(t)$  will go to extinction a.s.

(ii) If  $r = \frac{\sigma_2^2}{2}$  then  $z(t)$  is non-persistent in the mean a.s.

(iii) If  $r > \frac{\sigma_2^2}{2}$  then  $z(t)$  is strongly persistent in the mean a.s.

**Remark 4.3.6.** From (4.7), we have  $\limsup_{t \rightarrow \infty} \frac{\ln x(t)}{t} \leq a - \frac{\sigma_1^2}{2}$ . Then there exists a sufficiently large  $T_3 > 0$  such that  $\frac{\ln x(t)}{t} < a - \frac{\sigma_1^2}{2} \quad \forall t > T_3$ . Therefore,  $x(t) < e^{\left( a - \frac{\sigma_1^2}{2} \right) t} \quad \forall t > T_3$ . It shows that  $x$  is a monotonic decreasing function of time under the restriction  $a < \frac{\sigma_1^2}{2}$  and the extinction of susceptible prey will be faster as the noise,  $\sigma_1$ , becomes larger. Similarly, one can show from (4.9) that the infected prey  $y$  extinct monotonically under the restriction  $\lambda \left( a - \frac{\sigma_1^2}{2} \right) < b \left( \gamma + \frac{\sigma_2^2}{2} \right)$  and the extinction will be quicker if the corresponding noise  $\sigma_2$  grows faster. From (4.3), it is straightforward to show that increasing noise in predator population also ushers quicker extinction.

These results provide a quantitative measure on the system parameters and/or prescribe some limits on the environmental noises for which both the prey and predator populations can persist together or in isolation. It shows that species extinction may occur through many routes. For example, if the intrinsic growth rate of healthy prey is less than half of the corresponding noise intensity, then healthy prey cannot survive but can survive if its growth rate exceeds this critical value. It is obvious that infected prey also cannot survive in the absence of susceptible prey (see Theorem 4.3.4a). Theorem 4.3.4b says that infected prey  $y(t)$  will go extinct while sound prey  $x(t)$  may persist if the basic reproduction number  $R_0^S < 1$ , where  $R_0^S = \frac{\lambda \left( a - \frac{\sigma_1^2}{2} \right)}{b \left( \gamma + \frac{\sigma_2^2}{2} \right)}$ . This is an extremely important measure from the infection management point of view. It describes that disease control may be possible by tuning some system parameters as well as the noise parameters. The parameters  $b$  and  $\gamma$ , measuring the intra-species competition and removal rate of infected prey, have a negative correlation with the

#### 4. Persistence and extinction of species in a disease-induced ecological system under environmental stochasticity

---

basic reproduction number, and  $R_0^S$  can be reduced to below unity by increasing these rate parameters. In contrast, the infection rate parameter  $\lambda$  is positively correlated with  $R_0^S$ . Interestingly, both the noise parameters are negatively correlated with  $R_0^S$ . Thus, proper adjustment of environmental noise can potentially change the disease state of a system. The last theorem prescribes a relationship between the predator's intrinsic growth rate and noise intensity that allows its survival.

It is to be mentioned that most of the stochastic systems have no exact equilibrium, instead, it may have a time-independent probability distribution (May [1973]). The following theorem shows the existence of such stationary distribution for the populations of system (4.3).

**Theorem 4.3.7.** *Let  $(x(t), y(t), z(t)) \in \mathbb{R}^3$  be a solution of the stochastic system (4.3) with initial value  $(x(0), y(0), z(0)) \in \mathbb{R}^3$ . If the conditions (i)  $\frac{fz^*}{rm_2^2} > \max\left\{\frac{Ac}{m_1+\bar{x}+\bar{y}}, \frac{Ae}{m_1+\bar{x}+\bar{y}}\right\}$ , (ii)  $Ab > \frac{cz^*}{m_1} + \frac{fz^*}{2rm_2^2} + \frac{(c+e)z^*}{2m_1}$ , (iii)  $m + \frac{Ae}{m_1+\bar{x}+\bar{y}} > \frac{ez^*}{m_1} + \frac{fz^*}{2rm_2^2} + \frac{(c+e)z^*}{2m_1}$ , (iv)  $\frac{f}{r(m_2+\bar{x}+\bar{y})} + \frac{A(e+c)}{2(m_1+\bar{x}+\bar{y})} > \frac{fz^*}{rm_2^2}$  are satisfied, then*

$$\limsup_{t \rightarrow \infty} \frac{1}{t} \int_0^t [(x(s) - x^*)^2 + (y(s) - y^*)^2 + (z(s) - z^*)^2] ds \leq G\Theta \quad a.s.,$$

where  $A = m_1 + x^* + y^*$ ,  $\Theta = \frac{A\sigma_1^2 x^*}{2} + \frac{A\sigma_2^2 y^*}{2} + \frac{\sigma_3^2 z^*}{2r}$ ,  $G = \frac{1}{\min\{K, Q, T\}}$ ,  $K = Ab - \frac{cz^*}{m_1} - \frac{fz^*}{2rm_2^2} - \frac{(c+e)z^*}{2m_1}$ ,  $Q = m - \frac{ez^*}{m_1} - \frac{fz^*}{2rm_2^2} - \frac{(c+e)z^*}{2m_1} + \frac{Ae}{2(m_1+\bar{x}+\bar{y})}$  and  $T = \frac{f}{r(m_2+\bar{x}+\bar{y})} + \frac{A(e+c)}{2(m_1+\bar{x}+\bar{y})} - \frac{fz^*}{rm_2^2}$ ,  $\bar{x}$ ,  $\bar{y}$ ,  $\bar{z}$  are the stochastic bounds of  $x(t)$ ,  $y(t)$ ,  $z(t)$ , respectively, and  $(x^*, y^*, z^*)$  is the interior equilibrium point of the deterministic system (4.2).

**Proof** System (4.3) can be written as

$$\begin{aligned} d \begin{pmatrix} x(t) \\ y(t) \\ z(t) \end{pmatrix} &= \begin{pmatrix} x(a - bx) - \lambda xy - \frac{cxz}{m_1+x+y} \\ \lambda xy - my^2 - \gamma y - \frac{eyz}{m_1+x+y} \\ r - \frac{fz}{m_2+x+y} \end{pmatrix} dt + \begin{pmatrix} \sigma_1 x(t) \\ 0 \\ 0 \end{pmatrix} dW_1(t) \\ &+ \begin{pmatrix} 0 \\ \sigma_2 y(t) \\ 0 \end{pmatrix} dW_2(t) + \begin{pmatrix} 0 \\ 0 \\ \sigma_3 z(t) \end{pmatrix} dW_3(t) \end{aligned}$$

### 4.3. Mathematical results

---

and the diffusion matrix is

$$A' = \begin{pmatrix} \sigma_1^2 x^2 & 0 & 0 \\ 0 & \sigma_2^2 y^2 & 0 \\ 0 & 0 & \sigma_3^2 z^2 \end{pmatrix}.$$

Define  $\bar{V}(x, y, z) = V_1(x, y, z) + V_2(x, y, z) + V_3(x, y, z)$ , where

$$V_1 = A \left[ x - x^* - x^* \ln \frac{x}{x^*} \right], \quad V_2 = A \left[ y - y^* - y^* \ln \frac{y}{y^*} \right], \quad V_3 = \frac{1}{r} \left[ z - z^* - z^* \ln \frac{z}{z^*} \right].$$

At  $E^*$ , we have

$$a = bx^* + \lambda y^* + \frac{cz^*}{m_1 + x^* + y^*}, \quad \gamma = \lambda x^* - my^* - \frac{ez^*}{m_1 + x^* + y^*}, \quad \frac{f}{r} \left( \frac{z^*}{m_2 + x^* + y^*} \right) = 1. \quad (4.10)$$

Using (4.10), one can calculate

$$\begin{aligned} d\bar{V} &= A \left[ 1 - \frac{x^*}{x} \right] \left\{ \left[ ax - bx^2 - \lambda xy - \frac{cxz}{m_1 + x + y} \right] dt + \sigma_1 x dW_1(t) \right\} \\ &\quad + A \left[ 1 - \frac{y^*}{y} \right] \left\{ \left[ \lambda xy - my^2 - \frac{eyz}{m_1 + x + y} - \gamma y \right] dt + \sigma_2 y dW_2(t) \right\} \\ &\quad + \frac{1}{r} \left[ 1 - \frac{z^*}{z} \right] \left\{ \left[ rz - \frac{fz^2}{m_2 + x + y} \right] dt + \sigma_3 z dW_3(t) \right\} \\ &= L\bar{V} dt + A(x - x^*) dW_1(t) + A(y - y^*) dW_2(t) + \frac{1}{r}(z - z^*) dW_3(t), \end{aligned}$$

where

$$\begin{aligned} L\bar{V} &= - \left( Ab - \frac{cz^*}{m_1 + x + y} \right) (x - x^*)^2 - \left( m - \frac{ez^*}{m_1 + x + y} \right) (y - y^*)^2 - \frac{f(z - z^*)^2}{r(m_2 + x + y)} \\ &\quad + \left[ \frac{fz^*}{r(m_2 + x^* + y^*)(m_2 + x + y)} - \frac{Ac}{m_1 + x + y} \right] (z - z^*)(x - x^*) \\ &\quad + \left[ \frac{fz^*}{r(m_2 + x^* + y^*)(m_2 + x + y)} - \frac{Ae}{m_1 + x + y} \right] (z - z^*)(y - y^*) \\ &\quad + \frac{(c + e)z^*(x - x^*)(y - y^*)}{m_1 + x + y} + \Theta \\ &\leq - \left( Ab - \frac{cz^*}{m_1 + x + y} \right) (x - x^*)^2 - \left( m - \frac{ez^*}{m_1 + x + y} \right) (y - y^*)^2 - \frac{f(z - z^*)^2}{r(m_2 + x + y)} \\ &\quad + \left[ \frac{fz^*}{rm_2^2} - \frac{Ac}{m_1 + x + y} \right] (z - z^*)(x - x^*) + \left[ \frac{fz^*}{rm_2^2} - \frac{Ae}{m_1 + x + y} \right] (z - z^*)(y - y^*) \end{aligned}$$

#### 4. Persistence and extinction of species in a disease-induced ecological system under environmental stochasticity

---

$$\begin{aligned}
& + \frac{(c+e)z^*(x-x^*)(y-y^*)}{m_1+x+y} + \Theta \\
\leq & - \left( Ab - \frac{cz^*}{m_1+x+y} \right) (x-x^*)^2 - \left( m - \frac{ez^*}{m_1+x+y} \right) (y-y^*)^2 - \frac{f(z-z^*)^2}{r(m_2+x+y)} \\
& + \left[ \frac{fz^*}{rm_2^2} - \frac{Ac}{m_1+\bar{x}+\bar{y}} \right] (z-z^*)(x-x^*) + \left[ \frac{fz^*}{rm_2^2} - \frac{Ae}{m_1+\bar{x}+\bar{y}} \right] (z-z^*)(y-y^*) \\
& + \frac{(c+e)z^*(x-x^*)(y-y^*)}{m_1+x+y} + \Theta.
\end{aligned}$$

Let us assume  $\frac{fz^*}{rm_2^2} > \max \left\{ \frac{Ac}{m_1+\bar{x}+\bar{y}}, \frac{Ae}{m_1+\bar{x}+\bar{y}} \right\}$ . Hence

$$\begin{aligned}
L\bar{V} & \leq - \left( Ab - \frac{cz^*}{m_1} \right) (x-x^*)^2 - \left( m - \frac{ez^*}{m_1} \right) (y-y^*)^2 - \frac{f(z-z^*)^2}{r(m_2+x+y)} \\
& + \left[ \frac{fz^*}{rm_2^2} - \frac{Ac}{m_1+\bar{x}+\bar{y}} \right] |z-z^*||x-x^*| + \left[ \frac{fz^*}{rm_2^2} - \frac{Ae}{m_1+\bar{x}+\bar{y}} \right] |z-z^*||y-y^*| \\
& + \frac{(c+e)z^*|x-x^*||y-y^*|}{m_1} + \Theta \\
& \leq - \left[ Ab - \frac{cz^*}{m_1} - \frac{fz^*}{2rm_2^2} - \frac{(c+e)z^*}{2m_1} \right] (x-x^*)^2 - \left[ m - \frac{ez^*}{m_1} - \frac{fz^*}{2rm_2^2} - \frac{(c+e)z^*}{2m_1} \right. \\
& \left. + \frac{Ae}{2(m_1+\bar{x}+\bar{y})} \right] (y-y^*)^2 - \left[ \frac{f}{r(m_2+\bar{x}+\bar{y})} + \frac{A(e+c)}{2(m_1+\bar{x}+\bar{y})} - \frac{fz^*}{rm_2^2} \right] (z-z^*)^2 + \Theta.
\end{aligned}$$

Therefore, if  $Ab > \frac{cz^*}{m_1} + \frac{fz^*}{2rm_2^2} + \frac{(c+e)z^*}{2m_1}$ ,  $m + \frac{Ae}{2(m_1+\bar{x}+\bar{y})} > \frac{ez^*}{m_1} + \frac{fz^*}{2rm_2^2} + \frac{(c+e)z^*}{2m_1}$  and  $\frac{f}{r(m_2+\bar{x}+\bar{y})} + \frac{A(e+c)}{2(m_1+\bar{x}+\bar{y})} > \frac{fz^*}{rm_2^2}$  hold, we then have

$$\begin{aligned}
d\bar{V} & \leq - [K(x-x^*)^2 + Q(y-y^*)^2 + T(z-z^*)^2 - \Theta] dt + A(x-x^*)dW_1(t) \\
& \quad + A(y-y^*)dW_2(t) + \frac{1}{r}(z-z^*)dW_3(t) \\
& \leq - [\min \{K, Q, T\} (x-x^*)^2 + Q(y-y^*)^2 + T(z-z^*)^2 - \Theta] dt + A(x-x^*)dW_1(t) \\
& \quad + A(y-y^*)dW_2(t) + \frac{1}{r}(z-z^*)dW_3(t).
\end{aligned}$$

Integrating it from 0 to  $t$ , we obtain

$$\begin{aligned}
\bar{V}(t) - \bar{V}(0) & \leq -\min \{K, Q, T\} \int_0^t [(x(s) - x^*)^2 + (y(s) - y^*)^2 + (z(s) - z^*)^2] ds + \Theta t \\
& \quad + \int_0^t \left[ A(x(s) - x^*)dW_1(s) + A(y(s) - y^*)dW_2(s) + \frac{1}{r}(z(s) - z^*)dW_3(s) \right].
\end{aligned}$$

### 4.3. Mathematical results

---

Therefore,

$$\int_0^t [(x(s) - x^*)^2 + (y(s) - y^*)^2 + (z(s) - z^*)^2] ds \leq \frac{\bar{V}(0)}{\min \{K, Q, T\}} + \frac{\Theta t}{\min \{K, Q, T\}} + \frac{1}{\min \{K, Q, T\}} \int_0^t \left[ A(x(s) - x^*)dW_1(s) + A(y(s) - y^*)dW_2(s) + \frac{1}{r}(z(s) - z^*)dW_3(s) \right] \quad (4.11)$$

Assume  $M(t) = \int_0^t [A(x(s) - x^*)dW_1(s) + A(y(s) - y^*)dW_2(s) + \frac{1}{r}(z(s) - z^*)dW_3(s)]$ .

$M$  is a continuous martingale and  $M(0) = 0$ . Moreover,

$$\begin{aligned} \langle M, M \rangle_t &= \left( \int_0^t \left[ A(x(s) - x^*)dW_1(s) + A(y(s) - y^*)dW_2(s) + \frac{1}{r}(z(s) - z^*)dW_3(s) \right] \right)^2 \\ &= \left( \int_0^t \left[ A^2(x(s) - x^*)^2 ds + A^2(y(s) - y^*)^2 ds + \frac{1}{r^2}(z(s) - z^*)^2 ds \right] \right) \\ &\leq \left( A^2(\bar{x}^2 + \bar{y}^2) + \frac{1}{r^2}\bar{z}^2 \right) t \end{aligned}$$

and

$$\limsup_{t \rightarrow \infty} \frac{\langle M, M \rangle_t}{t} \leq A^2(\bar{x}^2 + \bar{y}^2) + \frac{1}{r^2}\bar{z}^2 < \infty \quad \text{a.s.}$$

Using the Lemma 1.7.7, one gets

$$\limsup_{t \rightarrow \infty} \frac{M(t)}{t} = 0 \quad \text{a.s.}$$

Therefore, from (4.11), we obtain

$$\limsup_{t \rightarrow \infty} \frac{1}{t} \int_0^t [(x(s) - x^*)^2 + (y(s) - y^*)^2 + (z(s) - z^*)^2] ds \leq G\Theta \quad \text{a.s.}$$

where  $G = \frac{1}{\min \{K, Q, T\}}$ .

It shows that  $\Theta \rightarrow 0$  if the noise intensities  $\sigma_1, \sigma_2, \sigma_3$  tend to zero, and we then have

$$\limsup_{t \rightarrow \infty} \frac{1}{t} \int_0^t [(x(s) - x^*)^2 + (y(s) - y^*)^2 + (z(s) - z^*)^2] ds \rightarrow 0,$$

yielding  $\lim_{t \rightarrow \infty} (x(t), y(t), z(t)) = (x^*, y^*, z^*)$ . Therefore, the stochastic solution will remain close and eventually approach the time-independent equilibrium solution of the deterministic system when noise intensities are negligible.

## 4. Persistence and extinction of species in a disease-induced ecological system under environmental stochasticity

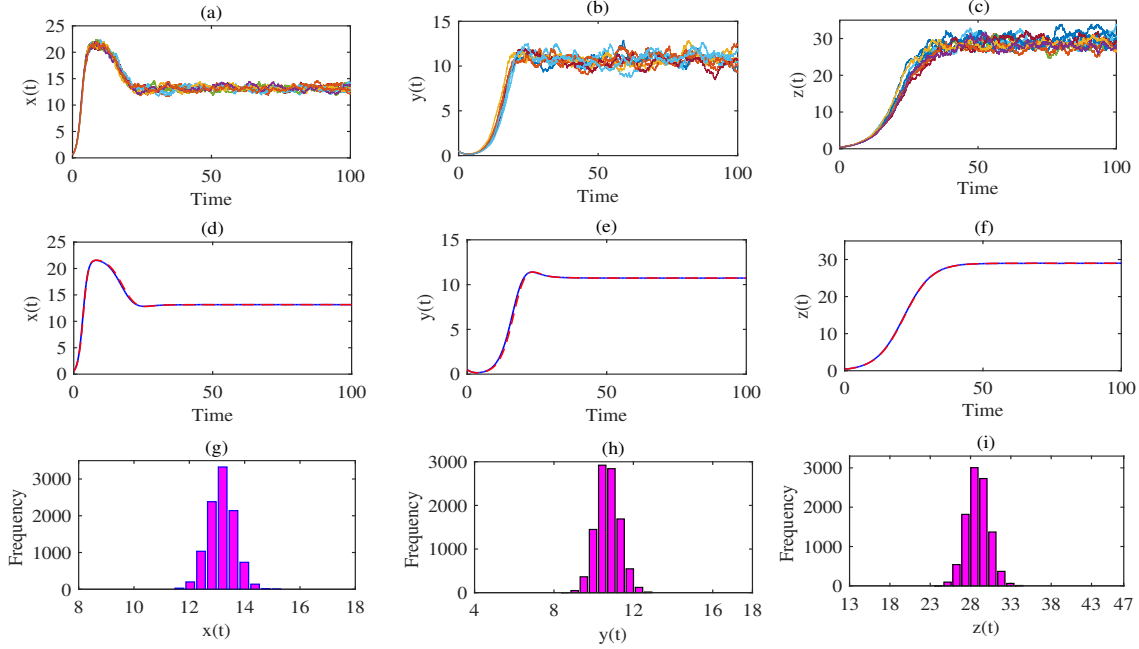


**Figure 4.1:** Upper panel: Time series solutions of 15 simulations of the stochastic system (4.3) with noise intensity  $\sigma_1 = 0.03$ ,  $\sigma_2 = 0.03$ ,  $\sigma_3 = 0.03$ . Middle panel: Average value of 1000 time series solutions with the same noise intensity. It shows that the stochastic solution (solid blue curve) and the deterministic solution (red broken line) are qualitatively and quantitatively similar. Lower panel: Frequency distribution of the populations at  $t = 100$  for 10,000 simulations of system (4.3). It shows small fluctuations in the population densities around the deterministic steady state value  $E^*(x^*, y^*, z^*) = (13.16, 10.73, 28.98)$ . Parameters are  $a = 1.1$ ,  $b = 0.05$ ,  $\lambda = 0.04$ ,  $c = 0.1$ ,  $e = 0.12$ ,  $f = 1.2$ ,  $m_1 = 200$ ,  $m = 0.001$ ,  $\gamma = 0.5$ ,  $r = 0.2$ ,  $m_2 = 150$  and the initial value is  $(0.6, 0.5, 0.4)$ .

### 4.4 Simulation results

Simulation study has been performed in two steps. First, we illustrate the theoretical results presented in the previous section, and in the second step, we consider an experimental data set to demonstrate how our stochastic model fits these data.

#### 4.4.1 Effect of environmental noise on the persistence and extinction of species

It is to be recalled that a deterministic model always gives a unique solution corresponding to a unique initial point when system parameters remain fixed. However, a stochastic solution of the same system gives different solutions for each simulation

#### 4.4. Simulation results

---

due to its inherent stochasticity even when the initial value and system parameters remain the same (see Fig. 4.1, first row). It will be, therefore, prudent to plot the mean value of such solutions corresponding to a fixed value of the noises to represent the overall behaviour of the system's solutions. We first demonstrate how different noise intensities can alter persistency of interacting species while the other system parameters remain unchanged. Choosing weak noise intensities like  $\sigma_1 = 0.03$ ,  $\sigma_2 = 0.03$ ,  $\sigma_3 = 0.03$  so that the conditions of stochastic persistence (see Theorems 4.3.3(iii), 4.3.4b(iii), 4.3.5(iii)) and stationary distribution (Theorem 4.3.7) are satisfied, one can observe that the stochastic and deterministic solutions (Fig. 4.1, middle row) show similar behaviour and the population densities of system (4.3) remain very close to the equilibrium solution  $E^*(13.16, 10.73, 28.98)$  of the deterministic system (4.2). In the lower panel of Fig. 4.1, we presented the frequency distribution, where the width of rectangles represent various classes, and its height indicates the frequency of the class. It is to be mentioned that the coefficient of variation of the time series solution of the stochastic system (4.3) is very low after  $t = 100$  and, therefore, the system was run for 100 to show the asymptotic behavior. The behaviour will remain the same for higher run. Distribution of the rectangles indicates how much the stochastic solutions will oscillate around the deterministic steady state for the considered noise intensity. It can be observed that  $x$ ,  $y$  and  $z$ -populations are distributed in the range (11.6, 15.2), (8.6, 12.8) and



## 4. Persistence and extinction of species in a disease-induced ecological system under environmental stochasticity

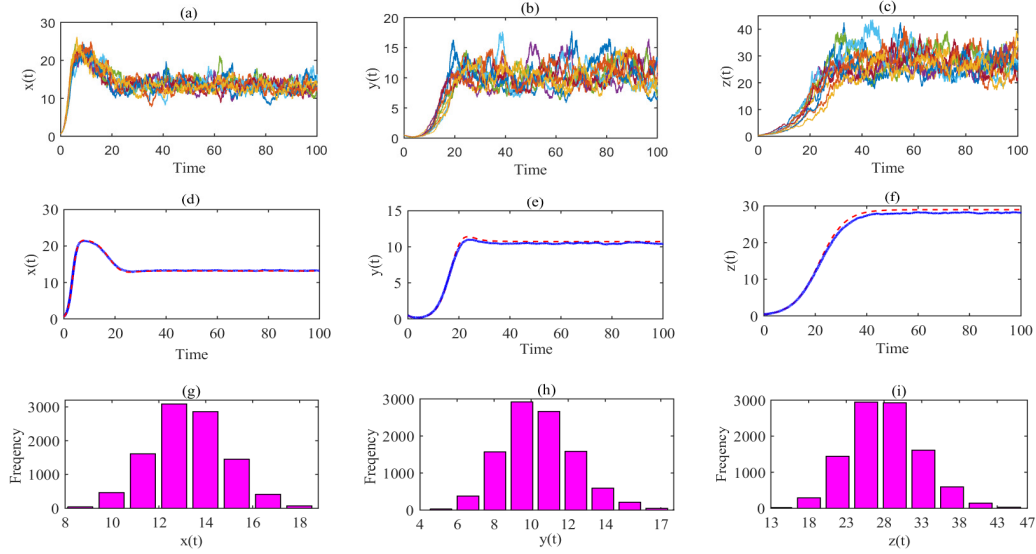


**Figure 4.2:** Upper panel: Time series solutions of 15 simulations of the stochastic system (4.3) with noise intensity  $\sigma_1 = 0.1$ ,  $\sigma_2 = 0.1$ ,  $\sigma_3 = 0.1$ . Middle panel: Average value of 1000 solutions of system (4.3) with the same noise intensity (solid blue line) and the solution of the deterministic system (4.2) (red broken line). Lower panel: Frequency distribution of the respective populations obtained at  $t = 100$  for 10,000 simulations of system (4.3). Parameters are as in Fig. 4.1.

(24, 34.1), respectively, and the highest frequency is observed at 13.2, 10.4, 28.5, which is very close to the deterministic steady state value  $E^*(x^*, y^*, z^*) = (13.16, 10.73, 28.98)$ . If we increase the strength of noises then the fluctuation increases. For higher values of  $\sigma_1 = 0.1$ ,  $\sigma_2 = 0.1$ ,  $\sigma_3 = 0.1$ , the population densities (Fig. 4.2) fluctuate more around the deterministic steady state  $E^*(x^*, y^*, z^*)$ . In this case, the frequency distribution of  $x(t)$ ,  $y(t)$  and  $z(t)$  populations are distributed over a larger range (8.6, 18), (5.1, 16.8), (13.4, 45.8) around the deterministic steady state values  $x^* = 13.16$ ,  $y^* = 10.73$  and  $z^* = 28.98$ . The 'probabilistic smoke cloud' of the system (4.3) for the above two sets of forcing intensities are shown in Fig. 4.3. For the lower value of noises, populations are distributed in a smaller region around the deterministic equilibrium value in comparison to the higher value of noises.

#### 4.4. Simulation results

---

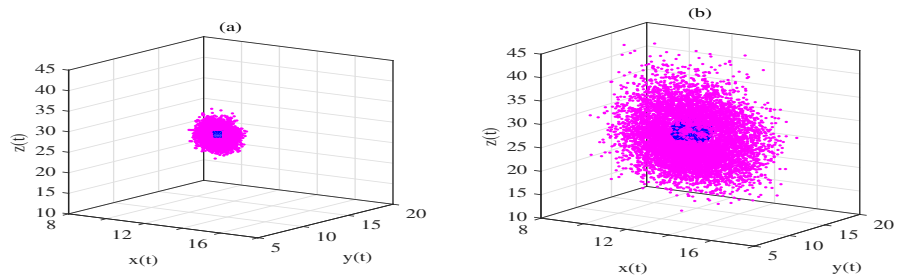


**Figure 4.3:** Stationary distribution of populations of the stochastic system (4.3) at  $t = 100$  is plotted (in pink dots) around the deterministic steady-state (in blue dot). It shows how population densities are distributed around the deterministic equilibrium value for lower and higher values of noise. Left panel:  $\sigma_1 = 0.03$ ,  $\sigma_2 = 0.03$ ,  $\sigma_3 = 0.03$ . Right panel:  $\sigma_1 = 0.1$ ,  $\sigma_2 = 0.1$ ,  $\sigma_3 = 0.1$ . Parameters are as in Fig. 4.1.

#### 4. Persistence and extinction of species in a disease-induced ecological system under environmental stochasticity

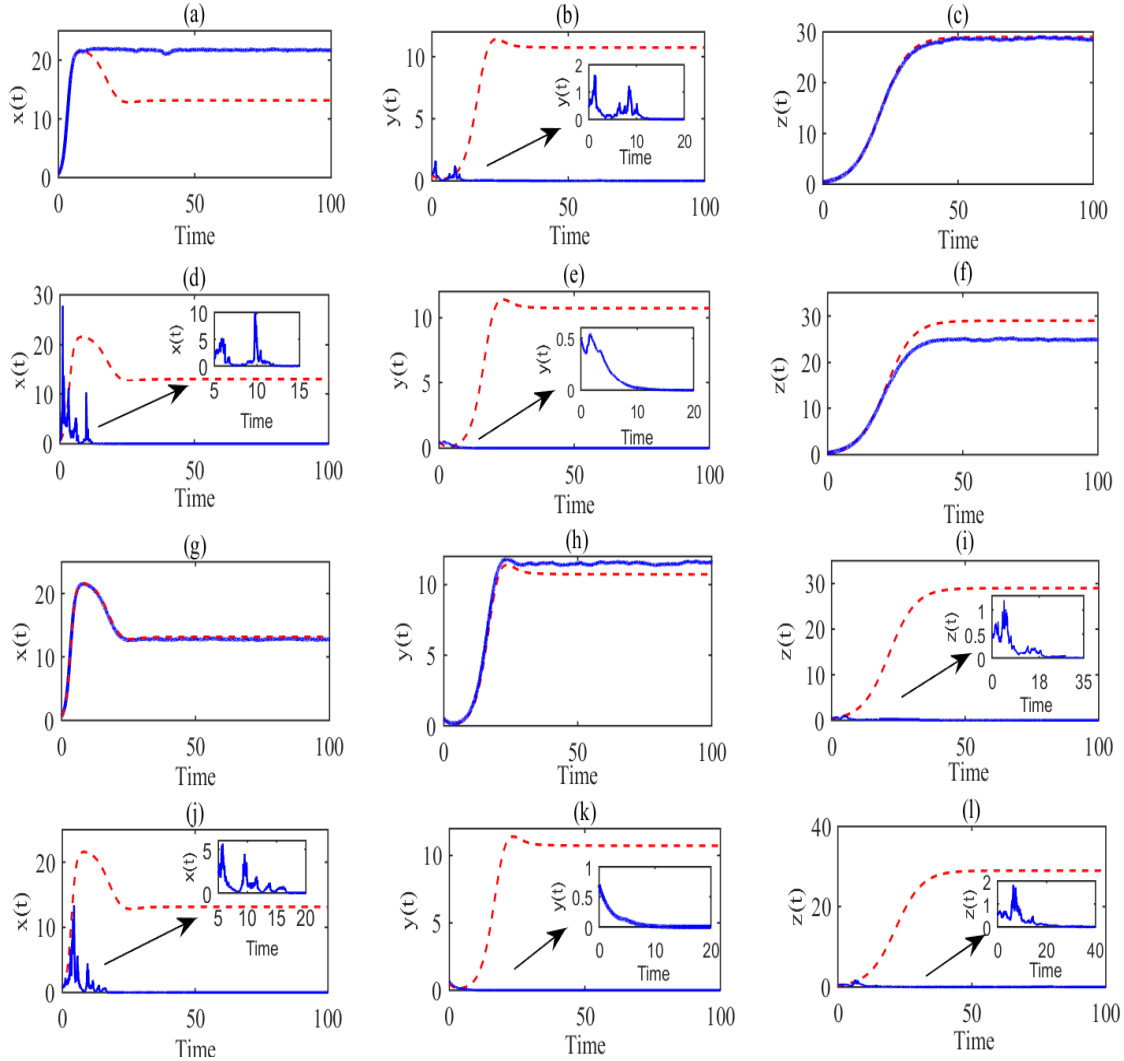


**Figure 4.4:** Solution of the stochastic system (4.3) with different noises. First row:  $y$ -population goes to extinction within a short period when  $\sigma_1 = 0.01$ ,  $\sigma_2 = 0.95$ ,  $\sigma_3 = 0.01$ . Second row:  $x$  and  $y$  populations extinct but  $z(t)$  survive at a lower density when  $\sigma_1 = 1.49$ ,  $\sigma_2 = 0.01$ ,  $\sigma_3 = 0.01$ . Third row:  $z$  population goes to extinction while  $x$  and  $y$  populations survive when  $\sigma_1 = 0.01$ ,  $\sigma_2 = 0.01$ ,  $\sigma_3 = 0.74$ . Last row: All species go to extinction due to higher environmental noise  $\sigma_1 = 1.49$ ,  $\sigma_2 = 0.01$ ,  $\sigma_3 = 0.74$ . Deterministic solution (dash line) of the system, however, reaches to the coexistence equilibrium value in each case. Parameters are as in Fig. 4.1.

Further increase of noise intensity may cause stochastic extinction of system populations. For example, an increase in the noise intensity of infected prey, say  $\sigma_2 = 0.95$ , so that the conditions of Theorems 4.3.3(iii), 4.3.4b(i), 4.3.5(iii) are satisfied then the infected population extinct (Fig. 4.4, upper row). Noticeably, when infected species die out then the susceptible population density lies above its deterministic steady-

#### 4.4. Simulation results

---

state value. Thus, environmental noise can make a system infection-free provided the noise intensity has a higher impact on the infected prey, however, the infection persists in an unvarying environment. If we increase the noise intensity in the growth rate of the susceptible population to  $\sigma_1 = 1.49$ , keeping all other noise intensities and parameters as in Fig. 4.1, to satisfy the condition of Theorem 4.3.3(i) (see also 4.3.4(a)) then both the susceptible and infected populations go to extinction but the predator survives with a lower density (Fig. 4.4, second row) by consuming its alternative food. It is to be recalled that the considered prey is the primary food of the predator and predator can survive in absence of its focal prey at a lower density by consuming its secondary prey. If the noise intensities are such that  $\sigma_1 = 0.01 = \sigma_2$  and  $\sigma_3 = 0.74$  so that the conditions of Theorems 4.3.3(iii), 4.3.4b(iii) and 4.3.5(i) are fulfilled then both the prey populations coexist but the extinction of predator population occurs (Fig. 4.4, third row) due to higher environmental noise on predator population. If the noise intensity on the predator,  $\sigma_3$ , is kept high ( $\sigma_3 = 0.74$ ) with  $\sigma_1 = 1.49$  and  $\sigma_2 = 0.01$ , then the extinction criteria of predator population (Theorem 4.3.5(i)) as well as the extinction criteria of prey population (Theorem 4.3.3(i)) are satisfied. In such a case, all populations die out due to environmental noise, however, populations of the deterministic system coexist in a stable state (Fig. 4.4, last row). It is mentionable that population persists and solutions (dash line) of the deterministic system in each case reach the coexistence equilibrium value, implying that stochasticity can destroy deterministic persistency and stability results. All these results support the fact that environmental noise has a profound influence on the persistence and extinction scenario of interacting species.

## 4. Persistence and extinction of species in a disease-induced ecological system under environmental stochasticity

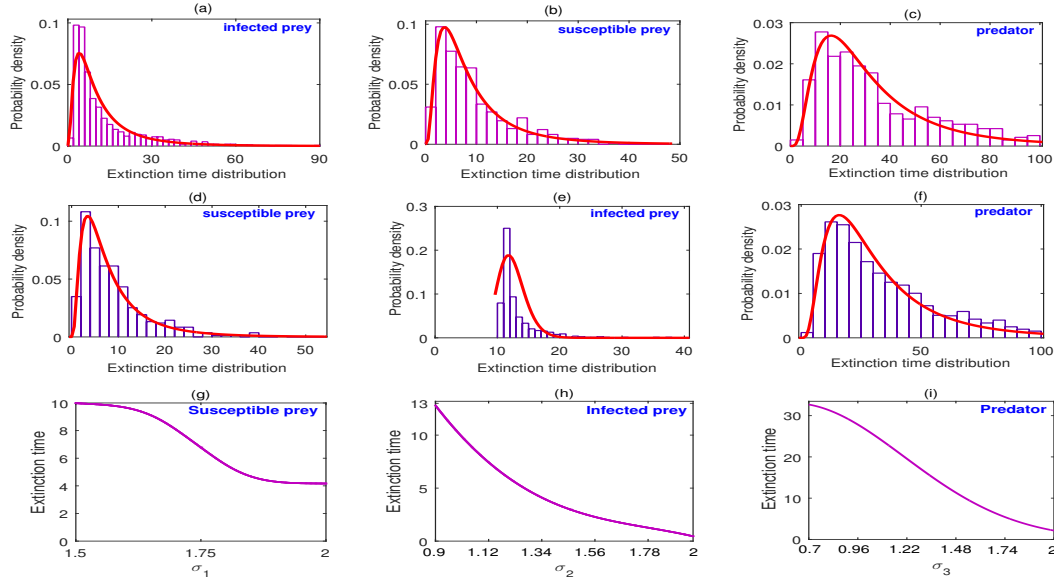


**Figure 4.5:** Probability density and the density curve of extinction time when the stochastic system was run 1000 times with the same set of parameter values of Fig. 4.4. Upper row: (a) Noise intensity as in the first row of Fig. 4.4. (b) Noise intensity as in the second row of Fig. 4.4. (c) Noise intensity as in the third row of Fig. 4.4. The red curve in all figures denotes the corresponding probability density curve, which satisfies the log-normal distribution function with  $p$ -value less than 0.0001. Middle row: Probability density of extinction times of (a) susceptible prey, (b) infected prey and (c) predator when noise intensities are as in the last row of Fig. 4.4 (where all populations extinct due to the noise). The red curve is the fitted log-normal probability distribution function. Here mean ( $\mu$ ) and standard deviation ( $\sigma$ ) of the fitted log-normal probability distribution functions are: (a)  $\mu = 1.95179, \sigma = 0.797037$ , (b)  $\mu = 2.17452, \sigma = 0.882333$ , (c)  $\mu = 3.29299, \sigma = 0.709178$ , (d)  $\mu = 1.87799, \sigma = 0.80553$ , (e)  $\mu = 2.49411, \sigma = 0.173672$ , (f)  $\mu = 3.26533, \sigma = 0.708356$ . Lower row: Extinction time plotted against the varying noise intensity for all three populations. When one noise intensity is varied, then the other two noise intensities remain fixed at 0.01.

In Fig. 4.4, we have deciphered the various extinction scenarios of the population taking the average of 1000 runs of the stochastic system with the same parameter set and initial value. It is obvious that the extinction time of the individual run of these 1000 simulations is different. It will be, therefore, interesting to see the probability distribution of extinction time. In the upper two panels of Fig. 4.5, we have presented the average extinction time distribution for susceptible, infected and predator populations for different fixed noise intensities (as in the Fig. 4.4) and the corresponding probability distribution curve. Figure 4.5(e) indicates that there is no extinction of the infected prey population before 10 units of time. In population ecology, it is a common phenomenon that extinction time of a large number

#### 4.4. Simulation results

---

of individuals of a population is more or less similar, but some others may survive a long time. It is also not unusual to observe that some infected individuals survive for a long time whereas most of the individuals infected with the same parasites die within some average time. In such a case, the data have a low mean and large variance. Data of such skewed distributions often fit log-normal distribution (Limpert et al. [2001]). We also observed here that the log-normal curve fits well the extinction time probability distributions. In the last row of Fig. 4.5, the average extinction times of 1000 simulations are estimated with varying noise intensity, showing that the extinction time of population decreases with increasing noise intensity. This is in accordance with our analytical result (Remark 4.3.6). Similar monotonic decreasing behaviour of extinction time was also observed in other studies (Ji et al. [2009], Li and Cui [2017]). However, nonmonotonic behaviour of the extinction time as a function of noise intensity was also observed in two competing species with stochastic resonance (Valenti et al. [2004b]) and in Verhulst model with Levy white noise (Dubkov and Spagnolo [2008]).

##### 4.4.2 Red grouse: A case study

The red grouse *Lagopus lagopus scoticus*, predominantly observed in heather dominated moorlands of upland Britain, has contributed largely to the long term study of population ecology (Martínez-Padilla et al. [2014]). Many private estates cultivate red grouse to use them as a game bird (Sharon A. Evans [2007]) and employ gamekeepers to maximize their number. The red grouse population is very much unstable and shows frequent fluctuations over time (Haydon et al. [2002], Moss [1996]). Long time field data of red grouse clearly shows such cyclic and quasi cycle behaviour (Moss [1996], Potts et al. [1984]). Fox is the main predator of the grouse population. Though red grouse is the focal prey of fox in the moorlands of Scotland, it also feeds on other species, like vole (Hewson and Kolb [1975], Harris [2015]). These ground-nesting birds are frequently infected by the parasites *trichostrongylus tenuis* (Hudson et al. [1992]). Even though red grouse develops various adaptation for its defence, detection and predation become easier for the fox as grouse emits a particular scent while parasite burden is higher in their bodies (Finnerty and Dunne [2007]). Thus our model assumptions perfectly match with the empirical examples of red grouse-fox interaction in presence of infection. We here examined how our stochastic model can effectively predict the long term dynamics of this PPP system.

#### 4. Persistence and extinction of species in a disease-induced ecological system under environmental stochasticity

---

The method for estimation of parameters of the deterministic system (4.2) and noise intensities for stochastic system (4.3) using the grouse and fox data set of the United Kingdom taken from the British Trust for Ornithology (<https://www.bto.org> [Accessed on August 21, 2020]) for the period 1995 to 2019 is given in 1.8.2.5. The initial values of grouse and fox populations were considered as 77 and 30 per square kilometre, which were their respective values in the year 1995. An adult female grouse lays 6 to 12 eggs per year (gro [2020]) and two-third of the grouse chicks survive (Redpath and Thirgood [1997], Baines et al. [2018]). Thus, the new recruitment of red grouse is between 4 to 9 per year per adult female grouse. In our estimation, we found the birth rate of grouse  $a$  as 0.56 per month, i.e., 6.7 newborn grouse per year. The estimated value of intra-species competition coefficient  $b$  is 0.00144. The death rate of grouse ( $\gamma$ ) is estimated to be 0.0864, which is very close to the field estimated value, 0.0875 (Jenkins et al. [1964]). Fox predation of red grouse ( $e$ ) has been observed to vary from one to two grouse per week (Hudson et al. [1992]), giving the average predation 4 to 8 in a month. We estimated the predation rate parameter  $e$  as 5.12 per month, which lies within the experimental range. Parasitic infection rate ( $\lambda$ ) in red grouse has been reported as 0.16 to 0.6 per year (Dobson and Hudson [1992]) (i.e, 0.0133 to 0.5 per month) and our estimated value is 0.036. The other parameters estimated through curve fitting are  $c = 0.21$ ,  $f = 0.0886$ ,  $m_1 = 101$ ,  $m = 0.0428$ ,  $r = 0.032$ ,  $m_2 = 41$ . Using these parameter values, we plotted (blue curve) the total red grouse population (susceptible and infected) (Fig. 4.6a) and fox population (Fig. 4.6b) obtained from the average of 1000 simulations of the stochastic system (4.3) with noise intensities  $\sigma_1 = 0.1$ ,  $\sigma_2 = 0.05$ ,  $\sigma_3 = 0.09$ . It shows that the stochastic model solutions well match the 25 years (1995 to 2019) field data. Furthermore, we extended our simulation results for another 5 years to predict the red grouse and fox population (red curve) beyond the study period. It shows that both the red grouse and fox populations coexist and will continue to do so if vital parameters and environmental noise are not perturbed significantly. Culling of foxes is an old practice in Great Britain. It was estimated that 190000 foxes were collectively killed annually by hounds, gamekeepers and farmers (Pye-Smith [1997]). Such culling can significantly reduce fox population on a regional scale (Devenish-Nelson et al. [2013]) and can eventually lower the intrinsic growth rate of fox population below some critical level, which can be determined from the Theorem 4.3.5. The effect of such a reduced growth rate may send the fox population to extinction on a local scale.

## 4.5. Discussion

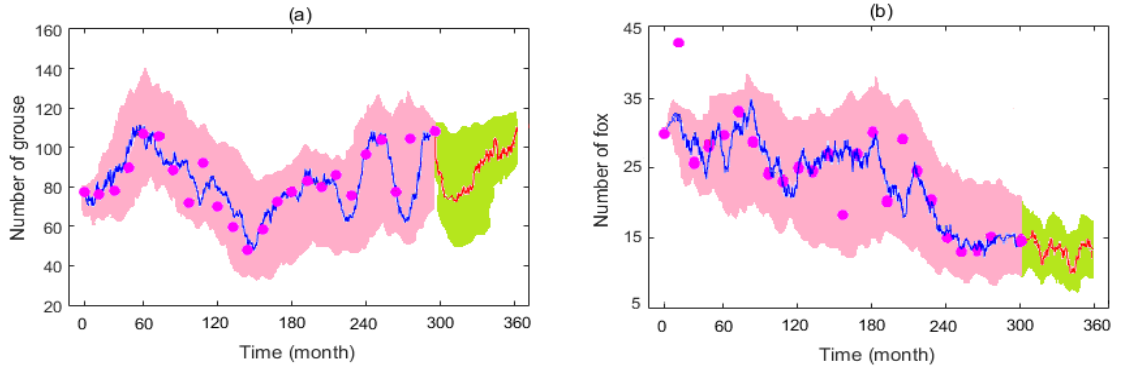


**Figure 4.6:** Comparison of time series solutions of the stochastic system (4.3) with the field data of red grouse and fox population. Left panel: Actual red grouse data for the period 1995 to 2019 are presented by solid circles in magenta colour. Simulated stochastic time series data of total grouse population are presented by a solid line in blue colour. Right panel: Actual fox population data is presented by solid circles and simulated stochastic time series data of fox density are presented by the blue line. Parameters are  $a = 0.56$ ,  $b = 0.00144$ ,  $\lambda = 0.036$ ,  $e = 5.12$ ,  $\gamma = 0.0875$ ,  $c = 0.21$ ,  $f = 0.0886$ ,  $m_1 = 101$ ,  $m = 0.0428$ ,  $r = 0.032$ ,  $m_2 = 41$  and initial value is  $(50, 27, 30)$ . Noise strengths are  $\sigma_1 = 0.1$ ,  $\sigma_2 = 0.05$ ,  $\sigma_3 = 0.09$ . In both figures, the red colour curve is the predicted population densities for the next 5 years. Shaded region represents the 95% confidence interval. The  $r$ -squared values for red grouse and fox data are, respectively, 0.7426 and 0.7231.

## 4.5 Discussion

The ubiquitous ecological phenomena predator-prey interaction is frequently influenced by parasites. Environmental stochasticity, on the other hand, may play a critical role in the persistence or extinction of any biological species. Study of such predator-prey models in presence of infection is extremely important because it encapsulates both the ecological and epidemiological issues simultaneously. Population extinction is a serious issue both from the theoretical and practical point of views. Interacting populations in a natural system may go to extinction in a variety of ways. Such extinction routes have been shown in single-species discrete systems (McLaughlin et al. [2002]) and two species continuous predator-prey (PP) systems by defining a master equation (Gottesman and Meerson [2012]). It is therefore interesting to know the routes to extinction in the higher-dimensional systems. In this chapter, we considered a predator-prey-parasite (PPP) model, where the interaction between prey and predator follows modified Leslie-Gower (or Holling-Tanner) type model with a type II functional response. A parasite infects the prey population and the predator



#### 4. Persistence and extinction of species in a disease-induced ecological system under environmental stochasticity

---

feeds on both the susceptible and infected preys. Environmental stochasticity was incorporated into the system by considering random perturbation, where an error term is added with the average value of a parameter in which perturbation has to be introduced. The error term, in general, follows a normal distribution, and therefore, can be approximated by a white noise (Liu and Wang [2011a]). Reproduction and death are frequently affected by the environmental noise (May [2019]) and consequently, the random perturbation was considered in the intrinsic growth rate of susceptible prey, the death rate of infected prey and growth rate of predator population.

The main objective of this work is to explore the population extinction routes in a PPP system due to environmental stochasticity even when the populations remain stable in its deterministic counterpart. We, therefore, restricted our deterministic analysis to the local stability of the coexisting or interior equilibrium point only. For the stochastic model, we first showed the non-negativity and global existence of a solution and proved its boundedness to mean that interacting populations will not grow abruptly for a long time and each population density will have some upper limit. It is also shown that there exists a stationary distribution of the populations under some parametric restrictions. We have proved that the asymptotic behaviour of the stochastic solution can be made very close to the coexistence equilibrium solution of the deterministic solution by choosing noise intensity small. Some sufficient conditions have been prescribed on some important parameters as well as on the noise intensities so that both the prey and predator populations persist together or in isolation for a long time. For example, Theorems 4.3.3(i) and 4.3.4(a) say that both the susceptible and infected preys cannot persist if the susceptible prey growth rate is lower than some critical value, measured by half of the corresponding noise intensity. This restriction may be satisfied in two ways: (i) by increasing the noise intensity of the system, keeping the other system parameters unaffected, or (ii) by decreasing the intrinsic birth rate, leaving the noise intensity unchanged. Susceptible prey can surely persist if its growth rate is significantly higher than the critical value (Theorem 4.3.3(iii)).

## 4.5. Discussion

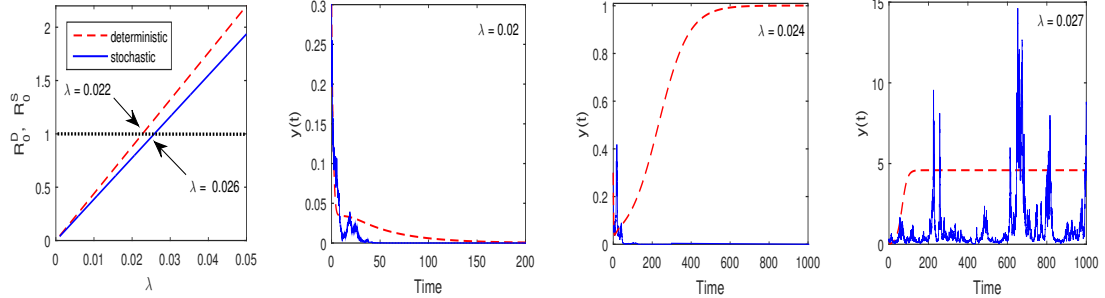


**Figure 4.7:** Comparison between stochastic and deterministic basic reproduction numbers for the varying force of infection. Left figure shows that infection will be eradicated from the deterministic system if  $\lambda < \lambda_1 = 0.022$  and for the stochastic system the range is  $0 < \lambda < \lambda_2 = 0.026$ . Disease persists in both the systems if  $\lambda > \lambda_2$ . This fact is demonstrated with the time series result for three different values of  $\lambda$  such that  $\lambda < \lambda_1$ ,  $\lambda_1 < \lambda < \lambda_2$  and  $\lambda > \lambda_2$ . It demonstrates that environmental noise can remove infection at higher force of infection. Here  $\sigma_1 = 0.3, \sigma_2 = 0.3, \sigma_3 = 0.01$  and other parameters are as in Fig. 4.1.

Eradication of infection from a system is an important issue in epidemiology and always a challenging task to the system manager. It would be really helpful if the system manager gets some insights, possibly by analyzing the disease dynamics of the system, regarding various avenues of disease eradication mechanisms. Our results show that the extinction of susceptible prey (as stated above) always leads to the extinction of the infected prey, causing resolution of infection from the system. This may be one of the possible ways of removing the infection from the system, which is straight forward but maybe, in many cases, unrealistic. Our analysis also prescribes some alternative way of disease eradication even when the susceptible prey growth is sufficiently high. In this case, the infection can be removed from the prey species and a healthy predator-prey system can be established, following the result of Theorem 4.3.4b(i), if the noise intensity on the infected prey is significantly high and/or the death/removal rate of infected prey ( $\gamma$ ) is high and/or the intra-species competition of infected prey ( $b$ ) is high. Infection can also be removed through parasites burden reduction (Hudson and Newborn [1995]) so that force of infection ( $\lambda$ ) becomes low and the corresponding extinction criterion is satisfied (cf. Theorem 4.3.4b(i)). One can relate these eradication criteria with the basic reproduction number of epidemic theory, which determines whether an infection will spread in a population or not. This threshold quantity may be used as a measure of intervention strategy and therefore has very important practical utility. It has been shown that the stochastic system (4.3)

#### 4. Persistence and extinction of species in a disease-induced ecological system under environmental stochasticity

---

will be disease free if  $R_0^S < 1$ , where  $R_0^S = \frac{\lambda \left( a - \frac{\sigma_1^2}{2} \right)}{b \left( \gamma + \frac{\sigma_2^2}{2} \right)}$  and the corresponding threshold for the deterministic system (4.2) is  $R_0^D < 1$ , where  $R_0^D = \frac{a\lambda}{b\gamma}$  (Sarwardi et al. [2011]). Thus,  $R_0^D > R_0^S$  for any nonzero value of the noises, implying that environmental noise plays a positive role in disease extinction. The parasitic infection can be eradicated even at higher infection rate with the right environmental noises (see Fig. 4.7).

The disease will always persist if susceptible prey has a high growth rate, or the disease has high infectivity (see Theorem 4.3.4b(iii)). On the other hand, predator population can not survive if its growth rate is lower than some critical value, where the critical predator's growth rate is defined by half of the corresponding noise intensity, even when its focal prey strongly persists (cf. Theorem 4.3.5(i)). Predator, however, almost surely persists if its growth rate exceeds the critical value. The predator can survive in absence of its focal prey at a lower density by consuming the nonpreferred secondary prey. It is interesting to observe that all these extinction scenarios occur in the stochastic system when the corresponding deterministic system shows stable persistence of all three populations. The average extinction time decreases with the increasing noise intensity and the probability distribution of the extinction time follows the log-normal density curve. Thus, environmental noise may play a critical role in population persistency as well as infection removal process by changing the physical property of the system.

The considered eco-epidemiological situation on which the model is based has similarity with the red grouse-fox interaction in presence of the parasites *trichostrongylus tenuis*. We, therefore, verified the field data of red grouse and fox populations with the time series solutions of our stochastic model. The solution of our model well fit the experimental data. Furthermore, the population densities of red grouse and fox populations have been predicted for the extended periods. Though both species have been coexisting for a long period and expected to do so in future if the environmental noises do not vary significantly, extinction of species can not be ruled out. For instance, foxes are regularly killed to maintain grouse population (Hudson and Newborn [1995]). This may be a potential threat to the fox population and may even send it to extinction if the fox killing rate increases and the intrinsic growth rate falls below the corresponding critical noise intensity.

This study, however, has not taken into account two important natural processes but may be considered in the future study, e.g. Allee effect, which generally enhances

## 4.5. Discussion

---

the extinction possibility (Stephan and Wissel [1994]), and immigration, which enhances the persistence of species, which is at the verge of extinction (Dey and Joshi [2013]). Despite these shortcomings, this study shows that environmental variability has significant influences on the persistence and extinction of interacting species in the natural environment. It also points out different routes to extinction, which may be beneficial to the system manager to take various control measures to prevent species extinction.

In the next chapter, we propose a deterministic model of the Covid-19 epidemic and then extend the deterministic system into a stochastic system through random parameter perturbations. We provided different analytical results and predicted the course of the outbreak with the Indian covid data from 1st March to 6th December 2020.



# Chapter 5

## Persistence and extinction criteria of Covid-19 pandemic: India as a case study<sup>3</sup>

### 5.1 Introduction

A highly infectious respiratory disease spread in Wuhan city of Hubei province, China, at the end of 2019. The disease crossed the international border of China and arrived in 23 other countries including USA, France, Italy, and India in the first month of January, 2020, and the World Health Organization (WHO) declared a public health emergency of international concern on January 30 (WHO [2019b]). Though the initial host of Covid-19 is assumed to be some animals, it spread rapidly among the human population of Wuhan and subsequently spread to the entire world through international travel. Realizing that the disease 2019-nCoV or Covid-19 caused by the novel coronavirus SARS-CoV-2 has a tremendous spreading ability, WHO declared the Covid-19 outbreak as pandemic on March 11 (Takian et al. [2020]). As of July 15, 2020, 216 countries or territories were affected with this novel coronavirus, with 13.15 million confirmed cases and 0.57 million deaths globally (WHO [2019a]). These numbers for India were, respectively, 970,169 and 24, 929 on the same date (cov [2020]).

Susceptible individuals get infection from COVID-19 infected individuals through

---

<sup>3</sup>The bulk of this chapter has been published in *Stochastic Analysis and Applications*, 40.2 (2022), 179-208.

## 5. Persistence and extinction criteria of Covid-19 pandemic: India as a case study

---

direct contact or inhaling the droplets caused due to coughing and sneezing by an infected person or through objects in the immediate environment around the infected person (Peeri et al. [2020]). Until now, there is no specific drug or vaccine for 2019-nCoV and therefore the non-pharmaceutical interventions (NPIs) like individual hygiene, cough etiquette, safe distancing, and lockdown are the only ways to contain this highly contagious disease (Cowling and Aiello [2020]). Such NPIs have been proven effective in slowing down community transmission and reducing the epidemic load (Lau et al. [2020]).

Mathematical models and computation techniques may play an important role in understanding this epidemic and may help a lot in policy making. In fact, policy-makers have used mathematical projections and taken various important decisions to curb the disease in more systematic and effective ways (Adam [2020]). Lots of mathematical models describe early transmission dynamics of Covid -19 and predict the future epidemic load. Most of them are deterministic SEIR (susceptible  $\rightarrow$  exposed  $\rightarrow$  infected  $\rightarrow$  recovered) models or its variants (Fanelli and Piazza [2020], Paul et al. [2020a], Mondal et al. [2020], Peng et al. [2020], Chen et al. [2020], Pang et al. [2020], Sardar et al. [2020], Zhou et al. [2020b], Rabajante [2020], Lin et al. [2020], Mandal et al. [2020], Paul et al. [2020b], Ivorra et al. [2020]) and few are stochastic models (Din et al. [2020], He et al. [2020], Adak et al. [2021], Yanev et al. [2020], Chatterjee et al. [2020]). A three-dimensional continuous time Markov Chain model was analyzed in Din et al. [2020]. Defining a suitable Lyapunov function, they studied the stationary distribution and extinction phenomena of the disease. He et al. [2020] used a discrete-time stochastic model taking into account the effect of different control measures. Using the epidemic data of Whuan city for the period 11 January to 13 February 2020, they predicted the rest course of Covid-19 epidemic. Adak et al. [2021] studied the pandemic situation of Italy with the help of a four dimensional stochastic model. Using Lyapunov functional method, they showed that the infected population tends to zero if the basic reproduction number is less than unity. A stochastic model with two types branching process was used in (Yanev et al. [2020]) to estimate the Covid-19 epidemic of Bulgaria and Italy. The model used only observed data of daily contaminated individuals and lab-confirmed cases to estimate the epidemic load. Monte Carlo simulation was used in a SEIR model to understand the early stage Covid-19 epidemic in India (Chatterjee et al. [2020]). Stochastic simulation models were also used for early transmission dynamics of Covid-19 epidemic for different countries (Plank et al. [2020], Kucharski et al. [2020], Girona [2020]).

## 5.1. Introduction

These simulation studies lead to an understanding of early transmission dynamics of Covid-19, however, did not provide any analytical criterion for persistence and extinction of this dreaded infection. Here we propose an extended version of SEIR epidemic model taking into consideration the different compartments that an individual has to be passed through if infected with Covid-19.

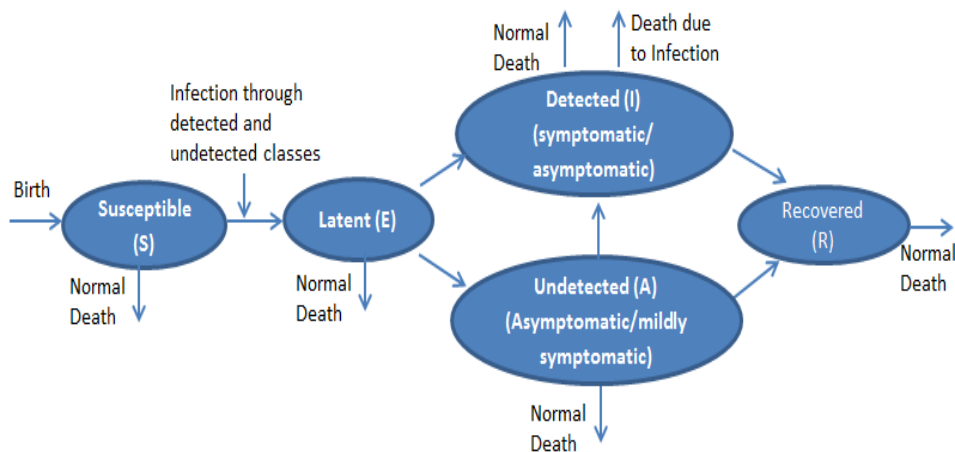


**Figure 5.1:** Schematic diagram of the model. An individual will move from left to right if infected with SARS-CoV-2.

We divide the total human population of a country or a geographical region into five disjoint groups, viz. susceptible, exposed, detected infectives, undetected infectives, and recovered classes denoted, respectively, by  $S$ ,  $E$ ,  $A$ ,  $I$  and  $R$ . Classification of populations and essential disease progression steps are represented in the schematic diagram (Fig. 5.1). Different studies report that a large number of Covid-19 patients do not show any symptoms or show mild symptoms, which are very similar to common flue (Day [2020], Hu et al. [2020], Lu et al. [2021]). Thus a significant number of Covid-19 patients may remain undetected and pose a challenge to containment (Yu and Yang [2020], Pedersen and Meneghini [2020], Giordano et al. [2020]). We, therefore, considered a detected class ( $I$ ), where all individuals (symptomatic or asymptomatic) are tested covid positive, and an undetected class ( $A$ ), whose members are asymptomatic or mildly symptomatic, and not tested. It is assumed that susceptible individuals are infected by both the detected and undetected infectious individuals, and the number of contacts is independent of population size. Assume that  $\kappa$  is the probability of disease transmission through a contact between an undetected infective and a susceptible individual, and the same for detected infective is  $(1 - \kappa)$ . If  $\beta$  is the



## 5. Persistence and extinction criteria of Covid-19 pandemic: India as a case study

---

average per capita daily contacts then the latent individuals that join newly in the  $E$  class is  $(\frac{\beta\kappa SA}{N} + \frac{\beta(1-\kappa)SI}{N})$ , where  $N(t) = S(t) + E(t) + A(t) + I(t) + R(t)$  is the total population at any time  $t$ . In the literature,  $\beta\kappa$  (and  $\beta(1-\kappa)$ ) is called the disease transmission efficiency or the force of infection (Lipsitch et al. [2003]). Thus, the effect of various NPIs to reduce human-to-human disease transmission are encapsulated through the parameters  $\beta$  and  $\kappa$ . The exit rate of  $E$  class is  $\omega$ . After exiting from  $E$  compartment, an individual either join the undetected infected class ( $A$ ) with probability  $\delta$  or join the detected class ( $I$ ) with probability  $(1-\delta)$ . It is important to note that an undetected individual may join the detected class if later on shows symptoms and/or tested positive. It is assumed that such a transfer from  $A$  to  $I$  class may occur at a rate  $\nu$ . A period  $\frac{1}{\gamma}$  is spent, on an average, by an individual of  $I$  class before moving to the recovered class  $R$  and the same for  $A$  class is  $\frac{1}{\gamma_1}$ . Natural death may occur in every compartment at a rate  $m$ , but disease related death occurs only in the  $I$  compartment at a rate  $d_i$ . It is notable that no disease related death is assumed in the asymptomatic class because, if such a serious condition arises, the individual will be tested and shifted immediately to the  $I$  class, if tested positive. The net inflow of susceptible individuals per unit of time, which includes birth, emigration, and immigration, is represented by  $\Lambda$ . The model is further extended to accommodate a death class ( $D$ ), which includes the disease-related death and quantify the virulence of the disease. This last class has been considered here to fit the available data only. These assumptions lead to the following deterministic model for the Covid-19 epidemic:

$$\begin{aligned}
 \frac{dS}{dt} &= \Lambda - mS - \frac{\beta S}{N} [\kappa A + (1-\kappa)I], \\
 \frac{dE}{dt} &= \frac{\beta S}{N} [\kappa A + (1-\kappa)I] - \omega E - mE, \\
 \frac{dA}{dt} &= \delta\omega E - (\gamma_1 + \nu + m)A, \\
 \frac{dI}{dt} &= (1-\delta)\omega E + \nu A - (\gamma + m + d_i)I, \\
 \frac{dR}{dt} &= \gamma_1 A + \gamma I - mR, \\
 \frac{dD}{dt} &= d_i I.
 \end{aligned} \tag{5.1}$$

It is reported that the average latent period during which an infected individual remain noninfectious is about 2 days (Peng et al. [2020]) and consequently the mean

## 5.1. Introduction

---

duration in the exposed class,  $\frac{1}{\omega+m}$ , is always assumed to be greater than unity. Moreover,  $\gamma_1 > \gamma$  as the recovery rate of asymptomatic or mildly symptomatic cases is higher than that of the symptomatic cases.

Uncertainty is obvious in the case of a growing epidemic and it multiplies if the disease etiology is unknown, as in the case of Covid-19. It is shown that there is substantial uncertainty in the reported Covid-19 infection rate (Manski and Molinari [2021a]). Uncertainty is also certain in the proportion of symptomatic and asymptomatic cases (Nishiura et al. [2020], Al-Tawfiq [2020]). Another uncertainty lies in the infectious period. It is reported that there is a large variation in the infectious period (Anderson et al. [2020]) and hence in the recovery rate (Zhang et al. [2020a]). It has been shown that there exists large uncertainty in the early stage of epidemic growth and suggested that real-time epidemiological prediction should include uncertainty (Alberti and Faranda [2020]). In the deterministic study, such variation is ignored and all rate parameters are assumed to be constant (Renshaw [2015]). We here introduce such randomness in the model parameters. For example, the per capita daily contact rate  $\beta$  will be replaced by an average value plus an error term, which is assumed to follow a normal distribution so that for a single infected individual, the probability of an event in  $[t, t + \Delta t]$  is approximately  $N(\beta\Delta t, \beta^2\Delta t) + \mathcal{O}(\Delta t)$ . One can, therefore, replace  $\beta$  by  $\beta + \sigma_1 \frac{dW(t)}{dt}$ , where  $\frac{dW(t)}{dt}$  is the white noise, i.e.,  $W(t)$  is a Brownian motion. Here  $\sigma_1 > 0$  is the intensity of the noise and small compare to  $\beta$ . This is a very popular technique to incorporate stochasticity into a deterministic model and is frequently used in the literature (Zhao et al. [2019], Ji et al. [2012b], Li et al. [2015], Liu and Mandal [2015], Zhou et al. [2020a], Majumder et al. [2020b], Lahrouz and Omari [2013], Li et al. [2019b], Yang and Mao [2014], Zhao and Jiang [2013]). Similar parametric perturbation is also considered in the other two parameters  $\gamma$  and  $\gamma_1$ , respectively, the recovery rates of symptomatic and asymptomatic classes. We therefore considered random perturbations in these parameters as

$$\mp\beta \rightarrow \mp\beta + \sigma_1 dB_1(t), \quad -\gamma_1 \rightarrow -\gamma_1 + \sigma_2 dB_2(t), \quad -\gamma \rightarrow -\gamma + \sigma_3 dB_3(t),$$

where  $B_i(t)$  are standard mutually independent Brownian motions and  $\sigma_i^2, i = 1, 2, 3$ , are the noise intensities. The system (5.1) under such stochastic perturbations reads

## 5. Persistence and extinction criteria of Covid-19 pandemic: India as a case study

---

$$\begin{aligned}
 dS &= \left[ \Lambda - mS - \frac{\beta S}{N} ((1 - \kappa)I + \kappa A) \right] dt - \frac{\sigma_1 S}{N} [(1 - \kappa)I + \kappa A] dB_1(t), \\
 dE &= \left[ \frac{\beta S}{N} ((1 - \kappa)I + \kappa A) - (\omega + m)E \right] dt + \frac{\sigma_1 S}{N} [(1 - \kappa)I + \kappa A] dB_1(t), \\
 dA &= [\delta\omega E - (\gamma_1 + \nu + m)A] dt - \sigma_2 A dB_2(t), \\
 dI &= [(1 - \delta)\omega E - (\gamma + m + d_i)I + \nu A] dt - \sigma_3 I dB_3(t), \\
 dR &= [\gamma_1 A + \gamma I - mR] dt + \sigma_2 A dB_2(t) + \sigma_3 I dB_3(t), \\
 dD &= d_i I dt.
 \end{aligned} \tag{5.2}$$

The initial values for the system (5.2) are assumed to be

$$S(0) \geq 0, E(0) \geq 0, A(0) \geq 0, I(0) \geq 0, R(0) = 0, D(0) = 0. \tag{5.3}$$

The remaining portion of this chapter is organized as follows. Deterministic and stochastic results are presented in the next Section 5.2. Indian case study for the period first march to sixth December 2020 is presented in the Section 5.3. The chapter ends with a discussion in Section 5.4.

## 5.2 Mathematical results

### 5.2.1 Deterministic results

#### 5.2.1.1 Basic reproduction number

Basic reproduction number is probably the most important measure of an epidemic model. Whether an epidemic will grow or not is determined by its basic reproduction number. Basically, it says about the average number of secondary infections caused by an infected individual in its infectious period when introduced into a group of susceptibles (Anderson and May [1992]). Certainly, the disease will grow if its value is greater than one and it dies out in the opposite case. Here we deduce the basic reproduction number  $R_0$  of the system (5.1) using the next generation matrix approach (Diekmann et al. [2010]). The infection subsystem of the deterministic system (5.1), which describes the production of new infections and makes change in the states, is given by

## 5.2. Mathematical results

---

$$\frac{dE}{dt} = \frac{\beta(1-\kappa)\left(\frac{\Lambda}{m}\right)I}{\frac{\Lambda}{m} + E + A + I + R} + \frac{\kappa\beta\left(\frac{\Lambda}{m}\right)A}{\frac{\Lambda}{m} + E + A + I + R} - (\omega + m)E, \quad (5.4)$$

$$\frac{dA}{dt} = \delta\omega E - \nu A - (\gamma_1 + m)A, \quad (5.5)$$

$$\frac{dI}{dt} = (1-\delta)\omega E + \nu A - (\gamma + m + d_i)I. \quad (5.6)$$

The transmission matrix and transition matrix associated with the system (5.4) are, respectively, given by  $\mathbf{T}$  and  $\mathbf{\Sigma}$ , where

$$\mathbf{T} = \begin{pmatrix} 0 & \beta\kappa & \beta(1-\kappa) \\ 0 & 0 & 0 \\ 0 & 0 & 0 \end{pmatrix}, \quad \mathbf{\Sigma} = \begin{pmatrix} -(\omega + m) & 0 & 0 \\ \delta\omega & -(\nu + \gamma_1 + m) & 0 \\ (1-\delta)\omega & \nu & -(\gamma + m + d_i) \end{pmatrix}. \quad (5.7)$$

According to the theory of next generation matrices,  $R_0$  is then given by the spectral radius (largest absolute eigenvalue) of the matrix  $-\mathbf{T}\mathbf{\Sigma}^{-1}$ , i.e.,  $R_0 = \rho(-\mathbf{T}\mathbf{\Sigma}^{-1})$ , where

$$\mathbf{\Sigma}^{-1} = \begin{pmatrix} -\frac{1}{\omega+m} & 0 & 0 \\ -\frac{\delta\omega}{(\omega+m)(\nu+\gamma_1+m)} & -\frac{1}{\nu+\gamma_1+m} & 0 \\ -\frac{\delta\omega\nu+(\nu+\gamma_1+m)(1-\delta)\omega}{(\omega+m)(\nu+\gamma_1+m)(\gamma+m+d_i)} & -\frac{\nu}{(\nu+\gamma_1+m)(\gamma+m+d_i)} & -\frac{1}{\gamma+m+d_i} \end{pmatrix}.$$

Therefore,

$$R_0 = \frac{\beta\kappa\delta\omega}{(\omega+m)(\nu+\gamma_1+m)} + \frac{\beta\delta\omega\nu(1-\kappa)}{(\omega+m)(\nu+\gamma_1+m)(\gamma+m+d_i)} + \frac{\beta\omega(1-\kappa)(1-\delta)}{(\omega+m)(\gamma+m+d_i)}. \quad (5.8)$$

From biological point of view, it is important to show that the solutions of the system (5.1) are positively bounded. In fact, it is trivial to prove the following lemma (Li et al. [2006]).

**Lemma 5.2.1.** *The system (5.1) is invariant in  $\mathbb{R}_+^5$  and its solutions are bounded in the region*

$$G = \left\{ (S, E, A, I, R) \in \mathbb{R}_+^5 : S + E + A + I + R \leq \frac{\Lambda}{m} \right\}.$$

## 5. Persistence and extinction criteria of Covid-19 pandemic: India as a case study

---

### 5.2.1.2 Existence and stability of equilibrium points

The system (5.1) has two equilibrium points, viz. the disease-free equilibrium  $E_0(\frac{\Lambda}{m}, 0, 0, 0, 0)$  and a unique coexistence (or endemic) equilibrium  $C^* = (S^*, E^*, A^*, I^*, R^*)$ , where  $S^* = \frac{\Lambda}{m + \frac{\beta}{N^*}((1-\kappa)I^* + \kappa A^*)}$ ,  $A^* = \frac{\delta\omega E^*}{\gamma_1 + m + \nu}$ ,  $I^* = \frac{(1-\delta)\omega E^*}{\gamma + m + d_i} + \frac{\delta\omega\nu E^*}{(\gamma_1 + m + \nu)(\gamma + m + d_i)}$ ,  $R^* = \frac{1}{m}(\gamma_1 A^* + \gamma I^*)$ , and satisfies the relation  $\frac{S^*}{N^*}R_0 = 1$ , where  $N^* = S^* + E^* + A^* + I^* + R^*$  is the total equilibrium population. The last relation shows that  $\frac{S^*}{N^*} < 1$  so far interior equilibrium is concerned, and  $\frac{S^*}{N^*}R_0 = 1$  holds only if  $R_0 > 1$ . Therefore, the system (5.1) has a unique endemic equilibrium point if  $R_0 > 1$  and no endemic equilibrium point if  $R_0 \leq 1$ .

**Theorem 5.2.2.** *If  $R_0 \leq 1$  then the disease-free equilibrium of the system (5.1) is globally asymptotically stable in  $G$ .*

*Proof.* Consider the Lyapunov function

$$V = \frac{\omega[(1-\kappa)(1-\delta)l_1 + (1-\kappa)\nu\delta + \kappa\delta l_2]}{l_1 l_2 l_3} E + \left( \frac{(1-\kappa)\nu}{l_1 l_2} + \frac{\kappa}{l_1} \right) A + \frac{1-\kappa}{l_2} I, \quad (5.9)$$

where  $l_1 = \gamma_1 + m + \nu$ ,  $l_2 = \gamma + m + d_i$ ,  $l_3 = \omega + m$ .

The time derivative of  $V$  along the solutions of (5.1) gives

$$\begin{aligned} \dot{V} &= \frac{\omega[(1-\kappa)(1-\delta)l_1 + (1-\kappa)\nu\delta + \kappa\delta l_2]}{l_1 l_2 l_3} \dot{E} + \left( \frac{(1-\kappa)\nu}{l_1 l_2} + \frac{\kappa}{l_1} \right) \dot{A} + \frac{1-\kappa}{l_2} \dot{I} \\ &= \frac{\omega[(1-\kappa)(1-\delta)l_1 + (1-\kappa)\nu\delta + \kappa\delta l_2]}{l_1 l_2 l_3} \left[ \frac{\beta S}{N} [(1-\kappa)I + \kappa A] - (\omega + m)E \right] \\ &\quad + \left( \frac{(1-\kappa)\nu}{l_1 l_2} + \frac{\kappa}{l_1} \right) [\delta\omega E - (\gamma_1 + \nu + m)A] \\ &\quad + \frac{1-\kappa}{l_2} [(1-\delta)\omega E + \nu A - (\gamma + m + d_a)I] \quad (5.10) \\ &\leq \frac{\omega\beta[(1-\kappa)(1-\delta)l_1 + (1-\kappa)\nu\delta + \kappa\delta l_2]}{l_1 l_2 l_3} [(1-\kappa)I + \kappa A] - \frac{\omega(1-\kappa)(1-\delta)}{l_2} E \\ &\quad - \frac{\omega(1-\kappa)\nu\delta}{l_1 l_2} E - \frac{\omega\kappa\delta}{l_1} E + \frac{\omega(1-\kappa)\nu\delta}{l_1 l_2} E + \frac{\omega\kappa\delta}{l_1} E - \frac{(1-\kappa)\nu}{l_2} A - \kappa A \\ &\quad + \frac{\omega(1-\kappa)(1-\delta)}{l_2} E - (1-\kappa)I + \frac{(1-\kappa)\nu}{l_2} A \\ &\leq (R_0 - 1)((1-\kappa)I + \kappa A) \\ &\leq 0, \quad \text{whenever } R_0 \leq 1. \end{aligned}$$

Using the fact that all the parameters and variables of the system (5.1) are non-

## 5.2. Mathematical results

negative, we have  $\dot{V} \leq 0$  whenever  $R_0 \leq 1$  with equality occurs at the disease-free equilibrium point. Therefore, by the LaSalle invariance principle (La Salle [1976]), one has  $(E(t), A(t), I(t)) \rightarrow (0, 0, 0)$  as  $t \rightarrow \infty$ . It gives  $\limsup_{t \rightarrow \infty} A(t) = 0$  and  $\limsup_{t \rightarrow \infty} I(t) = 0$ . Then for sufficiently small  $\epsilon > 0$ ,  $\exists$  constants  $M_1 > 0$  and  $M_2 > 0$  such that  $\limsup_{t \rightarrow \infty} A(t) \leq \epsilon \forall t > M_1$  and  $\limsup_{t \rightarrow \infty} I(t) \leq \epsilon \forall t > M_2$ . From the fifth equation of system (5.1), for  $t > \max \{M_1, M_2\}$ , one has

$$\frac{dR}{dt} \leq \gamma_1 \epsilon + \gamma \epsilon - mR. \quad (5.11)$$

Comparison theorem (Smith and Waltman [1995]) then allows

$$\limsup_{t \rightarrow \infty} R(t) \leq \frac{\gamma_1 \epsilon + \gamma \epsilon}{m}. \quad (5.12)$$

Letting  $\epsilon \rightarrow 0$ , one have  $\limsup_{t \rightarrow \infty} R(t) \leq 0$ . Again, using the fact that  $\liminf_{t \rightarrow \infty} A(t) = 0$  and  $\liminf_{t \rightarrow \infty} I(t) = 0$ , one can have  $\liminf_{t \rightarrow \infty} R(t) \geq 0$  and hence  $\lim_{t \rightarrow \infty} R(t) = 0$ . Similarly, one can show that  $\lim_{t \rightarrow \infty} S(t) = \frac{\Lambda}{m}$ . Therefore, it follows that all solutions of the system (5.1) with the initial condition in  $G$  converge to the disease-free equilibrium  $E_0$  as  $t \rightarrow \infty$  for  $R_0 \leq 1$ .  $\square$

**Theorem 5.2.3.** *If  $R_0 > 1$  then the interior equilibrium  $E^*$  is locally asymptotically stable.*

*Proof.* The proof is based on the line of Castillo-Chavez and Song [2004]. The variational matrix of the system (5.1) evaluated at  $E_0$  is given by

$$A' = \begin{pmatrix} -m & 0 & -\beta\kappa & -\beta(1-\kappa) & 0 \\ 0 & -(\omega+m) & \beta\kappa & \beta(1-\kappa) & 0 \\ 0 & \delta\omega & -(\gamma_1+m+\nu) & 0 & 0 \\ 0 & (1-\delta)\omega & \nu & -(\gamma+m+d_i) & 0 \\ 0 & 0 & \gamma_1 & \gamma & -m \end{pmatrix}.$$

We consider the force of infection,  $\beta$ , as the bifurcating parameter and apply the central manifold theorem to determine the local stability of  $E^*$ . The critical value  $\beta = \beta_*$  for which  $R_0 = 1$  holds is

$$\beta_* = \frac{(\gamma+m+d_i)(\gamma_1+m+\nu)(\omega+m)}{(1-\kappa)(1-\delta)\omega(\gamma_1+m+\nu) + (1-\kappa)\delta\omega\nu + \kappa\delta\omega(\gamma+m+d_i)}.$$

Now let at  $\beta = \beta_*$ , the Jacobian matrix  $J_{E_0}|_{\beta=\beta_*}$  has a right eigenvector  $u =$

## 5. Persistence and extinction criteria of Covid-19 pandemic: India as a case study

---

$(u_1, u_2, u_3, u_4, u_5)^T$  corresponding to the zero eigenvalue, where  $u_1 = -\frac{\omega+m}{m}u_2$ ,  $u_2 = u_2 > 0$ ,  $u_3 = \frac{\delta\omega}{\gamma_1+m+\nu}u_2$ ,  $u_4 = \frac{\omega(1-\delta)(\gamma_1+m+\nu)+\delta\omega\nu}{(\gamma+m+d_i)(\gamma_1+m+\nu)}u_2$ ,  $u_5 = \frac{\gamma_1\delta\omega(\gamma+m+d_i)+\gamma\omega(1-\delta)(\gamma_1+m+\nu)+\gamma\nu\delta\omega}{m(\gamma+m+d_i)(\gamma_1+m+\nu)}u_2$ . Similarly, a left eigenvector corresponding to the zero eigenvalue of the Jacobian matrix  $J_{E_0}|_{\beta=\beta_*}$  is  $w = (w_1, w_2, w_3, w_4, w_5)$ , where

$$w_1 = 0, w_2 = w_2, w_3 = \frac{\beta\nu(1-\kappa) + \beta\kappa(\gamma + m + d_i)}{(\gamma + m + d_i)(\gamma_1 + m + \nu)}w_2, w_4 = \frac{\beta(1-\kappa)}{\gamma + m + d_i}w_2, w_5 = 0.$$

With the transformations  $S = y_1, E = y_2, A = y_3, I = y_4, R = y_5$ , the system (5.1) can be expressed as

$$\frac{dy_i}{dt} = g_i(y_i),$$

where  $g_i \in C^2(\mathbb{R}^5 \times \mathbb{R})$ ,  $i = 1, \dots, 5$ . Then the second order partial derivatives of  $g_i$  at  $E_0$  are evaluated as

$$\frac{\partial^2 g_2}{\partial y_3 \partial y_2} = -\frac{\beta m \kappa}{\Lambda}, \frac{\partial^2 g_2}{\partial y_4 \partial y_2} = -\frac{\beta m (1 - \kappa)}{\Lambda}, \frac{\partial^2 g_2}{\partial y_3 \partial y_3} = -\frac{2\beta m \kappa}{\Lambda}, \frac{\partial^2 g_2}{\partial y_4 \partial y_3} = -\frac{\beta m}{\Lambda},$$

$$\frac{\partial^2 g_2}{\partial y_3 \partial y_4} = -\frac{\beta m}{\Lambda}, \frac{\partial^2 g_2}{\partial y_4 \partial y_4} = -\frac{2\beta m (1 - \kappa)}{\Lambda}, \frac{\partial^2 g_2}{\partial y_3 \partial y_5} = -\frac{\beta m \kappa}{\Lambda}, \frac{\partial^2 g_2}{\partial y_4 \partial y_5} = -\frac{\beta m (1 - \kappa)}{\Lambda}.$$

The signs of the quantities  $a$  and  $b$  evaluated at  $\beta = \beta_*$  determine the local stability of the system (Castillo-Chavez and Song [2004]), where

$$a = \sum_{l,m,n=1}^5 w_l u_m u_n \frac{\partial^2 g_l(0,0)}{\partial y_m \partial y_n} \text{ and } b = \sum_{l,m=1}^5 w_l u_m \frac{\partial^2 g_l(0,0)}{\partial y_m \partial \beta}.$$

Substituting all the values of the second order partial derivative evaluate at  $E_0$  and  $\beta = \beta_*$ , we have

$$a = -\frac{\beta m w_2}{\Lambda} [u_3 u_2 \kappa + u_4 u_2 (1 - \kappa) + 2u_3 u_3 \kappa + u_4 u_3 + u_3 u_4 + u_3 u_5 \kappa + 2u_4 u_4 (1 - \kappa) + u_4 u_5 (1 - \kappa)] < 0$$

and

$$b = w_2 (\kappa u_3 + (1 - \kappa) u_4) > 0.$$

Since  $a < 0$  and  $b > 0$  at  $\beta = \beta_*$ , by the Remark 1 of Theorem 4.1 in Castillo-Chavez and Song [2004], a transcritical bifurcation occurs at  $R_0 = 1$  and the unique endemic equilibrium exists and becomes locally asymptotically stable for  $R_0 > 1$ .  $\square$

## 5.2. Mathematical results

---

### 5.2.2 Stochastic results

Here we first prove that the solutions of the stochastic system exist not only locally but also globally. Also, we prove that the solutions are stochastically ultimately bounded and we have the following results.

**Theorem 5.2.4.** *For any initial value  $(S(0), E(0), A(0), I(0), R(0)) \in \mathbb{R}_+^5$ , there exists a unique solution  $(S(t), E(t), A(t), I(t), R(t)) \in \mathbb{R}_+^5$  for the system (5.2) for  $t \geq 0$  and the solution will remain in  $\mathbb{R}_+^5$  with probability 1, i.e.,  $(S(t), E(t), A(t), I(t), R(t)) \in \mathbb{R}_+^5$  for all  $t \geq 0$  almost surely (a.s).*

*Proof.* Since the coefficients of the equation are locally Lipschitz continuous, for any initial value  $(S(0), E(0), A(0), I(0), R(0)) \in \mathbb{R}_+^5$ , there is a unique local solution  $(S(t), E(t), A(t), I(t), R(t)) \in \mathbb{R}_+^5$  for all  $t \in [0, \tau_e)$ , where  $\tau_e$  is the explosion time (Mao [2007]). We now prove  $\tau_e = \infty$  a.s. so that the solution becomes global.

Let  $\kappa_0 > 0$  be sufficiently large for every coordinate  $(S(0), E(0), A(0), I(0), R(0))$  lying within the interval  $[\frac{1}{\kappa_0}, \kappa_0]$ . We then define, for every integer  $\kappa_1 > \kappa_0$ , the stopping time

$$\tau_{\kappa_1} = \inf \left\{ t \in [0, \tau_e) : S(t) \notin \left( \frac{1}{\kappa_1}, \kappa_1 \right) \text{ or } E(t) \notin \left( \frac{1}{\kappa_1}, \kappa_1 \right) \text{ or } A(t) \notin \left( \frac{1}{\kappa_1}, \kappa_1 \right) \right. \\ \left. \text{or } I(t) \notin \left( \frac{1}{\kappa_1}, \kappa_1 \right) \text{ or } R(t) \notin \left( \frac{1}{\kappa_1}, \kappa_1 \right) \right\}. \quad (5.13)$$

Thus,  $\tau_{\kappa_1}$  is increasing as  $\kappa_1 \rightarrow \infty$ . Set  $\lim_{\kappa_1 \rightarrow \infty} \tau_{\kappa_1} = \tau_\infty$ , when  $\tau_\infty \leq \tau_e$  a.s. We show that  $\tau_\infty = \infty$  with a contradiction. Let us assume that our claim is not true and there exist two constants  $T_2 > 0$  and  $\epsilon_3 \in (0, 1)$  such that

$$P(\tau_\infty \leq T_2) > \epsilon_3. \quad (5.14)$$

Thus, there exists an integer  $\kappa_2 \geq \kappa_0$  such that

$$P(\tau_{\kappa_1} \leq T_2) \geq \epsilon_3, \quad \forall \kappa_1 \geq \kappa_2. \quad (5.15)$$

At first, we can show that  $S(t), E(t), A(t), I(t), R(t)$  are bounded. From system (5.2), for  $t \leq \tau_{\kappa_1}$ , we have, for each  $\kappa_1$ ,

$$d(S + E + A + I + R) = (\Lambda - m(S + E + A + I + R)) dt.$$



## 5. Persistence and extinction criteria of Covid-19 pandemic: India as a case study

---

Therefore,

$$\frac{d(S + E + A + I + R)}{dt} = \Lambda - m(S + E + A + I + R)$$

and

$$S(t) + E(t) + A(t) + I(t) + R(t) = \frac{\Lambda}{m} + \left( S(0) + E(0) + A(0) + I(0) + R(0) - \frac{\Lambda}{m} \right) e^{-mt}.$$

Hence,

$$S(t) + E(t) + A(t) + I(t) + R(t) \leq \begin{cases} \frac{\Lambda}{m} & \text{if } S(0) + E(0) + A(0) + I(0) + R(0) \leq \frac{\Lambda}{m} \\ S(0) + E(0) + A(0) + I(0) + R(0) & \\ & \text{if } S(0) + E(0) + A(0) + I(0) + R(0) \geq \frac{\Lambda}{m} \end{cases}$$

Noticing that  $u + 1 - \ln u > 0$  for all  $u > 0$  and  $(S(t), E(t), A(t), I(t), R(t)) \in \mathbb{R}_+^5$ , we define the following positive definite function

$$U = (S + 1 - \ln S) + (E + 1 - \ln E) + (A + 1 - \ln A) + (I + 1 - \ln I) + (R + 1 - \ln R).$$

Applying Ito's formula, one can have

$$\begin{aligned} dU &= \left(1 - \frac{1}{S}\right) dS + \frac{1}{2S^2} (dS)^2 + \left(1 - \frac{1}{E}\right) dE + \frac{1}{2E^2} (dE)^2 + \left(1 - \frac{1}{A}\right) dA \\ &+ \frac{1}{2A^2} (dA)^2 + \left(1 - \frac{1}{I}\right) dI + \frac{1}{2I^2} (dI)^2 + \left(1 - \frac{1}{R}\right) dR + \frac{1}{2R^2} (dR)^2 \\ &= \left(1 - \frac{1}{S}\right) \left[ \left( \Lambda - mS - \frac{\beta S}{N} ((1 - \kappa)I + \kappa A) \right) dt - \frac{\sigma_1 S}{N} ((1 - \kappa)I + \kappa A) dB_1(t) \right] \\ &+ \frac{1}{2N^2} \sigma_1^2 ((1 - \kappa)I + \kappa A)^2 dt + \left(1 - \frac{1}{E}\right) \left[ \frac{\beta S}{N} ((1 - \kappa)I + \kappa A) \right. \\ &- \left. ((1 - \delta)\omega + \delta\omega + m)E \right] dt + \frac{\sigma_1 S}{N} ((1 - \kappa)I + \kappa A) dB_1(t) \\ &+ \frac{1}{2N^2 E^2} \sigma_1^2 ((1 - \kappa)I + \kappa A)^2 dt + \left(1 - \frac{1}{A}\right) [(\delta\omega E - (\gamma_1 + \nu + m)A) dt \end{aligned}$$

## 5.2. Mathematical results

---

$$\begin{aligned}
& - \sigma_2 AdB_2(t) + \frac{1}{2}\sigma_2^2 dt + \left(1 - \frac{1}{I}\right) [((1 - \delta)\omega E - (\gamma + m + d_i)I + \nu A) dt \\
& - \sigma_3 IdB_3(t) + \frac{1}{2}\sigma_3^2 dt + \left(1 - \frac{1}{R}\right) [(\gamma_1 A + \gamma I - mR) dt + \sigma_2 AdB_2(t) \\
& + \sigma_3 IdB_3(t)] + \frac{1}{2R^2}(\sigma_2 AdB_2(t) + \sigma_3 IdB_3(t))^2 \\
& = \left(\Lambda - mS - \frac{\beta S}{N}((1 - \kappa)I + \kappa A) - \frac{\Lambda}{S} + m + \frac{\beta S}{N}((1 - \kappa)I + \kappa A) - (\omega + m)E\right. \\
& - \frac{\beta S}{NE}((1 - \kappa)I + \kappa A) + (\omega + m) + \frac{1}{2N^2 E^2}\sigma_1^2((1 - \kappa)I + \kappa A)^2 + \delta\omega E \\
& - (\gamma_1 + m + d_i)I + \nu A - \frac{1}{I}(1 - \delta)\omega E + (\gamma + m + d_i) - \frac{\nu A}{I} + \frac{1}{2}\sigma_3^2 + \gamma_1 A + \gamma I \\
& - mR - \frac{\gamma_1 A}{R} - \frac{\gamma I}{R} + m + \frac{\sigma_2^2 A^2}{2R^2} + \frac{\sigma_3^2 I^2}{2R^2}\left. \right) dt + \left(\frac{\sigma_1}{N}((1 - \kappa)I + \kappa A) \left\{1 - \frac{S}{E}\right\} dB_1(t)\right. \\
& + \sigma_2 \left\{1 - \frac{A}{R}\right\} dB_2(t) + \sigma_3 \left\{1 - \frac{I}{R}\right\} dB_3(t)\left. \right). \tag{5.16}
\end{aligned}$$

Noting that  $N(t) \geq 1$ ,  $E(t) \geq 1$ ,  $R(t) \geq 1$  and  $u \leq 2(u + 1 - \ln u)$  for all  $u > 0$ , the above expression becomes

$$\begin{aligned}
dU & \leq \left[ \left( \Lambda + 5m + \beta + \omega + \gamma + \gamma_1 + \nu + d_i + \sigma_1^2 + \frac{1}{2}(\sigma_2^2 + \sigma_3^2) \left(1 + \frac{\Lambda^2}{m^2}\right) \right) \right. \\
& + 2(S + 1 - \ln S) + 2\delta\omega(E + 1 - \ln E) + 2\gamma_1(A + 1 - \ln A) + 2\gamma(I + 1 - \ln I) \\
& + \left. 2(R + 1 - \ln R) \right] dt + \left( \frac{\sigma_1}{N}((1 - \kappa)I + \kappa A) \left\{1 - \frac{S}{E}\right\} dB_1(t) \right. \\
& + \left. \sigma_2 \left\{1 - \frac{A}{R}\right\} dB_2(t) + \sigma_3 \left\{1 - \frac{I}{R}\right\} dB_3(t) \right). \tag{5.17}
\end{aligned}$$

Let  $\Delta_1 = \Lambda + 5m + \beta + \omega + \gamma + \gamma_1 + \nu + d_i + \sigma_1^2 + \frac{1}{2}(\sigma_2^2 + \sigma_3^2) \left(1 + \frac{\Lambda^2}{m^2}\right)$  and  $\Delta_2 = \max\{1, \delta\omega, \gamma, \gamma_1\}$ . Then

$$\begin{aligned}
dU & \leq (\Delta_1 + \Delta_2 U) dt + \left( \frac{\sigma_1}{N}((1 - \kappa)I + \kappa A) \left\{1 - \frac{S}{E}\right\} dB_1(t) + \sigma_2 \left\{1 - \frac{A}{R}\right\} dB_2(t) \right. \\
& + \left. \sigma_3 \left\{1 - \frac{I}{R}\right\} dB_3(t) \right).
\end{aligned}$$

## 5. Persistence and extinction criteria of Covid-19 pandemic: India as a case study

---

Defining  $\Delta_3 = \max\{\Delta_1, \Delta_2\}$ , we have

$$\begin{aligned} dU \leq & \Delta_3(1+U)dt + \left( \frac{\sigma_1}{N}((1-\kappa)I + \kappa A) \left\{ 1 - \frac{S}{E} \right\} dB_1(t) + \sigma_2 \left\{ 1 - \frac{A}{R} \right\} dB_2(t) \right. \\ & \left. + \sigma_3 \left\{ 1 - \frac{I}{R} \right\} dB_3(t) \right). \end{aligned} \quad (5.18)$$

Observe that  $\frac{\sigma_1}{N}((1-\kappa)I + \kappa A) \left\{ 1 - \frac{S}{E} \right\} \leq \sigma_1 \left( 1 - \frac{m}{\Lambda} \right)$ ,  $\sigma_2 \left( 1 - \frac{A}{R} \right) \leq \sigma_2 \left( 1 - \frac{m}{\Lambda} \right)$ ,  $\sigma_3 \left( 1 - \frac{I}{R} \right) \leq \sigma_3 \left( 1 - \frac{m}{\Lambda} \right)$ , we have  $\mathbb{E} \int_0^{\tau_{\kappa_1} \wedge T_2} \left| \sigma_2 \left( 1 - \frac{A}{R} \right) \right|^2 dt < \infty$ ,  $\mathbb{E} \int_0^{\tau_{\kappa_1} \wedge T_2} \left| \frac{\sigma_1}{N(t)}((1-\kappa)I(t) + \kappa A(t)) \left\{ 1 - \frac{S(t)}{E(t)} \right\} \right|^2 dt < \infty$ ,  $\mathbb{E} \int_0^{\tau_{\kappa_1} \wedge T_2} \left| \sigma_3 \left( 1 - \frac{I}{R} \right) \right|^2 dt < \infty$ . Now, since all these functions  $\frac{\sigma_1}{N}((1-\kappa)I + \kappa A) \left\{ 1 - \frac{S}{E} \right\}$ ,  $\sigma_2 \left( 1 - \frac{A}{R} \right)$ ,  $\sigma_3 \left( 1 - \frac{I}{R} \right)$  are continuous, bounded and non-anticipative, then for a sequence of partition of the interval  $[0, \tau_{\kappa_1} \wedge T_2]$  with mesh size  $\Delta t \rightarrow 0$ , we have

$$\begin{aligned} & \mathbb{E} \int_0^{\tau_{\kappa_1} \wedge T_2} \frac{\sigma_1}{N(t)}((1-\kappa)I(t) + \kappa A(t)) \left\{ 1 - \frac{S(t)}{E(t)} \right\} dB_1(t) \\ &= \lim_{\Delta t \rightarrow 0} \sum_j \mathbb{E} \left( \frac{\sigma_1}{N(t_j)}((1-\kappa)I(t_j) + \kappa A(t_j)) \left\{ 1 - \frac{S(t_j)}{E(t_j)} \right\} \right) \mathbb{E}(B_1(t_{j+1}) - B_1(t_j)), \\ & \text{since } \frac{\sigma_1}{N(t_j)}((1-\kappa)I(t_j) + \kappa A(t_j)) \left\{ 1 - \frac{S(t_j)}{E(t_j)} \right\} \text{ is independent of } B_1(t_{j+1}) - B_1(t_j). \end{aligned}$$

$$\begin{aligned} & \mathbb{E} \int_0^{\tau_{\kappa_1} \wedge T_2} \sigma_2 \left( 1 - \frac{A}{R} \right) dB_2(t) = \lim_{\Delta t \rightarrow 0} \sum_j \mathbb{E} \left( \sigma_2 \left( 1 - \frac{A(t_j)}{R(t_j)} \right) \right) \mathbb{E}(B_2(t_{j+1}) - B_2(t_j)), \\ & \text{since } \sigma_2 \left( 1 - \frac{A(t_j)}{R(t_j)} \right) \text{ is independent of } B_2(t_{j+1}) - B_2(t_j). \end{aligned}$$

and

$$\begin{aligned} & \mathbb{E} \int_0^{\tau_{\kappa_1} \wedge T_2} \sigma_3 \left( 1 - \frac{I}{R} \right) dB_3(t) = \lim_{\Delta t \rightarrow 0} \sum_j \mathbb{E} \left( \sigma_3 \left( 1 - \frac{I(t_j)}{R(t_j)} \right) \right) \mathbb{E}(B_3(t_{j+1}) - B_3(t_j)), \\ & \text{since } \sigma_3 \left( 1 - \frac{I(t_j)}{R(t_j)} \right) \text{ is independent of } B_3(t_{j+1}) - B_3(t_j). \end{aligned}$$

Using the fact that the increments of Brownian motion are normally distributed with

## 5.2. Mathematical results

---

mean zero and variance  $t_{j+1} - t_j$ , we have

$$\begin{aligned} & \mathbb{E} \int_0^{\tau_{\kappa_1} \wedge T_2} \frac{\sigma_1}{N(t)} ((1 - \kappa)I(t) + \kappa A(t)) \left\{ 1 - \frac{S(t)}{E(t)} \right\} dB_1(t) = 0, \\ & \mathbb{E} \int_0^{\tau_{\kappa_1} \wedge T_2} \sigma_2 \left( 1 - \frac{A}{R} \right) dB_2(t) = 0 \quad \text{and} \quad \mathbb{E} \int_0^{\tau_{\kappa_1} \wedge T_2} \sigma_3 \left( 1 - \frac{I}{R} \right) dB_3(t) = 0. \end{aligned}$$

Integrating both sides of (5.18) from 0 to  $\tau_{\kappa_1} \wedge T_2$ , taking the expectation and using the above fact, we obtain

$$\begin{aligned} & \mathbb{E}U\left(S(\tau_{\kappa_1} \wedge T_2), E(\tau_{\kappa_1} \wedge T_2), A(\tau_{\kappa_1} \wedge T_2), I(\tau_{\kappa_1} \wedge T_2), R(\tau_{\kappa_1} \wedge T_2)\right) \\ & \leq U\left(S(0), E(0), A(0), I(0), R(0)\right) + \Delta_3 \mathbb{E} \int_0^{\tau_{\kappa_1} \wedge T_2} (1 + U) dt \\ & \leq U\left(S(0), E(0), A(0), I(0), R(0)\right) + \Delta_3 T_2 + \Delta_3 \mathbb{E} \int_0^{\tau_{\kappa_1} \wedge T_2} U dt. \end{aligned} \quad (5.19)$$

Since  $U$  is increasing function on  $[0, \tau_{\kappa_1} \wedge T_2]$ , hence for any  $t \in [0, \tau_{\kappa_1} \wedge T_2]$   $U(S(t), E(t), A(t), I(t), R(t)) \leq U(S(\tau_{\kappa_1} \wedge T_2), E(\tau_{\kappa_1} \wedge T_2), A(\tau_{\kappa_1} \wedge T_2), I(\tau_{\kappa_1} \wedge T_2), R(\tau_{\kappa_1} \wedge T_2))$ .

$$\begin{aligned} \therefore & \mathbb{E}U\left(S(\tau_{\kappa_1} \wedge T_2), E(\tau_{\kappa_1} \wedge T_2), A(\tau_{\kappa_1} \wedge T_2), I(\tau_{\kappa_1} \wedge T_2), R(\tau_{\kappa_1} \wedge T_2)\right) \\ & \leq U\left(S(0), E(0), A(0), I(0), R(0)\right) + \Delta_3 T_2 \\ & + \Delta_3 \mathbb{E} \int_0^{\tau_{\kappa_1} \wedge T_2} U(S(\tau_{\kappa_1} \wedge T_2), E(\tau_{\kappa_1} \wedge T_2), A(\tau_{\kappa_1} \wedge T_2), I(\tau_{\kappa_1} \wedge T_2), R(\tau_{\kappa_1} \wedge T_2)) dt \\ & = U\left(S(0), E(0), A(0), I(0), R(0)\right) + \Delta_3 T_2 \\ & + \Delta_3 \int_0^{\tau_{\kappa_1} \wedge T_2} \mathbb{E}U(S(\tau_{\kappa_1} \wedge T_2), E(\tau_{\kappa_1} \wedge T_2), A(\tau_{\kappa_1} \wedge T_2), I(\tau_{\kappa_1} \wedge T_2), R(\tau_{\kappa_1} \wedge T_2)) dt. \end{aligned}$$

Gronwall's inequality then gives

$$\begin{aligned} & \mathbb{E}U(S(\tau_{\kappa_1} \wedge T_2), E(\tau_{\kappa_1} \wedge T_2), A(\tau_{\kappa_1} \wedge T_2), I(\tau_{\kappa_1} \wedge T_2), R(\tau_{\kappa_1} \wedge T_2)) \\ & \leq (U(S(0), E(0), A(0), I(0), R(0)) + \Delta_3 T_2) e^{\Delta_3 (\tau_{\kappa_1} \wedge T_2)} = \Delta_4 \text{ (say)}. \end{aligned} \quad (5.20)$$

Set  $\Omega_{\kappa_1} = \{\tau_{\kappa_1} \leq T_2\}$  for all  $\kappa_1 \geq \kappa_2$ . Thus, following (5.15), we get  $P(\Omega_{\kappa_1}) \geq \epsilon_3$  for all  $\omega_2 \in \Omega_{\kappa_1}$ . Clearly, at least one of  $S(\tau_{\kappa_1}, \omega_2)$ ,  $E(\tau_{\kappa_1}, \omega_2)$ ,  $A(\tau_{\kappa_1}, \omega_2)$ ,  $I(\tau_{\kappa_1}, \omega_2)$ ,  $R(\tau_{\kappa_1}, \omega_2)$  is equal to either  $\kappa_1$  or  $\frac{1}{\kappa_1}$ . Hence,  $V(S(\tau_{\kappa_1}), E(\tau_{\kappa_1}), A(\tau_{\kappa_1}), I(\tau_{\kappa_1}), R(\tau_{\kappa_1}))$  is no less

## 5. Persistence and extinction criteria of Covid-19 pandemic: India as a case study

---

than  $\min \left\{ \kappa_1 + 1 - \ln \kappa_1, \frac{1}{\kappa_1} + 1 + \ln \kappa_1 \right\}$ . From (5.14) and (5.20), we then obtain

$$\begin{aligned} \Delta_4 &\geq \mathbb{E}[1_{\Omega_{\kappa_1}} U(S(\tau_{\kappa_1}, \omega_2), E(\tau_{\kappa_1}, \omega_2), A(\tau_{\kappa_1}, \omega_2), I(\tau_{\kappa_1}, \omega_2), R(\tau_{\kappa_1}, \omega_2))] \\ &\geq \epsilon_3 \left[ (\kappa_1 + 1 - \ln \kappa_1) \wedge \left( \frac{1}{\kappa_1} + 1 + \ln \kappa_1 \right) \right], \end{aligned} \quad (5.21)$$

where  $1_{\Omega_{\kappa_1}}$  is the indicator function of  $\Omega_{\kappa_1}$ . Letting  $\kappa_1 \rightarrow \infty$ , we get  $\infty > \Delta_4 = \infty$ , a contradiction. Hence  $\tau_\infty = \infty$  a.s. Hence the theorem is proven.  $\square$

**Theorem 5.2.5.** *The solution  $(S(t), E(t), A(t), I(t), R(t)) \in \mathbb{R}_+^5$  of system (5.2) is stochastically ultimately bounded for any positive initial value  $(S(0), E(0), A(0), I(0), R(0)) \in \mathbb{R}_+^5$ .*

*Proof.* From the first two equations of (5.2), we have

$$\begin{aligned} dS + dE &= \Lambda - mS - ((1 - \delta)\omega + \delta\omega + m)E \\ &\leq \Lambda - m(S + E). \end{aligned}$$

Therefore,

$$\limsup_{t \rightarrow \infty} (S(t) + E(t)) \leq \frac{\Lambda}{m}. \quad (5.22)$$

We denote  $Q = A + I$  and define  $H(t) = Q + \frac{1}{Q}$ . We first define the differential operator  $L$ . The Ito differential equation has the form (Mao [2007])

$$dX(t) = P_1(X(t), t)dt + Q_1(X(t), t)dB(t), X(t_0) = X_0 \in \mathbb{R}_+^n \text{ for } t \geq t_0, \quad (5.23)$$

where  $P_1(X(t), t)$  is called drift function and  $Q_1(X(t), t)$  is called diffusion matrix. Let  $(\Omega, \mathbb{F}, \mathbb{P})$  be a complete probability space with a filtration  $\{\mathbb{F}_t\}_{t \geq 0}$ . The differential operator  $L$  of equation (5.23) is defined by

$$L = \frac{\partial}{\partial t} + \sum_{j=1}^n P_{1j}(X(t), t) \frac{\partial}{\partial P_{1j}} + \frac{1}{2} \sum_{i,j=1}^n [Q_1(X(t), t), Q_1(X(t), t)^T]_{i,j} \frac{\partial^2}{\partial Q_{1i} \partial Q_{1j}}.$$

## 5.2. Mathematical results

---

By Ito's formula and using the definition of  $L$  operator, we have

$$\begin{aligned} L(H(t)) &= [\omega E - (\gamma_1 + m)A - (\gamma + m + d_i)I] - \frac{\omega E - (\gamma_1 + m)A - (\gamma + m + d_i)I}{Q^2} \\ &\quad + \frac{\sigma_2^2 A^2 + \sigma_3^2 I^2}{Q^3} \\ &= \omega E - mQ - \gamma_1 A - (\gamma + d_i)I - \frac{\omega E}{Q^2} + \frac{m}{Q} + \frac{\gamma_1 A}{Q^2} + \frac{(\gamma + d_i)I}{Q^2} + \frac{\sigma_2^2 A^2 + \sigma_3^2 I^2}{Q^3}. \end{aligned}$$

Using the fact that  $Q > 1$ ,  $Q > A$  and  $Q > I$ , we have

$$\begin{aligned} L(H(t)) &\leq \omega E - m \left( Q + \frac{1}{Q} \right) + \frac{2m}{Q} + \frac{\gamma_1 A}{Q^2} + \frac{(\gamma + d_i)I}{Q^2} + \frac{\sigma_2^2 A^2 + \sigma_3^2 I^2}{Q^3} \\ &\leq \frac{\omega \Lambda}{m} + 2m + \gamma_1 + \gamma + d_i + \sigma_2^2 + \sigma_3^2 - m \left( Q + \frac{1}{Q} \right) \\ &= B - mH(t), \end{aligned} \tag{5.24}$$

where  $B = \frac{\omega \Lambda}{m} + 2m + \gamma_1 + \gamma + d_i + \sigma_2^2 + \sigma_3^2$ .

Again applying Ito's formula and using (5.24)

$$\begin{aligned} \mathbb{E}[e^{mt} H(t)] &= \mathbb{E}[H(0)] + \mathbb{E} \left[ \int_0^t e^{ms} (mH(s) + L(H(s))) ds \right] \\ &\leq \mathbb{E}[H(0)] + B \mathbb{E} \left[ \int_0^t e^{ms} ds \right] \\ &= \mathbb{E}[H(0)] + \frac{B}{m} (e^{mt} - 1). \end{aligned} \tag{5.25}$$

Therefore, we have

$$\begin{aligned} \mathbb{E}[H(t)] &\leq e^{-mt} \mathbb{E}[H(0)] + \frac{B}{m} (1 - e^{-mt}) \\ \therefore \limsup_{t \rightarrow \infty} \mathbb{E}[H(t)] &\leq \frac{B}{m} = C. \end{aligned}$$

We now chose a sufficiently large constant  $\alpha_1$  such that  $\frac{C}{\alpha_1} < 1$  and applying Chebyshev's inequality

$$P \left( Q + \frac{1}{Q} > \alpha_1 \right) \leq \frac{\mathbb{E} \left[ Q + \frac{1}{Q} \right]}{\alpha_1} \implies \limsup_{t \rightarrow \infty} P \left( Q + \frac{1}{Q} > \alpha_1 \right) \leq \frac{C}{\alpha_1}.$$

## 5. Persistence and extinction criteria of Covid-19 pandemic: India as a case study

---

Then for a positive constant  $\beta_1 > 0$ , we get a constant  $L_1 > 0$  such that

$$\limsup_{t \rightarrow \infty} P(A > \beta_1) \leq L_1 \quad \text{a.s.}$$

Hence,  $A(t)$  of the system (5.2) is stochastically ultimately bounded and there exists a positive constant  $\bar{A}$  such that for all  $t \in [0, \tau_e)$ ,  $\lim_{t \rightarrow \infty} \sup A(t) \leq \bar{A}$ . By the similar manner,  $I(t)$  of the system (5.2) is stochastically ultimately bounded and there exists a positive constant  $\bar{I}$  such that for all  $t \in [0, \tau_e)$ ,  $\lim_{t \rightarrow \infty} \sup I(t) \leq \bar{I}$ . Using the stochastic bounds of  $I(t)$  and  $A(t)$  in the fifth equation of (5.2), we have

$$R(t) \leq \frac{\gamma_1 \bar{A} + \gamma \bar{I}}{m} + e^{-mt} \left( R(0) - \frac{\gamma_1 \bar{A} + \gamma \bar{I}}{m} - \int_0^t e^{ms} (\sigma_2 A(s) dB_2(s) + \sigma_3 I(s) dB_3(s)) \right).$$

Using the fact that increment of Brownian motion is independent with both the functions  $e^{ms} \sigma_2 A(s)$  and  $e^{ms} \sigma_3 I(s)$  and also the increment of Brownian motion is normally distributed with mean zero, we have

$$\limsup_{t \rightarrow \infty} \mathbb{E}[R(t)] \leq \frac{1}{m} (\gamma_1 \bar{A} + \gamma \bar{I}) = L_3 \quad (\text{say}) \quad \text{a.s.} \quad (5.26)$$

and hence there exists a positive constant  $\bar{R}$  such that for all  $t \in [0, \tau_e)$

$$\limsup_{t \rightarrow \infty} R(t) \leq \bar{R}, \quad \forall t \in [0, \tau_e).$$

□

The following lemma will be used in the sequel.

**Lemma 5.2.6.** *Let  $(S(t), E(t), A(t), I(t), R(t)) \in \mathbb{R}_+^5$  be a solution of the system (5.2) with positive initial value  $(S(0), E(0), A(0), I(0), R(0)) \in \mathbb{R}_+^5$ . Then*

$$\lim_{t \rightarrow \infty} \frac{1}{t} \int_0^t \frac{\sigma_1 S(\tau) ((1 - \kappa) I(\tau) + \kappa A(\tau))}{E(\tau)} dB(\tau) = 0.$$

*Proof.* Let  $M(t) = \int_0^t \frac{\sigma_1 S(\tau) ((1 - \kappa) I(\tau) + \kappa A(\tau))}{E(\tau)} dB(\tau)$  and  $\theta > 2$ . By Burkholder-Davis-Gundy inequality (Mao [2007]) and Theorem 6.3.1, we get

## 5.2. Mathematical results

---

$$\begin{aligned} \mathbb{E} \left[ \sup_{0 \leq \tau \leq t} |M(\tau)|^\theta \right] &\leq C_\theta \mathbb{E} \left[ \int_0^t \frac{\sigma_1^2 S^2(\tau) ((1-\kappa)I(\tau) + \kappa A(\tau))^2}{E^2(\tau)} d\tau \right]^{\frac{\theta}{2}} \\ &\leq C_\theta t^{\frac{\theta}{2}} \mathbb{E} \left[ \sup_{0 \leq \tau \leq t} \frac{\sigma_1^\theta S^\theta(\tau) ((1-\kappa)I + \kappa A)^\theta}{E^\theta(0)} \right] \leq M_\theta C_\theta t^{\frac{\theta}{2}}, \end{aligned} \quad (5.27)$$

where  $M_\theta = \frac{\sigma_1^\theta (1+\kappa)^\theta \Lambda^{2\theta}}{m^{2\theta} E^\theta(0)}$ ,  $C_\theta = \left( \frac{\theta^{\theta+1}}{2(\theta-1)^{(\theta-1)}} \right)^{\frac{\theta}{2}}$ .

Then, for any  $0 < \epsilon_1 < \frac{\theta}{2} - 1$ , by Chebyshev's inequality (Mao [2007])

$$\begin{aligned} P \left\{ \omega_1 : \sup_{n\delta_1 \leq t \leq (n+1)\delta_1} |M(t)|^\theta > (n\delta_1)^{1+\epsilon_1+\frac{\theta}{2}} \right\} &\leq \frac{\mathbb{E} (|M(n+1)\delta_1|^\theta)}{(n\delta_1)^{1+\epsilon_1+\frac{\theta}{2}}} \leq \frac{M_\theta C_\theta [(n+1)\delta_1]^{\frac{\theta}{2}}}{(n\delta_1)^{1+\epsilon_1+\frac{\theta}{2}}} \\ &\leq \frac{2^{\frac{\theta}{2}} M_\theta C_\theta}{(n\delta_1)^{1+\epsilon_1}}. \end{aligned} \quad (5.28)$$

Using the Borel-Cantelli lemma (Mao [2007]), for almost all  $\omega_1 \in \Omega$ ,

$$\sup_{n\delta_1 \leq t \leq (n+1)\delta_1} |M(t)|^\theta \leq (n\delta_1)^{1+\epsilon_1+\frac{\theta}{2}}$$

hold for all except finitely many  $n$ . Then there exists a positive  $n_0(\omega_1)$ , for almost all  $\omega_1 \in \Omega$  and  $n \geq n_0(\omega_1)$ , such that  $\sup_{n\delta_1 \leq t \leq (n+1)\delta_1} |M(t)|^\theta \leq (n\delta_1)^{1+\epsilon_1+\frac{\theta}{2}}$  holds. If  $n \geq n_0(\omega_1)$  and  $n\delta_1 \leq t \leq (n+1)\delta_1$ , for almost all  $\omega_1 \in \Omega$ ,

$$\frac{\ln |M(t)|^\theta}{\ln t} \leq \frac{(1 + \epsilon_1 + \frac{\theta}{2}) \ln(n\delta_1)}{\ln(n\delta_1)} = 1 + \epsilon_1 + \frac{\theta}{2}.$$

We then have

$$\limsup_{t \rightarrow \infty} \frac{\ln |M(t)|}{\ln t} \leq \frac{1 + \epsilon_1 + \frac{\theta}{2}}{\theta}.$$

Let  $\epsilon_1 \rightarrow 0$ ,

$$\limsup_{t \rightarrow \infty} \frac{\ln |M(t)|}{\ln t} \leq \frac{1}{2} + \frac{1}{\theta} \text{ a.s.}$$

Then, for an arbitrary positive constant  $\delta_1$  ( $\delta_1 < \frac{1}{2} - \frac{1}{\theta}$ ), there exists a constant  $K(\omega_1)$



## 5. Persistence and extinction criteria of Covid-19 pandemic: India as a case study

---

and a set  $\Omega_{\delta_1}$  such that  $P(\Omega_{\delta_1}) \geq 1 - \delta_1$  and for  $t \geq K(\omega_1)$ ,  $\omega_1 \in \Omega_{\delta_1}$ ,

$$0 \leq \liminf_{t \rightarrow \infty} \frac{|M(t)|}{t} \leq \limsup_{t \rightarrow \infty} \frac{|M(t)|}{t} \leq \limsup_{t \rightarrow \infty} \frac{t^{\frac{1}{2} + \frac{1}{\theta} + \delta_1}}{t} = 0 \text{ a.s.}$$

$$\therefore \lim_{t \rightarrow \infty} \frac{|M(t)|}{t} = 0, \text{ a.s.} \implies \lim_{t \rightarrow \infty} \frac{M(t)}{t} = \lim_{t \rightarrow \infty} \frac{\int_0^t \frac{\sigma_1 S(\tau)((1-\kappa)I(\tau) + \kappa A(\tau))}{E(\tau)} dB(\tau)}{t} = 0 \text{ a.s.}$$

Hence the lemma is proven.  $\square$

**Definition 5.2.7.** For the system (5.2), the exposed class  $E(t)$  is said to be extinct (i.e., the system will be disease-free) if  $\lim_{t \rightarrow \infty} E(t) = 0$  a.s.

**Theorem 5.2.8.** Let  $R_0^S = \frac{\beta^2}{2\sigma_1^2(\omega+m)}$ . Then the exposed individuals of system (5.2) tend to zero exponentially almost surely if  $R_0^S < 1$ .

*Proof.* Assume that  $(S(t), E(t), A(t), I(t), R(t)) \in \mathbb{R}_+^5$  is a solution of system (5.2) satisfying the initial value  $(S(0), E(0), A(0), I(0), R(0)) \in \mathbb{R}_+^5$ . Following Ito's formula,

$$\begin{aligned} d(\ln E(t)) &= \left[ \frac{\beta S((1-\kappa)I + \kappa A)}{NE} - ((1-\delta)\omega + \delta\omega + m) \right. \\ &\quad \left. - \frac{1}{2N^2 E^2} \sigma_1^2 S^2 ((1-\kappa)I + \kappa A)^2 \right] dt + \frac{\sigma_1 \beta S((1-\kappa)I + \kappa A)}{NE} dB_1(t). \end{aligned} \quad (5.29)$$

Upon integration from 0 to  $t$ , we have

$$\begin{aligned} \ln E(t) &= \int_0^t \left( \frac{\beta S(\tau)((1-\kappa)I(\tau) + \kappa A(\tau))}{N(\tau)E(\tau)} - \frac{\sigma_1^2 S^2(\tau)((1-\kappa)I(\tau) + \kappa A(\tau))^2}{2N^2(\tau)E^2(\tau)} \right) \\ &\quad - ((1-\delta)\omega + \delta\omega + m)t + M_1(t) + \ln E(0), \end{aligned} \quad (5.30)$$

where  $M_1(t) = \int_0^t \frac{\sigma_1 \beta S((1-\kappa)I + \kappa A)}{NE} dB_1(t)$  and  $M_1(t)$  is the local continuous martingale with  $M_1(0) = 0$ .

Let  $x = \frac{S(\tau)((1-\kappa)I(\tau) + \kappa A(\tau))}{N(\tau)E(\tau)}$  and  $\frac{\beta S(\tau)((1-\kappa)I(\tau) + \kappa A(\tau))}{N(\tau)E(\tau)} - \frac{\sigma_1^2 S^2(\tau)((1-\kappa)I(\tau) + \kappa A(\tau))^2}{2N^2(\tau)E^2(\tau)} = \beta x - \frac{\sigma_1^2}{2} x^2 = f(x)$  (say). Then  $f'(x) = 0$  holds for  $x = \frac{\beta}{\sigma_1^2}$  and  $f''(x)|_{x=\frac{\beta}{\sigma_1^2}} = -\sigma_1^2 < 0$ .

Hence  $\max f(x) = f(\frac{\beta}{\sigma_1^2}) = \frac{\beta^2}{2\sigma_1^2}$ . Using the fact that

$$\max \left( \frac{\beta S(\tau)((1-\kappa)I(\tau) + \kappa A(\tau))}{N(\tau)E(\tau)} - \frac{\sigma_1^2 S^2(\tau)((1-\kappa)I(\tau) + \kappa A(\tau))^2}{2N^2(\tau)E^2(\tau)} \right) = \frac{\beta^2}{2\sigma_1^2} \text{ and } \beta M(t) > M_1(t), \quad (5.30)$$

## 5.2. Mathematical results

---

becomes

$$\ln E(t) \leq \left( \frac{\beta^2}{2\sigma_1^2} - ((1 - \delta)\omega + \delta\omega + m) \right) t + \beta M(t) + \ln E(0). \quad (5.31)$$

Taking the limit superior as  $t \rightarrow \infty$  after dividing both sides of (5.31) by  $t$  ( $> 0$ ) and using Lemma 5.2.6, we have

$$\limsup_{t \rightarrow \infty} \frac{\ln E(t)}{t} \leq \left( \frac{\beta^2}{2\sigma_1^2} - (\omega + m) \right) < 0. \quad (5.32)$$

If  $R_0^S = \frac{\beta^2}{2\sigma_1^2(\omega+m)} < 1$ , then  $\lim_{t \rightarrow \infty} E(t) = 0$  almost surely. Hence the proof is completed.  $\square$

In the following, we give a strong disease persistence condition.

**Theorem 5.2.9.** *Suppose the following holds*

$$\theta_1(\omega - \max\{\gamma_1 + m, \gamma + m + d_i\}) - \frac{\theta_1(\theta_1 + 1)}{2} \max\{\sigma_2^2, \sigma_3^2\} > l > 0,$$

where  $0 < \theta_1 < 2$ , for any initial value  $(S(0), E(0), A(0), I(0), R(0)) \in \mathbb{R}_+^5$ . Then the disease will be persistent in the system.

*Proof.* Define  $W(t) = A + I$ . Then

$$\begin{aligned} dW(t) &= [\{\delta\omega E - (\gamma_1 + \nu + m)A\} + \{(1 - \delta)\omega E - (\gamma + m + d_i)I + \nu A\}]dt \\ &\quad - \sigma_2 AdB_2(t) - \sigma_3 IdB_3(t). \end{aligned} \quad (5.33)$$

Let  $V_1(z) = \frac{1}{W(z)}$ . Ito's formula then gives

$$\begin{aligned} dV_1 &= \left( -V_1^2[\{\delta\omega E - (\gamma_1 + m)A\} + \{(1 - \delta)\omega E - (\gamma + m + d_i)I\}] \right. \\ &\quad \left. + V_1^3(\sigma_2^2 A^2 + \sigma_3^2 I^2) \right) dt + V_1^2(\sigma_2 AdB_2(t) + \sigma_3 IdB_3(t)). \end{aligned} \quad (5.34)$$

Define  $Z = (1 + V_1)^{\theta_1}$ . Again applying Ito's formula, one has

$$dZ = LZdt + \theta_1(1 + V_1)^{\theta_1-1} V_1^2(-\sigma_2 AdB_2 - \sigma_3 IdB_3),$$

## 5. Persistence and extinction criteria of Covid-19 pandemic: India as a case study

---

where

$$LZ = \theta_1(1 + V_1)^{\theta_1 - 1} \left( -V_1^2[\{\delta\omega E - (\gamma_1 + m)A\} + \{(1 - \delta)\omega E - (\gamma + m + d_i)I\}] \right. \\ \left. + V_1^3(\sigma_2^2 A^2 + \sigma_3^2 I^2) \right) + \frac{\theta_1(\theta_1 - 1)}{2}(1 + V_1)^{\theta_1 - 2} V_1^4(\sigma_2^2 A^2 + \sigma_3^2 I^2).$$

Now choose  $l > 0$  sufficiently small such that it satisfies  $\theta_1(\omega - \max\{\gamma_1 + m, \gamma + m + d_i\}) - \frac{\theta_1(\theta_1 + 1)}{2} \max\{\sigma_2^2, \sigma_3^2\} > l > 0$ . Noting that  $e^{\alpha t}$  is of finite variation so that  $L[e^{\alpha t}, Z] = 0$ , then by Ito's formula

$$\begin{aligned} L(e^{\alpha t} Z) &= e^{\alpha t} LZ + \alpha e^{\alpha t} Z + L[e^{\alpha t}, Z] \\ &= e^{\alpha t} L(1 + V_1)^{\theta_1} + \alpha e^{\alpha t} (1 + V_1)^{\theta_1} \\ &= e^{\alpha t} \left\{ \theta_1(1 + V_1)^{\theta_1 - 1} \left( -V_1^2[\{(1 - \delta)\omega E - (\gamma + m + d_i)I\}] \right. \right. \\ &\quad \left. \left. + \{\delta\omega E - (\gamma_1 + m + d_i)A\}] + V_1^3(\sigma_2^2 I^2 + \sigma_3^2 A^2) \right) \right. \\ &\quad \left. + \frac{\theta_1(\theta_1 - 1)}{2}(1 + V_1)^{\theta_1 - 2} V_1^4(\sigma_2^2 I^2 + \sigma_3^2 A^2) \right\} + \alpha e^{\alpha t} (1 + V_1)^{\theta_1} \\ &= e^{\alpha t} (1 + V_1)^{\theta_1 - 2} \{ \alpha(1 + V_1)^2 + P \}, \end{aligned}$$

where

$$\begin{aligned} P &= \theta_1(1 + V_1) \left\{ -V_1^2[\{\delta\omega E - (\gamma_1 + m)A\} + \{(1 - \delta)\omega E - (\gamma + m + d_i)I\}] \right. \\ &\quad \left. + V_1^3(\sigma_2^2 A^2 + \sigma_3^2 I^2) \right\} + \frac{\theta_1(\theta_1 - 1)}{2}(1 + V_1)^{\theta_1 - 2} V_1^4(\sigma_2^2 A^2 + \sigma_3^2 I^2) \\ &= -\theta_1 V_1^2[\{\delta\omega E - (\gamma_1 + m)\} + \{(1 - \delta)\omega E - (\gamma + m + d_i)\}] \\ &\quad -\theta_1 V_1^3[\{\delta\omega E - (\gamma_1 + m)\} + \{(1 - \delta)\omega E - (\gamma + m + d_i)\}] \\ &\quad + \theta_1 V_1^3(\sigma_2^2 A^2 + \sigma_3^2 I^2) + \frac{\theta_1(\theta_1 + 1)}{2} V_1^4(\sigma_2^2 A^2 + \sigma_3^2 I^2). \end{aligned}$$

Using the fact

$$\sigma_2^2 A^2 + \sigma_3^2 I^2 \leq \max(\sigma_2^2, \sigma_3^2)(A^2 + I^2) \leq \max(\sigma_2^2, \sigma_3^2) \frac{1}{V_1^2},$$

## 5.2. Mathematical results

---

one then obtain

$$\begin{aligned}
P &\leq -\theta_1 V_1^2 \left( \frac{\omega}{V_1} - \max\{\gamma_1 + m, \gamma + m + d_i\} \frac{1}{V_1} \right) \\
&\quad -\theta_1 V_1^3 \left( \frac{\omega}{V_1} - \max\{\gamma_1 + m, \gamma + m + d_i\} \frac{1}{V_1} \right) + \frac{\theta_1(\theta_1 + 1)}{2} V_1^4 \max(\sigma_2^2, \sigma_3^2) \frac{1}{V_1^2} \\
&\quad + \theta_1 V_1^3 \max(\sigma_2^2, \sigma_3^2) \frac{1}{V_1^2}.
\end{aligned}$$

Under the condition  $\theta_1(\omega - \max\{\gamma_1 + m, \gamma + m + d_i\}) - \frac{\theta_1(\theta_1 + 1)}{2} \max\{\sigma_2^2, \sigma_3^2\} > l > 0$  and  $0 < \theta_1 < 2$ , there exists a positive constant  $V_2$  such that

$$\begin{aligned}
L(e^{\alpha t} Z) &= e^{\alpha t} (1 + V_1)^{\theta_1 - 2} \{ \alpha (1 + V_1)^2 + P \} \\
&\leq e^{\alpha t} (1 + V_1)^{\theta_1 - 2} \left\{ \alpha + V_1 \left[ -\theta_1 \left( \frac{\omega}{V_1} - \max\{\gamma_1 + m, \gamma + m + d_i\} \frac{1}{V_1} \right) \right. \right. \\
&\quad \left. \left. + \theta_1 \max(\sigma_2^2, \sigma_3^2) + 2\alpha \right] - V_1^2 \left[ \theta_1 \left( \frac{\omega}{V_1} - \max\{\gamma_1 + m, \gamma + m + d_i\} \frac{1}{V_1} \right) \right. \right. \\
&\quad \left. \left. - \frac{\theta_1(\theta_1 + 1)}{2} \theta_1 \max(\sigma_2^2, \sigma_3^2) - \alpha \right] \right\} \\
&\leq V_2 e^{\alpha t}, \tag{5.35}
\end{aligned}$$

where  $V_2 = (1 + V_1)^{\theta_1 - 2} \left\{ \alpha + V_1 \left[ -\theta_1 \left( \frac{\omega}{V_1} - \max\{\gamma_1 + m, \gamma + m + d_i\} \frac{1}{V_1} \right) + \theta_1 \max(\sigma_2^2, \sigma_3^2) + 2\alpha \right] - V_1^2 \left[ \theta_1 \left( \frac{\omega}{V_1} - \max\{\gamma_1 + m, \gamma + m + d_i\} \frac{1}{V_1} \right) - \frac{\theta_1(\theta_1 + 1)}{2} \theta_1 \max(\sigma_2^2, \sigma_3^2) - \alpha \right] \right\}$ .

Taking expectation on both sides of (5.35), one gets

$$\begin{aligned}
\mathbb{E}(e^{\alpha t} (1 + V_1)^{\theta_1}) &\leq [1 + V_1(0)]^{\theta_1} + \frac{V_2}{\alpha} e^{\alpha t} \\
&= [1 + V_1(0)]^{\theta_1} + V_3 e^{\alpha t}, \text{ where } V_3 = \frac{V_2}{\alpha}.
\end{aligned}$$

Then

$$\limsup_{t \rightarrow \infty} \mathbb{E} V_1^{\theta_1}(t) \leq \limsup_{t \rightarrow \infty} \mathbb{E}(1 + V_1)^{\theta_1} \leq V_3.$$

Noting  $(A + I)^{\theta_1} \leq 2^{\theta_1} (A^2 + I^2)^{\frac{\theta_1}{2}} = 2^{\theta_1} |W|^{\theta_1}$ , one has

$$\limsup_{t \rightarrow \infty} \mathbb{E} \left( \frac{1}{|W(t)|^{\theta_1}} \right) \leq 2^{\theta_1} \limsup_{t \rightarrow \infty} \mathbb{E} V_1^{\theta_1}(t) \leq 2^{\theta_1} V_3 = V_4 \text{ (say)}.$$

## 5. Persistence and extinction criteria of Covid-19 pandemic: India as a case study

---

Therefore, by Chebyshev's inequality,

$$\mathbb{P} \left\{ \frac{1}{|W(t)|} > T_1 \right\} \leq \frac{1}{T_1 \mathbb{E}|W(t)|}.$$

$$\therefore \liminf_{t \rightarrow \infty} \mathbb{P} \left\{ |W(t)| > \frac{1}{T_1} \right\} \geq 1 - \epsilon_2, \text{ where } \epsilon_2 = \frac{2V_4}{T_1}.$$

Hence the theorem is proven.  $\square$

It is to be mentioned that the stochastic system (5.2) has no endemic or interior equilibrium, though this system has originated following the perturbation in the deterministic system (5.1), which has an endemic equilibrium. In the below, we show the asymptotic behaviour of the stochastic system around the endemic equilibrium  $E^*$  of the deterministic system. In the line of Ji et al. [2012a], we prove that if conditions of the following theorem hold, then the stochastic solutions will be around the nontrivial deterministic solution and the disease will prevail in the perturbed system (5.2).

**Theorem 5.2.10.** *Let  $(S(t), E(t), A(t), I(t), R(t)) \in \mathbb{R}_+^5$  be the solution of (5.2) with initial value  $(S(0), E(0), A(0), I(0), R(0)) \in \mathbb{R}_+^5$ . If  $R_0 > 1$ ,  $\gamma_1 + m + \frac{\nu}{2} > \frac{1}{2}\delta\omega$  and  $\gamma + m + d_i > \frac{1}{2}(1 - \delta)\omega + \frac{\nu}{2}$ , then*

$$\limsup_{t \rightarrow \infty} \frac{1}{t} \int_0^t [(S(u) - S^*)^2 + (E(u) - E^*)^2 + (I(u) - I^*)^2 + (A(u) - A^*)^2] \leq G_2 \text{ a.s.},$$

where  $S^*$ ,  $E^*$ ,  $A^*$ ,  $I^*$  are the components of the coexisting equilibrium  $C^*$  of the deterministic system (5.1),  $G_2 = \frac{c_1}{G_1} \left( \frac{1}{2}(A^* + I^*) + \gamma_1 \bar{A} + \gamma \bar{I} \right)$  and  $G_1 = \min \left\{ \frac{m}{2}, \omega + m, (\gamma_1 + m + \frac{\nu}{2}) - \frac{1}{2}\delta\omega, (\gamma + m + d_i) - \frac{1}{2}(1 - \delta)\omega - \frac{\nu}{2} \right\}$ ,  $c_1 = \max \{ \sigma_1^2, \sigma_2^2, \sigma_3^2 \}$ .

*Proof.* System (5.2) can be written as

## 5.2. Mathematical results

---

$$\begin{aligned}
 d \begin{pmatrix} S(t) \\ E(t) \\ A(t) \\ I(t) \\ R(t) \end{pmatrix} &= \begin{pmatrix} \Lambda - mS - \frac{\beta S}{N} ((1 - \kappa)I + \kappa A) \\ \frac{\beta S}{N} ((1 - \kappa)I + \kappa A) - ((1 - \delta)\omega + \delta\omega + m)E \\ \delta\omega E - (\gamma_1 + \nu + m)A \\ (1 - \delta)\omega E - (\gamma + m + d_i)I + \nu A \\ \gamma_1 A + \gamma I - mR \end{pmatrix} dt \\
 &+ \begin{pmatrix} -\frac{\sigma_1 S}{N} ((1 - \kappa)I + \kappa A) dB_1(t) \\ \frac{\sigma_1 S}{N} ((1 - \kappa)I + \kappa A) dB_1(t) \\ -\sigma_2 A dB_2(t) \\ -\sigma_3 I dB_3(t) \\ \sigma_2 A dB_2(t) + \sigma_3 I dB_3(t) \end{pmatrix} \quad (5.36)
 \end{aligned}$$

and the diffusion matrix is

$$A' = \begin{pmatrix} \frac{\sigma_1^2 S^2}{N^2} ((1 - \kappa)I + \kappa A)^2 & 0 & 0 & 0 & 0 \\ 0 & \frac{\sigma_1^2 S^2}{N^2} ((1 - \kappa)I + \kappa A)^2 & 0 & 0 & 0 \\ 0 & 0 & \sigma_2^2 A^2 & 0 & 0 \\ 0 & 0 & 0 & \sigma_3^2 I^2 & 0 \\ 0 & 0 & 0 & 0 & \sigma_2^2 A^2 + \sigma_3^2 I^2 \end{pmatrix}.$$

Define a  $C^2$ -function  $\bar{V} : \mathbb{R}_+^5 \rightarrow \mathbb{R}_+$

$$\bar{V}(S, E, A, I, R) = \frac{1}{2}(S - S^* + E - E^*)^2 + \left( A - A^* - A^* \ln \frac{A}{A^*} \right) + \left( I - I^* - I^* \ln \frac{I}{I^*} \right) + c_1 R$$

where  $c_1 = \max \{ \sigma_1^2, \sigma_2^2, \sigma_3^2 \}$ . Considering  $L$  to be the differential operator ([Mao \[2007\]](#)), one finds

$$\begin{aligned}
 L\bar{V} &= (S - S^* + E - E^*) [\Lambda - mS - (\omega + m)E] + \frac{A - A^*}{A} [\delta\omega E - (\gamma_1 + \nu + m)A] \\
 &+ \frac{1}{2} A^* \sigma_2^2 + \frac{I - I^*}{I} [(1 - \delta)\omega E - (\gamma + m + d_i)I + \nu A] + \frac{1}{2} I^* \sigma_3^2 \\
 &+ c_1 [\gamma_1 A + \gamma I - mR] \\
 &\leq -m(S - S^*)^2 - (\omega + 2m)(S - S^*)(E - E^*) - (\omega + m)(E - E^*)^2 \\
 &+ (1 - \delta)\omega(E - E^*)(I - I^*) - (\gamma + m + d_i)(I - I^*)^2 + \frac{1}{2} A^* \sigma_2^2 \\
 &+ \delta\omega(E - E^*)(A - A^*) + \nu(I - I^*)(A - A^*) - (\gamma_1 + \nu + m)(A - A^*)^2 \quad (5.37)
 \end{aligned}$$

**5. Persistence and extinction criteria of Covid-19 pandemic: India as a case study**

---

$$\begin{aligned}
& + \frac{1}{2}I^*\sigma_3^2 + c_1\gamma I + c_1\gamma_1 A - c_1 m R \\
& \leq -m(S - S^*)^2 + \frac{m}{2} |(S - S^*)(E - E^*)| - (\omega + m)(E - E^*)^2 \\
& + (1 - \delta)\omega|(E - E^*)(I - I^*)| - (\gamma + m + d_i)(I - I^*)^2 + \frac{1}{2}A^*\sigma_2^2 \\
& + \delta\omega|(E - E^*)(A - A^*)| + \nu|(I - I^*)(A - A^*)| - (\gamma_1 + \nu + m)(A - A^*)^2 \\
& + \frac{1}{2}I^*\sigma_3^2 + c_1\gamma I + c_1\gamma_1 A - c_1 m R \\
& \leq -\frac{m}{2}(S - S^*)^2 - \frac{1}{2}(\omega + m)(E - E^*)^2 - \left[ (\gamma + m + d_i) - \frac{1}{2}(1 - \delta)\omega - \frac{\nu}{2} \right] (I - I^*)^2 \\
& + \frac{1}{2}A^*\sigma_2^2 + \frac{1}{2}I^*\sigma_3^2 - \left[ \left( \gamma_1 + m + \frac{\nu}{2} \right) - \frac{1}{2}\delta\omega \right] (A - A^*)^2 + c_1\gamma\bar{I} + c_1\gamma_1\bar{A},
\end{aligned}$$

where  $\bar{A}, \bar{I}$  are the stochastic bounds of  $A(t)$  and  $I(t)$ .

Now, under the restrictions  $\gamma + m + d_i > \frac{1}{2}(1 - \delta)\omega + \frac{\nu}{2}$ ,  $\gamma_1 + m + \frac{\nu}{2} > \frac{1}{2}\delta\omega$ , we have

$$\begin{aligned}
d\bar{V} & \leq -\left[ \frac{m}{2}(S - S^*)^2 + (\omega + m)(E - E^*)^2 + \left( \left( \gamma_1 + m + \frac{\nu}{2} \right) - \frac{1}{2}\delta\omega \right) (A - A^*)^2 \right. \\
& + \left. \left( (\gamma + m + d_i) - \frac{1}{2}(1 - \delta)\omega - \frac{\nu}{2} \right) (I - I^*)^2 - \frac{1}{2}A^*\sigma_2^2 - \frac{1}{2}I^*\sigma_3^2 - c_1\gamma\bar{I} - c_1\gamma_1\bar{A} \right] dt \\
& + \sigma_2[(c_1 - 1)A + A^*]dB_2(t) + \sigma_3[(c_1 - 1)I + I^*]dB_3(t) \tag{5.38} \\
& \leq -\left[ \min \left\{ \frac{m}{2}, \omega + m, (\gamma + m + d_i) - \frac{1}{2}(1 - \delta)\omega - \frac{\nu}{2}, \left( \gamma_1 + m + \frac{\nu}{2} \right) - \frac{1}{2}\delta\omega \right\} \right. \\
& \quad \left. \left( (S - S^*)^2 + (E - E^*)^2 + (I - I^*)^2 + (A - A^*)^2 \right) - \frac{1}{2}A^*\sigma_2^2 - \frac{1}{2}I^*\sigma_3^2 \right. \\
& \quad \left. - c_1\gamma\bar{I} - c_1\gamma_1\bar{A} \right] dt + \sigma_2[(c_1 - 1)A + A^*]dB_2(t) + \sigma_3[(c_1 - 1)I + I^*]dB_3(t).
\end{aligned}$$

Let  $H_1(t) = \int_0^t \{ \sigma_2[(c_1 - 1)A + A^*]dB_2(t) + \sigma_3[(c_1 - 1)I + I^*]dB_3(t) \}$ , which is a continuous local martingale and  $H_1(0) = 0$ . Observe that  $\langle H_1, H_1 \rangle_t = \int_0^t \{ \sigma_2[(c_1 - 1)A + A^*]dB_2(t) + \sigma_3[(c_1 - 1)I + I^*]dB_3(t) \}^2 \leq c_1^2 \frac{\Lambda^2}{m^2} (\sigma_2^2 + \sigma_3^2)t$  and  $\limsup_{t \rightarrow \infty} \frac{\langle H_1, H_1 \rangle_t}{t} < \infty$ .

$\therefore \lim_{t \rightarrow \infty} \frac{H_1(t)}{t} = 0$  a.s. Define  $G_1 = \min \left\{ \frac{m}{2}, \omega + m, (\gamma + m + d_i) - \frac{1}{2}(1 - \delta)\omega - \frac{\nu}{2}, \right.$

### 5.3. Case study

---

$(\gamma_1 + m + \frac{\nu}{2}) - \frac{1}{2}\delta\omega$  } and integrate it from 0 to  $t$  so that

$$\begin{aligned} \bar{V}(t) - \bar{V}(0) &\leq -G_1 \int_0^t [(S(u) - S^*)^2 + (E(u) - E^*)^2 + (A(u) - A^*)^2 + (I(u) - I^*)^2] du \\ &\quad + \left( \frac{1}{2}A^*\sigma_2^2 + \frac{1}{2}I^*\sigma_3^2 + c_1\gamma\bar{I} + c_1\gamma_1\bar{A} \right) t + H_1(t). \end{aligned} \quad (5.39)$$

$$\begin{aligned} \therefore \int_0^t [(S(u) - S^*)^2 + (E(u) - E^*)^2 + (A(u) - A^*)^2 + (I(u) - I^*)^2] du &\leq \frac{\bar{V}(0)}{G_1} \\ &\quad + \frac{1}{G_1} \left( \frac{1}{2}A^*\sigma_2^2 + \frac{1}{2}I^*\sigma_3^2 + c_1\gamma\bar{I} + c_1\gamma_1\bar{A} \right) t + \frac{1}{G_1}H_1(t). \end{aligned} \quad (5.40)$$

$$\begin{aligned} \implies \limsup_{t \rightarrow \infty} \frac{1}{t} \int_0^t [(S(u) - S^*)^2 + (E(u) - E^*)^2 + (A(u) - A^*)^2 + (I(u) - I^*)^2] \\ \leq G_2 \text{ a.s.,} \end{aligned}$$

where  $G_2 = \frac{1}{G_1} \max \{ \sigma_1^2, \sigma_2^2, \sigma_3^2 \} \left( \frac{1}{2}(A^* + I^*) + \gamma_1\bar{A} + \gamma\bar{I} \right)$ . This completes the proof.  $\square$

**Remark 5.2.11.** *It is to be noted that  $G_2$  becomes zero if  $c_1$  is zero. It is worth mentioning that  $c_1$  would be zero when  $\max \{ \sigma_1^2, \sigma_2^2, \sigma_3^2 \} = 0$ , in other words, when there is no noise. Thus, the solution of the stochastic system will be equivalent to the solution of the deterministic system if the system's noise is too small.*

### 5.3 Case study

As a case study, we considered the Indian Covid-19 epidemic for which the data was taken from the freely available depository Covid19India.Org (<https://covid19india.org>). In this depository, the numbers of confirmed, recovered, and death cases are displayed in daily and cumulative basis. It reports only those cases which have been confirmed through various governmental and private agencies. These data were verified with the data of the Ministry of Health and Family Welfare (MoHFW), Government of India. The only difference between the two data sets is that MoHFW updates data only at a schedule time, whereas Covid19India.org updates data frequently in a day. For this case study, time series cumulative data of confirmed, recovered, and death cases for the period 1<sup>st</sup> March to 6<sup>th</sup> December, 2020 have been used to fit the model



## 5. Persistence and extinction criteria of Covid-19 pandemic: India as a case study

---

parameters. We have divided the total time span into three intervals: (i) from 1<sup>st</sup> March to 30<sup>th</sup> June, (ii) from 1<sup>st</sup> July to 16<sup>th</sup> September and (iii) from 17<sup>th</sup> September to 6<sup>th</sup> December. The `fminsearch` optimization toolbox and SDE toolbox of Matlab have been used in the estimation process. The `fminsearch` routine evaluates the least-squares error function starting from an initial guess of the parameter and the initial value in the starting vector to achieve a minimum value of the least square error function. The execution successfully terminates if the return value of the minimized function satisfy some stopping criteria (Li [2018]).

Both the deterministic model (5.1) and stochastic model (5.2) were considered to fit the data of the considered period. We initially estimated the parameters for the first time span and then keeping all parameters constant the fitting is done only by varying the parameter  $\beta$ . We, however, presented here only the best fit curves corresponding to the stochastic model only, which showed  $R^2$  value about 0.99 (see Fig. 5.2) compared to  $R^2$  value 0.91 of the deterministic model. The parameter values that best fit the actual data (magenta colour) with the solution of the stochastic model (blue curve), as shown in Fig. 5.2, are presented in the Table 5.1.

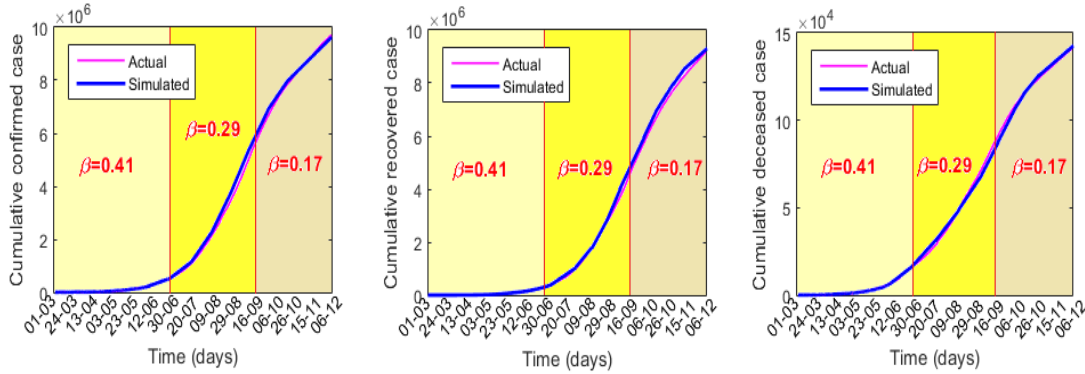


**Figure 5.2:** Covid-19 data fitting. The cumulative value of confirmed, recovered and death cases in India for the study period March 1 to December 6, 2020, are fitted by the solution of the stochastic model (5.2). Here the magenta line indicates the actual data and the blue line indicates the simulated data. Noise intensities are  $\sigma_1 = 0.1$ ,  $\sigma_2 = 0.12$ ,  $\sigma_3 = 0.15$ .

With the parameter values as in first row of Table 5.1, the basic reproduction number ( $R_0$ ) of the deterministic system is evaluated as 1.898. It is to be recalled that the spreading of infection from human-to-human can be controlled through NPIs in the absence of any specific drug/vaccine and the system parameter  $\beta$  encapsulates the effect of such NPIs. We, therefore, plotted a bifurcation diagram of  $R_0$  with

### 5.3. Case study

**Table 5.1:** Estimated parameter values for India

Period	$\Lambda$	$m$	$\beta$	$\kappa$	$\delta$	$\omega$	$\gamma$	$\gamma_1$	$d_i$	$\nu$
01.03-30.06	77500	$4.1 \times 10^{-5}$	0.41	0.92	0.66	0.37	0.11	0.13	$2.57 \times 10^{-2}$	0.002
01.07-16.09	77500	$4.1 \times 10^{-5}$	0.29	0.92	0.66	0.37	0.11	0.13	$2.57 \times 10^{-2}$	0.002
17.09-06.12	77500	$4.1 \times 10^{-5}$	0.17	0.92	0.66	0.37	0.11	0.13	$2.57 \times 10^{-2}$	0.002

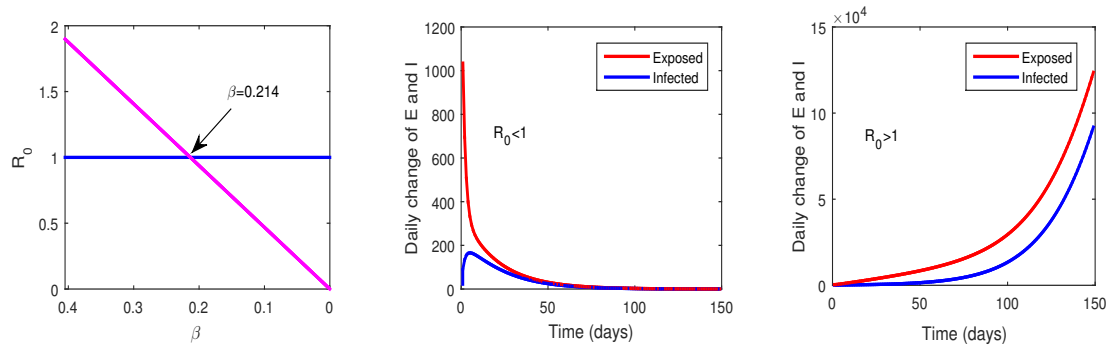


**Figure 5.3:** Bifurcation diagram (left figure) of the basic reproduction number  $R_0$  of the deterministic system (5.1) with respect to  $\beta$ . Both the exposed and infected individuals decline to zero (middle figure) for  $R_0 < 1$  (corresponding to  $\beta = 0.2 (< 0.214)$ ). Infection, however, steadily grows (right figure) for  $R_0 > 1$  (corresponding to  $\beta = 0.25 (> 0.214)$ ). Parameters are as in Table 5.1.

respect to  $\beta$  (Fig. 5.3) and it shows that  $R_0$  will be less than unity once the value of  $\beta$  goes below 0.214 from its existing value 0.41 (see Table 5.1). The number of individuals in the exposed class ( $E$ ) and infected class ( $I$ ) both will go to extinction if  $R_0 < 1$  and will gradually increase if  $R_0 > 1$  (see Fig. 5.3), satisfying the deterministic analytical results.

Following Theorem 5.2.8, a similar bifurcation diagram of  $R_0^S$  with respect to the force of infection,  $\beta$ , for the stochastic system (5.2) was plotted in Fig. 5.4. It shows that  $R_0^S$  will be less than unity for  $\beta = 0.085$  with the same parameter values, which is a much lower value compared to its deterministic counterpart. This value, however, depends on the noise intensity of the system. The critical values of  $\beta$  for which  $R_0^S = 1$  for  $\sigma_1 = 0.08, 0.1$  and  $0.12$  are, respectively,  $0.07, 0.085$  and  $0.105$ . The time series solutions of the exposed class for three noise intensities corresponding to three  $\beta$  values  $0.065 (< 0.07)$ ,  $0.08 (< 0.085)$  and  $0.1 (< 0.105)$ , such that it becomes less than its critical value, are plotted to show that the disease becomes extinct in each case (Fig. 5.4). It is notable that the number of days required for disease extinction increases with increasing noise.

## 5. Persistence and extinction criteria of Covid-19 pandemic: India as a case study

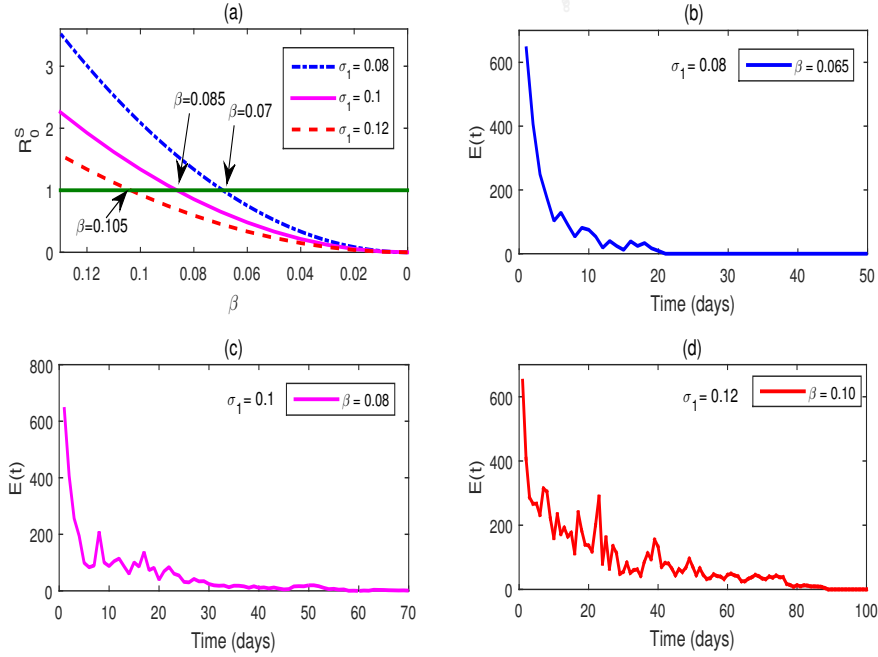
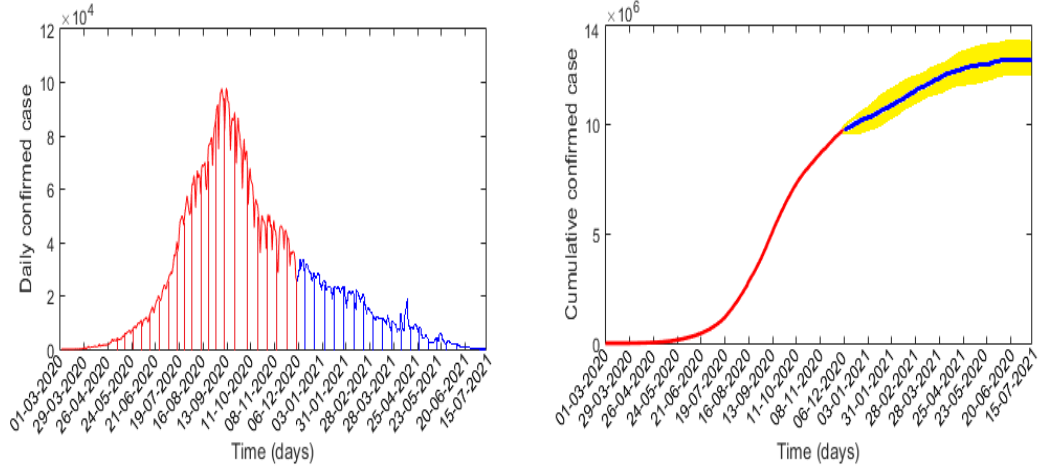


**Figure 5.4:** Left upper: Variation in  $R_0^s$  of the stochastic system (5.2) with respect to  $\beta$  for three different values of  $\sigma_1$ . Right upper: Time evolution of exposed class  $E$  of system (5.2) for  $\sigma_1 = 0.08$  and  $\beta = 0.065$  (less than the corresponding critical value 0.08). Here the extinction time is 20 days. Left lower: Similar time evolution of  $E$  for  $\sigma_1 = 0.1$  and  $\beta = 0.08$  (less than the corresponding critical value 0.085). The extinction time is 63 days. Right lower: Time evolution of  $E$  for  $\sigma_1 = 0.12$  and  $\beta = 0.10$  (less than the corresponding critical value 0.105). The extinction time is 88 days. Other parameters are as in the first row of Table 5.1.

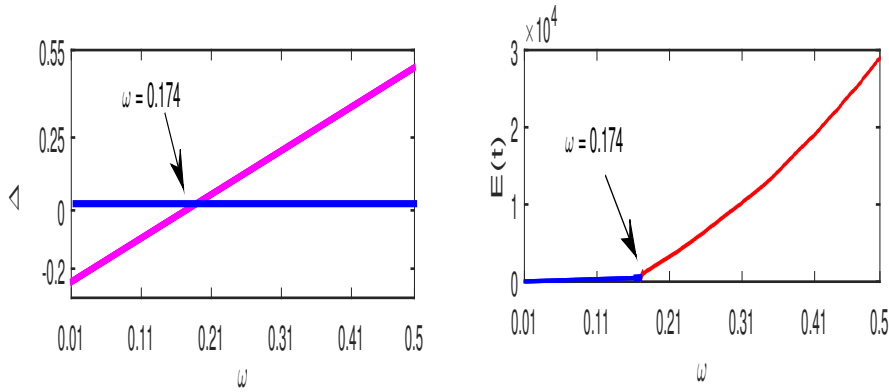
We also predicted the cumulative confirmed cases of Covid-19 individuals (i.e.,  $I$  class) in India (see Fig. 5.5) until the disease is controlled (for the period 7th December 2020 to 15th July 2021). To determine the future time course, we repeated the stochastic solution 1000 times and then averaged it to plot the estimated values (blue colour line) with 95% confidence interval. The curve becomes almost flat, indicating that no new case arises, at the third week of July 2021 with  $12.52 \times 10^6$  cumulative confirmed cases. However, the number may vary between  $12.13 \times 10^6$  and  $13.41 \times 10^6$  in the 95% confidence interval (yellow region).

Theorem 5.2.9 gives a strong disease persistence result. One can see that the conditions of this theorem will hold only if  $\omega$  is relatively high, i.e., if the average time spent ( $\frac{1}{\omega}$ ) in  $E$  class is relatively low. In case of Covid-19, it is about 2 days only (Peng et al. [2020]). The first bifurcation diagram in Fig. 5.6 shows that the value of  $\omega$  has to be higher than 0.174 to persist infection in the system. The right hand side

### 5.3. Case study



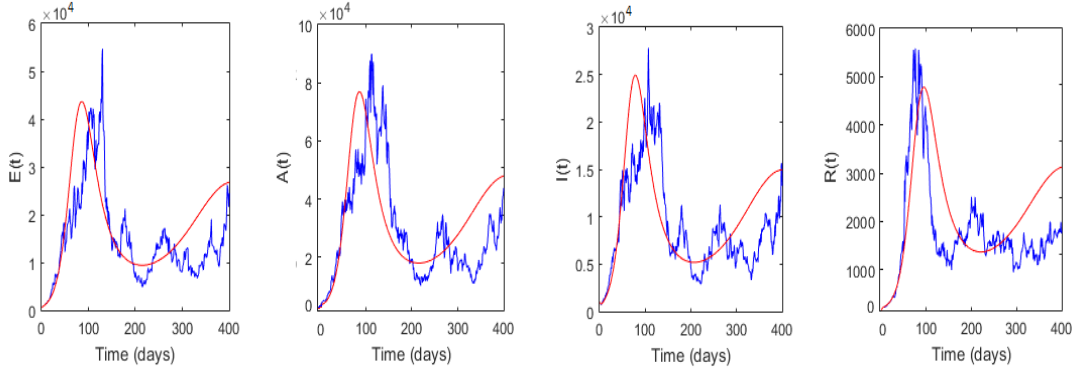
**Figure 5.5:** Predicted cumulative Covid-19 confirmed cases in India until the epidemic end. The simulation results of the system (5.2) (blue line) predict that India may observe  $12.52 \times 10^6$  positive cases until the disease is controlled in the third week of July 2021. The confidence interval (95%) is plotted with yellow shed. Parameters are as in the third row of Table 5.1 with similar noise intensities as in Fig. 5.2.



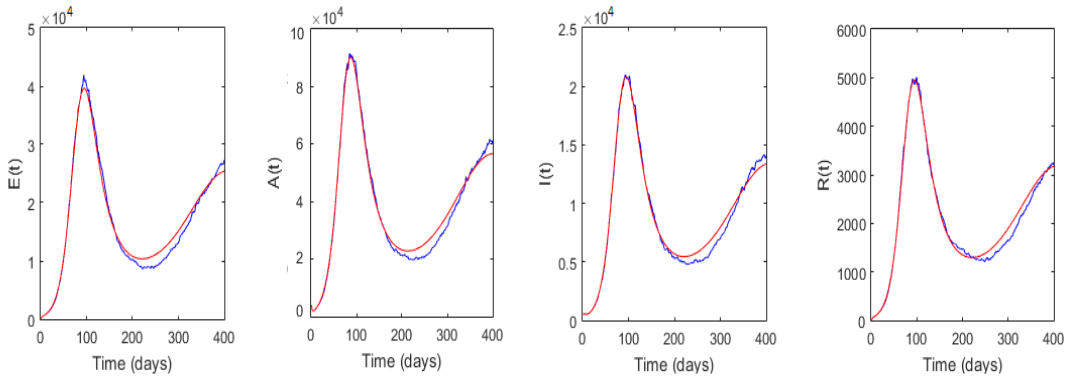
**Figure 5.6:** Left:  $\Delta$  becomes positive for  $\omega > 0.174$ , where  $\Delta = \theta_1(\omega - \max\{\gamma_1 + m, \gamma + m + d_i\}) - \frac{\theta_1(\theta_1 + 1)}{2} \max\{\sigma_2^2, \sigma_3^2\}$ . Right: Bifurcation of the exposed class,  $E$ , with respect to  $\omega$  shows that  $E$  becomes positive for  $\omega > 0.174$ . All parameters are as in first row of Table 5.1 with  $\theta_1 = 1.5$ .

figure shows that the exposed class becomes nonzero, indicating disease persistency, once  $\omega$  exceeds the said value.

## 5. Persistence and extinction criteria of Covid-19 pandemic: India as a case study



**Figure 5.7:** Time evolutions of system populations (5.1) and (5.2) when parameters satisfy the conditions of Theorem 5.2.10. Magenta colour represents the stochastic solutions and blue colour represents the deterministic solutions. Parameters are as in first row of Table 5.1 with  $\sigma_1 = 0.1$ ,  $\sigma_2 = 0.12$ ,  $\sigma_3 = 0.15$ .



**Figure 5.8:** Time evolutions of system populations (5.1) and (5.2) when noise intensities are small, implying the equivalence of the deterministic and stochastic systems. Magenta colour represents the stochastic solutions and blue colour represents the deterministic solutions. Parameters are as in Fig. 5.7 with  $\sigma_1 = \sigma_2 = \sigma_3 = 0.01$ .

To show the asymptotic behaviour of the stochastic system (5.2) around the endemic equilibrium  $E^*$  of the deterministic system (5.1), we computed  $R_0 = 1.5427 > 1$ ,  $\gamma_1 + m + \frac{\nu}{2} = 0.1354 > 0.1231 = \frac{1}{2}\delta\omega$  and  $\gamma + m + d_i = 0.1382 > 0.0648 = \frac{1}{2}(1 - \delta)\omega + \frac{\nu}{2}$ . Thus, conditions of the Theorem 5.2.10 are satisfied. The time series solutions of the stochastic system (magenta colour) show that it fluctuates around the deterministic solutions (blue colour) (see Fig. 5.7), showing that the disease will prevail in the system for a long time. However, the solution of the stochastic system will be equivalent to the solution of the deterministic system if the system's noise is too small (see Fig. 5.8).

## 5.4 Discussion

In this chapter, we have proposed an extended version of SEIR epidemic model to portrait the spread of coronavirus epidemic in a country or a region and analyzed the model to unveil different dynamic properties. We have considered a five dimensional epidemic model to classify the population of a designated area based on their epidemiological status. A rate equation for a deceased class has also been considered to encapsulate the severity of the disease and to better fit the model parameters on the basis of available data. Acknowledging the uncertainty that prevails in different rate parameters of a deterministic Covid-19 model, we considered the stochastic counterpart of the deterministic model with parameter perturbations. Perturbations were considered in three epidemiological parameters, viz. the per capita daily contacts, recovery rate of symptomatic class and recovery rate of asymptomatic class.

Basic reproduction number is probably the most important epidemiological measure that can delineate the occurrence and non-occurrence of an epidemic. We calculated this measure for our deterministic model and proved analytically that the disease cannot persists if  $R_0 \leq 1$  and prevails otherwise. In fact, we proved that the entire domain is the basin of attraction for the disease-free equilibrium if the basic reproduction number is less than unity. In the case of perturbed system, we proved several results for the existence of solutions and their boundedness, extinction criteria, and persistence of the disease. An equivalent extinction criterion, as it was in the case of the deterministic model, was also established for the stochastic model under which the exposed class goes to extinction. In epidemiological models, the extinction criterion is usually measured for which the  $I$  class goes to zero. Here we have found such conditions for  $E$  class because infection may still persist, at least in the case of Covid-19 infection, through undetected infectious individuals ( $A$ ) even if the detected infectives ( $I$ ) tend to zero.

It is to be mentioned that the stochastic system (5.2) has no endemic or interior equilibrium, though this system has originated following the parametric perturbation of the deterministic system (5.1), which has an endemic equilibrium. It is shown that the asymptotic solutions of the stochastic system fluctuate around the endemic equilibrium of the deterministic system (5.1) under some restriction and the infection remains endemic. Interestingly, the stochastic system will be equivalent to the deterministic system if noise is zero.

It is extremely difficult to predict the burden of an ongoing epidemic. This task

## 5. Persistence and extinction criteria of Covid-19 pandemic: India as a case study

---

becomes more difficult if the epidemic causes due to some pathogens of unknown etiology, like SARS-CoV-2. Scientists are trying to learn more and more about this dreaded pathogen, which has engulfed the entire globe within a short period. Our simulation results show that this epidemic will last for almost one year in India. Though we have considered uncertainty in our model, still it may be difficult to predict the number of infectives after a significant long time because you do not know what type of control measure will be imposed (or withdrawn) by the authority in the subsequent time which can significantly alter the current epidemiological trend. For example, the Indian Railway run 2813 special trains to shift 3.7 million migrant workers from one part of the country to the other part during the period May 1 to 23 (Rai [2020]). A good number of the migrant workers brought the infection to their home towns and villages (Hin [2020]). Due to this unknown perturbation, all earlier predictions on the India epidemic burden were failed. Such uncertainties may be captured if the noise term is very large. We, however, considered small noise term and predicted the cumulative number of confirmed cases of Covid-19 on the basis of current trend. The epidemic in India may continue up to third week of July 2021 if there is no additional perturbation, and the cumulative confirmed Covid-19 cases may vary from  $12.13 \times 10^6$  to  $13.41 \times 10^6$ . The Covid-19 infection, however, may not be controlled if any new variant of the virus appears with high infectivity.

The Covid-19 epidemic model analyzed here does not contain the vaccinated class. We propose and explore an epidemic model with a vaccinated class in the next chapter. There is uncertainty regarding the rate of immunity loss among the vaccinated population. We, therefore, consider such uncertainties in the SARS-CoV-2 epidemic models with vaccine-induced immunity loss and demonstrate the effect of vaccination in controlling the Covid-19 epidemic.

## Chapter 6

# Is large-scale vaccination sufficient for controlling the Covid-19 pandemic with uncertainties? A model-based study<sup>5</sup>

### 6.1 Introduction

Vaccination against SARS-CoV-2 infection started in the UK at the end of 2020 (Pritchard et al. [2021]). Presently, ten WHO-recommended vaccine candidates are in use throughout the globe (WHO [2021]). A good proportion of the population is vaccinated in the one year of its application (in Data [2020]). Though the covid pandemic has not been controlled, its morbidity and mortality have been reduced significantly due to vaccination (Rossman et al. [2021], Roghani [2021]). Numerous mathematical models have been proposed and analyzed to determine the course of the covid pandemic since the WHO's announcement of public health emergency of international concern (PHEIC) on January 30, 2020 (WHO [2020]) to restrict the spread of the novel coronavirus. These are mainly deterministic SEIR epidemic models or their variants (Prem et al. [2020], Paul et al. [2020b], Moore et al. [2021], Khajanchi and Sarkar [2020], Mondal et al. [2020], Sarkar et al. [2020], Anastassopoulou et al. [2020], Perc et al. [2020]) and a few are stochastic models (Majumder et al. [2021a], Karako et al. [2020], Zhang et al. [2020b], De Sousa et al. [2020], Adak et al. [2021]).

---

<sup>5</sup>*The bulk of this chapter has been communicated in a peer reviewed journal.*



## 6. Is large-scale vaccination sufficient for controlling the Covid-19 pandemic with uncertainties? A model-based study

---

Obviously, these earlier models did not consider the effect of vaccination and can no longer be used for the epidemic course once the full-fledged Covid-19 vaccination has started. Therefore, any current time epidemic model should contain a vaccinated class. Recently, some researchers have proposed and analyzed some Covid-19 vaccination models to find the effect of immunization on the disease dynamics (Musa and Iyaniwura [2021], De la Sen and Ibeas [2021], Furuse [2021], Rabi and Iyaniwura [2022], Zhai et al. [2021], Kurmi and Chouhan [2022], Ghostine et al. [2021], Paul et al. [2020a]). A case study of Japan shows that reduced vaccine efficacy and rollout of covid restriction may lead to a surge of covid cases (Furuse [2021]). Ghostine et al. [2021] have proposed an enhanced SEIR model including a vaccination compartment to mimic the spread of the coronavirus epidemic in Saudi Arabia. It is shown that intensifying the vaccination campaign can significantly decrease the number of confirmed cases and deaths. Kurmi and Chouhan [2022] analyzed a eight-compartment Covid-19 vaccination model using optimal control theory. They investigated the impact of vaccination on the spread of the disease and demonstrated that a combination of community mitigation strategies and vaccination can effectively minimize this pandemic. The simulations, however, were done with a hypothetical parameter set. A Covid-19 vaccination model was studied in Musa and Iyaniwura [2021] to show that the waning of vaccine-induced immunity greatly impacts the disease dynamics. Rabi and Iyaniwura [2022] developed a Covid-19 model to assess the impact of vaccination and immunity waning on the dynamics of the disease. Without considering a precise vaccination class, De la Sen and Ibeas [2021] analyzed an SEIR type epidemic model to observe the combined role of vaccination and antiviral drugs in controlling the Covid-19 pandemic. An SEIR type epidemic model with time delay and vaccination control was considered by Zhai et al. [2021]. They have considered the vaccination strategy based on feedback linearization techniques and showed that the disease would persist in the population if there is no vaccination control. All these models are deterministic types and do not consider any uncertainty in the rate parameters. None of these models studied the effect of vaccine-induced immunity loss on the persistence of the disease. However, understanding the dynamics of a novel virus is insufficient if the inherent noise in the rate parameters is not considered. It is reported that there is uncertainty in the covid infection rate (Merow and Urban [2020]). Due to spatial heterogeneity and other physical factors, there is a significant variation in the Covid-19 recovery time and rate (Desmet and Wacziarg [2021], Sanyaolu et al. [2020]). Most importantly, the efficacy of vaccines produced in the shortest time is primarily

## 6.2. The model

---

unknown. It is also unclear how long these vaccines will provide protection against covid infection and to what extent. Even after taking a total dose of the vaccine, it is now recommended for a booster dose, implying the loss of efficacy of the vaccine (Juno and Wheatley [2021], Croda and Ranzani [2021]). This indicates the existence of many uncertainties in the Covid-19 disease dynamics, its recovery rate, and vaccine efficacy. Here we study a six-dimensional stochastic epidemic model to demonstrate the effect of vaccination in controlling the Covid-19 epidemic. Due to the variability in the infection rate, recovery rate, and vaccine efficacy, we considered noise in these rate parameters and determined the disease persistence and eradication conditions. Using the Indian and Italian Covid-19 data, we estimated the best-fitted parameters and noise intensities for the considered model. We then observed the variational effects of the force of infection, vaccination and immunity waning rate parameters. Our analysis reveals that the Covid-19 disease will persist over the existing vaccine efficacy and transmissibility for a long time.

The remaining portion of this chapter is organized in the following sequence. The stochastic Covid-19 vaccination model is proposed in the next Section 6.2. Analytical results, including disease extinction conditions and stationary distribution of the solutions, are prescribed in Section 6.3. Parameter estimation and two case studies are done in Section 6.4. The chapter ends with a discussion in Section 6.5.

## 6.2 The model

We propose an extended SEIR stochastic compartmental epidemic model to investigate the Covid-19 disease under vaccination. The total human population,  $N(t)$ , of a region is divided into six mutually exclusive groups, viz., susceptible, exposed, detected infectives, undetected infectives, recovered, and vaccinated, which are denoted by  $S, E, I, A, R, V$ , respectively. The susceptible individuals are recruited through birth at a rate  $\Lambda$ . After the effective contact of a detected or undetected covid infected individual, susceptible individuals become infected and join the  $E$  class, who carry the virus but are not yet infectious. The transmission probability of covid infection from the detected and undetected individuals may differ. Assume that  $\kappa$  be the transmission probability of disease due to the contact between susceptible and undetected infected individuals. The same is  $(1 - \kappa)$  for the contact between susceptible and detected individuals. If  $\beta$  is the average per capita daily contact, then the

## 6. Is large-scale vaccination sufficient for controlling the Covid-19 pandemic with uncertainties? A model-based study

---

susceptible individual that joins the  $E$  class is given by  $\beta(\frac{(1-\kappa)SI}{N} + \frac{\kappa SA}{N})$ . The susceptible individuals are vaccinated at a rate  $q$  and join the  $V$  class. Since the vaccination of a susceptible individual does not give 100 % immunity against coronavirus, the vaccinated people may again be infected from the undetected and detected individuals, but possibly at a lower rate. Considering  $\eta$  as the vaccination-induced immunity loss, the portion of the vaccinated individuals who join the exposed class at time  $t$  is  $\eta(\frac{(1-\kappa)SI}{N} + \frac{\kappa SA}{N})$ . Observe that it gives the fraction of vaccinated individuals at time  $t$  losses immunity after effective interaction with the detected and undetected infected individuals. We call  $\eta$  as the vaccine-induced immunity loss parameter, or the vaccine efficacy parameter. If  $\eta = 0$ , then the vaccine will be 100% effective. An exposed class individual spends on an average  $\frac{1}{\omega}$  time in  $E$  class, and then joins either the undetected class with probability  $\delta$  or the detected class with probability  $(1 - \delta)$ . An average time of  $\frac{1}{\gamma_1}$  and  $\frac{1}{\gamma}$  are spent by the undetected and detected individuals, respectively, before moving to the recovered class. Recovered people can also lose immunity and join the susceptible class at a rate of  $g$ . Natural death at a rate  $m$  is incorporated in every compartment, and an additional disease-related death rate  $d_i$  is included in the detected class,  $I$ . We do not consider any disease-related death in the  $A$  class because critically ill individuals if any, may be shifted to the  $I$  class at a rate  $\nu$ . Since the coronavirus is a novel virus, there are substantial uncertainties in the rate constants, like infection rate (Manski and Molinari [2021a]), recovery rate (Bhapkar et al. [2020]) in  $A$  and  $I$  classes, and also in the rate of immunity loss (Dolgin et al. [2021]). To incorporate this uncertainty, we consider random perturbations to these parameters as follows:  $\mp\beta \rightarrow \mp\beta + \sigma_1 dB_1(t)$ ,  $\eta \rightarrow \eta + \sigma_2 dB_2(t)$ ,  $\gamma_1 \rightarrow \gamma_1 + \sigma_3 dB_3(t)$ ,  $\gamma \rightarrow \gamma + \sigma_4 dB_4(t)$ , where  $B_i(t)$  are standard mutually independent Brownian motions and  $\sigma_i^2, i = 1, 2, 3, 4$ , are the intensities of the white noises. Similar parametric perturbation has also been considered in other biological models (Zhou et al. [2020a], Majumder et al. [2021b], Yang and Mao [2014], Majumder et al. [2021c], Chen and Kang [2016]). Encapsulating all these assumptions, the stochastic compartmental model for Covid-19 reads

### 6.3. Results

---

$$\begin{aligned}
dS &= \left[ \Lambda - qS - \frac{\beta S}{N} ((1 - \kappa)I + \kappa A) - mS + gR \right] dt - \frac{\sigma_1 S}{N} [(1 - \kappa)I + \kappa A] dB_1(t), \\
dE &= \left[ \frac{\beta S}{N} ((1 - \kappa)I + \kappa A) + \frac{\eta V}{N} ((1 - \kappa)I + \kappa A) - \omega E - mE \right] dt \\
&\quad + \frac{[(1 - \kappa)I + \kappa A]}{N} (\sigma_1 S dB_1(t) + \sigma_2 V dB_2(t)), \\
dA &= [\delta\omega E - (\gamma_1 + \nu + m)A] dt - \sigma_3 A dB_3(t), \\
dI &= [(1 - \delta)\omega E - (\gamma + m + d_i)I + \nu A] dt - \sigma_4 I dB_4(t), \\
dR &= [\gamma_1 A + \gamma I - gR - mR] dt + \sigma_3 A dB_3(t) + \sigma_4 I dB_4(t), \\
dV &= \left[ qS - \frac{\eta V}{N} [(1 - \kappa)I + \kappa A] - mV \right] dt - \frac{\sigma_2 V}{N} [(1 - \kappa)I + \kappa A] dB_2(t).
\end{aligned} \tag{6.1}$$

The initial values for the state variables are considered as

$$S(0) \geq 0, E(0) \geq 0, A(0) \geq 0, I(0) \geq 0, R(0) = 0, V(0) = 0. \tag{6.2}$$

## 6.3 Results

### 6.3.1 Basic reproduction number of the deterministic system

One can easily write the deterministic version of the stochastic model (6.1) as

$$\begin{aligned}
\frac{dS}{dt} &= \Lambda - qS - \frac{\beta S}{N} [(1 - \kappa)I + \kappa A] - mS + gR, \\
\frac{dE}{dt} &= \frac{\beta S}{N} [(1 - \kappa)I + \kappa A] + \frac{\eta V}{N} [(1 - \kappa)I + \kappa A] - \omega E - mE, \\
\frac{dA}{dt} &= \delta\omega E - (\gamma_1 + \nu + m)A, \\
\frac{dI}{dt} &= (1 - \delta)\omega E + \nu A - (\gamma + m + d_i)I, \\
\frac{dR}{dt} &= \gamma_1 A + \gamma I - gR - mR, \\
\frac{dV}{dt} &= qS - \frac{\eta V}{N} [(1 - \kappa)I + \kappa A] - mV.
\end{aligned} \tag{6.3}$$

Using the next generation matrix method (Diekmann et al. [2010]), the infection subsystem of the system (6.3), which describes the production of new infections and

## 6. Is large-scale vaccination sufficient for controlling the Covid-19 pandemic with uncertainties? A model-based study

---

makes change in the states, reads

$$\begin{aligned}\frac{dE}{dt} &= \frac{\beta S}{N} [(1 - \kappa)I + \kappa A] + \frac{\eta V}{N} [(1 - \kappa)I + \kappa A] - (\omega + m)E, \\ \frac{dA}{dt} &= \delta\omega E - \nu A - (\gamma_1 + m)A, \\ \frac{dI}{dt} &= (1 - \delta)\omega E + \nu A - (\gamma + m + d_i)I,\end{aligned}\tag{6.4}$$

The transmission matrix ( $F$ ) and the transition matrix ( $\Sigma$ ) associated with the system (6.4) are given by

$$\begin{aligned}F &= \begin{pmatrix} 0 & \kappa \frac{(\beta m + \eta q)}{q+m} & (1 - \kappa) \frac{(\beta m + \eta q)}{q+m} \\ 0 & 0 & 0 \\ 0 & 0 & 0 \end{pmatrix}, \\ \Sigma &= \begin{pmatrix} -(\omega + m) & 0 & 0 \\ \delta\omega & -(\nu + \gamma_1 + m) & 0 \\ (1 - \delta)\omega & \nu & -(\gamma + m + d_i) \end{pmatrix}.\end{aligned}\tag{6.5}$$

Then the deterministic basic reproduction number (DBRN)  $R_{0V}^D$  of (6.3) is the spectral radius of the next generation matrix  $-F\Sigma^{-1}$ , i.e.,  $R_{0V}^D = \rho(-F\Sigma^{-1})$ , where

$$\Sigma^{-1} = \begin{pmatrix} -\frac{1}{\omega+m} & 0 & 0 \\ -\frac{\delta\omega}{(\omega+m)(\nu+\gamma_1+m)} & -\frac{1}{\nu+\gamma_1+m} & 0 \\ -\frac{\delta\omega\nu+(\nu+\gamma_1+m)(1-\delta)\omega}{(\omega+m)(\nu+\gamma_1+m)(\gamma+m+d_i)} & -\frac{\nu}{(\nu+\gamma_1+m)(\gamma+m+d_i)} & -\frac{1}{\gamma+m+d_i} \end{pmatrix}.$$

Thus,

$$R_{0V}^D = \frac{\omega(\beta m + \eta q)\{\kappa\delta(\gamma + m + d_i) + (1 - \kappa)\delta\nu + (1 - \kappa)(1 - \delta)(\nu + \gamma_1 + m)\}}{(q + m)(\gamma + m + d_i)(\nu + \gamma_1 + m)(\omega + m)}.$$

If  $R_{0V}^D > 1$  then the disease is established in the system.

### 6.3.2 Stochastic study

It is to be noted that the system (6.1) considers the human population as its variables which must be non-negative and bounded. Also, from a dynamical point of view, the solution of the system (6.1) should exist uniquely. The multiplicative noise considered in (6.1) may cause a population explosion. It is therefore imperative to show that the supposed system has a unique solution without any population explosion, i.e., the

### 6.3. Results

---

solution is global, and all the solutions are positive when starting with positive initial values. We have the following theorem for these results.

**Theorem 6.3.1.** *For any initial value  $(S(0), E(0), A(0), I(0), R(0), V(0)) \in \mathbb{R}_+^6$ , there exists a unique global solution of the system (6.1) such that  $(S(t), E(t), A(t), I(t), R(t), V(t)) \in \mathbb{R}_+^6$  for all  $t \geq 0$  and the solution remains in  $\mathbb{R}_+^6$  with probability 1, i.e., almost surely (a.s).*

*Proof.* This theorem can be proved similarly as presented in Theorem 5.2.4 in chapter 5.1. □

It is worth mentioning that the stochastic system (6.1) has no equilibrium point. However, it may have some stationary distribution, meaning that no significant change will occur in the asymptotic solution of the system when time is large. From an epidemic point of view, such distribution implies the long-term persistence of the disease. We show that the stationary distribution occurs if the following theorem holds good. We adopted the technique given in Han et al. [2017] to prove this result and will use the Lemma 1.7.5 in the sequel.

**Theorem 6.3.2.** *Assume that*

$$R_{0V}^S = \frac{\omega(\beta m + \eta q)}{(q + m + \frac{1}{2}\sigma_1^2)(\gamma + m + d_i + \frac{1}{2}\sigma_4^2)} \times \frac{\{\kappa\delta(\gamma + m + d_i) + (1 - \kappa)(\delta\nu + (1 - \delta)(\nu + \gamma_1 + m))\}}{(\nu + \gamma_1 + m + \frac{1}{2}\sigma_3^2)(\omega + m + \frac{1}{2}(\sigma_1^2 + \sigma_2^2))}.$$

*Then, for any initial value  $(S(0), E(0), A(0), I(0), R(0), V(0)) \in \mathbb{R}_+^6$ , a sufficient condition for existing a stationary distribution  $\pi(\cdot)$  of the system (6.1) is  $R_{0V}^S > 1$ .*

*Proof.* By Theorem 6.3.1, for any initial size of population  $(S(0), E(0), A(0), I(0), R(0), V(0)) \in \mathbb{R}_+^6$ , there exists a unique non-local global solution  $(S, E, A, I, R, V) \in \mathbb{R}_+^6$ . Let us

## 6. Is large-scale vaccination sufficient for controlling the Covid-19 pandemic with uncertainties? A model-based study

---

denote  $D = \frac{1}{N} [(1 - \kappa)I + \kappa A]$ . The diffusion matrix of the system (6.1) is given by

$$A' = \begin{pmatrix} \sigma_1^2 S^2 D^2 & 0 & 0 & 0 & 0 & 0 \\ 0 & \sigma_1^2 S^2 D^2 + \sigma_2^2 V^2 D^2 & 0 & 0 & 0 & 0 \\ 0 & 0 & \sigma_3^2 A^2 & 0 & 0 & 0 \\ 0 & 0 & 0 & \sigma_4^2 I^2 & 0 & 0 \\ 0 & 0 & 0 & 0 & \sigma_3^2 A^2 + \sigma_4^2 I^2 & 0 \\ 0 & 0 & 0 & 0 & 0 & \sigma_2^2 V^2 D^2 \end{pmatrix}.$$

Let  $\bar{D}_\alpha$  be a bounded domain in  $\mathbb{R}_+^6$  which excludes the origin. Choose  $M_1 = \min_{(S,E,A,I,R,V) \in \bar{D}_\alpha \in \mathbb{R}_+^6} \{\sigma_1^2 S^2 D^2, (\sigma_1^2 S^2 + \sigma_2^2 V^2) D^2, \sigma_3^2 A^2, \sigma_4^2 I^2, \sigma_3^2 A^2 + \sigma_4^2 I^2, \sigma_2^2 V^2 D^2\}$ . For  $\bar{\zeta} = (\bar{\zeta}_1, \bar{\zeta}_2, \bar{\zeta}_3, \bar{\zeta}_4, \bar{\zeta}_5, \bar{\zeta}_6) \in \mathbb{R}_+^6$ , we obtain

$$\begin{aligned} \sum_{i,j=1}^6 a_{ij}(S, E, A, I, R, V) \bar{\zeta}_i \bar{\zeta}_j &= \sigma_1^2 S^2 D^2 \bar{\zeta}_1^2 + (\sigma_1^2 S^2 + \sigma_2^2 V^2) D^2 \bar{\zeta}_2^2 + \sigma_3^2 A^2 \bar{\zeta}_3^2 \\ &+ \sigma_4^2 I^2 \bar{\zeta}_4^2 + (\sigma_3^2 A^2 + \sigma_4^2 I^2) \bar{\zeta}_5^2 + \sigma_2^2 V^2 D^2 \bar{\zeta}_6^2, \quad (S, E, A, I, R, V) \in \bar{D}_\alpha. \end{aligned} \quad (6.5)$$

Thus, the condition (a) of Lemma 1.7.5 holds. In order to prove the second assertion of the lemma, define a non-negative  $C^2$  function  $H_1$ , where  $H_1 : \mathbb{R}_+^6 \rightarrow \mathbb{R}$  be such that

$$H_1 = (S + E + A + I + R + V) - B_1 \ln S - B_2 \ln E - B_3 \ln A - B_4 \ln I,$$

where  $B_1, B_2, B_3, B_4$  are positive constants to be determined later.

Applying Ito formula, one gets

$$\begin{aligned} \mathcal{L}(S + E + A + I + R + V) &= \Lambda - m(S + E + A + I + R + V) - d_i I, \\ \mathcal{L}(-\ln S) &= -\frac{\Lambda}{S} + \frac{\beta}{N} [\kappa A + (1 - \kappa)I] + q + m - \frac{gR}{N} + \frac{1}{2N^2} \sigma_1^2 [\kappa A + (1 - \kappa)I]^2, \\ \mathcal{L}(-\ln E) &= -\frac{\beta S}{NE} [\kappa A + (1 - \kappa)I] - \frac{\eta V}{NE} [\kappa A + (1 - \kappa)I] \\ &+ \omega + m + \frac{1}{2N^2 E^2} (\sigma_1^2 S^2 + \sigma_2^2 V^2) [\kappa A + (1 - \kappa)I]^2, \end{aligned}$$

### 6.3. Results

$$\begin{aligned}\mathcal{L}(-\ln A) &= -\frac{\delta\omega E}{A} + (\gamma_1 + \nu + m) + \frac{1}{2}\sigma_3^2, \\ \mathcal{L}(-\ln I) &= -\frac{(1-\delta)\omega E}{I} - \frac{\nu A}{I} + (\gamma + m + d_i) + \frac{1}{2}\sigma_4^2.\end{aligned}$$

Therefore, we have

$$\begin{aligned}\mathcal{L}H_1 &= \Lambda - m(S + E + A + I + R + V) - d_i I + B_1 \left( -\frac{\Lambda}{S} + \frac{\beta}{N}[\kappa A + (1-\kappa)I] + q + m \right. \\ &\quad \left. - \frac{gR}{N} + \frac{1}{2N^2}\sigma_1^2[\kappa A + (1-\kappa)I]^2 \right) + B_2 \left( -\frac{\beta S}{NE}[\kappa A + (1-\kappa)I] + \omega + m \right. \\ &\quad \left. - \frac{\eta\beta V}{NE}[\kappa A + (1-\kappa)I] + \frac{1}{2N^2E^2}(\sigma_1^2 S^2 + \sigma_2^2 V^2)[\kappa A + (1-\kappa)I]^2 \right) + B_3 \left( -\frac{\delta\omega E}{A} \right. \\ &\quad \left. + (\gamma_1 + \nu + m) + \frac{1}{2}\sigma_3^2 \right) + B_4 \left( -\frac{(1-\delta)\omega E}{I} - \frac{\nu A}{I} + (\gamma + m + d_i) + \frac{1}{2}\sigma_4^2 \right) \quad (6.6) \\ &\leq -4 \left( m(S + E + A + I + R + V) \frac{\Lambda B_1 \beta S B_2 \kappa A \delta \omega B_3 E}{S N E A} \right)^{\frac{1}{4}} + \left( q + m + \frac{1}{2}\sigma_1^2 \right) B_1 \\ &\quad + \Lambda + \left( \omega + m + \frac{1}{2}(\sigma_1^2 + \sigma_2^2) \right) B_2 + \left( \gamma_1 + \nu + m + \frac{1}{2}\sigma_3^2 \right) B_3 + \left( \gamma + m + d_i + \frac{1}{2}\sigma_4^2 \right) B_4 \\ &\quad - d_i I + \frac{1}{N}\beta(\kappa A + (1-\kappa)I)B_1 - \frac{\beta(1-\kappa)SI}{NE}B_2 - \frac{gR}{N}B_1 - \frac{\beta V}{NE}(\kappa A + (1-\kappa)I)B_2 \\ &\quad - \frac{(1-\delta)\omega E}{I}B_4 - \frac{\nu A}{I}B_4.\end{aligned}$$

Define

$$B_1 = \frac{(\beta m + \eta q)(\kappa \delta(\gamma + m + d_i) + (1-\kappa)\delta\nu + (1-\kappa)(1-\delta)(\gamma_1 + \nu + m))}{(q + m + \frac{1}{2}\sigma_1^2)m\beta\kappa\delta(\gamma + m + d_i + \frac{1}{2}\sigma_4^2)}$$

$$\Lambda = \left( \omega + m + \frac{1}{2}(\sigma_1^2 + \sigma_2^2) \right) B_2 = \left( \gamma_1 + \nu + m + \frac{1}{2}\sigma_3^2 \right) B_3 = \left( \gamma + m + d_i + \frac{1}{2}\sigma_4^2 \right) B_4.$$

Therefore,

$$B_2 = \frac{\Lambda}{\left( \omega + m + \frac{1}{2}(\sigma_1^2 + \sigma_2^2) \right)}, \quad B_3 = \frac{\Lambda}{\left( \gamma_1 + \nu + m + \frac{1}{2}\sigma_3^2 \right)}, \quad B_4 = \frac{\Lambda}{\left( \gamma + m + d_i + \frac{1}{2}\sigma_4^2 \right)}.$$

Define

$$R_{0V}^S = \frac{\omega(\beta m + \eta q)\{\kappa\delta(\gamma + m + d_i) + (1-\kappa)(\delta\nu + (1-\delta)(\nu + \gamma_1 + m))\}}{(q + m + \frac{1}{2}\sigma_1^2)(\gamma + m + d_i + \frac{1}{2}\sigma_4^2)(\nu + \gamma_1 + m + \frac{1}{2}\sigma_3^2)(\omega + m + \frac{1}{2}(\sigma_1^2 + \sigma_2^2))} \quad (6.7)$$



## 6. Is large-scale vaccination sufficient for controlling the Covid-19 pandemic with uncertainties? A model-based study

---

so that (6.6) becomes

$$\begin{aligned} \mathcal{L}H_1 \leq & -4\Lambda \left[ (R_{0V}^S)^{\frac{1}{4}} - 1 \right] + (q + m + \frac{1}{2}\sigma_1^2) B_1 - d_i I + \frac{1}{N} \beta (\kappa A + (1 - \kappa) I) B_1 \\ & - \frac{\beta(1-\kappa)SI}{NE} B_2 - \frac{\nu A}{I} B_4 - \frac{\beta V}{NE} (\kappa A + (1 - \kappa) I) B_2 - \frac{(1-\delta)\omega E}{I} B_4. \end{aligned} \quad (6.8)$$

We further define

$$\begin{aligned} H_2 &= B_5((S + E + A + I + R + V) - B_1 \ln S - B_2 \ln E - B_3 \ln A - B_4 \ln I) - \ln S - \ln R \\ &\quad - \ln V + (S + E + A + I + R + V) \\ &= (B_5 + 1)(S + E + A + I + R + V) - (1 + B_1 B_5) \ln S - B_2 B_5 \ln E - B_3 B_5 \ln A \\ &\quad - \ln R - \ln V. \end{aligned} \quad (6.9)$$

Let  $W_{k_1} = \left(\frac{1}{k_1}, k_1\right) \times \left(\frac{1}{k_1}, k_1\right) \times \left(\frac{1}{k_1}, k_1\right) \times \left(\frac{1}{k_1}, k_1\right) \times \left(\frac{1}{k_1}, k_1\right) \times \left(\frac{1}{k_1}, k_1\right)$ . As  $k_1 \rightarrow \infty$ , it is evident that

$$\lim \inf_{(S,E,A,I,R,V) \in \mathbb{R}_+^6 \setminus W_{k_1}} H_2(S, E, A, I, R, V) = +\infty. \quad (6.10)$$

Now, we intend to prove that  $H_2(S, E, A, I, R, V)$  has the unique smallest value

$$H_2(S(0), E(0), A(0), I(0), R(0), V(0)).$$

Taking partial derivatives of the function  $H_2(S, E, A, I, R, V)$  with respect to each state variable, we get

$$\begin{aligned} \frac{\partial H_2(S, E, A, I, R, V)}{\partial S} &= 1 + B_5 - \frac{1 + B_1 B_5}{S}, \\ \frac{\partial H_2(S, E, A, I, R, V)}{\partial E} &= 1 + B_5 - \frac{B_2 B_5}{E}, \\ \frac{\partial H_2(S, E, A, I, R, V)}{\partial A} &= 1 + B_5 - \frac{B_3 B_5}{A}, \\ \frac{\partial H_2(S, E, A, I, R, V)}{\partial I} &= 1 + B_5 - \frac{B_4 B_5}{I}, \\ \frac{\partial H_2(S, E, A, I, R, V)}{\partial R} &= 1 + B_5 - \frac{1}{R}, \\ \frac{\partial H_2(S, E, A, I, R, V)}{\partial V} &= 1 + B_5 - \frac{1}{V}. \end{aligned} \quad (6.11)$$

Making each of these partial derivatives equal to zero, one gets  $S = \frac{1+B_1 B_5}{1+B_5}$ ,  $E =$

### 6.3. Results

---

$\frac{B_2 B_5}{1+B_5}$ ,  $A = \frac{B_3 B_5}{1+B_5}$ ,  $I = \frac{B_4 B_5}{1+B_5}$ ,  $R = \frac{1}{1+B_5}$ ,  $V = \frac{1}{1+B_5}$  as the unique stagnation point of  $H_2$ . Furthermore, the Hesse matrix of the function  $H_2(S, E, A, I, R, V)$  at the given initial population density reads

$$M_1 = \begin{pmatrix} \frac{1+B_1 B_5}{S^2(0)} & 0 & 0 & 0 & 0 & 0 \\ 0 & \frac{B_2 B_5}{E^2(0)} & 0 & 0 & 0 & 0 \\ 0 & 0 & \frac{B_3 B_5}{A^2(0)} & 0 & 0 & 0 \\ 0 & 0 & 0 & \frac{B_4 B_5}{I^2(0)} & 0 & 0 \\ 0 & 0 & 0 & 0 & \frac{1}{R^2(0)} & 0 \\ 0 & 0 & 0 & 0 & 0 & \frac{1}{V^2(0)} \end{pmatrix}.$$

Clearly, the matrix  $M_1$  is positive definite. Hence,  $H_2$  attains the smallest value at  $\left( \frac{1+B_1 B_5}{1+B_5}, \frac{B_2 B_5}{1+B_5}, \frac{B_3 B_5}{1+B_5}, \frac{B_4 B_5}{1+B_5}, \frac{1}{1+B_5}, \frac{1}{1+B_5} \right)$ . From the continuity of  $H_2$  and using equation (6.10), the function  $H_2(S, E, A, I, R, V)$  has the unique smallest value  $H_2(S(0), E(0), A(0), I(0), R(0), V(0))$  inside  $\mathbb{R}_+^6$ .

We, now define a non-negative  $C^2$  function  $H : \mathbb{R}_+^6 \rightarrow \mathbb{R}_+$  such that

$$H(S, E, A, I, R, V) = H_2(S, E, A, I, R, V) - H_2(S(0), E(0), A(0), I(0), R(0), V(0)).$$

Applying Ito formula on  $H$  and using the model (6.1), one obtains

$$\begin{aligned} \mathcal{L}(H) \leq & B_5 \left\{ -4\Lambda \left[ (R_{0V}^S)^{\frac{1}{4}} - 1 \right] + \left( q + m + \frac{1}{2}\sigma_1^2 \right) B_1 - d_i I - \frac{gR}{N} B_1 - \frac{\beta(1-\kappa)SI}{NE} B_2 \right. \\ & + \frac{1}{N} \beta (\kappa A + (1-\kappa)I) B_1 - \frac{\nu A}{I} B_4 - \frac{\beta V}{NE} (\kappa A + (1-\kappa)I) B_2 - \frac{(1-\delta)\omega E}{I} B_4 \left. \right\} - \frac{\Lambda}{S} \\ & + \frac{\beta}{N} (\kappa A + (1-\kappa)I) + q + m - \frac{gR}{N} + \frac{1}{2}\sigma_1^2 - \frac{\gamma_1 A}{R} - \frac{\gamma I}{R} + g + m + \frac{1}{2}\sigma_3^2 \frac{A^2}{R^2} + \frac{1}{2}\sigma_4^2 \frac{I^2}{R^2} \\ & - \frac{qS}{V} + m + \frac{1}{2}\sigma_2^2 + \Lambda + \frac{\beta}{V} [\kappa A + (1-\kappa)I] - d_i I - m(S + E + A + I + R + V). \end{aligned} \tag{6.12}$$

## 6. Is large-scale vaccination sufficient for controlling the Covid-19 pandemic with uncertainties? A model-based study

---

Under the assumption  $B_6 = 4\Lambda \left[ (R_{0V}^S)^{\frac{1}{4}} - 1 \right] > 0$ , (6.12) becomes

$$\begin{aligned}
 \mathcal{L}(H) \leq & -B_5 B_6 - (B_5 + 1)d_i I + B_1 B_5 \left( q + m + \frac{1}{2}\sigma_1^2 \right) + (1 + B_1 B_5) \frac{\beta}{N} (\kappa A + (1 - \kappa)I) \\
 & - (1 + B_1 B_5) \frac{gR}{N} - \frac{\beta(1 - \kappa)SI}{NE} B_2 B_5 - \frac{B_4 B_5 \nu A}{I} - \frac{\gamma_1 A}{R} - \frac{\gamma I}{R} - \frac{\Lambda}{S} + g \\
 & - \frac{\beta V}{NE} (\kappa A + (1 - \kappa)I) B_2 B_5 - \frac{(1 - \delta)\omega E}{I} B_4 B_5 - \frac{qS}{V} + q + 3m + \Lambda + \frac{1}{2}\sigma_1^2 + \\
 & \frac{1}{2}\sigma_2^2 + \frac{1}{2}\sigma_3^2 \frac{A^2}{R^2} + \frac{1}{2}\sigma_4^2 \frac{I^2}{R^2} - mN.
 \end{aligned} \tag{6.13}$$

Consider now the following bounded subset

$$U = \left\{ \delta_1 < S < \frac{1}{\delta_2}, \delta_1 < E < \frac{1}{\delta_2}, \delta_1 < A < \frac{1}{\delta_2}, \delta_1 < I < \frac{1}{\delta_2}, \delta_1 < R < \frac{1}{\delta_2}, \delta_1 < V < \frac{1}{\delta_2} \right\},$$

where  $\delta_i > 0$ , for  $i = 1, 2$ , are negligibly small constants to be chosen later on. Now, we divide the domain  $\mathbb{R}_+^6 \setminus U$  into the following sub-domains:

$$\begin{aligned}
 U_1 &= \{(S, E, A, I, R, V) : 0 < S \leq \delta_1\}, \\
 U_2 &= \{(S, E, A, I, R, V) : 0 < E \leq \delta_1, S > \delta_2\}, \\
 U_3 &= \{(S, E, A, I, R, V) : 0 < A \leq \delta_1, E > \delta_2\}, \\
 U_4 &= \{(S, E, A, I, R, V) : 0 < I \leq \delta_1, A > \delta_2\}, \\
 U_5 &= \{(S, E, A, I, R, V) : 0 < R \leq \delta_2, I > \delta_1\}, \\
 U_6 &= \{(S, E, A, I, R, V) : 0 < V \leq \delta_1, R > \delta_2\}, \\
 U_7 &= \left\{ (S, E, A, I, R, V) : S \geq \frac{1}{\delta_2} \right\}, \\
 U_8 &= \left\{ (S, E, A, I, R, V) : E \geq \frac{1}{\delta_2} \right\}, \\
 U_9 &= \left\{ (S, E, A, I, R, V) : A \geq \frac{1}{\delta_2} \right\}, \\
 U_{10} &= \left\{ (S, E, A, I, R, V) : I \geq \frac{1}{\delta_2} \right\}, \\
 U_{11} &= \left\{ (S, E, A, I, R, V) : R \geq \frac{1}{\delta_2} \right\}, \\
 U_{12} &= \left\{ (S, E, A, I, R, V) : V \geq \frac{1}{\delta_2} \right\}.
 \end{aligned} \tag{6.14}$$

### 6.3. Results

We have to prove that  $\mathcal{L}H(S, E, A, I, R, V) < 0$  on  $\mathbb{R}_+^6 \setminus U$ , or equivalently,  $\mathcal{L}H < 0$  in all of the above twelve regions. We provide proofs of the first two cases. The other cases can be proved with a similar argument.

**Case 1.** Suppose  $(S, E, A, I, R, V) \in U_1$ , then (6.13) becomes

$$\begin{aligned} \mathcal{L}(H) \leq & -B_5B_6 - (B_5 + 1)d_iI + B_1B_5 \left( q + m + \frac{1}{2}\sigma_1^2 \right) + (1 + B_1B_5) \frac{\beta}{N} (\kappa A + (1 - \kappa)I) \\ & - (1 + B_1B_5) \frac{gR}{N} - \frac{\beta(1 - \kappa)SI}{NE} B_2B_5 - \frac{B_4B_5\nu A}{I} - \frac{\Lambda}{\delta_1} - \frac{\gamma_1 A}{R} - \frac{\gamma I}{R} + g \\ & - \frac{\beta V}{NE} (\kappa A + (1 - \kappa)I) B_2B_5 - \frac{(1 - \delta)\omega E}{I} B_4B_5 - \frac{qS}{V} + q + 3m + \Lambda + \frac{1}{2}\sigma_1^2 + \frac{1}{2}\sigma_2^2 + \\ & \frac{1}{2}\sigma_3^2 \frac{A^2}{R^2} + \frac{1}{2}\sigma_4^2 \frac{I^2}{R^2} - mN. \end{aligned}$$

Choosing  $\delta_1 > 0$  sufficiently small, one obtains  $\mathcal{L}(H) < 0$  for every  $(S, E, A, I, R, V) \in U_1$ .

**Case 2.** If  $(S, E, A, I, R, V) \in U_2$ , then from (6.13), we obtain

$$\begin{aligned} \mathcal{L}(H) \leq & -B_5B_6 - (B_5 + 1)d_iI + B_1B_5 \left( q + m + \frac{1}{2}\sigma_1^2 \right) + (1 + B_1B_5) \frac{\beta}{N} (\kappa A + (1 - \kappa)I) \\ & - (1 + B_1B_5) \frac{gR}{N} - \frac{\beta(1 - \kappa)SI}{NE} B_2B_5 - \frac{B_4B_5\nu A}{I} - \frac{\Lambda}{S} - \frac{\gamma_1 A}{R} - \frac{\gamma I}{R} + g \\ & - \frac{\beta V}{NE} (\kappa A + (1 - \kappa)I) B_2B_5 - \frac{(1 - \delta)\omega E}{I} B_4B_5 - \frac{qS}{V} + q + 3m + \Lambda + \frac{1}{2}\sigma_1^2 + \frac{1}{2}\sigma_2^2 \\ & + \frac{1}{2}\sigma_3^2 \frac{A^2}{R^2} + \frac{1}{2}\sigma_4^2 \frac{I^2}{R^2} - \frac{m\delta_2}{\delta_1}. \end{aligned}$$

Letting  $\delta_2^2 = \delta_1$  and choosing large positive value of  $B_5$  and sufficiently small value of  $\delta_2$ , one have  $\mathcal{L}(H) < 0$  for every  $(S, E, A, I, R, V) \in U_2$ . Similarly, by selecting sufficiently small values of either  $\delta_1 > 0$  or  $\delta_2 > 0$ , it can be easily shown that  $\mathcal{L}(H) < 0$  for the rest cases. Thus,  $\mathcal{L}(H) < 0$  can be attained for every  $(S, E, A, I, R, V) \in U_{12}$ . Therefore, condition (b) of Lemma 1.7.5 is satisfied and hence Theorem 6.3.2 is proved, following Lemma 1.7.5.  $\square$

**Remark 6.3.3.** Here,  $R_{0V}^S$  defined in (6.7) may be called as the stochastic basic reproduction number (SBRN), which ensures the disease establishment in the stochastic system (6.1) when  $R_{0V}^S > 1$ .

**Remark 6.3.4.** We have deduced the deterministic basic reproduction number (DBRN)

## 6. Is large-scale vaccination sufficient for controlling the Covid-19 pandemic with uncertainties? A model-based study

---

as

$$R_{0V}^D = \frac{\omega(\beta m + \eta q)\{\kappa\delta(\gamma + m + d_i) + (1 - \kappa)\delta\nu + (1 - \kappa)(1 - \delta)(\nu + \gamma_1 + m)\}}{(q + m)(\gamma + m + d_i)(\nu + \gamma_1 + m)(\omega + m)}.$$

If  $R_{0V}^D > 1$ , then disease can be established in the corresponding deterministic system. Observe that the basic reproduction number of the stochastic system ( $R_{0V}^S$ ) is smaller than that of the corresponding deterministic system ( $R_{0V}^D$ ). Furthermore, if  $\sigma_i = 0, i = 1, \dots, 4$ , then  $R_{0V}^S$  coincides with  $R_{0V}^D$ .

Observe that both the infected classes (symptomatic and asymptomatic) originate from the exposed class. Thus, the infection will eventually be eradicated if the individuals of the exposed class go extinct. For the system (6.1), the exposed class  $E(t)$  is said to be extinct (i.e., the system will be disease-free) if  $\lim_{t \rightarrow \infty} E(t) = 0$  a.s. (Majumder et al. [2021a]). We give here some sufficient conditions for which the exposed class dies out over time. In proving the extinction criterion, the result of the strong law of large number given in the Lemma 1.7.7 will be used.

**Theorem 6.3.5.** *The exposed individuals of the system (6.1) tend to zero exponentially almost surely if  $R_{0V}^{ext} < 1$ , where  $R_{0V}^{ext} = \frac{1}{\omega+m} \left( \frac{\beta^2}{2\sigma_1^2} + \frac{\eta^2}{2\sigma_2^2} \right)$ .*

*Proof.* Assume that  $(S(t), E(t), A(t), I(t), R(t), V(t)) \in \mathbb{R}_+^6$  is a solution of system (6.1) satisfying the initial value  $(S(0), E(0), A(0), I(0), R(0), V(0)) \in \mathbb{R}_+^6$ . Following Ito's formula, we have

$$\begin{aligned} d(\ln E(t)) &= \left( \frac{\beta S(\tau)((1 - \kappa)I(\tau) + \kappa A(\tau))}{N(\tau)E(\tau)} - \frac{\sigma_1^2 S^2(\tau)((1 - \kappa)I(\tau) + \kappa A(\tau))^2}{2N^2(\tau)E^2(\tau)} \right) dt \\ &+ \left( \frac{\eta V(\tau)((1 - \kappa)I(\tau) + \kappa A(\tau))}{N(\tau)E(\tau)} - \frac{\sigma_2^2 V^2(\tau)((1 - \kappa)I(\tau) + \kappa A(\tau))^2}{2N^2(\tau)E^2(\tau)} \right) dt - (\omega + m) \\ &+ \frac{\sigma_1 S}{NE}((1 - \kappa)I + \kappa A) dB_1(t) + \frac{\sigma_2 V}{NE}((1 - \kappa)I + \kappa A) dB_2(t). \end{aligned} \tag{6.15}$$

Upon integration from 0 to  $t$ , we have

$$\begin{aligned} \ln E(t) &= \int_0^t \left( \frac{\beta S(\tau)((1 - \kappa)I(\tau) + \kappa A(\tau))}{N(\tau)E(\tau)} - \frac{\sigma_1^2 S^2(\tau)((1 - \kappa)I(\tau) + \kappa A(\tau))^2}{2N(\tau)^2 E^2(\tau)} \right) dt \\ &+ \int_0^t \left( \frac{\eta V(\tau)((1 - \kappa)I(\tau) + \kappa A(\tau))}{N(\tau)E(\tau)} - \frac{\sigma_2^2 V^2(\tau)((1 - \kappa)I(\tau) + \kappa A(\tau))^2}{2N^2(\tau)E^2(\tau)} \right) dt \\ &- (\omega + m)t + M_1(t) + M_2(t) + \ln E(0), \end{aligned} \tag{6.16}$$

## 6.4. Case study

---

where  $M_1(t) = \int_0^t \frac{\sigma_1 S}{NE} ((1 - \kappa)I + \kappa A) dB_1(\tau)$ ,  $M_2(t) = \int_0^t \frac{\sigma_2 V}{NE} ((1 - \kappa)I + \kappa A) dB_2(\tau)$  are the local continuous martingale with  $M_1(0) = 0$ ,  $M_2(0) = 0$ . We, then have  $\langle M_1, M_1 \rangle_t = \int_0^t \frac{\sigma_1^2 S^2}{N^2 E^2} ((1 - \kappa)I + \kappa A)^2 dt < \sigma_1^2$  and  $\langle M_2, M_2 \rangle_t = \int_0^t \frac{\sigma_2^2 V^2}{N^2 E^2} ((1 - \kappa)I + \kappa A)^2 dt < \sigma_2^2$ . Using the fact

$$\max \left( \frac{\beta S(\tau)((1 - \kappa)I(\tau) + \kappa A(\tau))}{N(\tau)E(\tau)} - \frac{\sigma_1^2 S^2(\tau)((1 - \kappa)I(\tau) + \kappa A(\tau))^2}{2N(\tau)^2 E^2(\tau)} \right) = \frac{\beta^2}{2\sigma_1^2}$$

and

$$\left( \frac{\eta V(\tau)((1 - \kappa)I(\tau) + \kappa A(\tau))}{N(\tau)E(\tau)} - \frac{\sigma_2^2 V^2(\tau)((1 - \kappa)I(\tau) + \kappa A(\tau))^2}{2N^2(\tau)E^2(\tau)} \right) = \frac{\eta^2}{2\sigma_2^2},$$

then (6.16) can be written as

$$\ln E(t) \leq \left( \frac{\beta^2}{2\sigma_1^2} + \frac{\eta^2}{2\sigma_2^2} - (\omega + m) \right) t + M_1(t) + M_2(t) + \ln E(0). \quad (6.17)$$

Taking the limit superior as  $t \rightarrow \infty$ , after dividing both sides of (6.17) by  $t (> 0)$  and using Lemma 1.7.7, we have

$$\limsup_{t \rightarrow \infty} \frac{\ln E(t)}{t} \leq \left( \frac{\beta^2}{2\sigma_1^2} + \frac{\eta^2}{2\sigma_2^2} - (\omega + m) \right) < 0. \quad (6.18)$$

If  $\frac{1}{\omega+m} \left( \frac{\beta^2}{2\sigma_1^2} + \frac{\eta^2}{2\sigma_2^2} \right) < 1$ , then  $\lim_{t \rightarrow \infty} E(t) = 0$  almost surely. Hence the theorem.  $\square$

It is observable that  $R_{0V}^{ext}$  is an increasing function of  $\beta$  and  $\eta$ . Thus, if the infection rate increases or the vaccine-induced immunity loss increases, the inequality  $R_{0V}^{ext} < 1$  may not be held, and consequently, the disease eradication may not be possible.

## 6.4 Case study

For the case study, we considered the covid data of two countries, India and Italy. The parameters estimation and other detailed analysis were done using the Indian Covid-19 epidemic data available from the repositories Covid19India.Org (<https://covid19india.org>) and Worldometers.info (<https://www.worldometers.info/coronavirus/country/india/>). The daily and cumulative numbers of infected, recovered, deceased, and vaccinated cases are reported and updated daily in these depositories. The results of Italy were obtained following a similar analysis.

## 6. Is large-scale vaccination sufficient for controlling the Covid-19 pandemic with uncertainties? A model-based study

**Table 6.1:** Estimated parameter values of system (6.1) for Indian Covid data for the periods: **(1)** 2<sup>nd</sup> February to 6<sup>th</sup> May, 2021; **(2)** 7<sup>th</sup> May to 27<sup>th</sup> December 2021; **(3)** 28<sup>th</sup> December 2021 to 20<sup>th</sup> January 2022; **(4)** from 21<sup>st</sup> January 2022 to 15<sup>th</sup> April 2022; **(5)** from 16<sup>th</sup> April 2022 to 7<sup>th</sup> July 2022.

Period	$\Lambda$	$m$	$\beta$	$\kappa$	$\delta$	$\omega$	$\gamma$	$\gamma_1$	$g$	$d_i$	$\nu$	$\eta$	$q$	$\sigma_1$	$\sigma_2$	$\sigma_3$	$\sigma_4$
1	77756	$4.1 \times 10^{-5}$	0.115	0.92	0.66	0.18	0.03	0.032	0.004	0.007	0.002	0.11	$1.6 \times 10^{-3}$	0.03	0.02	.035	0.04
2	77756	$4.1 \times 10^{-5}$	0.109	0.92	0.66	0.18	0.014	0.16	0.064	0.018	0.002	0.23	$2.1 \times 10^{-3}$	0.06	0.05	0.04	0.05
3	77756	$4.1 \times 10^{-5}$	0.57	0.92	0.97	0.18	0.004	0.205	0.14	0.017	0.002	0.23	$4 \times 10^{-3}$	0.09	0.08	0.12	0.1
4	77756	$4.1 \times 10^{-5}$	0.090	0.92	0.99	0.18	0.004	0.364	0.42	0.024	0.002	0.12	$4.8 \times 10^{-3}$	0.14	0.11	0.07	0.4
5	77756	$4.1 \times 10^{-5}$	0.134	0.92	0.66	0.18	0.029	0.030	0.0004	0.013	0.002	0.15	$2.5 \times 10^{-3}$	0.015	0.023	0.031	0.03

We have considered India's covid data for February 2, 2021, to July 7, 2022. It is to be mentioned that different variants of SARS-Cov-2 have different infectivity and virulence. Furthermore, the vaccination rate was low initially but increased subsequently. We, therefore, divided the data set of the study period into five intervals to obtain a good fit parameter set: **(1)** from 2<sup>nd</sup> February to 6<sup>th</sup> May 2021 (the date when the peak is attained in the second wave); **(2)** from 7<sup>th</sup> May to 27<sup>th</sup> December 2021 (end of the second wave); **(3)** from 28<sup>th</sup> December 2021 to 20<sup>th</sup> January 2022 (the date when the peak of the third wave is attained); **(4)** from 21<sup>st</sup> January 2022 to 15<sup>th</sup> April 2022 (end of third wave); **(5)** from 16<sup>th</sup> April 2022 to 7<sup>th</sup> July 2022, where study period ends. We fitted (see Fig. 6.1) the actual covid data (in red colour) for the considered period with the stochastic model solution (in blue colour). The best-fitted parameters and the optimal noise intensities are provided in Table 6.1. The parameters and noise estimation techniques are given in 1.8.2.5.

Indian Covid-19 vaccination program started on January 16, 2021 (Choudhary et al. [2021]). Though the initial vaccination rate was slow, it intensified later on. We demonstrated how the vaccination rate ( $q$ ) and the immunity loss rate ( $\eta$ ) jointly influence the disease burden. We also explained why the covid positive cases increased during the third wave even after mass vaccination. To elucidate, we considered the parameter values of the third row (see Table 6.1), representing the increasing phase of the third wave, and plotted (Fig. 6.2) the per day covid positive cases ( $A + I$ ) from the solution of system (6.1) for simultaneous variation in  $q$  and  $\eta$ . The parameters  $q$  and  $\eta$  were varied in the range 0-0.024 and 0.1-0.25, respectively. The lower range value of each parameter was considered smaller than all the estimated values of the said parameter (see Table 6.1), and the value at the higher range was considered larger than all the estimated values. It shows that daily covid positive cases increase with the increasing vaccination rate ( $q$ ) when the vaccine-induced immunity loss ( $\eta$ ) exceeds the value 0.23, i.e., if the vaccine efficacy is lower than 77%. On the contrary,

## 6.4. Case study

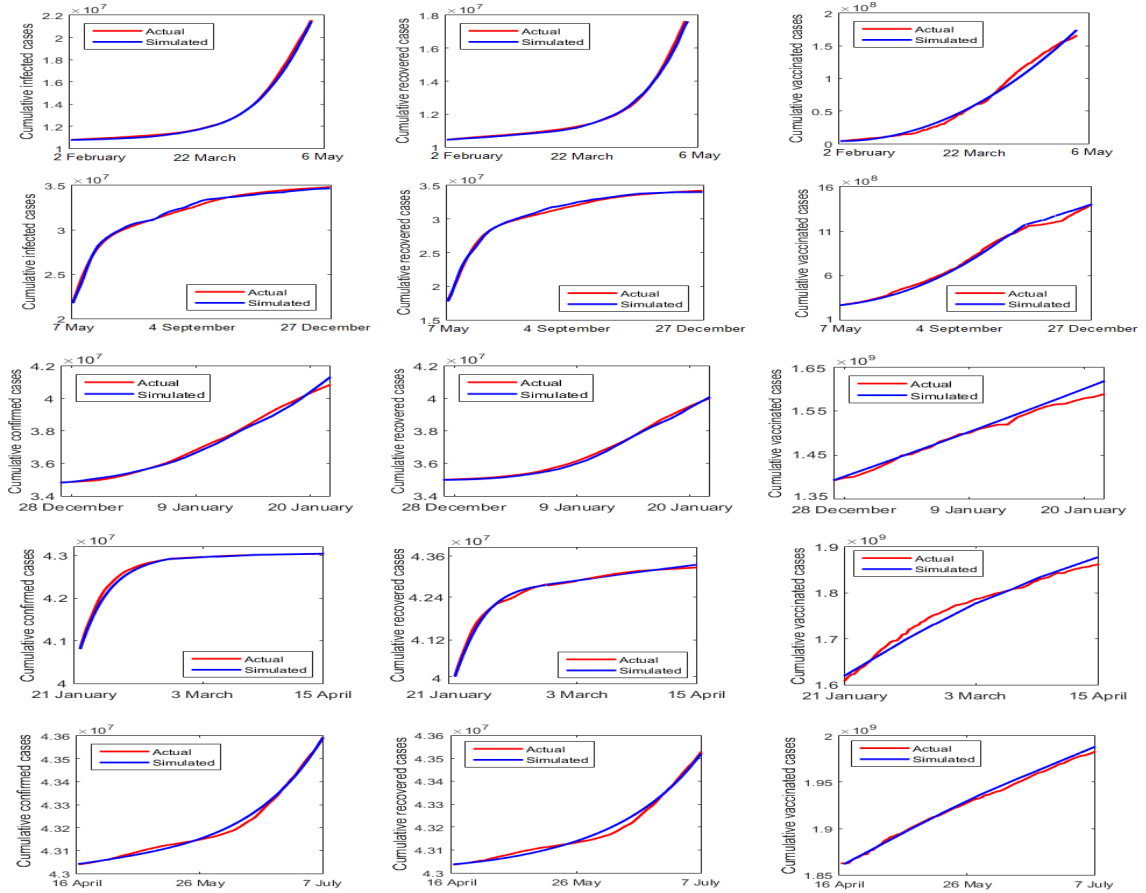


**Figure 6.1:** Covid-19 data fitting with the parameter values and noise intensities as in the Table 6.1. The first row provides the cumulative actual Covid-19 data (red colour curve) of the confirmed, recovered, and vaccinated cases in India from February 2 to May 6, 2021. The other rows represent the same consecutive periods mentioned in the Table 6.1. The solution (blue colour curve) of the stochastic model (6.1) is the fitted curve with the parameter values of the first row of Table 6.1.

if vaccine efficacy is higher than 77% (or  $\eta < 0.23$ ), then daily covid positive cases decrease with increasing immunization. Observe that the per day cases become as high as 0.397 million when  $\eta = 0.25$  and  $q = 0.22$ . It is to be mentioned that Indian covid positive cases during the peak (20<sup>th</sup> January) of the third wave were reported as 0.34 million per day ([https:// www.worldometers.info/coronavirus/country/india/](https://www.worldometers.info/coronavirus/country/india/)). Thus, increased vaccination cannot eradicate covid infection if the vaccine efficacy is low; instead, it increases the covid cases. However, infection eradication is possible with a higher vaccination rate if the vaccine immunity is more than 77%. It is to be mentioned that  $R_{0V}^S < 1$  holds for the lower values of  $q$  and  $\eta$  and  $R_{0V}^S > 1$  for its



## 6. Is large-scale vaccination sufficient for controlling the Covid-19 pandemic with uncertainties? A model-based study

---

higher values.

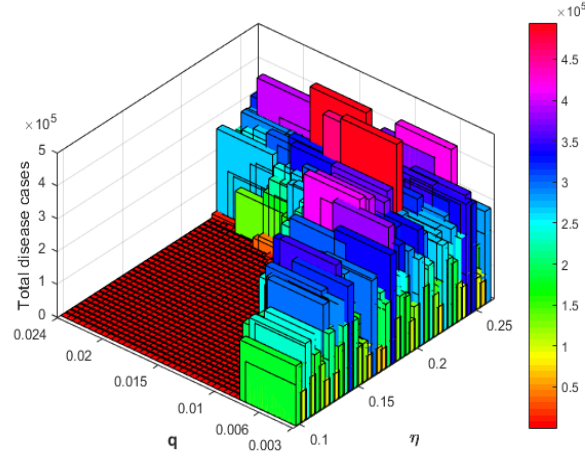


**Figure 6.2:** Per day covid positive cases in India for the variation in the rate parameters  $\eta$  and  $q$ , representing the immunity loss and vaccination rate, respectively. The total disease cases (asymptomatic plus symptomatic) are the end values of the solutions for 1000 time steps. Noise intensities and other parameter values remain fixed from December 28, 2021, to January 20, 2022 (see Table 6.1, third row), the increasing phase of covid cases of the last wave.

A similar phenomenon is plotted in Fig. 6.3 (left) when the vaccination rate ( $q$ ) and force of infection ( $\beta$ ) are varied simultaneously. The covid positive cases gradually increase if  $\beta$  is high and  $q$  is low. The number of positive cases may be as high as 0.5 million per day at the low vaccination and high transmission rates (below figure). In the opposite case, the disease is eradicated. The lower figure represents the newly infected per day covid cases when the force of infection ( $\beta$ ) and the vaccine efficacy ( $\eta$ ) parameters are jointly varied. The infection spreads rapidly when  $\beta > 0.25$  and  $\eta > 0.2$  (Fig. 6.3, right). The covid cases in this parametric range may be as high as 0.532 million per day. It is also to be noted that the number of covid cases will be few if  $\beta$  is high and  $\eta$  is low. It demonstrates that vaccine effectiveness is crucial in controlling the covid cases. The disease may be controlled even at a very high infection rate if the vaccine efficacy is close to 100% (i.e.,  $\eta$  is closed to zero). On the other hand, daily covid cases will remain under control if  $\beta$  is low and  $\eta$  is significantly high. Thus, a strain of coronavirus with low infectivity would not sustain in the present immunization rate.

## 6.4. Case study

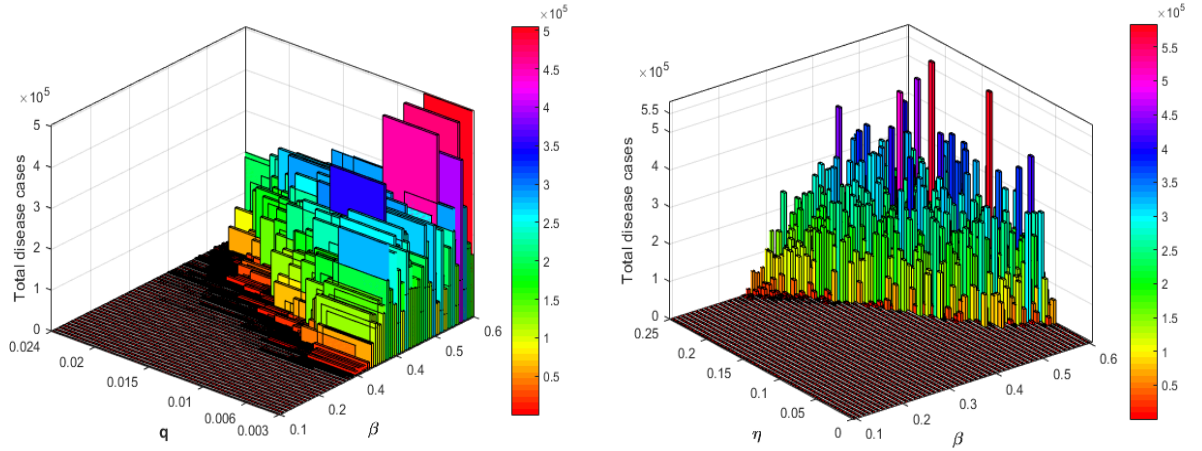


**Figure 6.3:** Per day covid positive cases with respect to  $\beta$  and  $q$  (left) and  $\beta$  and  $\eta$  (right). Noise intensities and other parameter values remain fixed for the period of December 28, 2021, to January 20, 2022, see Table 6.1.

**Table 6.2:** Estimated parameter values of system (6.3) for Italian Covid data for the periods: **(1)** 11<sup>th</sup> October 2021 to 18<sup>th</sup> January 2022; **(2)** 19<sup>th</sup> January 2022 to 20<sup>th</sup> April 2022; **(3)** 21<sup>st</sup> April 2022 to 7<sup>th</sup> July 2022.

Period	$\Lambda$	$m$	$\beta$	$\kappa$	$\delta$	$\omega$	$\gamma$	$\gamma_1$	$g$	$d_i$	$\nu$	$\eta$	$q$	$\sigma_1$	$\sigma_2$	$\sigma_3$	$\sigma_4$
1	1428	$3.35 \times 10^{-5}$	0.228	0.88	0.66	0.16	0.025	0.035	0.035	0.003	0.004	0.32	$4.2 \times 10^{-4}$	0.12	0.50	.23	0.21
2	1428	$3.35 \times 10^{-5}$	0.118	0.88	0.66	0.16	0.025	0.035	0.065	0.003	0.004	0.45	$1 \times 10^{-4}$	0.11	0.10	0.08	0.10
3	1428	$3.35 \times 10^{-5}$	0.208	0.88	0.66	0.16	0.025	0.038	0.065	0.0026	0.004	0.45	$5 \times 10^{-5}$	0.10	0.07	0.18	0.16

We here considered the Covid-19 dataset of Italy to explore the critical value of the vaccine-induced immunity loss. First, we estimate the system parameters for Italian Covid-19 data. The Italian covid data (available from the repository our-worldindata.org (<https://ourworldindata.org/covid-cases>)) for the study period 11<sup>th</sup> October, 2021 to July 7, 2022, were divided into three time segments: **(1)** from 11<sup>th</sup> October, 2021 to 18<sup>th</sup> January, 2022 (the date when the peak is attained in the second wave); **(2)** from 18<sup>th</sup> January, 2022 to 20<sup>th</sup> April 2022 (peak is attained in third wave); **(3)** from 21<sup>st</sup> April 2022 to 7<sup>th</sup> July 2022 (where the study period ends). As previously, we fitted (see Fig. 6.4) the actual covid data (red colour) of Italy with the model generated data (blue colour).

## 6. Is large-scale vaccination sufficient for controlling the Covid-19 pandemic with uncertainties? A model-based study

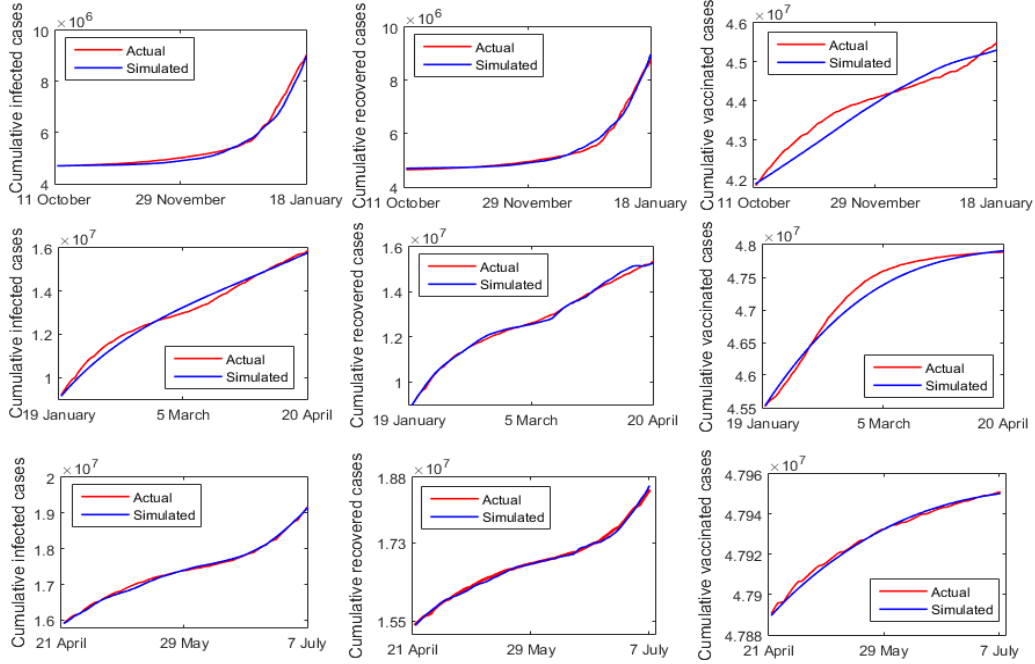


**Figure 6.4:** Covid-19 data fitting with the parameter values and noise intensities as in the Table 6.2. The first row provides the cumulative actual Covid-19 data (red colour curve) of the confirmed, recovered, and vaccinated cases in Italy for the period October 11, 2021 to January 18, 2022. The other rows represent the same with the consecutive periods mentioned in the Table 6.2. The solution (blue colour curve) of the stochastic model (6.1) is the fitted curve with the parameter values of the first row of Table 6.2.

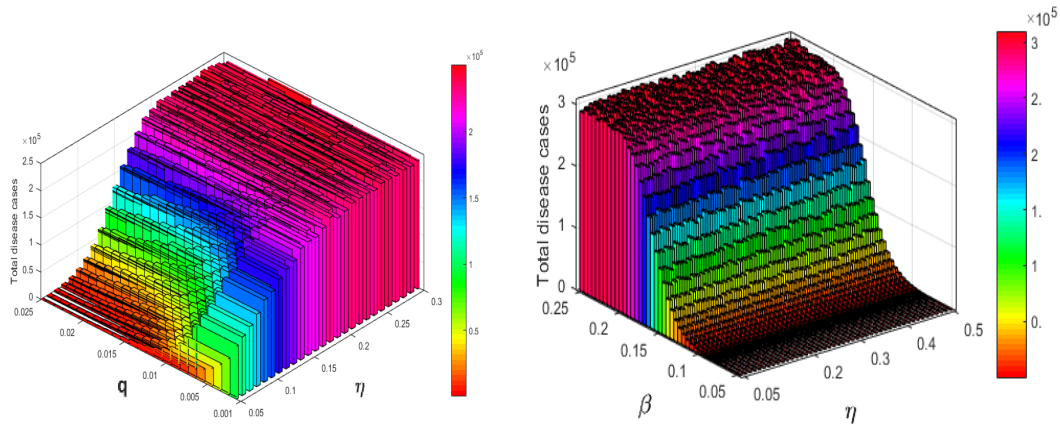


**Figure 6.5:** Left: Per day Covid positive cases in Italy for the variation in the rate parameters  $\eta$  and  $q$ , representing the immunity loss and vaccination rate, respectively. The total disease cases (asymptomatic plus symptomatic) are the end values of the solutions for 1000 time steps. Right: same for the variation of  $\beta$  and  $\eta$ . Noise intensities and other parameter values remain fixed in the period from 21<sup>st</sup> April 2022 to 7<sup>th</sup> July 2022 (see Table 6.2).

## 6.4. Case study

We plotted a similar figure like in the case study for India to explore how the number of disease cases of Italy would change under the variation of parameters  $q$  and  $\eta$ . In the case of Italy, we observe (Figure 6.5, left) that if the vaccination induced immunity loss is higher than 12%, then the epidemic will grow rapidly. In case of variation of  $\beta$  and  $\eta$ , it is observed that when  $\beta$  is low ( $< 0.1$ ), number of confirmed cases is low (Fig. 6.5, right). However, for a higher transmission rate, number of confirmed cases increase rapidly.

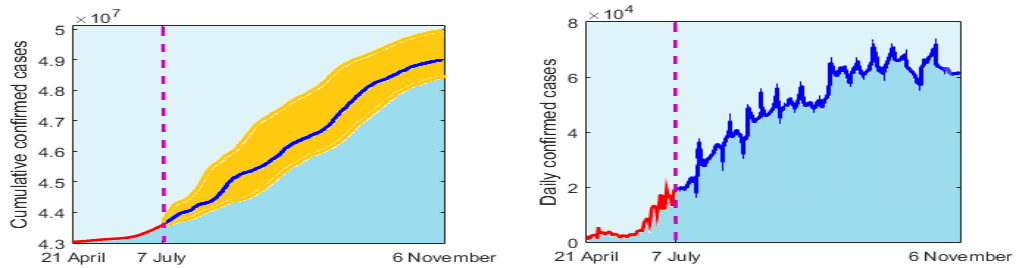


**Figure 6.6:** Left: Predicted cumulative Covid-19 confirmed cases in India for the next 150 days starting from July 7, 2022. The simulation results of the system (6.1) (blue line) predict that India may observe  $4.88 \times 10^7$  positive cases until the first week of November 2022. The confidence interval (95%) is plotted with a yellow shed. Right: Predicted daily confirmed cases for the same period. The red curve in both figures indicates the actual cases, and the dotted vertical line indicates July 7, 2022. Parameters and noise intensities as in the last row of Table 6.1.

Indian covid cases are again in increasing mode. We predicted the cumulative confirmed covid positive cases for the next 150 days based on the current epidemiological status of India. To provide a forecast, we repeated the stochastic system's solution 1000 times and then took the mean to get the estimated values with a 95% confidence interval (blue line of Fig. 6.6, left). The curve is increasing and will continue till the first week of November 2022, indicating that the newly infected cases are surging gradually. The cumulative number of the predicted infected case till the first week of November 2022 might be between  $4.82 \times 10^7$  to  $5.01 \times 10^7$  in the 95% confidence interval. The predicted daily covid confirmed cases in India till the first week of November 2022 is presented in Fig. 6.6, right.

The covid cases in Italy are also in a increasing trend. Fig. 6.7 indicates that the daily case may be around 37,142 and the cumulative cases might be between  $2.41 \times 10^7$  to  $2.54 \times 10^7$  till the first week of November, 2022. It is, however, to be mentioned that the accurate prediction for a significantly long period is quite impossible in the case of SARS CoV-2 infection because this novel virus can mutate to some strains

## 6. Is large-scale vaccination sufficient for controlling the Covid-19 pandemic with uncertainties? A model-based study

with high infectivity (Haque et al. [2021]). Also, a change in the control measure imposed by the authority can change the trend.

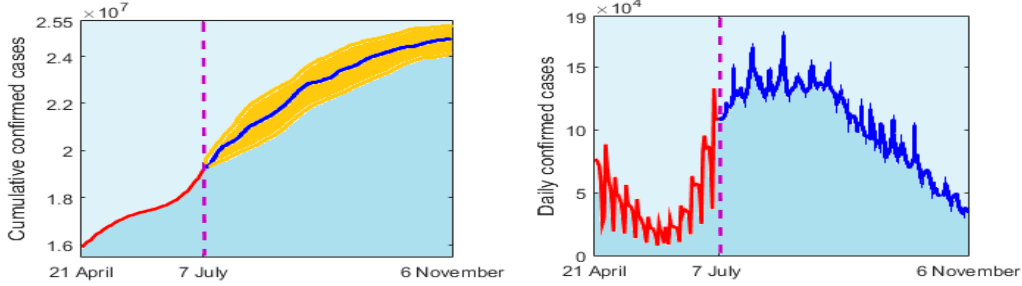


**Figure 6.7:** Left: Predicted cumulative Covid-19 confirmed cases in Italy for the next 150 days starting from July 7, 2022. The simulation results of the system (6.1) (blue line) predict that Italy may observe  $2.49 \times 10^7$  positive cases until the first week of November 2022. The confidence interval (95%) is plotted with a yellow shed. Right: Predicted daily confirmed cases for the same period. The red curve in both figures indicates the actual cases, and the dotted vertical line means July 7, 2022. Parameters and noise intensities as in the last row of Table 6.2.

### 6.5 Discussion

The SARS-CoV-2 infection has put the world under pressure for more than two years. Most countries have experienced several waves of this infection at the cost of millions of lives. A massive vaccination program started at the end of 2020, hoping that the disease would be controlled. Though the morbidity and mortality of the covid disease reduced significantly, the disease eradication even of its control is far from expected. In the second and third waves, many countries have experienced higher positive cases than the previous peak values. Several European countries, the UK, and the USA have fully vaccinated a significant proportion of their population but cannot resist further covid infection. This fact has put the efficacy of the vaccine under question. Recent studies show that vaccine-induced immunity is significantly reduced after six to eight months post-vaccination. The level of a covid antibody that persists after this period may not be sufficient to prevent reinfection. There is, however, uncertainty regarding the rate of immunity loss among the vaccinated population. Uncertainty also exists in different rate parameters, e.g., the force of infection and recovery rates. It is undoubtedly true that the infectivity of the omicron variant is much higher than the previous strains. Also, the severity of the disease is relatively

## 6.5. Discussion

---

low, and the recovery rate is high in the current wave caused due to the omicron variant of coronavirus. Considering such uncertainties in the rate parameters, we have proposed and analyzed a six-dimensional stochastic Covid-19 epidemic model in the presence of vaccination. Theories of the asymptotic behaviour of the nonlinear stochastic system are used to analyze this noise-induced dynamical system. The objective was to understand the effect of vaccination on the disease dynamics in the presence of uncertainties. We here prescribed both the disease persistence and eradication conditions. It is shown that the disease persists for a long time almost surely if the stochastic basic reproduction number (SBRN) is greater than unity. It is noticed that this value of SBRN is smaller than the DBRN (deterministic basic reproduction number) of the corresponding deterministic model, which is usually used as a measure of disease establishment in the latter type of epidemic models. A sufficient condition ( $R_{0V}^{ext} < 1$ ) is established for the disease eradication from the system. Noticeably, this condition may not hold if the disease's infectivity increases or/and the vaccine-induced immunity loss increases (that is, if the vaccine efficacy is reduced). Both issues are probably real for many countries, where vaccination starts in the initial months of 2021, implying that vaccinated people will significantly lose their immunity from July/August onwards (seven to eight months post-vaccination). Furthermore, the new variant, omicron, is highly infectious. These two reasons are probably responsible for the second, third and subsequent waves in different countries. We used the Indian and Italian Covid-19 data to demonstrate the variational effects of the rate parameters  $q$ ,  $\eta$ , and  $\beta$ . Noticeably, if the vaccine-induced immunity loss rate,  $\eta$ , is higher than 0.23 for India, eradicating infection is practically impossible. The same value of  $\eta$  for Italy is 0.12. The covid positive cases will surge in India if the force of infection is high ( $> 0.25$ ) and vaccine-induced immunity loss is higher than 23%. For Italy, these values are 0.1 and 12%, respectively. It implies that the disease will last long unless a long-lasting vaccine candidate appears or a low infectious variant replaces the highly infectious variant.

There are, however, some limitations of this model. For example, this model does not consider the population's age structure. It is to be mentioned that a higher age group population is more prone to covid infection. Secondly, there are many variants of coronavirus with different infectivity and virulence. Therefore, a multi-strain epidemic model would be more appropriate to represent the ongoing pandemic. Despite such limitations, our theoretical and simulation results justify the reason for long-lasting disease persistence even when a large-scale immunization process has

## **6. Is large-scale vaccination sufficient for controlling the Covid-19 pandemic with uncertainties? A model-based study**

---

been implemented. To our knowledge, such effects have not been reported earlier using a dynamic mathematical model. Our study reveals that eradicating Covid-19 infection is challenging if the vaccine-induced immunity loss or the infectivity of the virus strain is high. Therefore the disease will last long unless a long-lasting vaccine candidate appears or a low infectious variant replaces the highly contagious variant.

# Chapter 7

## Future Work

In this thesis, we have considered the stochasticity in the deterministic system in two ways. Firstly, we have considered random white noise perturbation of some system parameters. Secondly, we have regarded stochastic perturbation as proportional to the distance between the state variable and the corresponding deterministic equilibrium. However, this kind of randomness helps us to realize the physical phenomena better, but still, this method has a drawback. Due to the white noise perturbation (Wiener process) of the parameter, the variance of the parameter becomes a function of time where the time variable occurs at the denominator. As a result, the fluctuation of the perturbed parameter becomes very high for a small time value which is physically not very realistic. However, such unrealistic fluctuation in the perturbed parameter can be removed by considering a mean-reverting Ornstein–Uhlenbeck process.

Additionally, a time delay is a significant factor in many ecological and epidemiological models. Therefore, a delay-induced stochastic model would be better for modelling real-world biological phenomena. It has also been observed that the noise is not always white in all environments. It is reported that terrestrial noise tends to be white while the marine environment’s noise tends to be red or brown ([Vasseur and Yodzis \[2004\]](#)). But due to the lack of mathematical tools and tractability, these colour noises haven’t gained much attention from researchers to model biological events. We look forward to studying the stochastic population models with suitable colour noise. We also want to study stochastic models, where the stochasticity in the deterministic model will be incorporated through the Markov process. In this thesis, we have included stochasticity in an isolated deterministic system. In the future, we would like to study spatial and multi-patch ecological models with stochasticity. Thus, our



future study will focus on, but not limited to, the following topics:

- To study the dynamical behaviour of the stochastic ecological and epidemiological models with mean-reverting Ornstein–Uhlenbeck processes.
- To study the dynamical behaviour of biological models in the presence of coloured noise.
- To include both the delay and stochasticity in deterministic ecological, epidemiological and eco-epidemiological models and explore their dynamics.
- To study stochastic spatial models.
- To analyze the multi-patch ecological system in the presence of noise.

# References

- (1975). Statistical problems in diffraction theory, author=Kravtsov, Yu A and Rytov, Sergei Mikhailovich and Tatarskiĭ, vi. *Soviet Physics Uspekhi*, 18(2), 118. [1.1](#)
- (2019a). WHO Coronavirus Disease (COVID-19) Dashboard, in: WHO Coronavirus Disease (Covid-19) Dashboard. In *Available from: <https://covid19.who.int/>, 2020 (accessed on December 6, 2020)*. [5.1](#)
- (2019b). World health organization coronavirus disease. In *World Health Organization Coronavirus disease. Available from: <https://www.who.int/emergencies/diseases/novel-coronavirus->*. [5.1](#)
- (2020). *<https://www.northyorkmoors.org.uk/discover/moorland/moorland-plants-and-wildlife/red-grouse>*. [4.4.2](#)
- (2020). Covid19.org: <https://www.covid19india.org/> (accessed on July 16, ). [5.1](#)
- (2020). Hindustantime,large number of covid-19 cases being observed in migrant workers: Top uttar pradesh health official. large number of covid-19 cases being observed in migrant workers 2020. In *Available from: <https://www.hindustantimes.com/india-news/large-number-of-covid-19-cases-being-observed-in-migrant-workers-top-uttar-pradesh-health-official/story-9yPKobgBXHYr5p4ULtPeoK.html>*. [5.4](#)
- (2020). <https://www.mohfw.gov.in/pdf/revisedvaccinationguidelines.pdf>. :text=COVID%20vaccination%20in%20the%20country,18%20years%20of%20age,.
- (2020). Ministry of railways, press release, prid=1626576,. In *Available from: <https://pib.gov.in/PressReleaseIframePage.aspx?>* [5.4](#)

- 
- Adak, D., Bairagi, N., and Hakl, R. (2020). Chaos in delay-induced leslie–gower prey–predator–parasite model and its control through prey harvesting. *Nonlinear Analysis: Real World Applications*, 51, 102998. [4.2.1](#)
- Adak, D., Majumder, A., and Bairagi, N. (2021). Mathematical perspective of covid-19 pandemic: disease extinction criteria in deterministic and stochastic models. *Chaos, Solitons & Fractals*, 142, 110381. [5.1](#), [6.1](#)
- Adam, D. (2020). Special report: The simulations driving the world’s response to COVID-19. *Nature*, 580(7803), 316. [1.9](#), [5.1](#)
- Adnani, J., Hattaf, K., and Yousfi, N. (2013). Stability analysis of a stochastic sir epidemic model with specific nonlinear incidence rate. *International Journal of Stochastic Analysis*, 2013. [1.9](#)
- Afanasev, V.N., Kolmanovskij, V.B., and Nosov, V.R. (1996). *Mathematical theory of control systems design*. Springer. [2.5.2](#)
- Al-Tawfiq, J.A. (2020). Asymptomatic coronavirus infection: MERS-CoV and SARS-CoV-2 (COVID-19). *Travel Medicine and Infectious Disease*. [5.1](#)
- Alberti, T. and Faranda, D. (2020). On the uncertainty of real-time predictions of epidemic growths: a COVID-19 case study for China and Italy. *Communications in Nonlinear Science and Numerical Simulation*, 90, 105372. [5.1](#)
- Allen, E. (2007). *Modeling with Itô stochastic differential equations*, volume 22. Springer Science & Business Media. [1.6](#)
- Allen, L.J. (2010). *An introduction to stochastic processes with applications to biology*. CRC press. [1.7.3](#)
- Anastassopoulou, C., Russo, L., Tsakris, A., and Siettos, C. (2020). Data-based analysis, modelling and forecasting of the covid-19 outbreak. *PloS One*, 15(3), e0230405. [6.1](#)
- Anderson, R.M., Anderson, B., and May, R.M. (1992). *Infectious diseases of humans: dynamics and control*. Oxford University Press. [3.3](#)
- Anderson, R.M., Heesterbeek, H., Klinkenberg, D., and Hollingsworth, T.D. (2020). How will country-based mitigation measures influence the course of the COVID-19 epidemic? *The Lancet*, 395(10228), 931–934. [1.9](#), [5.1](#)

## References

---

- Anderson, R.M. and May, R.M. (1992). Infectious diseases of humans: dynamics and control. *Oxford university press*. [5.2.1.1](#)
- Anderson, R.M. and May, R.M. (1981). The population dynamics of microparasites and their invertebrate hosts. *Philosophical Transactions of the Royal Society of London. B, Biological Sciences*, 291(1054), 451–524. [1.9](#)
- Antonovics, J., Wilson, A.J., Forbes, M.R., Hauffe, H.C., Kallio, E.R., Leggett, H.C., Longdon, B., Okamura, B., Sait, S.M., and Webster, J.P. (2017). The evolution of transmission mode. *Philosophical Transactions of the Royal Society B: Biological Sciences*, 372(1719), 20160083. [3.1](#)
- Armitage, P. and Doll, R. (1957). A two-stage theory of carcinogenesis in relation to the age distribution of human cancer. *British Journal of Cancer*, 11(2), 161. [1.1](#)
- Bailey, N.T. et al. (1975). *The mathematical theory of infectious diseases and its applications*. Charles Griffin & Company Ltd, 5a Crendon Street, High Wycombe, Bucks HP13 6LE. [1.1](#)
- Baines, D., Allinson, H., Duff, J.P., Fuller, H., Newborn, D., and Richardson, M. (2018). Lethal and sub-lethal impacts of respiratory cryptosporidiosis on red grouse, a wild gamebird of economic importance. *Ibis*, 160(4), 882–891. [4.4.2](#)
- Bairagi, N. and Adak, D. (2015). Complex dynamics of a predator–prey–parasite system: An interplay among infection rate, predator’s reproductive gain and preference. *Ecological Complexity*, 22, 1–12. [3.3](#)
- Bairagi, N. and Adak, D. (2016). Switching from simple to complex dynamics in a predator–prey–parasite model: An interplay between infection rate and incubation delay. *Mathematical Biosciences*, 277, 1–14. [4.2.1](#)
- Bairagi, N., Roy, P.K., and Chattopadhyay, J. (2007). Role of infection on the stability of a predator–prey system with several response functions—a comparative study. *Journal of Theoretical Biology*, 248(1), 10–25. [4.1](#)
- Bairagi, N., Sarkar, R.R., and Chattopadhyay, J. (2008a). Impacts of incubation delay on the dynamics of an eco-epidemiological system—a theoretical study. *Bulletin of Mathematical Biology*, 70, 2017–2038. [4.1](#)

- 
- Bairagi, N., Pal, S., Chatterjee, S., and Chattopadhyay, J. (2008b). Nutrient, non-toxic phytoplankton, toxic phytoplankton and zooplankton interaction in an open marine system. In *Aspects of Mathematical Modelling*, 41–63. Springer. [2.1](#)
- Bairagi, N., Saha, S., Chaudhuri, S., and Dana, S.K. (2019). Zooplankton selectivity and nutritional value of phytoplankton influences a rich variety of dynamics in a plankton population model. *Physical Review E*, 99(1), 012406. [1.9](#), [2.1](#), [2.1](#)
- Bandyopadhyay, M. and Chattopadhyay, J. (2005). Ratio-dependent predator–prey model: effect of environmental fluctuation and stability. *Nonlinearity*, 18(2), 913. [1.9](#)
- Baron, C., Domke, N., Beinhofer, M., and Hapfelmeier, S. (2001). Elevated temperature differentially affects virulence, virb protein accumulation, and t-pilus formation in different agrobacterium tumefaciens and agrobacterium vitis strains. *Journal of Bacteriology*, 183(23), 6852–6861. [1.9](#)
- Bartlett, M. (1949). Some evolutionary stochastic processes. *Journal of the Royal Statistical Society. Series B (Methodological)*, 11(2), 211–229. [1.1](#)
- Beddington, J.R. and May, R.M. (1977). Harvesting natural populations in a randomly fluctuating environment. *Science*, 197(4302), 463–465. [1.1](#), [1.9](#)
- Beltrami, E. and Carroll, T. (1994). Modeling the role of viral disease in recurrent phytoplankton blooms. *Journal of Mathematical Biology*, 32(8), 857–863. [2.1](#)
- Benedetti, F., Jalabert, L., Sourisseau, M., Beker, B., Cailliau, C., Desnos, C., Elineau, A., Irisson, J.O., Lombard, F., Picheral, M., et al. (2019). The seasonal and inter-annual fluctuations of plankton abundance and community structure in a north atlantic marine protected area. *Frontiers in Marine Science*, 6, 214. [2.8](#)
- Beretta, E., Carletti, M., and Solimano, F. (2000). On the effects of environmental fluctuations in a simple model of bacteria-bacteriophage infection. *Canad. Appl. Math. Quart*, 8, 321–366. [1.9](#)
- Beretta, E., Kolmanovskii, V., and Shaikhet, L. (1998). Stability of epidemic model with time delays influenced by stochastic perturbations. *Mathematics and Computers in Simulation*, 45(3-4), 269–277. [1.9](#)

## References

---

- Bhapkar, H., Mahalle, P.N., Dey, N., and Santosh, K. (2020). Revisited covid-19 mortality and recovery rates: are we missing recovery time period? *Journal of Medical Systems*, 44(12), 1–5. [6.2](#)
- Bixon, M. and Zwanzig, R. (1969). Boltzmann-langevin equation and hydrodynamic fluctuations. *Physical Review*, 187(1), 267. [1.1](#)
- Blanford, S., Thomas, M.B., Pugh, C., and Pell, J.K. (2003). Temperature checks the red queen? resistance and virulence in a fluctuating environment. *Ecology Letters*, 6(1), 2–5. [1.9](#)
- Bloch, F. (1946). Nuclear induction. *Physical Review*, 70(7-8), 460. [1.1](#)
- Blower, S.M. and Dowlatabadi, H. (1994). Sensitivity and uncertainty analysis of complex models of disease transmission: an HIV model, as an example. *International Statistical Review/Revue Internationale de Statistique*, 229–243. [1.8.2.4](#)
- Braumann, C.A. (2019). *Introduction to stochastic differential equations with applications to modelling in biology and finance*. John Wiley & Sons. [1.7.4.1](#), [1.7.5.2](#), [3.4](#)
- Brooks, J.L. and Dodson, S.I. (1965). Predation, body size, and composition of plankton. *Science*, 150(3692), 28–35. [2.1](#)
- Capocelli, R. and Ricciardi, L. (1974). A diffusion model for population growth in random environment. *Theoretical Population Biology*, 5(1), 28–41. [1.1](#)
- Carletti, M. (2002). On the stability properties of a stochastic model for phage–bacteria interaction in open marine environment. *Mathematical Biosciences*, 175(2), 117–131. [1.9](#)
- Carletti, M. (2006). Numerical simulation of a campbell-like stochastic delay model for bacteriophage infection. *Mathematical Medicine and Biology: a Journal of the IMA*, 23(4), 297–310. [1.9](#)
- Caruso, A., Gargano, M., Valenti, D., Fiasconaro, A., and Spagnolo, B. (2005). Cyclic fluctuations, climatic changes and role of noise in planktonic foraminifera in the mediterranean sea. *Fluctuation and Noise Letters*, 5(02), L349–L355. [4.1](#)

- 
- Castillo-Chavez, C. and Song, B. (2004). Dynamical models of tuberculosis and their applications. *Mathematical Biosciences & Engineering*, 1(2), 361. [5.2.1.2](#), [5.2.1.2](#)
- Chakraborty, S., Pal, S., and Bairagi, N. (2012). Predator-prey fishery model under deterministic and stochastic environments: a mathematical perspective. *International Journal of Dynamical Systems and Differential Equations*, 4(3), 215–241. [1.9](#)
- Chatterjee, K., Chatterjee, K., Kumar, A., and Shankar, S. (2020). Healthcare impact of COVID-19 epidemic in India: A stochastic mathematical model. *Medical Journal Armed Forces India*, 76(2), 147–155. [1.9](#), [5.1](#)
- Chatterjee, S., Isaia, M., Bona, F., Badino, G., Venturino, E., et al. (2008). Modelling environmental influences on wanderer spiders in the langhe region (piemonte-nw italy). *Journal of Numerical Analysis, Industrial and Applied Mathematics*, 3(3-4), 193–209. [1.9](#)
- Chattopadhyay, J. and Bairagi, N. (2001). Pelicans at risk in salton sea—an eco-epidemiological model. *Ecological Modelling*, 136(2-3), 103–112. [4.1](#)
- Chattopadhyay, J. and Pal, S. (2002). Viral infection on phytoplankton–zooplankton system—a mathematical model. *Ecological Modelling*, 151(1), 15–28. [4.1](#)
- Chattopadhyay, J., Sarkar, R.R., and El Abdllaoui, A. (2002). A delay differential equation model on harmful algal blooms in the presence of toxic substances. *Mathematical Medicine and Biology: A Journal of the IMA*, 19(2), 137–161. [2.1](#)
- Chen, C. and Kang, Y. (2016). The asymptotic behavior of a stochastic vaccination model with backward bifurcation. *Applied Mathematical Modelling*, 40(11-12), 6051–6068. [6.2](#)
- Chen, F., Li, Z., Chen, X., and Laitochová, J. (2007). Dynamic behaviors of a delay differential equation model of plankton allelopathy. *Journal of Computational and Applied Mathematics*, 206(2), 733–754. [2.1](#)
- Chen, T.M., Rui, J., Wang, Q.P., Zhao, Z.Y., Cui, J.A., and Yin, L. (2020). A mathematical model for simulating the phase-based transmissibility of a novel coronavirus. *Infectious Diseases of Poverty*, 9(1), 1–8. [1.9](#), [5.1](#)

## References

---

- Chen, Y., Evans, J., and Feldlaufer, M. (2006). Horizontal and vertical transmission of viruses in the honey bee, *Apis mellifera*. *Journal of Invertebrate Pathology*, 92(3), 152–159. [1.9](#), [3.1](#)
- Chernov, L.A., Silverman, R.A., and Morse, P.M. (1960). Wave propagation in a random medium. *Physics Today*, 13(12), 50. [1.1](#)
- Choudhary, O.P., Choudhary, P., and Singh, I. (2021). India's covid-19 vaccination drive: key challenges and resolutions. *The Lancet Infectious Diseases*, 21(11), 1483–1484. [6.4](#)
- Clancy, D. (2014). Sir epidemic models with general infectious period distribution. *Statistics & Probability Letters*, 85, 1–5. [1.9](#)
- Clayton, D.H. and Tompkins, D.M. (1994). Ectoparasite virulence is linked to mode of transmission. *Proceedings of the Royal Society of London. Series B: Biological Sciences*, 256(1347), 211–217. [1.9](#), [3.1](#)
- Coleman, T.F. and Li, Y. (1994). On the convergence of interior-reflective Newton methods for nonlinear minimization subject to bounds. *Mathematical Programming*, 67(1), 189–224. [1.8.2.2](#)
- Coleman, T.F. and Li, Y. (1996). An interior trust region approach for nonlinear minimization subject to bounds. *SIAM Journal on Optimization*, 6(2), 418–445. [1.8.2.2](#)
- Cowling, B.J. and Aiello, A.E. (2020). Public health measures to slow community spread of coronavirus disease 2019. *The Journal of Infectious Diseases*, 221(11), 1749–1751. [5.1](#)
- Croda, J. and Ranzani, O.T. (2021). Booster doses for inactivated covid-19 vaccines: if, when, and for whom. *The Lancet Infectious Diseases*. [6.1](#)
- Day, M. (2020). Covid-19: four fifths of cases are asymptomatic, China figures indicate. *British Medical Journal Publishing Group*. [5.1](#)
- De la Sen, M. and Ibeas, A. (2021). On an SE(Is)(Ih)AR epidemic model with combined vaccination and antiviral controls for covid-19 pandemic. *Advances in Difference Equations*, 2021(1), 1–30. [6.1](#)



- 
- De Sousa, L.E., De Oliveira Neto, P.H., and Da Silva Filho, D.A. (2020). Kinetic monte carlo model for the covid-19 epidemic: Impact of mobility restriction on a covid-19 outbreak. *Physical Review E*, 102(3), 032133. [6.1](#)
- Denaro, G., Valenti, D., La Cognata, A., Spagnolo, B., Bonanno, A., Basilone, G., Mazzola, S., Zgozi, S., Aronica, S., and Brunet, C. (2013a). Spatio-temporal behaviour of the deep chlorophyll maximum in mediterranean sea: Development of a stochastic model for picophytoplankton dynamics. *Ecological Complexity*, 13, 21–34. [4.1](#)
- Denaro, G., Valenti, D., Spagnolo, B., Basilone, G., Mazzola, S., Zgozi, S.W., Aronica, S., and Bonanno, A. (2013b). Dynamics of two picophytoplankton groups in mediterranean sea: Analysis of the deep chlorophyll maximum by a stochastic advection-reaction-diffusion model. *PLoS One*, 8(6), e66765. [4.1](#)
- Desmet, K. and Wacziarg, R. (2021). Jue insight: Understanding spatial variation in covid-19 across the united states. *Journal of Urban Economics*, 103332. [6.1](#)
- Devenish-Nelson, E.S., Harris, S., Soulsbury, C.D., Richards, S.A., and Stephens, P.A. (2013). Demography of a carnivore, the red fox, *vulpes vulpes*: what have we learnt from 70 years of published studies? *Oikos*, 122(5), 705–716. [4.4.2](#)
- Dexter, N. (2003). Stochastic models of foot and mouth disease in feral pigs in the australian semi-arid rangelands. *Journal of Applied Ecology*, 40(2), 293–306. [1.9](#)
- Dey, S. and Joshi, A. (2013). Effects of constant immigration on the dynamics and persistence of stable and unstable drosophila populations. *Scientific Reports*, 3, 1405. [4.5](#)
- Diekmann, O., Heesterbeek, J., and Roberts, M.G. (2010). The construction of next-generation matrices for compartmental epidemic models. *Journal of the Royal Society Interface*, 7(47), 873–885. [5.2.1.1](#), [6.3.1](#)
- Din, A., Khan, A., and Baleanu, D. (2020). Stationary distribution and extinction of stochastic coronavirus (COVID-19) epidemic model. *Chaos, Solitons & Fractals*, 139, 110036. [5.1](#)
- Djéballi, N. and Belhassen, T. (2010). Field study of the relative susceptibility of eleven potato (*Solanum tuberosum* L.) varieties and the efficacy of two fungicides against rhizoctonia solani attack. *Crop Protection*, 29(9), 998–1002. [3.1](#)

## References

---

- Dobson, A.P. and Hudson, P.J. (1992). Regulation and stability of a free-living host-parasite system: *Trichostrongylus tenuis* in red grouse. II. population models. *Journal of Animal Ecology*, 487–498. [4.4.2](#)
- Dolgin, E. et al. (2021). Covid vaccine immunity is waning-how much does that matter. *Nature*, 597(7878), 606–607. [6.2](#)
- Doob, J.L. (1953). *Stochastic processes*, volume 7. Wiley New York. [1.1](#)
- Dubkov, A. and Spagnolo, B. (2008). Verhulst model with lévy white noise excitation. *The European Physical Journal B*, 65(3), 361–367. [4.4.1](#)
- Dunkel, J. and Hänggi, P. (2009). Relativistic Brownian motion. *Physics Reports*, 471(1), 1–73. [1.1](#)
- Dunn, A.M. and Smith, J.E. (2001). Microsporidian life cycles and diversity: the relationship between virulence and transmission. *Microbes and Infection*, 3(5), 381–388. [1.9](#)
- Ebert, D., Lipsitch, M., and Mangin, K.L. (2000). The effect of parasites on host population density and extinction: experimental epidemiology with *Daphnia* and six microparasites. *The American Naturalist*, 156(5), 459–477. [1.9](#), [3.1](#)
- Edelstein-Keshet, L. (2005). *Mathematical models in biology*. SIAM. [1.9](#)
- Einstein, A. (1956). *Investigations on the Theory of the Brownian Movement*. Courier Corporation. [1.1](#)
- Engen, S., Bakke, Ø., and Islam, A. (1998). Demographic and environmental stochasticity-concepts and definitions. *Biometrics*, 840–846. [1.9](#)
- Ewald, P.W. et al. (1994). *Evolution of infectious disease*. Oxford University Press on Demand. [1.9](#), [3.1](#)
- Fanelli, D. and Piazza, F. (2020). Analysis and forecast of COVID-19 spreading in China, Italy and France. *Chaos, Solitons & Fractals*, 134, 109761. [1.9](#), [5.1](#)
- Fayer, R. (1994). Effect of high temperature on infectivity of *Cryptosporidium parvum* oocysts in water. *Applied and Environmental Microbiology*, 60(8), 2732–2735. [1.9](#)

- 
- Feynman, R.P., Leighton, R.B., and Sands, M. (1965). The Feynman lectures on physics. *American Journal of Physics*, 33(9), 750–752. [1.9](#)
- Finnerty, E.J. and Dunne, J. (2007). Trichostrongylus tenuis found in red grouse lagopus lagopus scoticus in the connemara national park. *The Irish Naturalists' Journal*, 28(11), 471–471. [4.4.2](#)
- Fisher, J. (1958). Multiple-mutation theory of carcinogenesis. *Nature*, 181(4609), 651–652. [1.1](#)
- Fistarol, G.O., Legrand, C., and Granéli, E. (2003). Allelopathic effect of prymnesium parvum on a natural plankton community. *Marine Ecology Progress Series*, 255, 115–125. [2.1](#)
- Foppa, I.M. (2016). *A historical introduction to mathematical modeling of infectious diseases: Seminal Papers in Epidemiology*. Academic Press. [1.9](#)
- Fox, R.F. and Uhlenbeck, G.E. (1970). Contributions to nonequilibrium thermodynamics. II. Fluctuation theory for the Boltzmann equation. *The Physics of Fluids*, 13(12), 2881–2890. [1.1](#)
- Furuse, Y. (2021). Simulation of future covid-19 epidemic by vaccination coverage scenarios in japan. *Journal of Global Health*, 11. [6.1](#)
- Gao, M. and Jiang, D. (2019). Stationary distribution of a stochastic food chain chemostat model with general response functions. *Applied Mathematics Letters*, 91, 151–157.
- Gao, N., Song, Y., Wang, X., and Liu, J. (2019). Dynamics of a stochastic SIS epidemic model with nonlinear incidence rates. *Advances in Difference Equations*, 2019(1), 1–19. [3.2](#)
- Garay, R.P. and Lefever, R. (1978). A kinetic approach to the immunology of cancer: Stationary states properties of effector-target cell reactions. *Journal of Theoretical Biology*, 73(3), 417–438. [1.1](#)
- Gard, T.C. (1988). Introduction to Stochastic Differential Equations. Monographs and Text-books in pure and applied mathematics. [1.6](#)

## References

---

- Gardiner, C.W. et al. (1985). *Handbook of stochastic methods*, volume 3. springer Berlin. [1.6](#)
- Ghostine, R., Gharamti, M., Hassrouny, S., and Hoteit, I. (2021). An extended seir model with vaccination for forecasting the covid-19 pandemic in saudi arabia using an ensemble kalman filter. *Mathematics*, 9(6), 636. [6.1](#)
- Gibbs, J.W. (1906). *Scientific Papers of J. Willard Gibbs, in Two Volumes*, volume 1. Longmans, Green. [1.1](#)
- Gilpin, M.E. and Rosenzweig, M.L. (1972). Enriched predator-prey systems: theoretical stability. *Science*, 177(4052), 902–904. [1.9](#), [2.1](#)
- Giordano, G., Blanchini, F., Bruno, R., Colaneri, P., Di Filippo, A., Di Matteo, A., and Colaneri, M. (2020). Modelling the COVID-19 epidemic and implementation of population-wide interventions in Italy. *Nature Medicine*, 26(6), 855–860. [5.1](#)
- Girona, T. (2020). Confinement Time Required to Avoid a Quick Rebound of COVID-19: Predictions From a Monte Carlo Stochastic Model. *Frontiers in Physics*, 8, 186. [5.1](#)
- Giuffrida, A., Valenti, D., Ziino, G., Spagnolo, B., and Panebianco, A. (2009). A stochastic interspecific competition model to predict the behaviour of listeria monocytogenes in the fermentation process of a traditional sicilian salami. *European Food Research and Technology*, 228(5), 767–775. [4.1](#)
- Gottesman, O. and Meerson, B. (2012). Multiple extinction routes in stochastic population models. *Physical Review E*, 85(2), 021140. [4.5](#)
- Gounand, I., Mouquet, N., Canard, E., Guichard, F., Hauzy, C., and Gravel, D. (2014). The paradox of enrichment in metaecosystems. *The American Naturalist*, 184(6), 752–763. [1.9](#), [2.1](#)
- Grassly, N.C. and Fraser, C. (2008). Mathematical models of infectious disease transmission. *Nature Reviews Microbiology*, 6(6), 477–487. [1.9](#), [3.2](#)
- Gray, A., Greenhalgh, D., Hu, L., Mao, X., and Pan, J. (2011). A stochastic differential equation SIS epidemic model. *SIAM Journal on Applied Mathematics*, 71(3), 876–902. [1.9](#)

- 
- Greenhalgh, D., Khan, Q.J., and Pettigrew, J.S. (2017). An eco-epidemiological predator–prey model where predators distinguish between susceptible and infected prey. *Mathematical Methods in the Applied Sciences*, 40(1), 146–166. [4.1](#)
- Greenman, J. and Hoyle, A. (2010). Pathogen exclusion from eco-epidemiological systems. *The American Naturalist*, 176(2), 149–158. [4.1](#)
- Grigoriu, M. (2013). *Stochastic calculus: applications in science and engineering*. Springer Science & Business Media. [1.9](#)
- Haken, H. and Weidlich, W. (1969). Quantum theory of the laser. *Quantum Optics*, 630. [1.1](#)
- Haken, H. (1970). Laser theory. In *Light and Matter Ic/Licht und Materie Ic*, 1–304. Springer. [1.1](#)
- Han, Q., Chen, L., and Jiang, D. (2017). A note on the stationary distribution of stochastic seir epidemic model with saturated incidence rate. *Scientific Reports*, 7(1), 1–9. [6.3.2](#)
- Haque, A., Pranto, T.H., Noman, A.A., and Mahmood, A. (2021). Insight about detection, prediction and weather impact of coronavirus (covid-19) using neural network. *ArXiv preprint arXiv:2104.02173*. [6.4](#)
- Haque, M. and Venturino, E. (2006). The role of transmissible diseases in the holling–tanner predator–prey model. *Theoretical Population Biology*, 70(3), 273–288. [4.1](#), [4.2.1](#)
- Harris, S. (2015). The utility of killing foxes in scotland. *Commissioned and published by the League Against Cruel Sports Scotland*. [4.4.2](#)
- Havens, K.E., Elia, A.C., Taticchi, M.I., and Fulton, R.S. (2009). Zooplankton–phytoplankton relationships in shallow subtropical versus temperate lakes apopka (florida, usa) and trasimeno (umbria, italy). *Hydrobiologia*, 628(1), 165–175. [2.7](#)
- Haydon, D.T. et al. (2002). Analysing noisy time–series: describing regional variation in the cyclic dynamics of red grouse. *Proceedings of the Royal Society of London. Series B: Biological Sciences*, 269(1500), 1609–1617. [4.4.2](#)

## References

---

- He, S., Tang, S., Rong, L., et al. (2020). A discrete stochastic model of the COVID-19 outbreak: Forecast and control. *Mathematical Biosciences and Engineering*, 17(4), 2792–2804. [5.1](#)
- Heelan, P.A. (2012). *Quantum mechanics and objectivity: A study of the physical philosophy of Werner Heisenberg*. Springer. [1.9](#)
- Hernandez-Suarez, C.M. (2002). A markov chain approach to calculate R0 in stochastic epidemic models. *Journal of Theoretical Biology*, 215(1), 83–93. [1.9](#)
- Hewson, R. and Kolb, H. (1975). The food of foxes (*vulpes vulpes*) in scottish forests. *Journal of Zoology*, 176(2), 287–292. [4.4.2](#)
- Higham, D.J. (2001). An algorithmic introduction to numerical simulation of stochastic differential equations. *SIAM Review*, 43(3), 525–546. [2.4](#)
- Holmes, J.C. (1972). Modification of intermediate host behaviour by parasites. *Behavioural Aspects of Parasite Transmission*. [3.2](#)
- Horton Sr, C. (1969). Signal processing of underwater acoustic waves. Technical report, TEXAS UNIV AT AUSTIN. [1.1](#)
- Hritonenko, N., Yatsenko, Y., et al. (1999). *Mathematical modeling in economics, ecology and the environment*. Springer. [1.9](#)
- <https://www.bto.org> (Accessed on August 21, 2020). British trust for ornithology. [4.4.2](#)
- Hu, Z., Song, C., Xu, C., Jin, G., Chen, Y., Xu, X., Ma, H., Chen, W., Lin, Y., Zheng, Y., et al. (2020). Clinical characteristics of 24 asymptomatic infections with COVID-19 screened among close contacts in Nanjing, China. *Science China Life Sciences*, 63(5), 706–711. [5.1](#)
- Hua, J. and Relyea, R. (2014). Chemical cocktails in aquatic systems: Pesticide effects on the response and recovery of > 20 animal taxa. *Environmental Pollution*, 189, 18–26. [3.1](#)
- Hudson, P.J., Dobson, A.P., and Newborn, D. (1992). Do parasites make prey vulnerable to predation? red grouse and parasites. *Journal of Animal Ecology*, 681–692. [4.1](#), [4.2.1](#), [4.4.2](#)

- 
- Hudson, P. and Newborn, D. (1995). A manual of red grouse and moorland management. Fordingbridge, UK. [4.5](#)
- Hunt, G. (1957). Markoff processes and potentials I. *Illinois Journal of Mathematics*, 1(1), 44–93. [1.1](#)
- Ibe, O. (2013). *Markov processes for stochastic modeling*. Newnes. [1.7.5.2](#)
- Iman, R.L. and Conover, W.J. (1982). A distribution-free approach to inducing rank correlation among input variables. *Communications in Statistics-Simulation and Computation*, 11(3), 311–334. [1.8.2.4](#)
- Iman, R.L. and Davenport, J.M. (1982). Rank correlation plots for use with correlated input variables. *Communications in Statistics-Simulation and Computation*, 11(3), 335–360. [1.8.2.4](#)
- in Data, O.W. (2020). The our world in data covid vaccination data. In *ourworldindata.org/covid-vaccinations? country=OWID WRL*. [6.1](#)
- Itô, K. (1944). Stochastic integral. *Proceedings of the Imperial Academy*, 20(8), 519–524. [1.1](#)
- Itô, K. (1951). *On stochastic differential equations*. 4. American Mathematical Society. [1.1](#)
- Ivorra, B., Ferrández, M.R., Vela-Pérez, M., and Ramos, A. (2020). Mathematical modeling of the spread of the coronavirus disease 2019 (COVID-19) taking into account the undetected infections. The case of China. *Communications in Nonlinear Science and Numerical Simulation*, 88, 105303. [1.9](#), [5.1](#)
- Jang, S.R.J. and Baglama, J. (2009). Continuous-time predator–prey models with parasites. *Journal of Biological Dynamics*, 3(1), 87–98. [4.1](#)
- Jenkins, D., Watson, A., and Miller, G. (1964). Predation and red grouse populations. *Journal of Applied Ecology*, 183–195. [4.4.2](#)
- Jernigan, R. and Tsokos, C. (1980). A linear stochastic model for phytoplankton production in a marine ecosystem. *Ecological Modelling*, 10(1), 1–12. [1.1](#)
- Ji, C. and Jiang, D. (2013). Analysis of a predator–prey model with disease in the prey. *International Journal of Biomathematics*, 6(03), 1350012. [4.1](#)

## References

---

- Ji, C., Jiang, D., and Li, X. (2011a). Qualitative analysis of a stochastic ratio-dependent predator–prey system. *Journal of Computational and Applied Mathematics*, 235(5), 1326–1341. [1.9](#)
- Ji, C., Jiang, D., and Shi, N. (2009). Analysis of a predator–prey model with modified leslie–gower and holling-type ii schemes with stochastic perturbation. *Journal of Mathematical Analysis and Applications*, 359(2), 482–498. [4.1](#), [4.4.1](#)
- Ji, C., Jiang, D., and Shi, N. (2011b). A note on a predator–prey model with modified leslie–gower and holling-type ii schemes with stochastic perturbation. *Journal of Mathematical Analysis and Applications*, 377(1), 435–440. [4.1](#)
- Ji, C., Jiang, D., and Shi, N. (2012a). The behavior of an SIR epidemic model with stochastic perturbation. *Stochastic Analysis and Applications*, 30(5), 755–773. [5.2.2](#)
- Ji, C., Jiang, D., Yang, Q., and Shi, N. (2012b). Dynamics of a multigroup SIR epidemic model with stochastic perturbation. *Automatica*, 48(1), 121–131. [5.1](#)
- Jiang, D., Shi, N., and Li, X. (2008). Global stability and stochastic permanence of a non-autonomous logistic equation with random perturbation. *Journal of Mathematical Analysis and Applications*, 340(1), 588–597. [2.3.2](#)
- Jonsson, A. and Wennergren, U. (2019). Approximations of population growth in a noisy environment: on the dichotomy of non-age and age structure. *Theoretical Ecology*, 12(1), 99–110. [2.8](#)
- Juno, J.A. and Wheatley, A.K. (2021). Boosting immunity to covid-19 vaccines. *Nature Medicine*, 27(11), 1874–1875. [6.1](#)
- Kabata, Z. et al. (1985). Parasites and diseases of fish cultured in the tropics. *Taylor & Francis Ltd.* [4.1](#), [4.2.1](#)
- Kaiser, J. (1999). Salton sea: Battle over a dying sea. *Science*, 28–30. [4.1](#), [4.2.1](#)
- Kampe de Feriet, J. (1955). Introduction to the statistical theory of turbulence. iv. *Journal of the Society for Industrial and Applied Mathematics*, 3(2), 90–117. [1.1](#)
- Karako, K., Song, P., Chen, Y., and Tang, W. (2020). Analysis of covid-19 infection spread in japan based on stochastic transition model. *Bioscience Trends*. [6.1](#)



- 
- Keller, J.B., Bellman, R., et al. (1964). *Stochastic equations and wave propagation in random media*, volume 16. American Mathematical Society Providence, RI. [1.1](#)
- Kermack, W.O. and McKendrick, A.G. (1927). A contribution to the mathematical theory of epidemics. *Proceedings of the Royal Society of London. Series A, Containing Papers of a Mathematical and Physical Character*, 115(772), 700–721. [3.6](#)
- Khajanchi, S. and Sarkar, K. (2020). Forecasting the daily and cumulative number of cases for the covid-19 pandemic in india. *Chaos: An Interdisciplinary Journal of Nonlinear Science*, 30(7), 071101. [1.9](#), [6.1](#)
- Khalatnikov, M., Abrikosov, A., and Exptl, J. (1958). Theory of diffuse scattering of X-rays and thermal neutrons in solid solutions. III. Account of geometrical distortions of the lattice. *Soviet Physics JETP*, 34(7). [1.1](#)
- Khasminskii, R. (2011). *Stochastic stability of differential equations*, volume 66. Springer Science & Business Media. [1.7.6](#), [1.7.4](#)
- Klebaner, F.C. (2012). *Introduction to stochastic calculus with applications*. World Scientific Publishing Company. [1.1](#)
- Knudson Jr, A.G. (1971). Mutation and cancer: statistical study of retinoblastoma. *Proceedings of the National Academy of Sciences*, 68(4), 820–823. [1.1](#)
- Kohler, W.E. (1975). Wave propagation with stochastically coupled propagating and evanescent modes. *Journal of Mathematical Physics*, 16(3), 536–543. [1.1](#)
- Kot, M. (2001). *Elements of mathematical ecology*. Cambridge University Press. [3.3](#)
- Kucharski, A.J., Russell, T.W., Diamond, C., Liu, Y., Edmunds, J., Funk, S., Eggo, R.M., Sun, F., Jit, M., Munday, J.D., et al. (2020). Early dynamics of transmission and control of COVID-19: a mathematical modelling study. *The Lancet Infectious Diseases*, 20(5), 553–558. [5.1](#)
- Kurmi, S. and Chouhan, U. (2022). A multicompartment mathematical model to study the dynamic behaviour of covid-19 using vaccination as control parameter. *Nonlinear Dynamics*, 1–17. [6.1](#)
- La Salle, J.P. (1976). The stability of dynamical systems. *SIAM*. [5.2.1.2](#)

## References

---

- Lafferty, K.D. (1992). Foraging on prey that are modified by parasites. *The American Naturalist*, 140(5), 854–867. [4.1](#), [4.2.1](#)
- Lafferty, K.D. and Morris, A.K. (1996). Altered behavior of parasitized killifish increases susceptibility to predation by bird final hosts. *Ecology*, 77(5), 1390–1397. [3.2](#), [4.1](#), [4.2.1](#)
- Lagarias, J.C., Reeds, J.A., Wright, M.H., and Wright, P.E. (1998). Convergence properties of the nelder–mead simplex method in low dimensions. *SIAM Journal on Optimization*, 9(1), 112–147. [1.8.2.1](#)
- Lahrouz, A. and Omari, L. (2013). Extinction and stationary distribution of a stochastic SIRS epidemic model with non-linear incidence. *Statistics & Probability Letters*, 83(4), 960–968. [5.1](#)
- Lan, G., Huang, Y., Wei, C., and Zhang, S. (2019). A stochastic SIS epidemic model with saturating contact rate. *Physica A: Statistical Mechanics and its Applications*, 529, 121504. [3.2](#)
- Landau, L.D. and Lifshitz, E. (1960). *Course of theoretical physics. vol. 8: Electrodynamics of continuous media*. Oxford. [1.1](#)
- Laskey, K.B. and Myers, J.W. (2003). Population markov chain monte carlo. *Machine Learning*, 50(1-2), 175–196. [1.9](#)
- Lau, H., Khosrawipour, V., Kocbach, P., Mikolajczyk, A., Schubert, J., Bania, J., and Khosrawipour, T. (2020). The positive impact of lockdown in Wuhan on containing the COVID-19 outbreak in China. *Journal of Travel Medicine*, 27(3), taaa037. [5.1](#)
- Lavenda, B.H. (1985). Brownian motion. *Scientific American*, 252(2), 70–85. [1.1](#)
- Legendre, S. (1999). Demographic stochasticity: a case study using the ulm software. *Bird study*, 46(sup1), S140–S147. [1.9](#)
- Lemons, D.S. and Gythiel, A. (1997). Paul langevin’s 1908 paper “on the theory of Brownian motion” [“sur la théorie du mouvement brownien,” *cr acad. sci.(paris)* 146, 530–533 (1908)]. *American Journal of Physics*, 65(11), 1079–1081. [1.1](#)
- Leslie, P. and Gower, J. (1960). The properties of a stochastic model for the predator-prey type of interaction between two species. *Biometrika*, 47(3/4), 219–234. [1.1](#)

- 
- Levins, R. (1969). The effect of random variations of different types on population growth. *Proceedings of the National Academy of Sciences*, 62(4), 1061–1065. [1.1](#)
- Li, D., Liu, M., Liu, S., et al. (2015). The evolutionary dynamics of stochastic epidemic model with nonlinear incidence rate. *Bulletin of Mathematical Biology*, 77(9), 1705–1743. [3.2](#), [5.1](#)
- Li, D. and Cui, X. (2017). Dynamics of virus infection model with nonlytic immune response induced by stochastic noise. *Chaos, Solitons & Fractals*, 99, 124–132. [4.4.1](#)
- Li, F., Zhang, S., and Meng, X. (2019a). Dynamics analysis and numerical simulations of a delayed stochastic epidemic model subject to a general response function. *Computational and Applied Mathematics*, 38(2), 1–30.
- Li, G., Wang, W., and Jin, Z. (2006). Global stability of an SEIR epidemic model with constant immigration. *Chaos, Solitons & Fractals*, 30(4), 1012–1019. [5.2.1.1](#)
- Li, M.Y. (2018). Parameter estimation and nonlinear least-squares methods: An Introduction to Mathematical Modeling of Infectious Diseases. 103–124. Springer. [5.3](#)
- Li, S. and Wang, X. (2015). Analysis of a stochastic predator-prey model with disease in the predator and beddington-deangelis functional response. *Advances in Difference Equations*, 2015(1), 224. [4.1](#)
- Li, X., Song, G., Xia, Y., and Yuan, C. (2019b). Dynamical behaviors of the tumor-immune system in a stochastic environment. *SIAM Journal on Applied Mathematics*, 79(6), 2193–2217. [1.9](#), [5.1](#)
- Liang, Y., Greenhalgh, D., and Mao, X. (2016). A stochastic differential equation model for the spread of hiv amongst people who inject drugs. *Computational and Mathematical Methods in Medicine*, 2016. [1.9](#)
- Liao, X. and Mao, X. (1996a). Stability of stochastic neural networks. *Neural, Parallel & Scientific Computations*, 4(2), 205–224. [1.1](#)
- Liao, X. and Mao, X. (1996b). Exponential stability and instability of stochastic neural networks. *Stochastic Analysis and Applications*, 14(2), 165–185. [1.1](#)

## References

---

- Lighthill, M. (1953). On the energy scattered from the interaction of turbulence with sound or shock waves. In *Mathematical Proceedings of the Cambridge Philosophical Society*, volume 49, 531–551. Cambridge University Press. [1.1](#)
- Limpert, E., Stahel, W.A., and Abbt, M. (2001). Log-normal distributions across the sciences: keys and clues: on the charms of statistics, and how mechanical models resembling gambling machines offer a link to a handy way to characterize log-normal distributions, which can provide deeper insight into variability and probability—normal or log-normal: that is the question. *BioScience*, 51(5), 341–352. [4.4.1](#)
- Lin, Q., Zhao, S., Gao, D., Lou, Y., Yang, S., Musa, S.S., Wang, M.H., Cai, Y., Wang, W., Yang, L., et al. (2020). A conceptual model for the coronavirus disease 2019 (COVID-19) outbreak in Wuhan, China with individual reaction and governmental action. *International Journal of Infectious Diseases*, 93, 211–216. [1.9](#), [5.1](#)
- Lipsitch, M., Cohen, T., Cooper, B., Robins, J.M., Ma, S., James, L., Gopalakrishna, G., Chew, S.K., Tan, C.C., Samore, M.H., et al. (2003). Transmission dynamics and control of severe acute respiratory syndrome. *Science*, 300(5627), 1966–1970. [5.1](#)
- Lipsitch, M., Nowak, M.A., Ebert, D., and May, R.M. (1995). The population dynamics of vertically and horizontally transmitted parasites. *Proceedings of the Royal Society of London. Series B: Biological Sciences*, 260(1359), 321–327. [1.9](#), [3.3](#)
- Lipsitch, M., Siller, S., and Nowak, M.A. (1996). The evolution of virulence in pathogens with vertical and horizontal transmission. *Evolution*, 50(5), 1729–1741. [1.9](#), [3.1](#), [3.5](#)
- Liu, M. and Mandal, P.S. (2015). Dynamical behavior of a one-prey two-predator model with random perturbations. *Communications in Nonlinear Science and Numerical Simulation*, 28(1-3), 123–137. [5.1](#)
- Liu, M., Qiu, H., and Wang, K. (2013). A remark on a stochastic predator–prey system with time delays. *Applied Mathematics Letters*, 26(3), 318–323. [1.7.3](#)
- Liu, M. and Wang, K. (2011a). Global stability of a nonlinear stochastic predator–prey system with beddington–deangelis functional response. *Communications in Nonlinear Science and Numerical Simulation*, 16(3), 1114–1121. [1.9](#), [2.1](#), [3.6](#), [4.5](#)

- 
- Liu, M. and Wang, K. (2011b). Global stability of a nonlinear stochastic predator–prey system with Beddington–DeAngelis functional response. *Communications in Nonlinear Science and Numerical Simulation*, 16(3), 1114–1121.
- Liu, M. and Wang, K. (2011c). Persistence and extinction in stochastic non-autonomous logistic systems. *Journal of Mathematical Analysis and Applications*, 375(2), 443–457. [1.7.2](#), [1.9](#), [2.3.3](#)
- Liu, M. and Wang, K. (2011d). Persistence and extinction in stochastic non-autonomous logistic systems. *Journal of Mathematical Analysis and Applications*, 375(2), 443–457. [3.4](#)
- Lotka, A.J. (1925). *Elements of physical biology*. Williams & Wilkins. [1.9](#)
- Lu, S., Lin, J., Zhang, Z., Xiao, L., Jiang, Z., Chen, J., Hu, C., and Luo, S. (2021). Alert for non-respiratory symptoms of coronavirus disease 2019 patients in epidemic period: A case report of familial cluster with three asymptomatic COVID-19 patients. *Journal of Medical Virology*, 93(1), 518–521. [5.1](#)
- Majumder, A., Adak, D., and Bairagi, N. (2020a). Phytoplankton-zooplankton interaction under environmental stochasticity: Survival, extinction and stability. *Applied Mathematical Modelling*. [1.9](#)
- Majumder, A., Adak, D., and Bairagi, N. (2021a). Persistence and extinction criteria of covid-19 pandemic: India as a case study. *Stochastic Analysis and Applications*, 1–125. [6.1](#), [6.3.2](#)
- Majumder, A., Adak, D., and Bairagi, N. (2021b). Persistence and extinction of species in a disease-induced ecological system under environmental stochasticity. *Physical Review E*, 103(3), 032412. [6.2](#)
- Majumder, A., Adak, D., and Bairagi, N. (2021c). Phytoplankton-zooplankton interaction under environmental stochasticity: Survival, extinction and stability. *Applied Mathematical Modelling*, 89, 1382–1404. [6.2](#)
- Majumder, A., Bala, T.K., Adak, D., N’Guérékata, G.M., and Bairagi, N. (2020b). Evaluating the current epidemiological status of Italy: Insights from a stochastic epidemic model. *Nonlinear Studies*, 27(4). [5.1](#)

## References

---

- Malchow, H., Petrovskii, S.V., and Medvinsky, A.B. (2002). Numerical study of plankton–fish dynamics in a spatially structured and noisy environment. *Ecological Modelling*, 149(3), 247–255. [2.1](#)
- Malthus, T.R. (1798). An essay on the theory of population. [1.9](#)
- Mandal, S., Bhatnagar, T., Arinaminpathy, N., Agarwal, A., Chowdhury, A., Murhekar, M., Gangakhedkar, R.R., and Sarkar, S. (2020). Prudent public health intervention strategies to control the coronavirus disease 2019 transmission in India: A mathematical model-based approach. *The Indian Journal of Medical Research*, 151(2-3), 190. [1.9](#), [5.1](#)
- Manski, C.F. and Molinari, F. (2021a). Estimating the covid-19 infection rate: Anatomy of an inference problem. *Journal of Econometrics*, 220(1), 181–192. [1.9](#), [5.1](#), [6.2](#)
- Manski, C.F. and Molinari, F. (2021b). Estimating the COVID-19 infection rate: Anatomy of an inference problem. *Journal of Econometrics*, 220(1), 181–192.
- Manski, C.F. and Molinari, F. (2021c). Estimating the covid-19 infection rate: Anatomy of an inference problem. *Journal of Econometrics*, 220(1), 181–192.
- Mao, X. (2007). Stochastic differential equations and applications. [2.3.1](#), [3.4](#), [5.2.2](#), [5.2.2](#), [5.2.2](#), [5.2.2](#), [5.2.2](#)
- Mao, X. (2011). Stationary distribution of stochastic population systems. *Systems & Control Letters*, 60(6), 398–405. [1.9](#)
- Mao, X., Marion, G., and Renshaw, E. (2002). Environmental brownian noise suppresses explosions in population dynamics. *Stochastic Processes and Their Applications*, 97(1), 95–110.
- Marino, S., Hogue, I.B., Ray, C.J., and Kirschner, D.E. (2008). A methodology for performing global uncertainty and sensitivity analysis in systems biology. *Journal of Theoretical Biology*, 254(1), 178–196. [1.8.2.3](#), [1.8.2.4](#)
- Martcheva, M. (2015). *An introduction to mathematical epidemiology*, volume 61. Springer. [2.2.2](#)

- 
- Martínez-Padilla, J., Redpath, S.M., Zeineddine, M., and Mougeot, F. (2014). Insights into population ecology from long-term studies of red grouse lagopus lagopus scoticus. *Journal of Animal Ecology*, 83(1), 85–98. [4.4.2](#)
- May, R.M. (1972). Limit cycles in predator-prey communities. *Science*, 177(4052), 900–902. [1.9](#), [2.1](#)
- May, R.M. (1973). Stability in randomly fluctuating versus deterministic environments. *The American Naturalist*, 107(957), 621–650. [4.3](#)
- May, R.M. (2019). *Stability and complexity in model ecosystems*, volume 1. Princeton university press. [3.5](#), [4.5](#)
- May, R.M. (2001). *Stability and complexity in model ecosystems*, volume 6. Princeton university press. [1.9](#), [4.1](#)
- McKay, M., Beckman, R., and Conover, W. (1979). A comparison of three methods for selecting values of input variables in the analysis of output from a computer code. *Technometrics*, 21(2), 239–245. [1.8.2.4](#)
- McKendrick, A. (1925). Applications of mathematics to medical problems. *Proceedings of the Edinburgh Mathematical Society*, 44, 98–130. [1.1](#)
- McLaughlin, J.F., Hellmann, J.J., Boggs, C.L., and Ehrlich, P.R. (2002). The route to extinction: population dynamics of a threatened butterfly. *Oecologia*, 132(4), 538–548. [4.5](#)
- Memarzadeh, F. (2012). Literature review of the effect of temperature and humidity on viruses. *ASHRAE Transactions*, 118(1). [1.9](#)
- Merow, C. and Urban, M.C. (2020). Seasonality and uncertainty in global covid-19 growth rates. *Proceedings of the National Academy of Sciences*, 117(44), 27456–27464. [6.1](#)
- Miao, A., Zhang, T., Zhang, J., and Wang, C. (2018). Dynamics of a stochastic SIR model with both horizontal and vertical transmission. *Journal of Applied Analysis and Computation*, 8(4), 1108–1121. [3.2](#)
- Mikhailov, A.S. and Loskutov, A.Y. (2012). *Foundations of synergetics II: Complex patterns*, volume 52. Springer Science & Business Media. [3.2](#)

## References

---

- Mikhailov, A.S. and Loskutov, A.Y. (2013). *Foundations of synergetics II: Chaos and Noise*, volume 52. Springer Science & Business Media. [1.9](#)
- Miller, M.R., White, A., and Boots, M. (2007). Host life span and the evolution of resistance characteristics. *Evolution*, 61(1), 2–14. [1.9](#)
- Mondal, C., Adak, D., Majumder, A., and Bairagi, N. (2020). Mitigating the transmission of infection and death due to SARS-CoV-2 through non-pharmaceutical interventions and repurposing drugs. *ISA transactions*. [1.9](#), [5.1](#), [6.1](#)
- Moore, J. (2002). Parasites and the behavior of animals. *Oxford University Press, USA*. [4.1](#), [4.2.1](#)
- Moore, S., Hill, E.M., Tildesley, M.J., Dyson, L., and Keeling, M.J. (2021). Vaccination and non-pharmaceutical interventions for covid-19: a mathematical modelling study. *The Lancet Infectious Diseases*, 21(6), 793–802. [6.1](#)
- Moré, J.J. (1978). The Levenberg-Marquardt algorithm: implementation and theory. In *Numerical analysis*, 105–116. Springer. [1.8.2.2](#)
- Moss, R., W.A..P.R. (1996). Experimental prevention of a population cycle in red grouse. volume 77, 1512–1530. [4.4.2](#)
- Motulsky, H. and Christopoulos, A. (2004). *Fitting models to biological data using linear and nonlinear regression: a practical guide to curve fitting*. Oxford University Press. [1.8.2.5](#)
- Mukherjee, D. (2003). Stability analysis of a stochastic model for prey-predator system with disease in the prey. *Nonlinear Analysis: Modelling and Control*, 8(2), 83–92. [4.1](#)
- Mukhopadhyay, A., Chattopadhyay, J., and Tapaswi, P. (1998). A delay differential equations model of plankton allelopathy. *Mathematical Biosciences*, 149(2), 167–189. [2.1](#)
- Musa, M.R. and Iyaniwura, S. (2021). Assessing the potential impact of immunity waning on the dynamics of covid-19: an endemic model of covid-19. *MedRxiv*. [6.1](#)
- Nariai, H. (1975). On characteristic turbulent quantities at the bounce epoch in our hadron-dominated model of the universe. *Progress of Theoretical Physics*, 53(1), 287–289. [1.1](#)



- Nariai, H.N. (1974). On the average effect of a highly turbulent gravito-hydrodynamic field in the hadron era of the universe. *Progress of Theoretical Physics*, 52(5), 1539–1553. [1.1](#)
- Nelson, E. (1966). Derivation of the schrödinger equation from newtonian mechanics. *Physical Review*, 150(4), 1079. [1.1](#)
- Nishiura, H., Kobayashi, T., Miyama, T., Suzuki, A., Jung, S.m., Hayashi, K., Kinoshita, R., Yang, Y., Yuan, B., Akhmetzhanov, A.R., et al. (2020). Estimation of the asymptomatic ratio of novel coronavirus infections (COVID-19). *International Journal of Infectious Diseases*, 94, 154. [5.1](#)
- Nordling, C. (1953). A new theory on the cancer-inducing mechanism. *British Journal of Cancer*, 7(1), 68. [1.1](#)
- O'Brien, J. and Wroblewski, J. (1971). Analysis of a nutrient-limited phytoplankton model. In *National Center for Atmospheric Research Manuscript No. 71-146*. [1.1](#)
- Øksendal, B. (2003). Stochastic differential equations. In *Stochastic differential equations*, 65–84. Springer. [1.6](#)
- Olinick, M. (1978). *introduction to mathematical models in the social and life sciences*. Addison-Wesley Pub. Co. [1.9](#)
- Pang, L., Liu, S., Zhang, X., Tian, T., and Zhao, Z. (2020). Transmission dynamics and control strategies of COVID-19 in Wuhan, China. *Journal of Biological Systems*, 28(03), 543–560. [1.9](#), [5.1](#)
- Panik, M.J. (2017). *Stochastic Differential Equations: An Introduction with Applications in Population Dynamics Modeling*. [1.1](#)
- Parker, R.A. (1974). Some consequences of stochasticizing an ecological system model. In *Mathematical Problems in Biology*, 174–183. Springer. [1.1](#)
- Paul, A., Chatterjee, S., and Bairagi, N. (2020a). Covid-19 transmission dynamics during the unlock phase and significance of testing. *Journal of Vaccines & Vaccination*, 6. [1.9](#), [5.1](#), [6.1](#)
- Paul, A., Chatterjee, S., and Bairagi, N. (2020b). Prediction on Covid-19 epidemic for different countries: Focusing on South Asia under various precautionary measures. *Medrxiv*. [1.9](#), [5.1](#), [6.1](#)

## References

---

- Pearl, R. and Reed, L.J. (1920). On the rate of growth of the population of the United States since 1790 and its mathematical representation. *Proceedings of the national academy of sciences*, 6(6), 275–288. [1.9](#)
- Pedersen, M.G. and Meneghini, M. (2020). Quantifying undetected COVID-19 cases and effects of containment measures in Italy. *ResearchGate Preprint (online 21 March 2020)* DOI, 10. [5.1](#)
- Peeri, N.C., Shrestha, N., Rahman, M.S., Zaki, R., Tan, Z., Bibi, S., Baghbanzadeh, M., Aghamohammadi, N., Zhang, W., and Haque, U. (2020). The SARS, MERS and novel coronavirus (COVID-19) epidemics, the newest and biggest global health threats: what lessons have we learned? *International Journal of Epidemiology*, 49(3), 717–726. [5.1](#)
- Peng, L., Yang, W., Zhang, D., Zhuge, C., and Hong, L. (2020). Epidemic analysis of COVID-19 in China by dynamical modeling. *ArXiv preprint arXiv:2002.06563*. [1.9](#), [5.1](#), [5.1](#), [5.3](#)
- Perc, M., Gorišek Miksić, N., Slavinec, M., and Stožer, A. (2020). Forecasting covid-19. *Frontiers in Physics*, 8, 127. [6.1](#)
- Perrin, F. (1934). Mouvement Brownien d'un ellipsoïde-I. Dispersion diélectrique pour des molécules ellipsoïdales. *J. Phys. Radium*, 5(10), 497–511. [1.1](#)
- Petrov, V.V. (1969). On the strong law of large numbers. *Theory of Probability & Its Applications*, 14(2), 183–192. [1.7.7](#), [3.4](#), [3.4](#)
- Pierce, A.D. and Maglieri, D.J. (1972). Effects of atmospheric irregularities on sonic-boom propagation. *The Journal of the Acoustical Society of America*, 51(2C), 702–721. [1.1](#)
- Plank, M.J., Binny, R.N., Hendy, S.C., Lustig, A., James, A., and Steyn, N. (2020). A stochastic model for COVID-19 spread and the effects of Alert Level 4 in Aotearoa New Zealand. *MedRxiv*. [5.1](#)
- Potts, G., Tapper, S., and Hudson, P.J. (1984). Population fluctuations in red grouse: analysis of bag records and a simulation model. *The Journal of Animal Ecology*, 21–36. [4.4.2](#)

- Prem, K., Liu, Y., Russell, T.W., Kucharski, A.J., Eggo, R.M., Davies, N., Flasche, S., Clifford, S., Pearson, C.A., Munday, J.D., et al. (2020). The effect of control strategies to reduce social mixing on outcomes of the covid-19 epidemic in wuhan, china: a modelling study. *The Lancet Public Health*, 5(5), e261–e270. [1.9](#), [6.1](#)
- Pritchard, E., Matthews, P.C., Stoesser, N., Eyre, D.W., Gethings, O., Vihta, K.D., Jones, J., House, T., VanSteenHouse, H., Bell, I., et al. (2021). Impact of vaccination on new SARS-CoV-2 infections in the united kingdom. *Nature Medicine*, 1–9. [6.1](#)
- Pye-Smith, C. (1997). Fox-hunting: beyond the propaganda. *Wildlife Network*. [4.4.2](#)
- Rabajante, J.F. (2020). Insights from early mathematical models of 2019-nCoV acute respiratory disease (COVID-19) dynamics. *ArXiv preprint arXiv:2002.05296*. [1.9](#), [5.1](#)
- Rabiu, M. and Iyaniwura, S.A. (2022). Assessing the potential impact of immunity waning on the dynamics of covid-19 in South Africa: an endemic model of covid-19. *Nonlinear Dynamics*, 1–21. [6.1](#)
- Rand, D.A. and Wilson, H.B. (1991). Chaotic stochasticity: a ubiquitous source of unpredictability in epidemics. *Proceedings of the Royal Society of London. Series B: Biological Sciences*, 246(1316), 179–184. [1.9](#)
- Rasconi, S., Winter, K., and Kainz, M.J. (2017). Temperature increase and fluctuation induce phytoplankton biodiversity loss—evidence from a multi-seasonal mesocosm experiment. *Ecology and Evolution*, 7(9), 2936–2946. [2.8](#)
- Redpath, S.M. and Thirgood, S.J. (1997). Birds of prey and red grouse. [4.4.2](#)
- Renshaw, E. (1993). *Modelling biological populations in space and time*, volume 11. Cambridge University Press. [1.9](#)
- Renshaw, E. (2015). Stochastic population processes: analysis, approximations, simulations. *OUP Oxford*. [5.1](#)
- Restif, O. and Koella, J.C. (2003). Shared control of epidemiological traits in a co-evolutionary model of host-parasite interactions. *The American Naturalist*, 161(6), 827–836. [1.9](#)

## References

---

- Reynolds, C.S. (2006). *The ecology of phytoplankton*. Cambridge University Press. [2.7](#)
- Rhodes, C. and Martin, A. (2010). The influence of viral infection on a plankton ecosystem undergoing nutrient enrichment. *Journal of Theoretical Biology*, 265(3), 225–237. [2.1](#)
- Ripa, J. and Lundberg, P. (2000). The route to extinction in variable environments. *Oikos*, 90(1), 89–96. [1.9](#), [4.1](#)
- Roghani, A. (2021). The influence of covid-19 vaccine on daily cases, hospitalization, and death rate in tennessee: A case study in the united states. *JMIRx Med*, 2(3):e29324. [6.1](#)
- Rosenzweig, M.L. (1971). Paradox of enrichment: destabilization of exploitation ecosystems in ecological time. *Science*, 171(3969), 385–387. [1.9](#), [2.1](#)
- Rossmann, H., Shilo, S., Meir, T., Gorfine, M., Shalit, U., and Segal, E. (2021). Covid-19 dynamics after a national immunization program in israel. *Nature Medicine*, 1–7. [6.1](#)
- Roy, S. and Chattopadhyay, J. (2007). The stability of ecosystems: a brief overview of the paradox of enrichment. *Journal of Biosciences*, 32(2), 421–428. [1.9](#), [2.1](#)
- Ruokolainen, L., Lindén, A., Kaitala, V., and Fowler, M.S. (2009a). Ecological and evolutionary dynamics under coloured environmental variation. *Trends in Ecology & Evolution*, 24(10), 555–563. [1.9](#)
- Ruokolainen, L., Lindén, A., Kaitala, V., and Fowler, M.S. (2009b). Ecological and evolutionary dynamics under coloured environmental variation. *Trends in Ecology & Evolution*, 24(10), 555–563. [4.1](#)
- Saha, P. and Bairagi, N. (2018). Dynamics of vertically and horizontally transmitted parasites: Continuous vs discrete models. *International Journal of Difference Equations*, 13(2), 139–156. [3.3](#)
- Saha, T. and Bandyopadhyay, M. (2008). Dynamical analysis of a delayed ratio-dependent prey–predator model within fluctuating environment. *Applied Mathematics and Computation*, 196(1), 458–478. [1.9](#)

- Sanyaolu, A., Okorie, C., Marinkovic, A., Patidar, R., Younis, K., Desai, P., Hosein, Z., Padda, I., Mangat, J., and Altaf, M. (2020). Comorbidity and its impact on patients with covid-19. *SN Comprehensive Clinical Medicine*, 1–8. [6.1](#)
- Sardar, T., Nadim, S., and Chattopadhyay, J. (2020). Assessment of 21 Days Lock-down Effect in Some States and Overall India: A Predictive Mathematical Study on COVID-19 Outbreak, arXiv preprint 2020. *ArXiv preprint arXiv:2004.03487 v1 [q-bio. PE]*. [1.9](#), [5.1](#)
- Sarkar, K., Khajanchi, S., and Nieto, J.J. (2020). Modeling and forecasting the covid-19 pandemic in india. *Chaos, Solitons & Fractals*, 139, 110049. [6.1](#)
- Sarwardi, S., Haque, M., and Venturino, E. (2011). A leslie-gower holling-type ii ecoepidemic model. *Journal of Applied Mathematics and Computing*, 35(1-2), 263–280. [4.2.1](#), [4.2.2](#), [4.2.2](#), [4.5](#)
- Scheffer, M. (1991). Fish and nutrients interplay determines algal biomass: a minimal model. *Oikos*, 271–282. [2.1](#), [2.1](#), [2.1](#), [2.1](#), [2.8](#)
- Scheffer, M., Rinaldi, S., and Kuznetsov, Y.A. (2000). Effects of fish on plankton dynamics: a theoretical analysis. *Canadian Journal of Fisheries and Aquatic Sciences*, 57(6), 1208–1219. [2.1](#)
- Sharon A. Evans, Steve M. Redpath, F.L.F.M. (2007). Alternative methods for estimating density in an upland game bird: the red grouse *lagopus lagopus scoticus*. volume 13, 130–139. [4.4.2](#)
- Sibly, R.M. and Hone, J. (2002). Population growth rate and its determinants: an overview. *Philosophical Transactions of the Royal Society of London. Series B: Biological Sciences*, 357(1425), 1153–1170. [1.9](#)
- Sieber, M., Malchow, H., and Hilker, F.M. (2014). Disease-induced modification of prey competition in eco-epidemiological models. *Ecological Complexity*, 18, 74–82. [4.1](#)
- Smith, H.L. and Waltman, P. (1995). The theory of the chemostat: dynamics of microbial competition. *Cambridge University Press*, 13. [5.2.1.2](#)
- Sobczyk, K. (2001). *Stochastic differential equations: with applications to physics and engineering*, volume 40. Springer Science & Business Media. [1.1](#)

## References

---

- Sorensen, R.E. and Minchella, D.J. (1998). Parasite influences on host life history: *Echinostoma revolutum* parasitism of *Lymnaea elodes* snails. *Oecologia*, 115(1), 188–195. [3.1](#)
- Spagnolo, B., Valenti, D., and Fiasconaro, A. (2004). Noise in ecosystems: a short review. *arXiv preprint q-bio/0403004*. [4.3](#)
- Stephan, T. and Wissel, C. (1994). Stochastic extinction models discrete in time. *Ecological Modelling*, 75, 183–192. [4.5](#)
- Suttle, C.A. and Chan, A.M. (1993). Marine cyanophages infecting oceanic and coastal strains of synechococcus: abundance, morphology, cross-infectivity and growth characteristics. *Marine Ecology-Progress Series*, 92, 99–99. [2.1](#)
- Takian, A., Raoofi, A., and Kazempour-Ardebili, S. (2020). COVID-19 battle during the toughest sanctions against Iran. *Lancet (London, England)*, 395(10229), 1035. [5.1](#)
- Tapaswi, P. and Mukhopadhyay, A. (1999). Effects of environmental fluctuation on plankton allelopathy. *Journal of Mathematical biology*, 39(1), 39–58. [1.9](#)
- Tatarski, V.I. (2016). *Wave propagation in a turbulent medium*. Courier Dover Publications. [1.1](#)
- Tompkins, D. and Begon, M. (1999). Parasites can regulate wildlife populations. *Parasitology Today*, 15(8), 311–313. [1.9](#), [3.1](#)
- Tuckwell, H.C. (2018). *Elementary applications of probability theory: With an introduction to stochastic differential equations*. Chapman and Hall/CRC. [1.9](#)
- Turchin, P. (2003). Complex population dynamics: a theoretical/empirical synthesis. *Princeton University Press*, 35. [4.1](#)
- Turelli, M. (1977). Random environments and stochastic calculus. *Theoretical Population Biology*, 12(2), 140–178. [1.6](#)
- Ubbink, J. (1971). The relation between the correlations of the incident photons and the noise in a photoconductor. *Physica*, 52(2), 253–278. [1.1](#)
- Ullersma, P. (1966). An exactly solvable model for Brownian motion: I. Derivation of the Langevin equation. *Physica*, 32(1), 27–55. [1.1](#)

- 
- Valenti, D., Fiasconaro, A., and Spagnolo, B. (2004a). Stochastic resonance and noise delayed extinction in a model of two competing species. *Physica A: Statistical Mechanics and its Applications*, 331(3-4), 477–486. [3.4](#)
- Valenti, D., Fiasconaro, A., and Spagnolo, B. (2004b). Stochastic resonance and noise delayed extinction in a model of two competing species. *Physica A: Statistical Mechanics and its Applications*, 331(3-4), 477–486. [4.3](#), [4.4.1](#)
- Van den Driessche, P. and Watmough, J. (2002). Reproduction numbers and sub-threshold endemic equilibria for compartmental models of disease transmission. *Mathematical Biosciences*, 180(1-2), 29–48. [3.3](#), [3.3](#)
- Van Kampen, N.G. (1976). Stochastic differential equations. *Physics Reports*, 24(3), 171–228. [1.1](#)
- Vanni, M.J. (1987). Effects of food availability and fish predation on a zooplankton community. *Ecological Monographs*, 57(1), 61–88. [2.1](#)
- Vasseur, D.A. and Yodzis, P. (2004). The color of environmental noise. *Ecology*, 85(4), 1146–1152. [7](#)
- Venturino, E. (2002). Epidemics in predator–prey models: disease in the predators. *Mathematical Medicine and Biology*, 19(3), 185–205. [4.1](#)
- Verhulst, P. (1838). Notice on the law that the population follows in its growth. *Corresp Math Phys*, 10, 113–26. [1.9](#)
- Volterra, V. (1926). Fluctuations in the abundance of a species considered mathematically. *Nature*, 118(2972), 558–560. [1.9](#)
- Wang, H. and Liu, M. (2020). Stationary distribution of a stochastic hybrid phytoplankton–zooplankton model with toxin-producing phytoplankton. *Applied Mathematics Letters*, 101, 106077. [4.1](#)
- Wangsness, R.K. and Bloch, F. (1953). The dynamical theory of nuclear induction. *Physical Review*, 89(4), 728. [1.1](#)
- Wei, C., Liu, J., and Zhang, S. (2018). Analysis of a stochastic eco-epidemiological model with modified leslie-gower functional response. *Advances in Difference Equations*, 2018(1), 119. [4.1](#)

## References

---

- Wenzel, A.R. (1975). Propagation of transients in a random medium. *Journal of Mathematical Physics*, 16(1), 44–49. [1.1](#)
- WHO (2020). Covid-19 public health emergency of international concern (phecic). In *Global Research and Innovation Forum*. [6.1](#)
- WHO (2021). Who - prequalification of medical products (ivds, medicines, vaccines and immunization devices, vector control). In *COVID-19 vaccines WHO EUL issued*, <https://extranet.who.int/pqweb/vaccines/vaccinescovid-19-vaccine-eul-issued>. WHO. [6.1](#)
- Wu, R., Zou, X., and Wang, K. (2014). Dynamical behavior of a competitive system under the influence of random disturbance and toxic substances. *Nonlinear Dynamics*, 77(4), 1209–1222. [4.1](#)
- Xiao, Y. and Chen, L. (2002). A ratio-dependent predator–prey model with disease in the prey. *Applied Mathematics and Computation*, 131(2-3), 397–414. [4.1](#)
- Yanev, N.M., Stoimenova, V.K., and Atanasov, D.V. (2020). Stochastic modeling and estimation of COVID-19 population dynamics. *ArXiv preprint arXiv:2004.00941*. [5.1](#)
- Yang, Q. and Mao, X. (2014). Stochastic dynamical behavior of SIRS epidemic models with random perturbation. *Mathematical Biosciences and Engineering*, 11(4), 1003–1025. [5.1](#), [6.2](#)
- Yongzhen, P., Shuping, L., and Changguo, L. (2011). Effect of delay on a predator–prey model with parasitic infection. *Nonlinear Dynamics*, 63(3), 311–321. [4.1](#)
- Yu, J., Jiang, D., and Shi, N. (2009). Global stability of two-group sir model with random perturbation. *Journal of Mathematical Analysis and Applications*, 360(1), 235–244. [1.9](#)
- Yu, X., Yuan, S., and Zhang, T. (2018). The effects of toxin-producing phytoplankton and environmental fluctuations on the planktonic blooms. *Nonlinear Dynamics*, 91(3), 1653–1668. [4.1](#)
- Yu, X., Yuan, S., and Zhang, T. (2019). Survival and ergodicity of a stochastic phytoplankton–zooplankton model with toxin-producing phytoplankton in an im-



- 
- pulsive polluted environment. *Applied Mathematics and Computation*, 347, 249–264. [4.1](#)
- Yu, X. and Yang, R. (2020). COVID-19 transmission through asymptomatic carriers is a challenge to containment. *Influenza and Other Respiratory Viruses*, 14(4), 474–475. [5.1](#)
- Zhai, S., Luo, G., Huang, T., Wang, X., Tao, J., and Zhou, P. (2021). Vaccination control of an epidemic model with time delay and its application to Covid-19. *Nonlinear Dynamics*, 106(2), 1279–1292. [6.1](#)
- Zhang, X., Li, Y., and Jiang, D. (2017). Dynamics of a stochastic holling type ii predator–prey model with hyperbolic mortality. *Nonlinear Dynamics*, 87(3), 2011–2020.
- Zhang, Y., Yu, X., Sun, H., Tick, G.R., Wei, W., and Jin, B. (2020a). COVID-19 infection and recovery in various countries: Modeling the dynamics and evaluating the non-pharmaceutical mitigation scenarios. *ArXiv preprint arXiv:2003.13901*. [1.9](#), [5.1](#)
- Zhang, Y., You, C., Cai, Z., Sun, J., Hu, W., and Zhou, X.H. (2020b). Prediction of the covid-19 outbreak based on a realistic stochastic model. *MedRxiv*. [6.1](#)
- Zhao, W., Liu, J., Chi, M., and Bian, F. (2019). Dynamics analysis of stochastic epidemic models with standard incidence. *Advances in Difference Equations*, 2019(1), 1–16. [5.1](#)
- Zhao, Y. and Jiang, D. (2013). Dynamics of stochastically perturbed SIS epidemic model with vaccination. *Hindawi*, 2013. [5.1](#)
- Zhao, Y., Yuan, S., and Zhang, T. (2016). The stationary distribution and ergodicity of a stochastic phytoplankton allelopathy model under regime switching. *Communications in Nonlinear Science and Numerical Simulation*, 37, 131–142. [4.1](#)
- Zhou, D., Liu, M., and Liu, Z. (2020a). Persistence and extinction of a stochastic predator–prey model with modified Leslie–Gower and Holling-type II schemes. *Advances in Difference Equations*, 2020(1), 1–15. [5.1](#), [6.2](#)

## References

---

- Zhou, J. and Shi, J. (2013). The existence, bifurcation and stability of positive stationary solutions of a diffusive leslie–gower predator–prey model with holling-type ii functional responses. *Journal of Mathematical Analysis and Applications*, 405(2), 618–630. [4.1](#)
- Zhou, X., Wu, Z., Yu, R., Cao, S., Fang, W., Jiang, Z., Yuan, F., Yan, C., and Chen, D. (2020b). Modelling-based evaluation of the effect of quarantine control by the Chinese government in the coronavirus disease 2019 outbreak. *Science China Life Sciences*, 63, 1257–1260. [1.9](#), [5.1](#)
- Zhu, C. and Yin, G. (2007). Asymptotic properties of hybrid diffusion systems. *SIAM Journal on Control and Optimization*, 46(4), 1155–1179. [1.7.6](#)



## List of Papers Included in the Thesis

1. **Abhijit Majumder**, Debadatta Adak, and Nandadulal Bairagi. "Phytoplankton-zooplankton interaction under environmental stochasticity: Survival, extinction and stability." *Applied Mathematical Modelling*, 89(2021), 1382 – 1404.
2. **Abhijit Majumder**, Debadatta Adak, and Nandadulal Bairagi. "Persistence and extinction of species in a disease-induced ecological system under environmental stochasticity." *Physical Review E*, 103.3 (2021), 032412.
3. **Abhijit Majumder**, Debadatta Adak, and Nandadulal Bairagi. "Persistence and extinction criteria of Covid-19 pandemic: India as a case study." *Stochastic Analysis and Applications*, 40.2 (2022), 179 – 208.
4. **Abhijit Majumder**, Debadatta Adak, Nandadulal Bairagi, and Adeline Samson. "Persistence and extinction of infection in stochastic SIS host-parasite epidemic model with horizontal and imperfect vertical transmissions." *Communicated*.
5. **Abhijit Majumder**, and Nandadulal Bairagi. "Is large-scale vaccination sufficient for controlling the Covid-19 pandemic with uncertainties? A model-based study." *Communicated*.

## Published/Accepted Papers not Included in the Thesis

1. Debadatta Adak, **Abhijit Majumder**, and Nandadulal Bairagi. "Mathematical perspective of COVID-19 pandemic: disease extinction criteria in deterministic and stochastic models." *Chaos, Solitons & Fractals*, 142 (2021), 110381.
2. **Abhijit Majumder**, Tapas Kumar Bala, Debadatta Adak, Gaston M. N'Guérékata and Nandadulal Bairagi. "Evaluating the current epidemiological status of Italy: Insights from a stochastic epidemic model." *Nonlinear Studies*, 27, no. 4 (2020).
3. Chittaranjan Mondal, Debadatta Adak, **Abhijit Majumder** and Nandadulal Bairagi. "Mitigating the transmission of infection and death due to SARS-CoV-2 through non-pharmaceutical interventions and repurposing drugs." *ISA Transactions* (2020), 124 (2020) 236 – 246.
4. **Abhijit Majumder**, Debadatta Adak, Tapas Kumar Bala and Nandadulal Bairagi. "Global picture of Covid-19 pandemic with emphasis on European Sub-continent.", *Springer Nature*. (Accepted).